Synthetic Studies of Amide-functionalized Helicene-like Molecules

アミド基を持つヘリセン様分子の合成研究

2020

Yongning Xing

Table of Contents

Theoretical Section

Experimental Section

List of abbreviation

AcOEt	ethyl acetate
aq.	aqueous
*n*Bu	normal butyl
cat.	catalyst
DBU	diazabicycloundecene
DCC	dicyclohexylcarbodiimide
DIPEA	diisopropylethylamine
DPPA	diphenylphosphoryl azide
DMA	dimethylacetamide
DMAP	4-dimethylaminopyridine 4-dimethylaminopyridine
DMF	*N*, *N*-dimethylformamide
DMSO	dimethylsulfoxide
ee	enantiomeric excess
ESI	electrospray ionization
FAB	fast-atom ionization
HOBT	1-hydroxybenzotriazole
HPLC	high performance liquid chromatography
HRMS	high resolution mass spectrometer
IR	infrared
Me	methyl
min	minute
mp	melting point
ND	not detected
NMR	nuclear magnetic resonance
PTLC	preparative thin-layer chromatography
PMB	*p*-methoxybenzene
PMP	*p*-mehoxyphenyl
TFA	trifluoroacetic acid
THF	tetrahydrofuran
TS	transition state
UV	ultraviolet

Theoretical Section

Foreword

During the past one hundred and twenty years, helicenes gradually draw more and more attention because of the diversity of helical aromatic structures and various functionalizations,[1] which make helicenes to be unique π-conjugated systems provided with special chemical properties[2] and wide range of applications.[3] Possessing inherent chirality, helicenes are believed to be chiral elements and show particular chiroptical properties with introduction of different functional groups. The ability of self-assembly promotes helicenes to be highlighted in the area of organic materials.[4]

A specific attention has been paid to heterohelicenes and heterohelicene-like molecules, bearing hetero-functional groups as constituent moieties in helical backbones, generally because of their special properties, interesting chemical behaviors and therefore varieties of potential applications as chiral elements in organic materials, chiral catalysts,[5] and bioactive compounds.[6] Since there's a growing demand of these attractive helical molecules, it becomes highly desirable to synthesize hetero-functionalized helicenes or helicene-like molecules with concise synthetic strategies.

Among heterohelicenes and heterohelicene-like molecules, amide-functionalized helicenes and helicene-like molecules, bearing the amide functional group at the periphery of the helical backbones especially draw the author's interests, as shown below, through the synthetic background as described in **Chapter 1**.

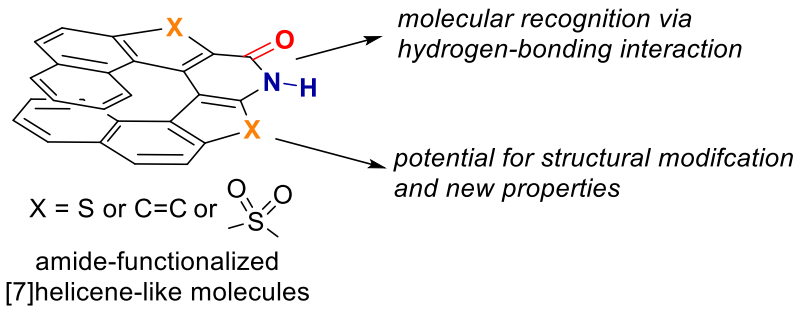

Compared with carbohelicenes, the amide group inserted into helix will offer the potential to obtain a variety of functionalized helical structures, and there will be a possibility of adding sulfonyl groups on the helicene outer core which might change the acidity of amide, induce new molecular recognition areas and change other helical properties by the replacement of thiophene ring instead of benzene ring. These amide-functionalized molecules might also show special self-assembly phenomenon with amide groups through intramolecular hydrogen-bonding interaction.

The self-assembling property is a key feature for exhibiting the functions of helicene molecules.[7] Therefore, the amide-functionalized helicene and helicene-like molecules would be promising as functionalized structures which exhibit special properties through molecular assembly. Therefore, the author motivated development of the new and concise synthetic methods towards heterohelicenes and heterohelicene-like molecules.

Chapter 1
Introduction

1.1 General introduction of helicenes and heterohelicenes

Helicenes are a kind of unique π-conjugated and characteristically helical polyaromatic compounds, which mainly consist of *ortho*-fused benzene or other aromatic rings with nonplanar screw-shaped skeletons and show a distinctive helical chirality (**Figure 1-1**).[8,9] Particularly, heterohelicenes are a significant class of helicenes, which are usually represented as helical heteroaromatics and generally considered to be composed of *ortho* (or mostly *ortho*) condensed benzene, pyridine, pyrrole, thiophene, furan and other heterocyclic rings to form a helical backbone. Additionally, they can be fused and functionalized.

Besides the traditional definition of helicene and heterohelicene molecules, there also exist helical structures (**Figure 1-1**), called helicene-like molecules. Helicene-like molecules usually contain at least one saturated atom as a part of the fused rings in the helicene-type core system. In the case of the author's target compounds **1a** and **1b**, since the tautomerism configuration of amide is not definite, whilst pyridin-2(1*H*)-one moiety is not an aromatic ring, the molecules therefore are called [7]helicene-like molecules.

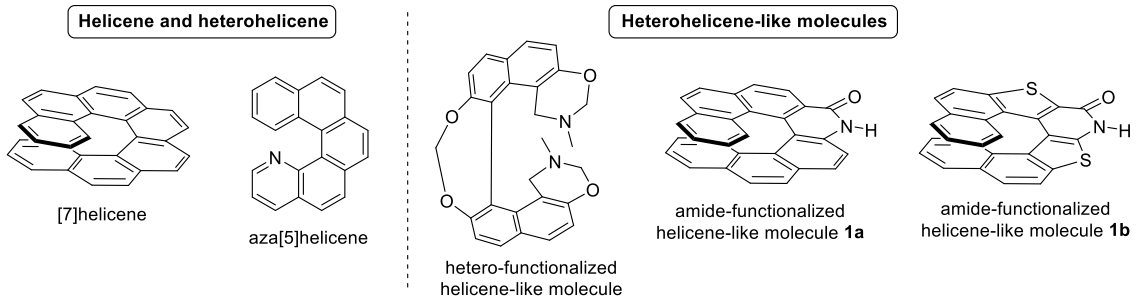

Figure 1-1. Examples of helicene, heterohelicene and helicene-like molecules
(for selected examples see: ref. 8, 9)

The structural features and helicity are described with [6]helicene as example (**Figure 1-2**). The helicene's inner core can be distinguished that the helix experiences steric clashes towards the inner side. On the contrary, the outer skeleton of the helicene is called the helicene's outer core. The benzene rings at the beginning and at the end of the helical arrangement are called the terminal or peripheral rings. This structural organization results in a helical chiral cavity (**Figure 1-2A**).

In general, helicene exists as helically chiral molecule in the case of the terminal aromatic moieties, leading to steric repulsion. The helical structure is assigned the name (*P*)-enantiomer

observed as right-handed helix (clockwise moving from up to down) or (*M*)-enantiomer observed as left-handed helix (anti clockwise moving from up to down) (**Figure 1-2B**).

Due to the *ortho*-fusion mode, each aromatic ring contributes to the total helicity of the structure through an in-plane turn angle (**Figure 1-2C**). The molecule is forced to adopt a helically chiral structure when the sum of the in-plane angles of the rings in helicene core becomes 360° or more, caused by the corresponding steric clashes among the terminal/peripheral rings.

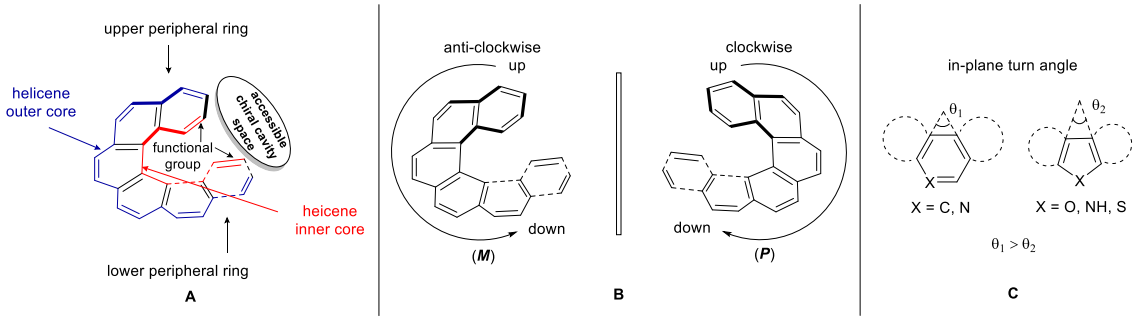

Figure 1-2. (A) Explanation of terms used for helicene structures and chiral cavity; (B) Helicity and enantiomers of [6]helicene; (C) Comparison of the in-plane turn angles (θ) of different rings.

Helicenes show particularly attractive chiroptical properties because of their helical shape, π-electronic conjugation, self-assembly and other features, such as circular dichroism (CD) which gives the structural information about the electronic ground state. Because of inherent chirality and functional groups, heterohelicenes have the potential of a series of promising applications in asymmetric catalysis,[3i,5] enantioselective molecular recognition and chiroptical or electro-optical functional materials.[4] Besides, heterohelicenes, especially thiahelicenes, might show biological activities such as protein inhibitors and interactions with DNA acting as a new scaffold for new drugs.[6] Several examples are displayed in **Figure 1-3**.

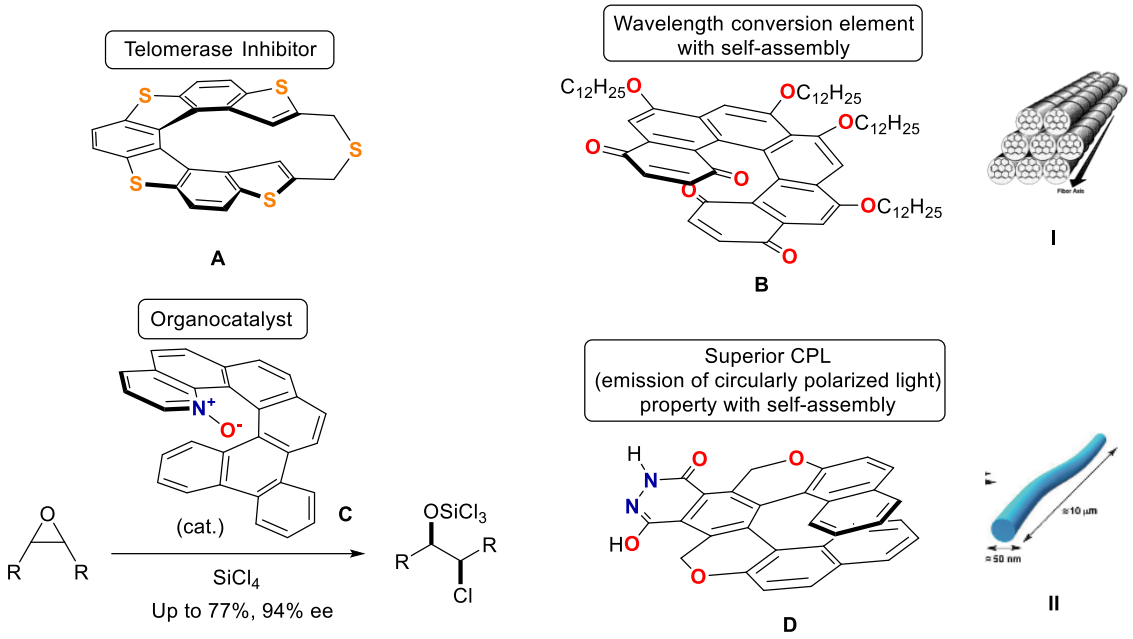

Figure 1-3. Representative applications of helicenes (For **A**, see ref. 6f; Figure I is the schematic representation of column of stacked helicene molecules **B** as observed in solid bulk samples, see ref. 4b; For **C**, see ref. 3i; Figure II is the schematic representation of the formation of fibrous aggregations from the trimeric disk of compound **D** dissolved in toluene, see ref. 4c)

1.2 Examples of synthesis of amide-functionalized helicenes and helicene-like molecules

Since the first helicene was synthesized, there has been 120 years. Till now, more and more new methods of synthesis of helicenes with satisfactory results have been developed. However, the examples of synthesis of amide-functionalized helicenes and helicene-like molecules have been reported in the limited examples as summarized below. Espeically for multiple fused helical structures, one of the challenges in synthesis is to overcome the steric repulsion at terminal part. Compound **1a** is taken as example to show steric clash at peripheral rings (**Figure 1-4**), as well as contributing to the formation of helical shape and unique properties such as high racemization barriers, which will be discussed in detail in **Chapter 4**.

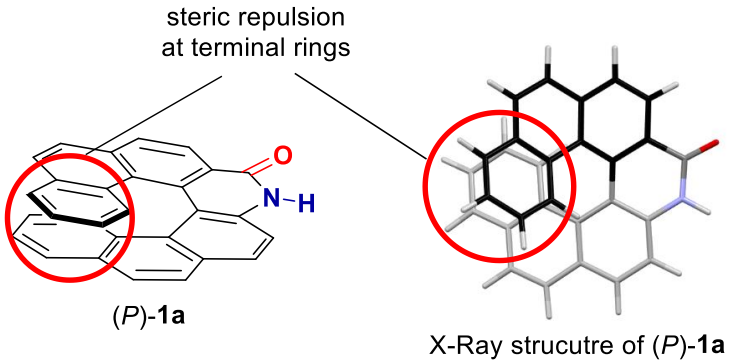

Figure 1-4. One example of steric clash in helical structure

To achieve the cyclization to sterically hindered helical structures in these amide-functionalized molecules, a photo-induced cyclization has been adapted, which is originally applied in carbohelicene synthesis.[1h,1n,1o,1p] In 2000, Branda prepared terminal amide-functionalized [7]helicene, in minor amounts through irradiation of an isomeric mixture with iodine as an oxidizing agent and propylene oxide as an HI scavenger and the following removal of the benzyl groups (**Scheme 1-1**).[7d] However, this method is not readily applicable to gram-scale syntheses because high-dilution conditions and special apparatuses for the photo-irradiation were needed and a undesirable isomer was obtained as the main product.

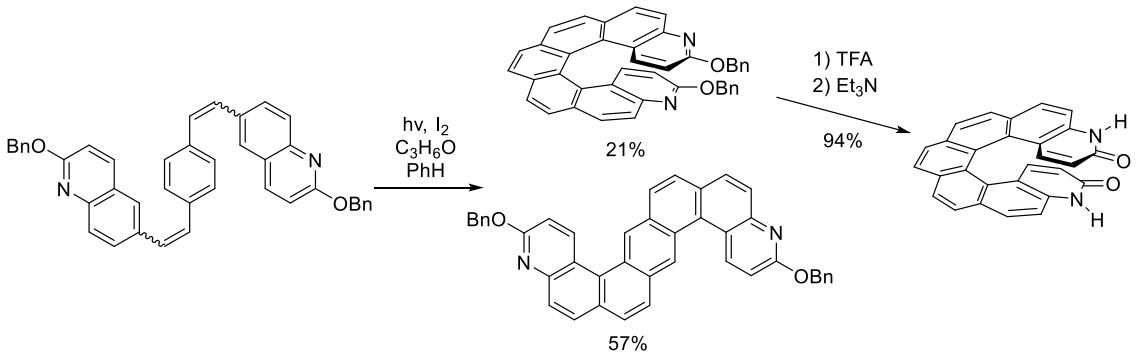

Scheme 1-1. Synthesis of terminal amide-functionalized [7]helicene-like molecule by Branda

Reported by Suzuki and Murase, a continuous flow strategy was performed to furnish amide-type aza[6]helicene by virtue of the borate structure, in which the phenyl group located in close to the fused cyclic rings. The oxidative photocyclization and easy brokenness of nitrogen-oxygen bond gave the amide-functionalized helicene-like molecule (**Scheme 1-2**).[10] Cumbersome experimental operations, harsh reaction conditions, and low yield make it difficult to obtain the desired product conveniently and efficiently.

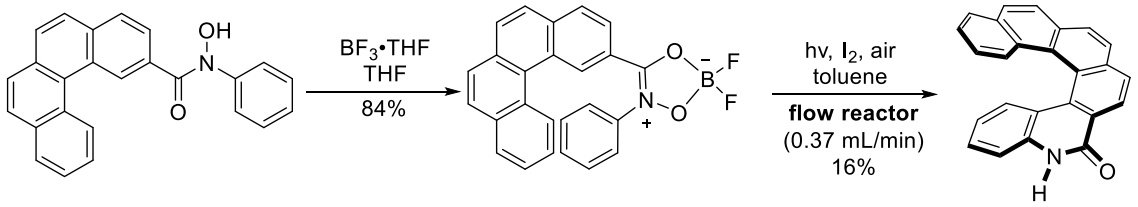

Scheme 1-2. Synthesis of amide-type aza[6]helicene by Suzuki and Murase

Transition-metal catalyzed reactions represent another promising pathway for asymmetric synthesis of heterohelicenes and heterohelicene-like molecules,[1s,4c,11] which have been proved to be powerful enough to overcome the terminal steric repulsion, especially in highly fused systems.

A highly efficient method for the enantioselective synthesis of azahelicenes has been achieved through the Au-catalyzed sequential intramolecular hydroarylation of alkynes by Tanaka in 2014. The amide-type [6]helicene was afforded in 92% yield with 74% ee value by Au-catalyzed enantioselective sequential intramolecular hydroarylation from a diyne substrate with two naphthyl groups (**Scheme 1-3**).[11b] Although this method is quite powful, further improvement of the enantioselectivity would be needed.

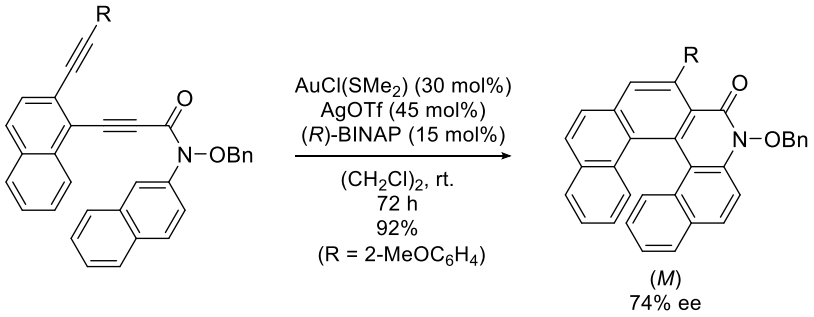

Scheme 1-3. Synthesis of (*M*)-amide-type [6]helicene by Tanaka

With the short review of synthesis of amide-functionalized helicene-like molecules, it has been realized that very limited methods have been developed to achieve the cyclization by overcoming terminal steric effect, especially in highly fused systems. Furthermore, photocyclization methods are hardly applied to the scaled-up preparation of heterohelicenes and heterohelicene-like molecules. Therefore, simple cyzliation conditions that do not use photocyclization are required.

1.3 Background and design of the synthetic strategies to amide-functionalized [7]helicene-like molecules

Previously, a synthetic investigation of axially chiral biary δ-amino acid **2** processing aniline-type amino and carboxy groups at 2,2'-position has been conducted in the author's group (**Scheme 1-4**).[12] In the course of this research, it has been discovered that there exists a spontaneous cyclization of (*S*)-binaphthyl-type δ-amino acid molecule, furnishing an (*dl*)-amide-functionalized [5]helicene-like molecule. In this process, the amide group was incorporated into the fused heterocyclic system as a constituent moiety.[12a] Moreover, the properties of *N*-PMP substituted amide-functionalized [5]helicene-like molecule, for instance, its twisted aromatic system, were also revealed by X-Ray analysis. However, the racemization barrier is too low (24.6 kcal/mol at 60°C) to permit it to exist in a configurationally stable form at ambient temperature.

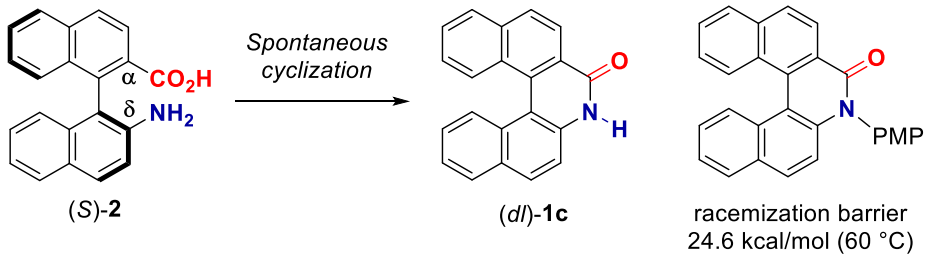

Scheme 1-4. Discovery of spontaneous cyclization process

It's envisioned that if the racemization barrier energy was increased sufficiently, such amide-functionalized molecules could become promising chiral functionalized heterohelicene-like molecules. To the best of my knowledge, there is no precedent for employing an lactamization for a cyclization reaction that yields a heterhelicene-like molecule except for our example.[12a] Therefore, it was intended to prepare amide-functionalized [7]helicene-like molecules, with the expectation that it would exhibit stable helical chirality.

Furthermore, a series of palladium-catalyzed domino reaction of *ortho*-halobenzamide to phenanthridinone derivatives have been conducted by Catellani (**Scheme 1-5A**),[13] our group (**Scheme 1-5B and C**)[12a, 14] and Chen (**Scheme 1-5D**).[15] Early in 2006, Catellani discovered that a catalytic multistep process sequence combining the palladium-catalyzed homocoupling of *ortho*-bromobenzothiophene amide in the presence of $Pd(OAc)_2$/TFP as the catalyst leads to *N*-PMB sulfur-containing fused cyclic compound, that can be recognized as an amide-functionalized [5]helicene-type molecule, under mild conditions (**Scheme 1-5A**). Our group also developed this-type of coupling in the presence of biaryl phosphine ligand (**Scheme 1-5B**).[14] Further investigation in our group found the phosphine-ligand-free conditions (cat. $Pd_2(dba)_3$, K_2CO_3 in

DMF), which led to amide-functionalized [5]helicene-like molecule in excellent yield in a single step (**Scheme 1-5C**).[12a]

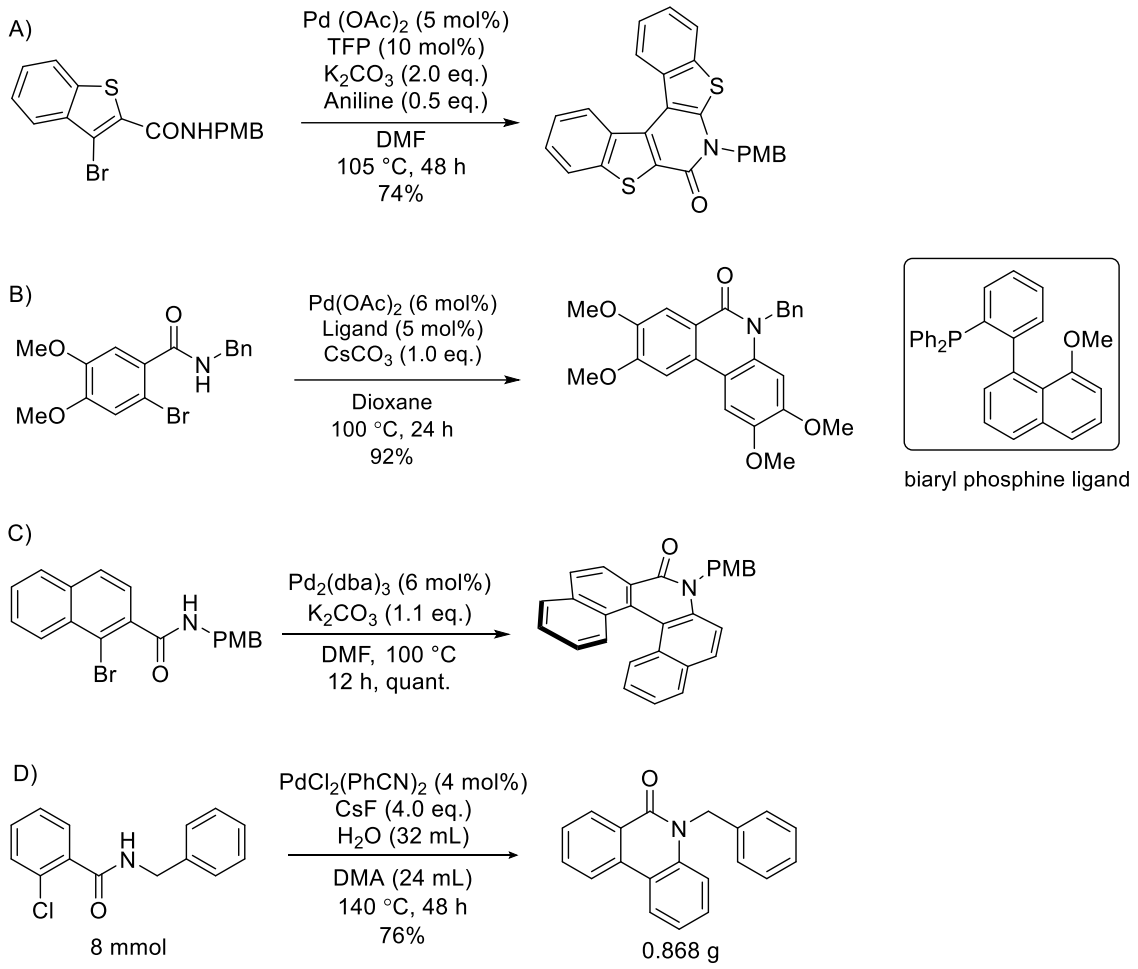

Scheme 1-5. Palladium-catalyzed domino reactions to phenanthridione derivatives

The domino reaction of *ortho*-chlorobenzamides was further investigated by Chen (**Scheme 1-5D**).[15] After optimization of conditions, the catalytic system was established to be $PdCl_2(PhCN)_2$ as catalyst, CsF as base, water as additive at 140 °C in DMA. A broad substrate scope of *N*-substituted 2-chlorobenzamides as well as a scaled-up experiment were exemplified in this protocol.

However, to my best knowledge, there is no report for this domino approach applied with the highly fused cyclic system such as naphtho[2,1-*b*]thiophene **3** towards amide-functionalized [7]helicene-like molecules which are also regarded as optically active helical molecules (**Scheme 1-6**). Thus, an strategy for the synthesis of sulfur containing amide-functionalized [7]helicene-like molecule **1a** and **1b** via palladium-catalyzed domino reaction would be worthy to examine.

Taking these backgrounds into account, basically two strategies were proposed to achieve the synthesis, including lactamization and palladium catalyzed domino reaction (**Scheme 1-6**).

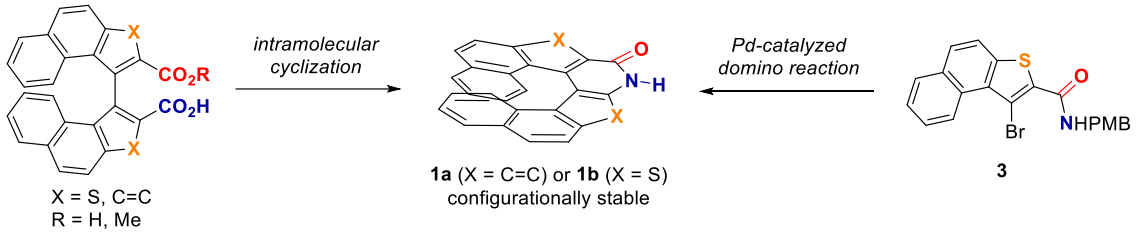

Scheme 1-6. Synthetic strategies towards amide-functionalized [7]helicene-like molecules

In **Chapter 2**, the author designed the lactamization as a key to amide-functionalized [7]helicene-like molecules. After being prepared the monomethyl ester of biphenanthryl dicarboxylic acid **4**, helicene-like molecule **1a** was obtained under Curtius reaction conditions with DPPA and subsequent addition of H_2O via the lactamization of the intermediary aniline-type δ-amino acid derivative **5**. This cyclization was readily expanded to the preparation of optically active (*M*)- and (*P*)-helicene-like molecules **1a** from (*R*)- and (*S*)-biphenanthryl monomethyl ester **4**, respectively (**Scheme 1-7**).

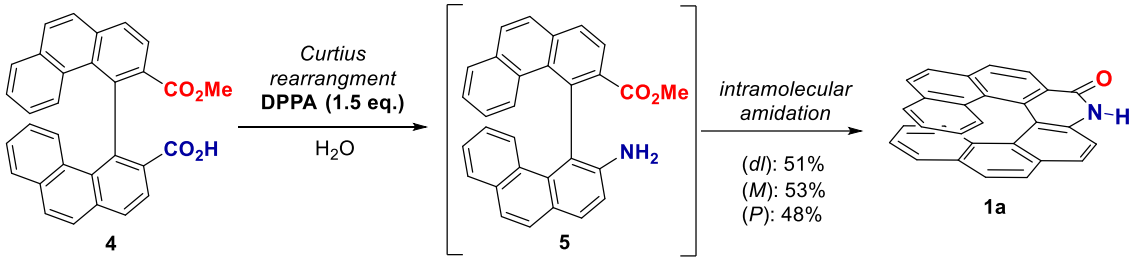

Scheme 1-7. Lactamization strategy

In **Chapter 3**, a novel and efficient direct one-pot cyclization protocol has been developed to furnish phenanthridinones and amide-functionalized [7]helicene-like molecules **1** (**Scheme 1-8**). The author envisioned that direct cyclization from the dicarboxylic acid **6** to helicene-like molecules as well as phenanthridinone derivatives would be possible, if the *in-situ* generated amino group undergoes cyclization with the alternative carboxy group under Curtius reaction conditions. By the survey of the reaction conditions, use of 2 equivalents of DPPA gave the desired product. This reaction conditions can be applicable to the preparation of optically active (*M*)- and (*P*)-amide-functionalized [7]helicene-like molecules including sulfur containing derivatives from the corresponding (*R*)- and (*S*)-biaryl dicarboxylic acids **6**. During the survey of the conditions, the author noticed the phosphate ester derivatives **7** were generated under Curtius

conditions in the case of the substrates including chalcogen atoms and subsequent treatment of the basic conditions gave the corresponding helicene-like molecules.

Furthermore, these conditions were applicable to the biaryl dicarboxylic acid derivatives to furnish phenanthridinone derivatives bearing a variety of substituents.

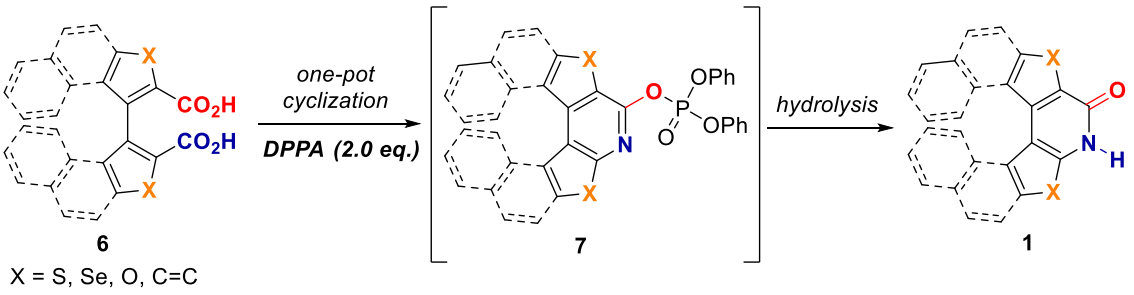

Scheme 1-8. Direct one-pot cyclization strategy

A palladium-catalyzed domino reaction through C–C and C–N bond formation involving *ipso* substitution is described in **Chapter 4** to obtain a sulfur containing amide-functionalized [7]helicene-like molecule **1b** efficiently. In the strategies described in **Chapter 2** and **Chapter 3**, the key intramolecular amide bond formations were proceeded from the biaryl substrates prepared in prior to the cyclization. Further straightforward way to access amide-functionalized helicene-like molecules would be the domino process through the biaryl formation and the lactamization. The author envisioned that the Pd catalyzed domino process previously developed in our laboratory can be applicable to this strategy. After the survey of the reaction conditions, **8** was obtained from the bromo naphthothiophene amide **3** through subsequent C–C and C–N bond formations (shown in the green bonds). The PMB-protecting group was readily deprotected to give **1b** (**Scheme 1-9**).

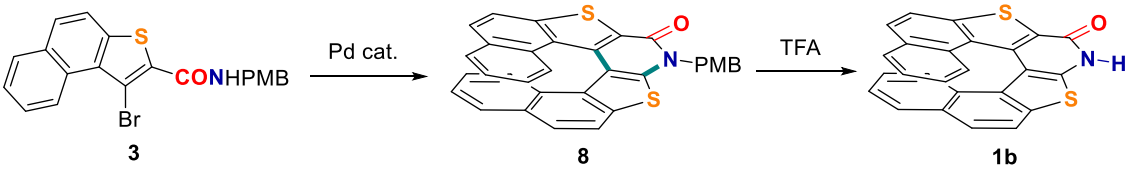

Scheme 1-9. Palladium-catalyzed domino reaction strategy

Details on the three strategies will be described in the following chapters.

Chapter 2
Synthesis of an amide-functionalized [7]helicene-like molecule via lactamization of biphenanthryl monomethyl ester and its structural analysis

In this Chapter, it was intended to prepare amide-functionalized [7]helicene-like molecule **1a**, through an lactamization of the intermediary axialy chiral δ-amino acids formed by the Curtius rearrangement of biphenanthryl monomethyl ester **4** (**Scheme 2-1**). Furthermore, the author reports the crystal structure of **1a**.

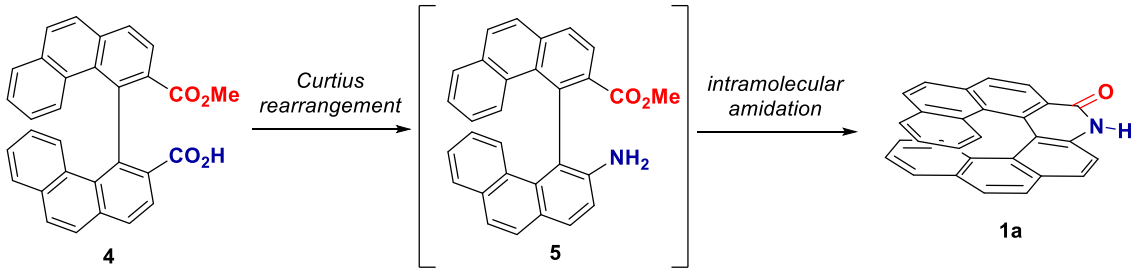

Scheme 2-1. Synthetic strategies of **1a** via lactamization

2.1 Preparation of monomethyl ester for the lactamization

We explored a synthetic pathway to monomethyl ester **4** of biphenanthryl dicarboxylic acid. Firstly, it was intended to prepare 3-methoxyphenanthrene **9**. A versatile method[16] has been developed by Kwong in 2017, which is a three-component cross-coupling of aryl halides, 2-haloarylcarboxylic acids, and nobornadiene. According to this method, compound **9** was directly obtained with the yield of 64% in large scale under almost the same conditions in Kwong's paper except for changing reaction temperature 130 °C to reflux in dioxane (**Scheme 2-2**).

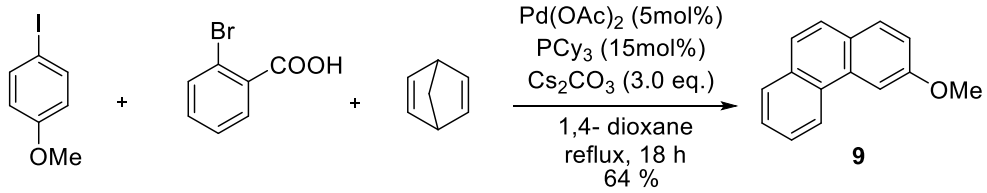

Scheme 2-2. Synthesis of 3-methoxyphenanthrene **9**

With large amount of **9** in hand, racemic ditriflate (*dl*)-**12** of biphenanthrenediol can be furnished smoothly through the demethylation by BBr_3, oxidative coupling in the presence of

$CuCl_2$ and phenylethylamine, and the triflation with Tf_2O in pyridine according to the reported method as shown in **Scheme 2-3**.[17]

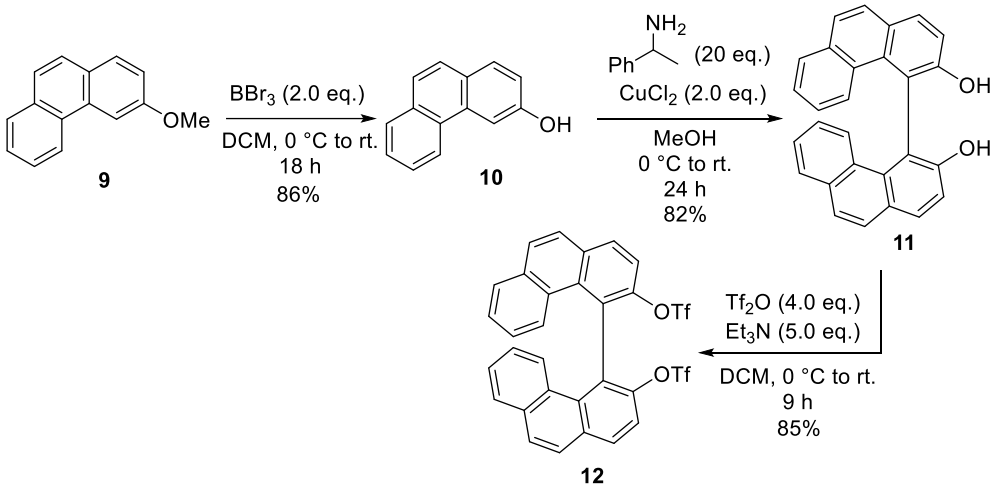

9 **10** **11** **12**

Scheme 2-3. Synthesis of (*dl*)-ditriflate **12**

The optical resolution of (*dl*)-diol **11** was conducted according to the literature procedure by the use of (1*S*)-10-camphorsulfonyl chloride as chiral resolution reagent (**Scheme 2-4**).[18] The diastereomers of **13** was readily separated by column chromatography (SiO_2, toluene : AcOEt = 10 : 1). Then hydrolysis of the camphor ester gave (*S*)-**11** and (*R*)-**11** respectively in enantiopure form. The absolute configuration of compounds **11** has been determined by comparing with the reported ^{1}H NMR data of corresponding compound **13**.[18]

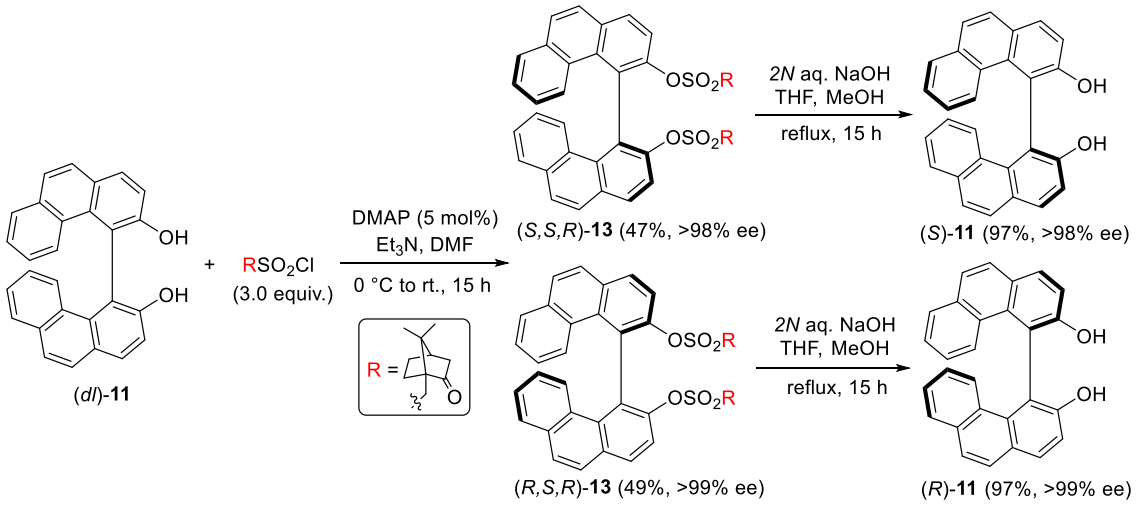

Scheme 2-4. Optical resolution of (*dl*)-**11**

Related to synthesis of the dicarboxylic acid from the ditriflate, Manabe reported a practical synthetic method,[19] palladium-catalyzed external CO-free carbonylation reaction with phenyl formate as a CO surrogate. Claiming the prepared biphenanthryl ditriflate substrate **12**, diphenyl ester **14a** was synthesized. Then, desired dicarboxylic acid (*dl*)-**6a** was obtained by hydrolysis (**Scheme 2-5**).

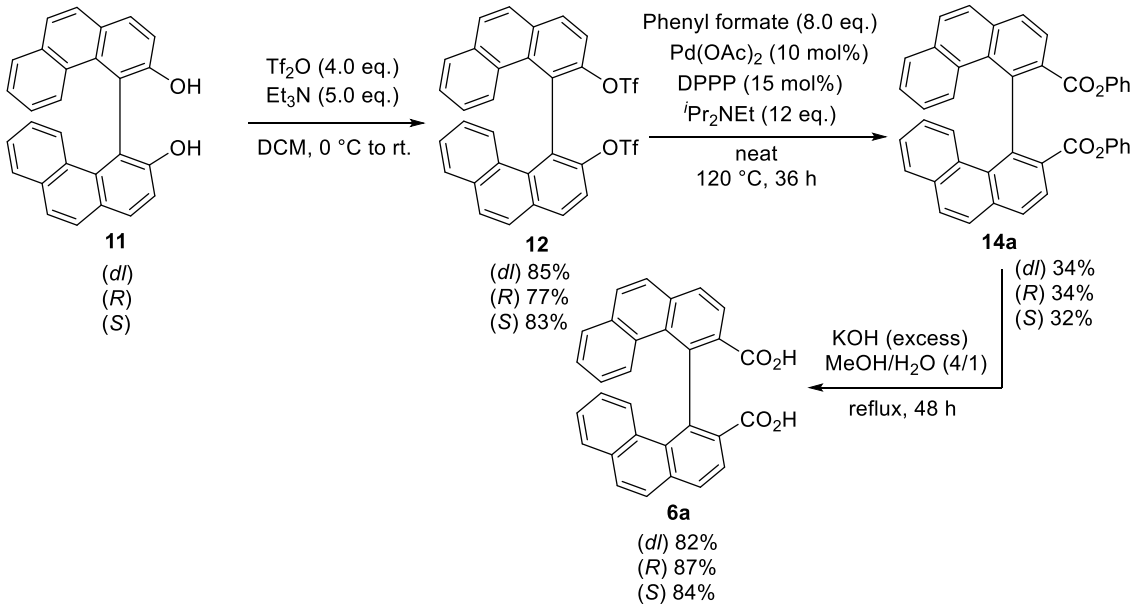

Scheme 2-5. Optimization for synthesis of dicarboxylic acid **6a**

With dicarboxylic acid (*dl*)-**6a** in hand, selective monomethylation was easily achieved with controlled equivalence of MeI (3.0 equiv.) and Ag_2CO_3 (0.5 equiv.) developed by our group in

54% yield (**Scheme 2-6**),[12b] The same procedure afforded (*R*)-**4** and (*S*)-**4** in 40% and 43% yields, respectively.

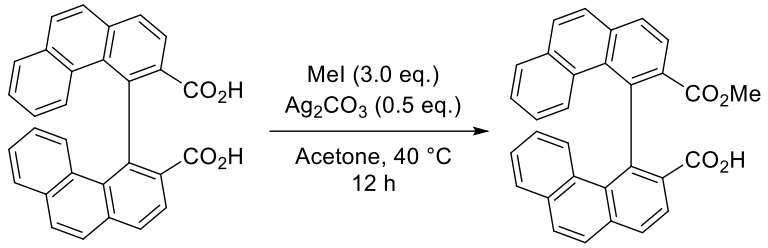

6a
(*dl*)
(*R*)
(*S*)

4
(*dl*) 54%
(*R*) 40%
(*S*) 43%

Scheme 2-6. Selective monomethylation of biphenanthryl dicarboxylic acids (*dl*)-, (*R*)-, and (*S*)-**6a**

2.2 Transformation to amide-functionalized [7]helicene-like molecules via lactamization

With monomethyl ester **4** in hand, the cyclization reaction via lactamization of *in-situ* generated δ-amino acids **5** prepared from the Curtius rearrangement was conducted (**Scheme 2-7**). Treatment of **4** with DPPA (1.5 equiv.) and Et_3N (3.0 equiv.) in toluene at 90 °C completed the Curtius rearrangement. Subsequently, H_2O was added to hydrolyze the isocyanate intermediate to furnish the intermediate **5**. And finally the target amide-functionalized helicene-like molecule **1a** was obtained after further hearting and stirring for 42 hours in 51% yield.

In order to confirm intermediate **5**, the reaction of (*dl*)-**4** was stopped in 1.5 hours after adding H_2O. Compound **5** was successfully isolated in 64% yield. This proved that the cyclization to **1a** proceeded through lactamization of **5**.

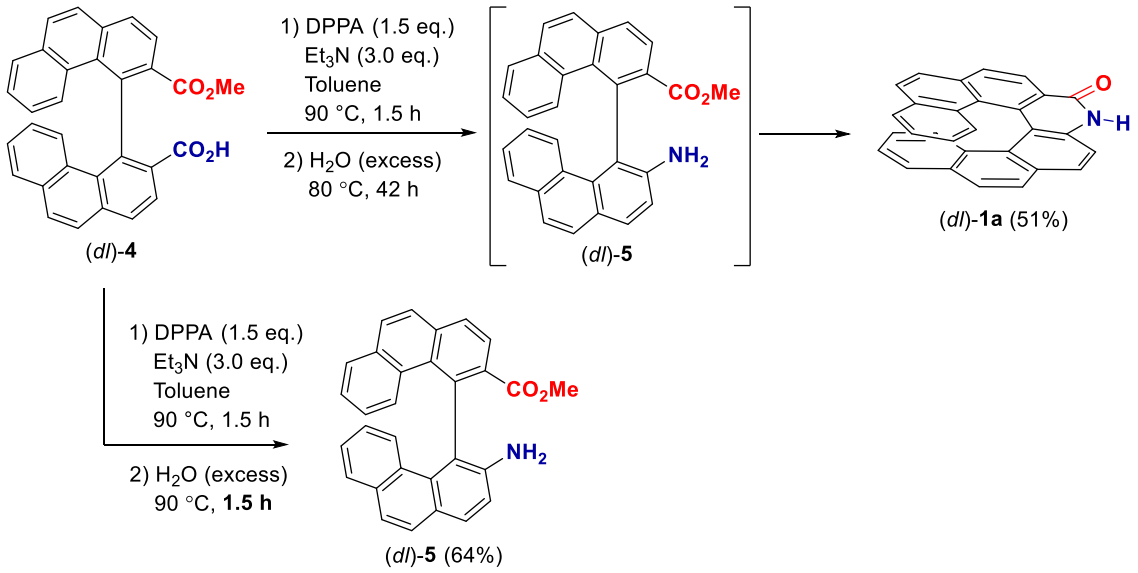

Scheme 2-7. Synthesis of (*dl*)-**1a** via lactamization and isolation of (*dl*)-**5**

Under the same Curtius rearrangement and lactamization procedure, the optically pure (*M*)- and (*P*)-amide-functionalized [7]helicene **1a** were obtained respectively (**Scheme 2-8**). It has been proved that there's no racemization taking place during the lactamization procedure based on the high ee value (> 99% ee for (*M*)-**1a**; >98% ee for (*P*)-**1a**) of each isomer of resulted **1a**. The specific rotation of (*M*)-**1a** was also measured to show large value as described in **Chapter 4** ($[\alpha]_D^{20}$ = -1336, c = 0.01, $CHCl_3$).

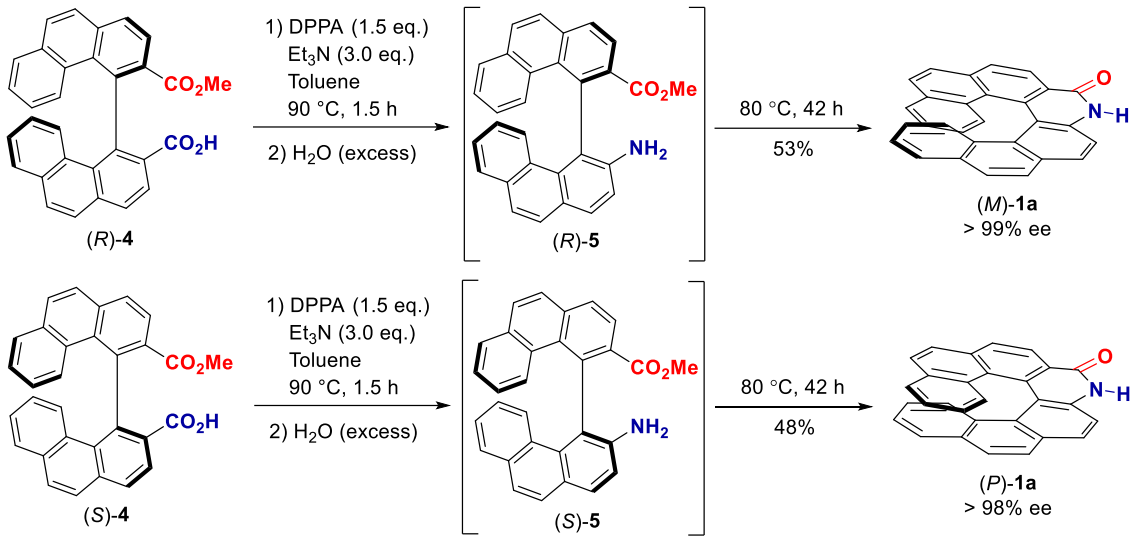

Scheme 2-8. Synthesis of optically pure **1a** via lactamization

2.3 The X-Ray analysis of racemic mixture of amide-functionalized [7]helicene-like molecule

An X-Ray diffraction analysis of racemic helicene-like molecule **1a** has been conducted. Although significant disorder over two different geometries of the molecules was observed as shown in **Figure 2-1(A)**, the helicene-like structure of **1a** was clearly confirmed. To make the discussion simple, one of the disordered structure was extracted and depicted in **Figure 2-1(B)**.

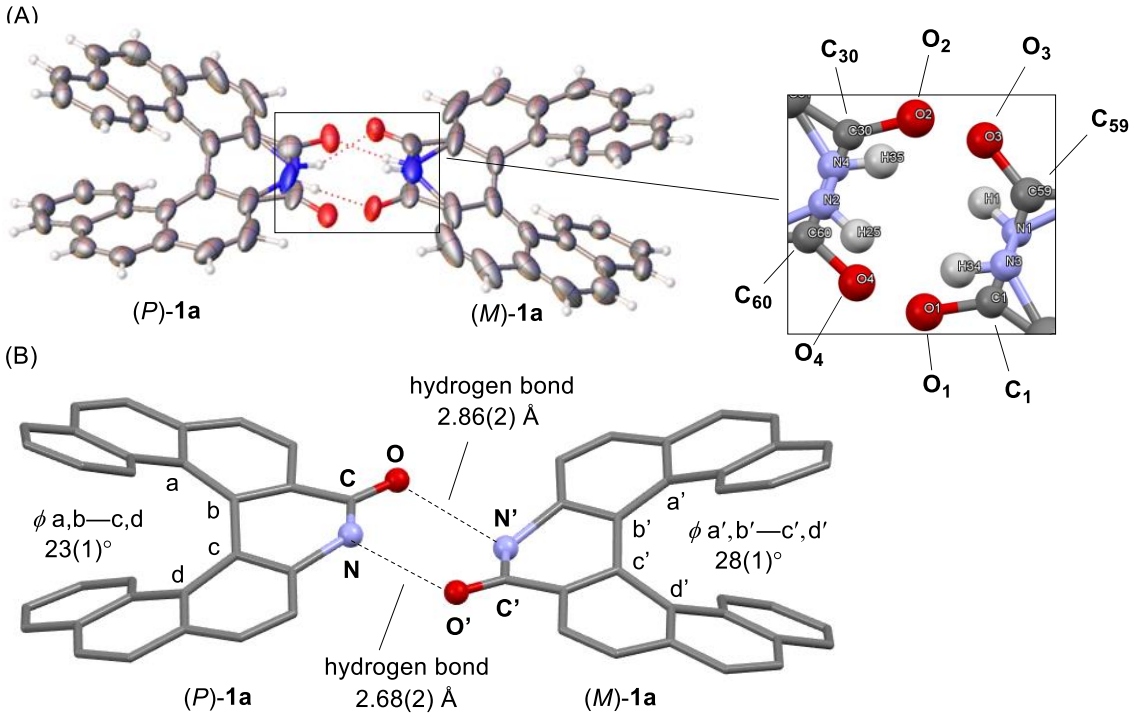

Figure 2-1. The crystal structure of (*dl*)-**1a**. (A) The disordered structure of associated pair of (*P*)- and (*M*)-**1a** through hydrogen bonding. (B) One of the disordered structure.

In **Figure 2-1(B)**, it is clearly confirmed that **1a** revealed a typical helicene structure with a twisted π-system (*ϕ*a,b–c,d: 23(1)° for the (*P*)-enantiomer and *ϕ*a',b'–c',d': –28(1)° for the (*M*)-enantiomer) and an amide group as a constituent moiety of the molecular framework. It is worth noting that the amide group functions as a molecular recognition moiety that manifests in pairwise association between the (*P*)- and (*M*)-enantiomers via hydrogen-bonding interactions (O···N' = 2.86(2) Å; O'···N = 2.68(2) Å).

This paired complex furthermore forms alternatingly aligned *M, P, M, P* columnar packs (**Figure 2-2A, B**), in which each column is created by the π-π stacking of a homochiral enantiomer (**Figure 2-2C**). Generally, π-π stacking interaction plays an important role in the self-assembly behavior of helicenes. In our case, it is typically supported by short contacts between the π-faces

of a homochiral enantiomer such as (*P*)-**1** (e.g., 3.19(2) Å and 3.49(1) Å) (**Figure 2-2C**), acting as one of the foundational driving forces toward aggregations.

Thus, along *a* axis, in a lengthwise way of the packing form, the single enantiomer aggregates vertically based on regular π-π stacking interactions to give the columnar packing constructed by homo chiral molecules. Rarely, along *b* axis, in a crosswise way, each homochiral column is connected horizontally by hydrogen bonding interactions between the amide groups in pairwise enantiomers, leading to an uncommon aggregation style. Hydrogen bonding functionalized packing structure with a particular width makes the racemic mixture of amide-functionalized helicene-like molecule **1a** to form a wider and larger molecular network which is different from usual single columnar aggregations of most helicenes.

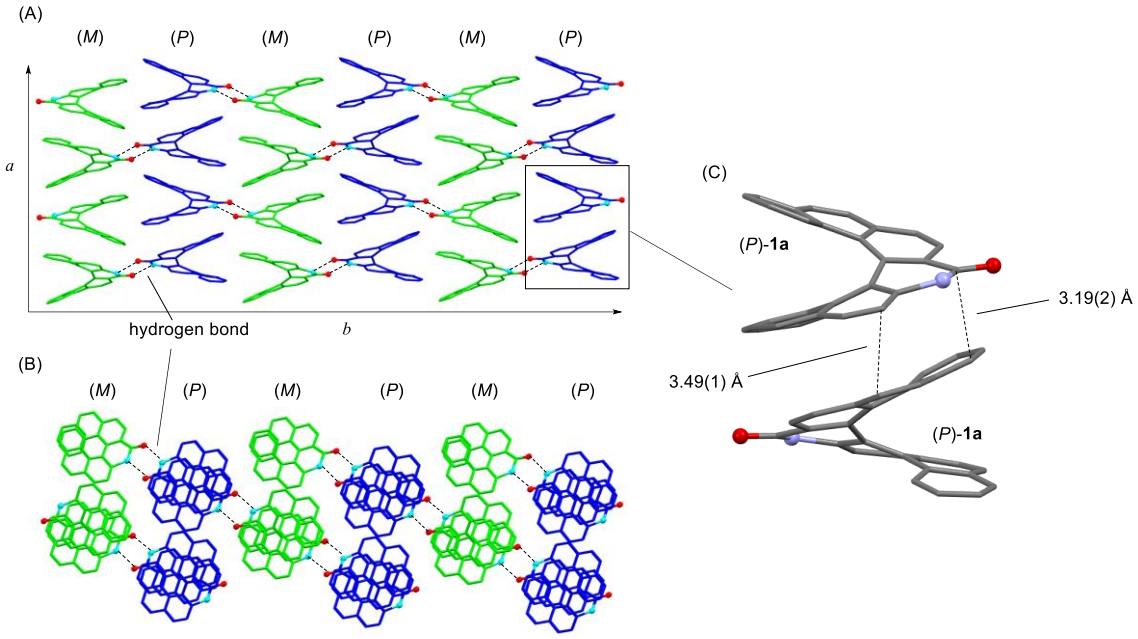

Figure 2-2. The packing diagram of (*dl*)-**1a**

The formation of homochiral or heterochiral dimers of helicene compounds have been studied by Yamaguchi and Wùrthner.[20] The [4]helicene (**Figure 2-3**) dimers might be in an alternating-orientation arrangement (*anti*) or a same-orientation arrangement (*syn*), especially that the *syn*-homochiral dimer is the most stable form (**Figure 2-3**). With regard to chiral recognition phenomenon in noncovalent bonding interactions (π-π stacking interaction in helicene case), the summary was also provided by Prof. Yamaguchi's study: The interactions between helical molecules show a tendency for pairs of the same configuration of the helicenes to form more stable complexes than pairs of enantiomeric helicenes. There was also a finding that in π-π

stacking dimerization of perylene bisimides (PBIs) with π-core, chiral self-recognition (*PP* and *MM* homodimer formation) prevails over self-discrimination (*PM* heterodimer formation).

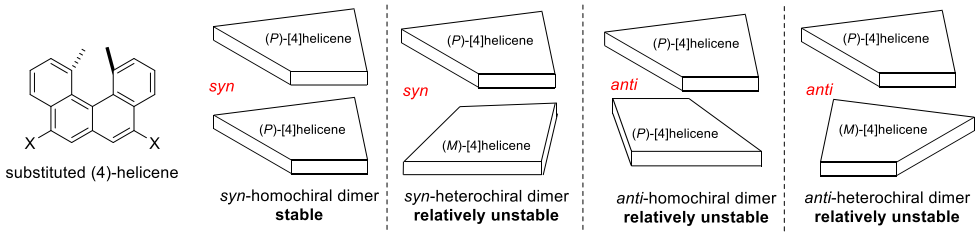

Figure 2-3. *Syn*- and *anti*-dimer aggregation of helicenes with flexible π-core

However, the model used by Prof. Yamaguchi is basically [4]helicenes without large steric repulsion at terminal rings. In the case of **1a** which is much sterically hindered at terminal part, the situation of π-π stacking interactions and aggregation behavior is totally different as discussed below.

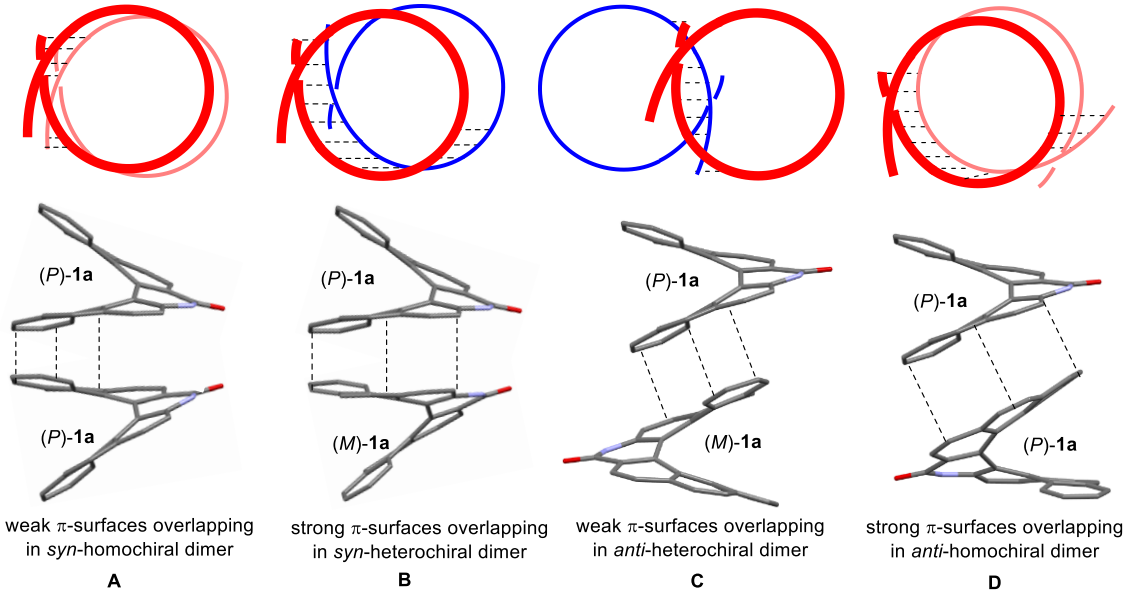

Figure 2-4. π-Overlapping analysis of *syn*- and *anti*-dimers of **1a** ((*P*)-**1a** red; (*M*)-**1a** blue)

***Syn*-dimer form:**

With a sterically hindered terminal part, the π overlapping area of *syn*-homochiral dimer of **1a** is less tight. Since the directions of radians are opposite between the close two π-faces, the overlapping is worst in *syn*-homochiral dimer (**Figure 2-4A**). In *syn*-heterochiral dimer form, the overlapping of the close two π-surfaces is strong (**Figure 2-4B**). However, in this form, only ordinary columnar packing along *a* axis (lengthwise way) is formed by the paired complexed

dimers with associated (*P*)- and (*M*)-enantiomers by hydrogen bonds at amide groups. Since *syn*-dimers are formed, amide groups will be located tightly in the center of each packing column, failing to align molecules in *b* axis (crosswise way). Therefore, it's difficult for *syn*-heterochiral dimers to form aggregation net. In my opinion, the separated columnar packing form should be less stable than the staggered combined net construction as shown in **Figure 2-2** (formed by *anti*-homochiral dimers) because of weaker π-π stacking interactions in separated column form. Further powerful evidences or special-purpose calculation are needed to prove the idea.

***Anti*-dimer form:**

In *anti*-heterochiral dimer form, between the close two twisted π surfaces, the directions of radians are also opposite. Thus, a relatively weak π overlapping extent is formed. The stability of *anti*-heterochiral dimer is still relatively low (**Figure 2-4C**). Finally, in *anti*-homochiral dimer, the two directions of radians in close π-faces are the same, leading to a large π overlapping area. At the same time, because of *anti*-dimer formation, they can further be connected by hydrogen bonds along *b* axis (crosswise way) to form an aggregation net (**Figure 2-2**). Thus, the highest stability is formed (**Figure 2-4D**).

In conclusion, *anti*-homochiral dimer arrangement is the best aggregation way.

The similar molecular assembly through hydrogen-bonding interaction has also been reported by Branda with amide-functionalized helicene bearing amide groups at the ends of the twisted backbone (**Figure 2-5A**).[7d] **Figure 2-5C** shows the packing diagrams. In these molecular assembly, there's a diastereoselective recognition process and only homochiral dimers where the acetyl groups exist exclusively in a *cis*-relationship appear in the crystal. Homochiral dimers arrange into offset racemic columns with face to face π-stacking interactions.

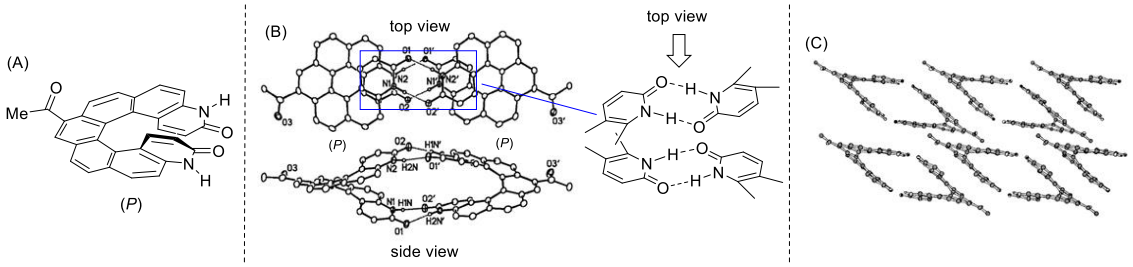

Figure 2-5. (A) Structure of acetyl group and amide-functionalized [7]helicene; (B) Side and up views of the X-Ray diagram of one of the enantiomerically pure hydrogen-bonded dimers (N···O distance of 2.740 and 2.829 Å); (C) Packing diagram (an average distance of 3.64 Å) (see ref. 7d)

Our X-Ray results and this reported observation indicated that molecular assembling property was considered as a typical feature of amide-functionalized helicenes and helicene-like molecules.

Furthermore, the columnar assemblies of helicene have been recognized to be the source of unusual optical properties in helicene-type materials as well as to be a key for potential applications in material chemistry. Especially, one-dimensional stacked chiral columnar aggregations of helicens are particularly attractive due to their unique chiroptical properties in the crystalline state.[4a,4b,4f]

The helicenebisquinone derivative (**Figure 2-6A**)[4b] were reported to form one-dimensional columnar aggregates with the aid of long alkyl side chains. The donor-acceptor interactions between the electron-rich inner rings of one molecule and the electron-poor outer rings of another might stabilize a columnar stack. This aggregate might contribute to the application of electro-optical functional material for helicenebisquinone molecules.

The use of dipole-dipole interactions with inherent π-π stacking interactions in helicenes can also produce a one-dimensional columnar arrangement. One of the examples is the columnar aggregation of λ^5-Phospha [7]helicene with one-way chirality (**Figure 2-6B**).[7c] The dipole moment vectors that are perpendicular to the helical axis compensate with each other by the two interacting molecules, while in the orientation of being parallel to the helical axis, the vectors are aligned in one column. The most notable is that each column has a single enantiomer of either (*P*) or (*M*) in the packing of racemate. Other example was found in coumarin-fused [6]helicene (**Figure 2-6C**).[7a] The packing structure of enantiopure (*M*)-coumarin-fused helicene in the single crystals exhibits a one-dimensionally stacked columnar alignment resulted from antiparallel face-to-tail π-π stacking interactions (**Figure 2-6C**). In the helical axis, the dipole moment vectors compensate for each and the vectors which are parallel to the helical axis are aligned into one column.

The one-dimensionally stacked columnar organization was also found in carbo[5]helicene containing bromide substituted benzylmaleimide group (**Figure 2-6D**).[7b] The peripheral benzyl groups result in weak steric interactions that are responsible for the formation of columnar stacked arrangements by keeping less steric clash at terminal rings as well as the interaction between bromine and oxygen. The formation of (*P*)- and (*M*)-racemic dimers in its unit cell from the pair of bromine and oxygen leads to an alternating array of (*P*)- and (*M*)-columns.

In the author's amide-functionalized helicene-like molecule, the columnar packing was found to be caused from the interactions not only through the π-π interaction between the π-faces, which is well known for helicene molecular assembly, but also through the hydrogen-bonding interactions via the amide groups (**Figure 2-6E**). This indicated that the amide functional group modified at the outer sphere of the helicene and/or helicene-like molecules would also be a promising way to have these special packing modes. Foreseeable, our columnar, as well as row packing of racemic **1a** would thus represent an attractive starting point for potential applications in chiral organic materials.

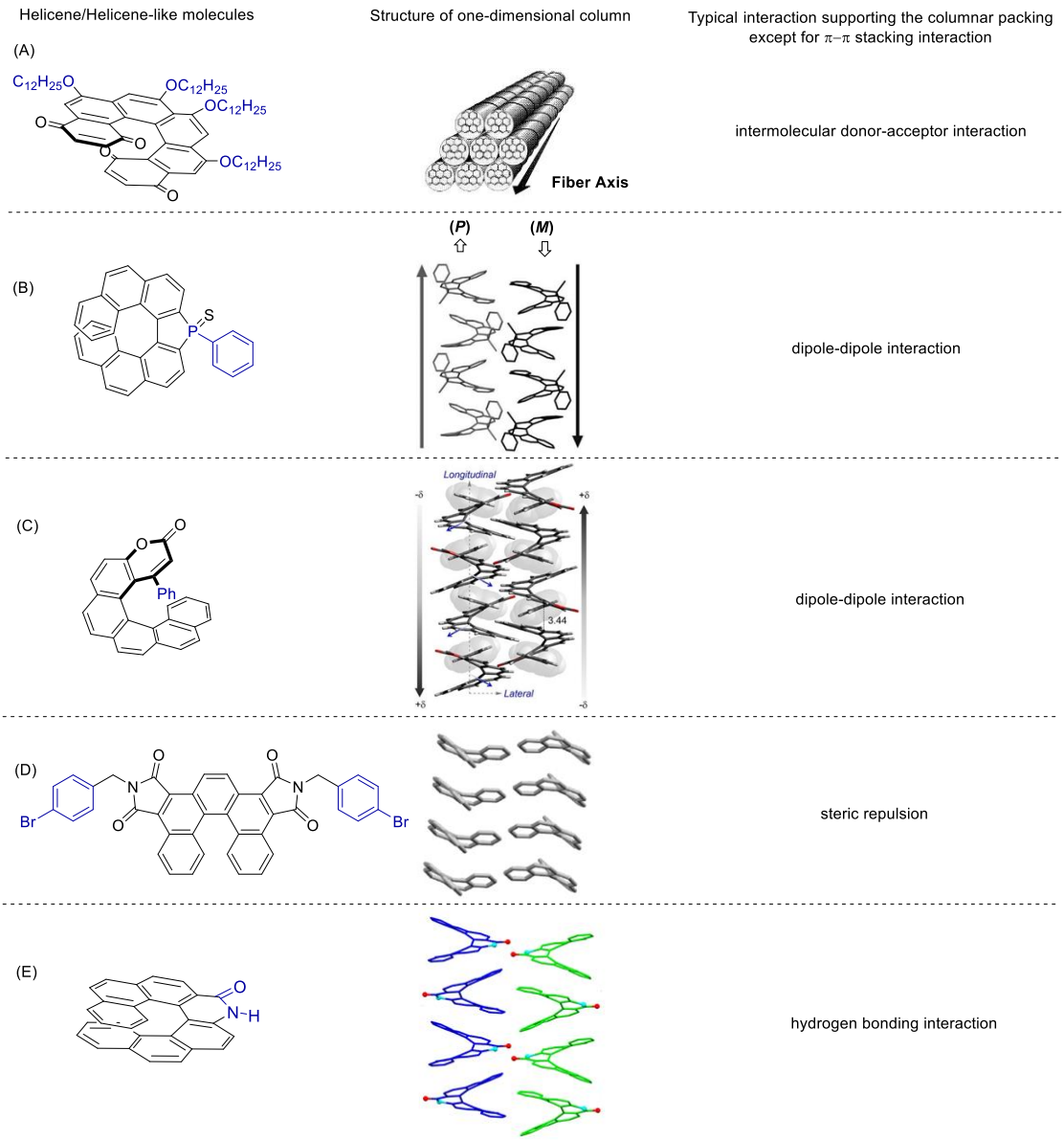

Figure 2-6. (A) Chemical structure of helicenebiquinone and schematic representation of columns of stacked helicene molecules as observed in solid bulk samples. (The side chains have been deleted for clarity, and the first helicenes are arbitrarily shown to be in the same rotational phase) (See ref. 4b) (B) Structure of λ^5 -phospha[7]helicene and columnar arrangement of (*P*) and (*M*) in the single-crystal structure of racemate. (The closest intermolecular contact between homochiral dimers is 3.35 Å.) (See ref.7c) (C) Structure of coumarin-fused helicene and one-dimensionally stacked packing structure of (*M*)-coumarin-fused helicene. (The closest intermolecular contact between homochiral dimers is 3.44 Å) (See ref. 7a) (D) Chemical structure of *p*-bromobenzylmaleimide functionalized carbo[5]helicene and the packing diagram. (The *p*-bromobenzylmaleimide groups and hydrogen atoms are omitted for clarity) (See ref.7b) (E) Packing diagram of **1a**

Furthermore, the discussion on the amide functionalized groups at the terminal rings exist as pyridin-2(1*H*)-one moiety or 2-hydroxypyridine would be important. However, the crystal structure of racemic **1a** is disordered over two positions actually, shown in **Figure 2-1(A)**. Two possible directions, located in the associated structure for each (*P*) or (*M*) enantiomer result in the mixed outcome which might bring some deviation into the crystal data. For example, the bond lengths of C–O bonds were obtained from the X-Ray analysis as following: C1–O1 (124 pm), C60–O4 (124 pm), C59–O3 (129 pm), C30–O2 (127 pm) (**Figure 2-1A**). Based on general experience, it should be predicted that the C–O bond in **1a** is double bond.[21] However, the data might not be reliable or accurate because of its severe disordered structure. Besides, In the case of 2-pyridone, oxo- form **B** mainly exists in both weakly polar solvent (e.g. $CHCl_3$) or polar solvent (e.g. DMSO) (**Figure 2-7**).[21] However, the substituents show large effects on the equilibrium. There's no study for the amide-[7]helicene so far. For the time being, detailed discussion on such tautomeric structures is quite difficult. Further study is needed to make sure the structural details. 2-pyridone form is used in DFT calculation of racemization barrier (**Chapter 4**).

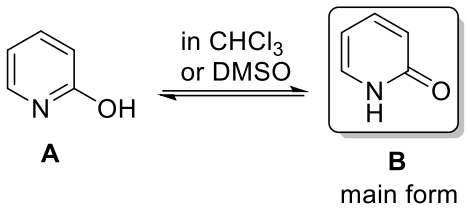

Figure 2-7. Tautomerization of 2-pyridone and 2-hydroxypyridine

In summary, since such special and interesting properties of **1a** shown by an X-Ray analysis have been discovered for the first time, our attentions were drawn even more to its unique molecular behaviors and added promising chiroptical properties of amide-functionalized [7]helicene-like molecules are expected to be checked. Thus, a demand of more efficient, easier and broader synthetic method towards various amide-functionalized [7]helicene-like molecules remains.

Chapter 3
One-pot access to amide-functionalized [7]helicene-like molecules and phenanthridinone derivatives from biaryl dicarboxylic acids

In **chapter 2**, the lactamization of axially chiral biphenanthryl δ-amino acid derivative **5** was prepared from the corresponding monomethyl ester **4** (**Scheme 3-1A**). In this strategy, for discrimination of the carboxy groups modified on the biphenanthrene framework, monoesterification of the dicaboxylic acid should be carried out prior to the key lactamization.

For further streamlining the synthesis of amide-functionalized helicene-like molecules, the author envisioned that direct cyclization from the dicarboxylic acid to helicene-like molecules would be possible without esterification, if the intermediary δ-amino acid can be yielded *in-situ* and its amino group undergoes cyclization with the alternative carboxy group under Curtius reaction conditions (**Scheme 3-1B**). Thus, the author examined this hypothesis starting from simple and readily available substrate.

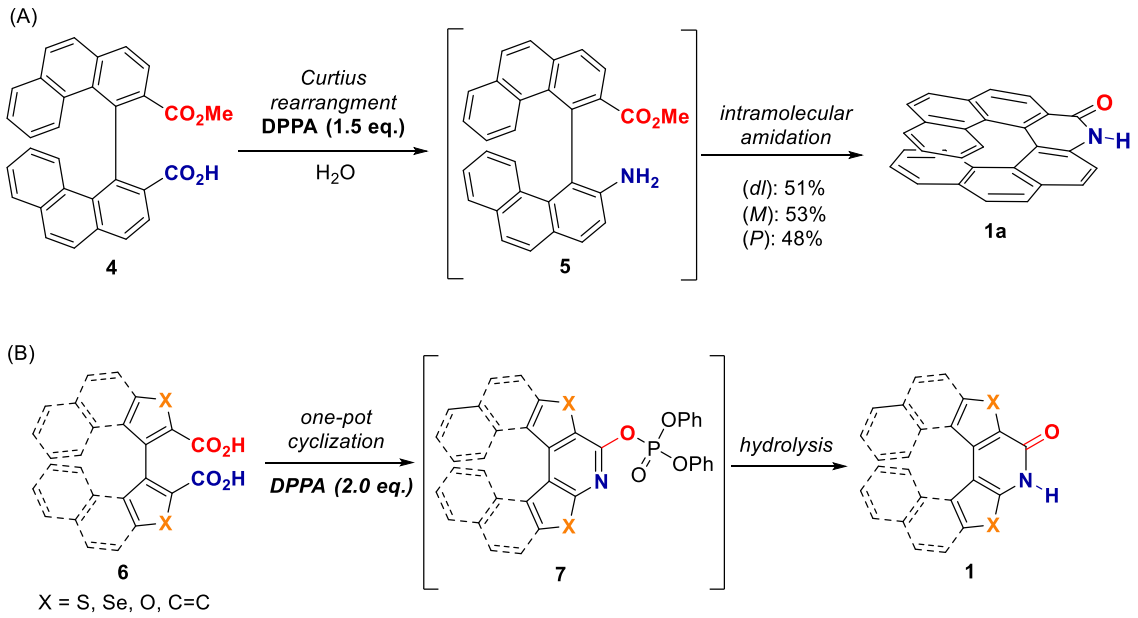

Scheme 3-1. Discovery of direct one-pot cyclization

3.1 Optimization of reaction conditions and extension to phenanthridinone synthesis

Initially, we examined the one-pot cyclization of diphenic acid **6d** to phenanthridinone **1d** (**Table 3-1**). As the author expected, the cyclization through lactamization proceeded to give **1d**. Under Curtius rearrangement conditions using DPPA (1.0 equiv.) and DIPEA (2.0 equiv.) in toluene and successive treatment of 2*N* aq. NaOH in one-pot, phenanthridinone **1d** was obtained with 17% yield (**Table 3-1, Entry 1**). The amount of DPPA was found to be important for this cyclization. When the amount of DPPA increased to 2.0 equivalent, the yield dramatically increased to 72% yield (**Entry 2**).

Table 3-1. Reaction conditions screening of one-pot cyclization

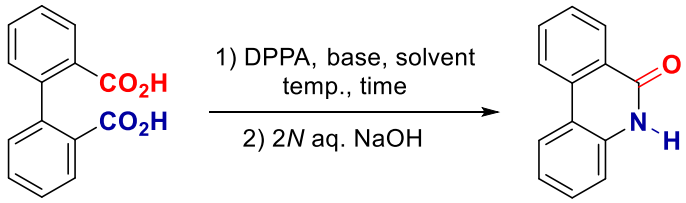

6d **1d**

Entry	DPPA (eq.)	Base (eq.)	Time	Temp.	Solvent	Yield[a]
1	1.0	DIPEA (2.0)	12 h	reflux	toluene	17%
2	2.0	DIPEA (2.0)	12 h	reflux	toluene	72%
3	3.0	DIPEA (2.0)	12 h	reflux	toluene	38%
4	4.0	DIPEA (2.0)	12 h	reflux	toluene	26%
5	2.0	DIPEA (4.0)	12 h	reflux	toluene	73%
6	2.0	DIPEA (6.0)	12 h	reflux	toluene	80%
7	2.0	Dibutylpyridine (6.0)	12 h	reflux	toluene	ND
8	2.0	Et_3N (6.0)	12 h	reflux	toluene	33%
9	2.0	TMP (6.0)	12 h	reflux	toluene	47%
10	2.0	DBU (6.0)	12 h	reflux	toluene	52%
11	2.0	DIPEA (6.0)	12 h	reflux	THF	30%
12	2.0	DIPEA (6.0)	12 h	reflux	PhCl	69%

a) isolated yields.

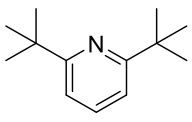

Dibutylpyridine
(2,6-Di-*tert*-butylpyridine)

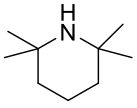

TMP
(2,2,6,6-Tetramethylpiperidine)

On the other hand, increasing the amount of DPPA to 3.0 or 4.0 equivalents, the yields were decreased to 38% and 26% yields, respectively (**Entries 3** and **4**). After surveying reaction conditions further on bases (**Entries 5-10**) and solvent (**Entries 11** and **12**), the best condition was determined to be the combination of DPPA (2.0 equiv.) and DIPEA (6.0 equiv.) in toluene

under refluxing conditions. This best condition gave **1d** in 80% yield (**Entry 6**). This proper equivalent of DPPA (2.0 equiv.) offer evidence for the mechanistic study of this cyclization, which will be discussed in **Section 3.3**.

Besides, this reaction was also successfully performed in gram-scale. With the optimized conditions (**Table 3-1, entry 6**), product **1d** (1.3 g, 6.6 mmol) was obtained from **6d** (2.0 g, 8.3 mmol) in 80% yield (**Scheme 3-2**).

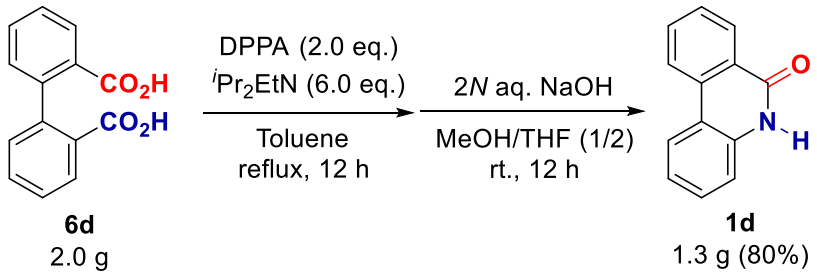

6d
2.0 g

1d
1.3 g (80%)

Scheme 3-2. Scaled-up experiment of one-pot cyclization

The importance of phenanthridinones as bioactive compounds has been widely realized. Phenanthridinone core and its derivatives, as one of the important structural units for the development of therapeutic agents, have shown a variety of biological activities, such as anti-tumor activity, inhibitors for human poly (ADP-ribose) polymerase-3, selective estrogen receptor modulators (**Figure 3-1**).[22]

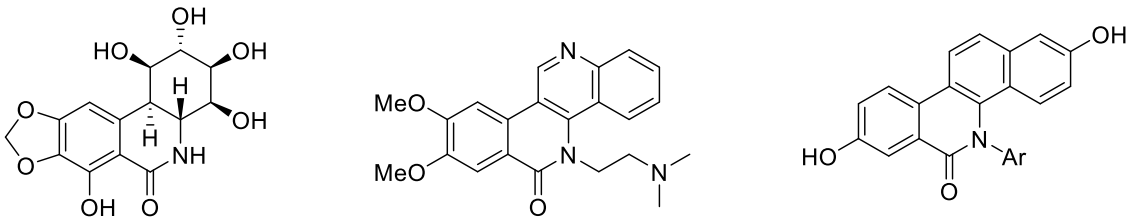

anti-tumor activity

ADP-ribose polymerase-3 inhibitor

selective estrogen receptor modulators (SERMs)

Figure 3-1. Selected examples of phenanthridinone derivatives as natural products or key skeleton of bioactivity

With the importance of phenanthridinone derivatives in mind, the author extended the reaction to a variety of substrates to furnish corresponding phenanthridinone derivatives. After preparing a series of biaryl dicarboxylic acids through Ullmann coupling reaction of *ortho*-bromo or chloro aryl methylester and the following hydrolysis (see the experimental part), construction of a variety of phenanthridinone derivatives including heteroaromatic rings have been examined by this one-pot cyclization method (**Table 3-2**).

It was proved that the one-pot cyclization was applicable to a variety of biaryl dicarboxylic acid derivatives, although the substrates bearing methyl groups at 5,5' positions only gave relarively low yield (41%). Fluorine substituted substrates **1f** and **1i** gave 76% and 73% yields, respectively. Nitro- and methoxyl groups were found to be applicatble in this reaction. The heteroaromatic rings containing O, S, and Se were also accepted and furnished the corresponding products **1m**, **1n**, and **1o** in good yields. One case did not give the expected product was the reaction with **6l**. This reaction gave unexpected cyclic urea **15** instead of expected **1l**. This could be due to the steric repulsion between the methyl groups at the bay region of expected **1l** as discussed below.

Table 3-2. Synthesis of phenanthridinone derivatives via one-pot cyclization

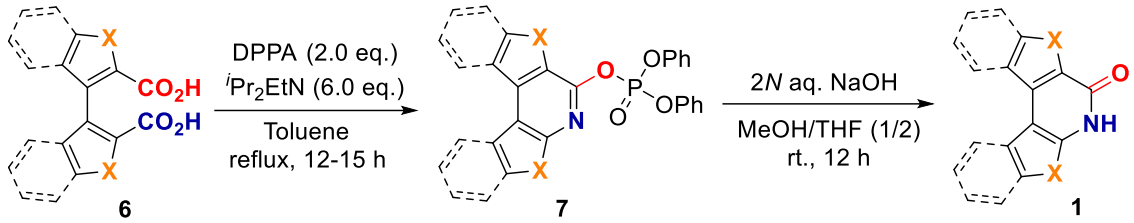

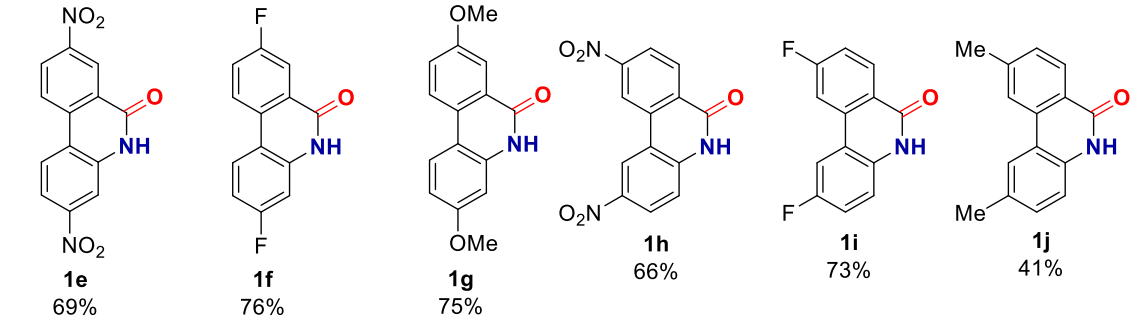

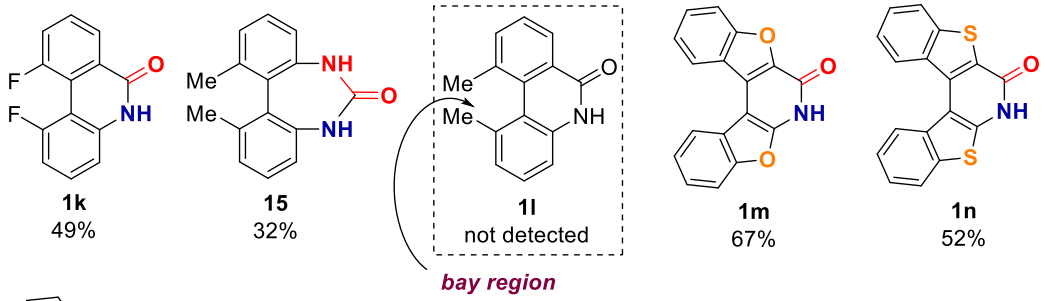

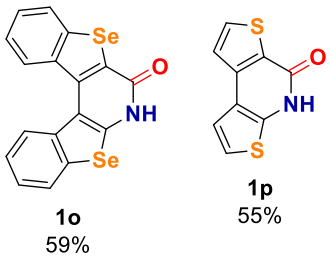

Although the result of the cyclization to **1l** suggested this reaction relatively sensitive to the steric congestion, the author moved to preparation of amide-functionalized helicene derivatives with the best conditions for one-pot access to phenanthridinone derivatives.

3.2 Synthesis of racemic and enantiopure amide-functionalized [7]helicene-like molecules via direct one-pot cyclization

Recently, an emerging trend in the helicene chemistry is the fusion of thiophenes into the helical skeleton, giving birth to various thiahelicenes (**Figure 3-2**).[1a] The presence of sulfur along the outer ridge of the helicene offers new opportunities to modify the electronic and optical properties.[1a,1f] Another exciting property of thiaheterohelicenes revealed to date is their interaction with biologically important macromolecules as discussed in **Chapter 1**.

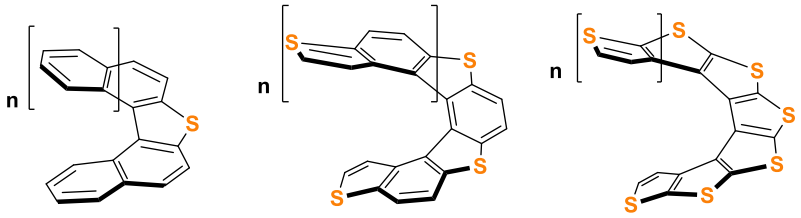

Figure 3-2. Examples of thiahelicenes

Despite that the advances for thiahelicene synthesis have been well developed, the classic method of carbohelicene synthesis involving photocyclization of stilbene precursors has been developed for decades of years, remaining as the most popular method for preparing thiahelicenes of various sizes and functionalization (**Scheme 3-3**).[1a] It is clear that a general and highly enantioselective route to thiahelicenes remains a synthetic challenge. Therefore, the author also applied the developed one-pot cyclization into sulfur containing [7]helicene-like molecule.

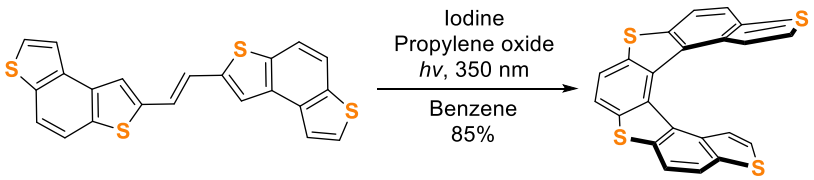

Scheme 3-3. Photocyclization of stilbenoid precursor as a route to thiahelicene

Firstly, both racemic and optically pure biphenanthryl dicarboxylic acids obtained in **Chapter 2** were applied to the developed one-pot cyclization conditions. As the author expected, both corresponding racemic and optically active amide-functionalized [7]helicene-like molecule **1a** was afforded directly although the yields were not satisfactory (**Scheme 3-4**). The HPLC analysis of [7]helicene-like compound (*M*)- and (*P*)-**1a** proved no racemization proceeded during the one-pot cyclization.

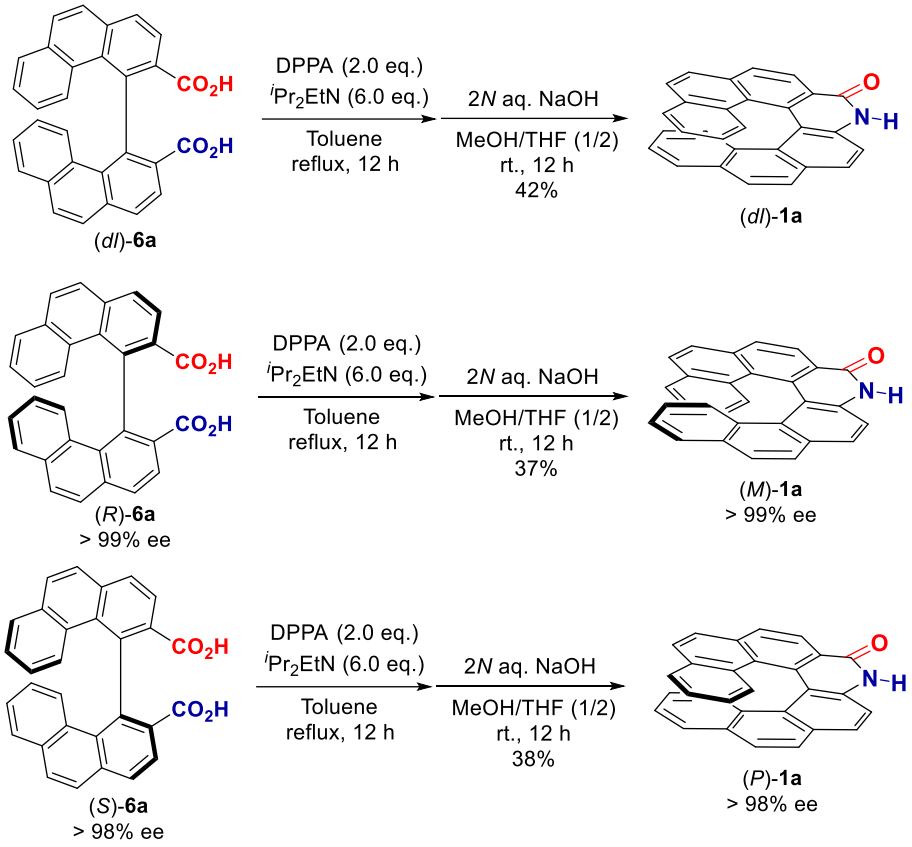

Scheme 3-4. Synthesis of racemic and enantiopure **1a** via direct one-pot cyclization

Based on previous study, a new sulfur and amide-functionalized [7]helicene **1b** was designed and synthesized with the newly developed Curtius-rearrangement type one-pot cyclization strategy.

Since the previous conditions did not fit the racemic binaphthothiophene dicarboxylic acid substrate **5b** well, a preliminary optimization for the bases has been conducted (**Table 3-3**). With DIPEA as base, target helicene-like molecule **1b** was obtained with a low yield (15%) (**Table 3-3, entry 1**). A further screening of bases was performed and finally it was discovered that Et_3N as base improved the reaction situation, with the yield increased to 25% and a relatively clean system on TLC (**Table 3-3, entry 3**). Above all, the racemic sulfur and amide-functionalized [7]helicene-like molecule **1b** was synthesized with DPPA (2.0 equiv.) and Et_3N (6.0 equiv.) via the one-pot cyclization method.

Table 3-3. Base screening of one-pot cyclization from **6b**

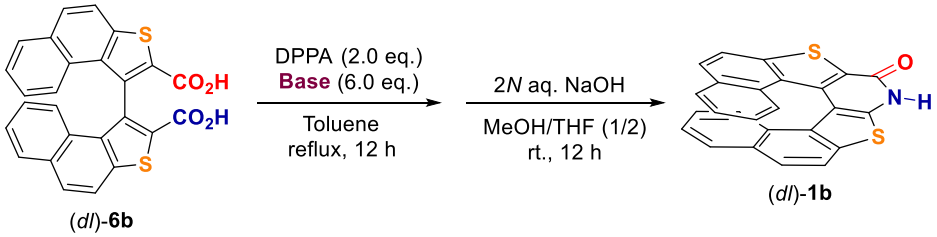

(*dl*)-**6b** (*dl*)-**1b**

Entry	Base	Yield[a]
1	$^{i}Pr_2EtN$	15%
2	DBU	24%
3	Et_3N	25%

a) isolated yields

With the optimized conditions, optically active (*M*)- and (*P*)-sulfur containing amide-functionalized [7]helicene-like molecule **1b** has been successfully obtained from (*R*)- and (*S*)-enantiomers of binaphthothiophene dicarboxylic acid **6b** as substrates, respectively (**Scheme 3-5**). Optical rotation for (*M*)-**1b** was measured: $[\alpha]_D^{19}$ = –1869.4 (c = 0.50, DMSO). Racemization barrier energy of **1b** was checked and determined by observation of decrease of ee value of (*P*)-**1b** in chlorobenzene under refluxing: $\Delta G^{\ddagger}_{rac}$ = 34.3 kcal/mol (132 °C in PhCl) as discussed in **Chapter 4**.

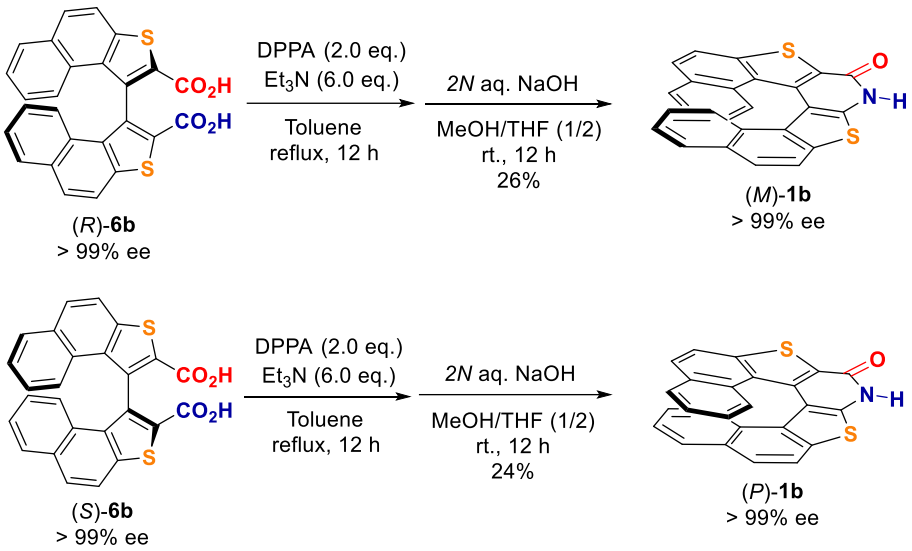

Scheme 3-5. Synthesis of optically pure **1b** via direct one-pot cyclization

During this investigation, the author noticed that the formation of phosphate ester derivatives was observed prior to addition of aq. NaOH, especially in the case of the reaction with the substrates **6a**, **6b**, **6m**, **6n**, **6o** and **6p** including chalcogen atoms in their fused cyclic systems (**Figure 3-3**).

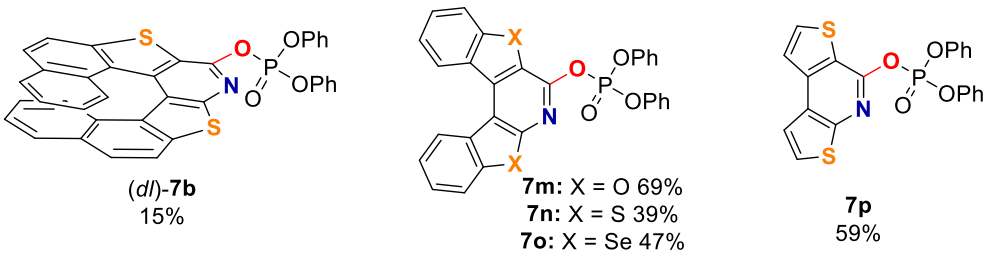

Figure 3-3. Structures of diphenylphosphoryl esters

For example, **7b** was successfully isolated and analyzed, after applying **6b** to the optimized one-pot cyclization condition for 4 hours. **7b** was isolated and purified by column chromatography, resulted as green solid with the yield of 15%. At the same time, **1b** was furnished in 10% yield directly. Then, **7b** was quantitatively converted to **1b** with aqueous NaOH in the mixture solvent of MeOH and THF at room temperature. The total yield of **1b** (25%) is consistent with the one-pot procedure (**Table 3-3, entry 3**). This proved **7b** was the product in the first Curtius reaction step prior to the treatment of aqueous NaOH.

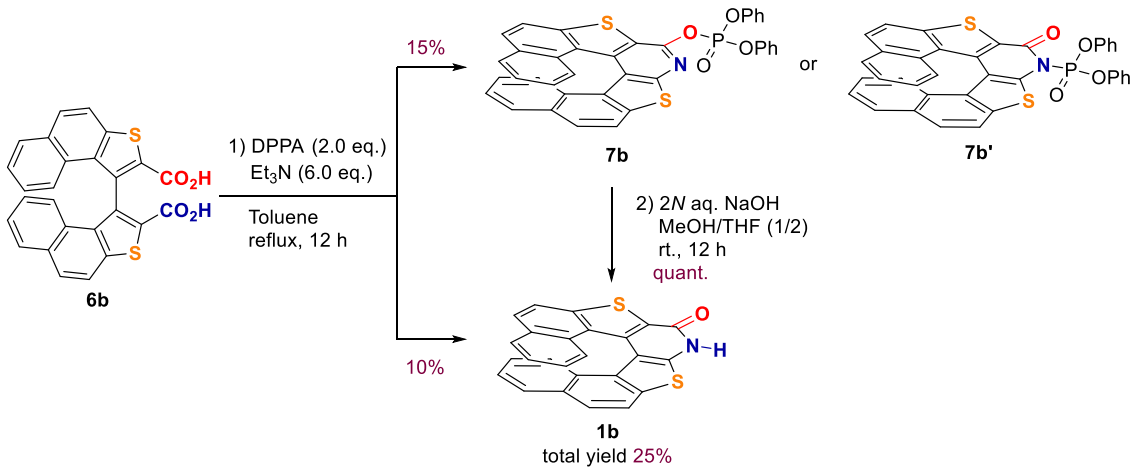

Scheme 3-6. Isolation of **7b** and its conversion to **1b**

^{1}H NMR and mass spectral analysis of **7b** indicated that the structure should be phosphoryl ester or phosphoryl amide **7b'**. However, it was difficult to obtain its single crystal for further structural analysis because of the instability. Thus, in the initial stage of the research, it kept

unclear whether the phosphoryl group was connected to oxygen in amide group or linked with nitrogen atom. The *O*-phosphoryl ester structure was deduced by the X-Ray analysis of sulfur containing **7n** and selenium containing **7o** (**Figure 3-4A, B**).

From the X-Ray analysis of sulfur containing **7n**, *O*-phosphorus ester structure, in which diphenylphosphoryl group is connected to the oxygen atom instead of nitrogen atom in the amide group, was clearly determined. Furtherore, the helically twisted structure was observed (ϕa,b–c,d: -15.9(6)°). Interestingly, the top view of the crystal structure indicated that the C–O bond of the phosphate and the π-faces of thiophene ring seem to be almost in the same plane without any remarkable twist (**Figure 3-4**, side view, the N–C, C–O and O–P bonds aligned in the almost same plane: ϕN,C–O,P: –7.3(4)°). The coplanar arrangement seems to come from the conformational restriction around the C–O bond between the pyridine moiety and the diphenylphosphate group. This conformational lock might come from the pnictogen-bonding interaction between the nitrogen and the phosphorus atoms. The length between the nitrogen and the phosphorus atoms (2.928(3) Å) which is shorter than sum of the van der Waals radii of nitrogen and phosphorus atoms (3.35 Å) suggested the presence of the pnictogen-bonding interaction (**Figure 3-4**, side view).[23] Furthermore, the length between the sulfur of thiophene moiety and the oxygen of phosphate group (3.003(2) Å) which is shorter than sum of the van der Waals radii of sulfur and oxygen atoms (3.32 Å) indicated the presence of chalcogen-bonding interaction occurred between these atoms (**Figure 3-4**, side view).[23]

In the crystal structure of selenium containing **7o**, its π-system was also found to be helically twisted with the dihedral angle (ϕa,b–c,d: -16.4(5)°), which is slightly bigger than that of **7n**. This compound also showed the coplanar geometry of the C–O–P bond of the phosphate and the π-face of selenophene ring, that also might derive from the pnictogen-bonding interaction between the nitrogen and the phosphorus atoms (**Figure 3-4**, side view, the N–C, C–O and O–P bonds aligned in the almost same plane: ϕN,C–O,P: 5.5(3)°). Furthermore, the chalcogen-bonding interaction also occurred between the selenium atom of selenophene moiety and the oxygen of phosphate group (3.101(2) Å), which is shorter than sum of the van der Waals radii of selenium and oxygen atoms (3.42 Å). (**Figure 3-4**, side view).[23] These additional non-covalent bonding interactions contribute to make these phosphorus esters to be isolable.

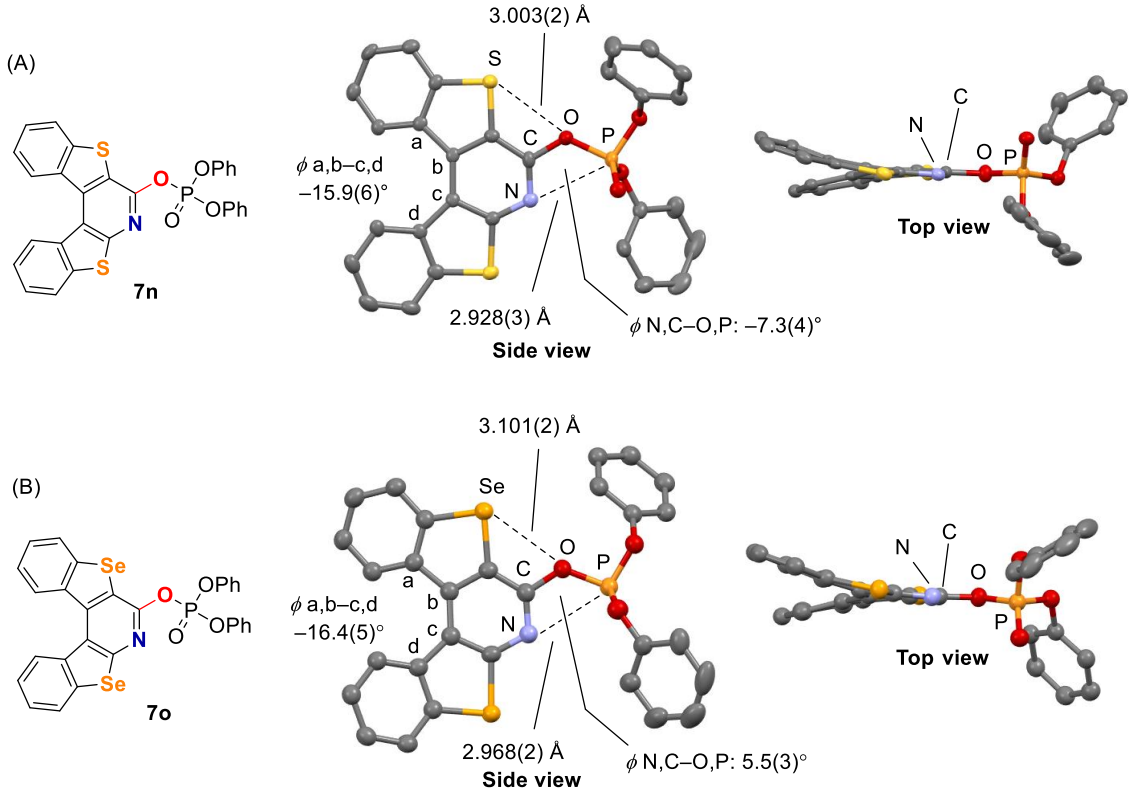

Figure 3-4. Crystal structures of **7n** and **7o**

The packing diagrams of **7n** and **7o** are also shown in **Figure 3-5**. In both of the packing of **7n** and **7o**, *M*- and *P*-enantiomers were alternatively associated through π-π stacking interations to form the columnar aggregations. In the case of **7n**, the π-π stacking interations were observed between the helical backbone of the enantiomers (3.361(4) Å) and between the helical backbone of one enantiomer and the phenoxy group of the other enantiomer (3.184(5) Å). In the case of **7o**, the π-π stacking interations were observed between the helical backbone and the phenoxy group of each enantiomeric pair (3.338(3) Å and 3.342(3) Å). Furthermore, CH–O interations were observed between the oxygen atom of the phenoxy group of *M*-enantiomer and the helical backbone of *P*-enantiomer (2.717 Å). The formation of heterochiral colums in case of **7n** and **7o** should be controlld by strong π-π stacking interactions between phenoxy groups and helical backbone and CH–O interactions.

It is worth noting that homochiral columnar packing was not formed in the both cases as observed in **1a**. This might support the key role of the hydrogen-bonding interactions through the amide functional group of **1a** and the rigid helical π-core for its columner aggregation composed of the homochiral molecules (**Chapter 2.3**, **Figure 2-2**).

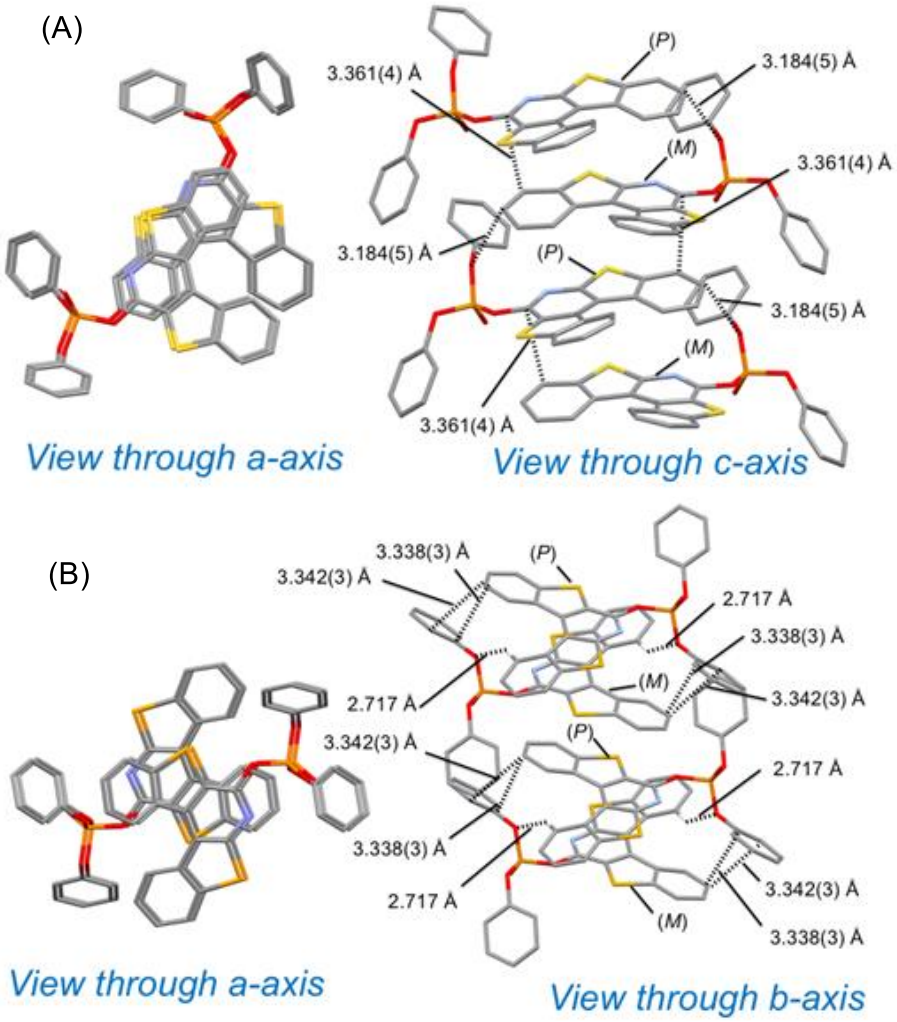

Figure 3-5. (A) Packing diagrams of **7n**; (B) Packing diagrams of **7o**

3.3 Mechanistic consideration of the direct cyclization from dicarboxylic acid

Based on the information on generating *O*-phosphorus esters bearing a partial structure of DPPA as the product in the first operation, and requirement of 2.0 equivalents of DPPA for reasonable yield, a reaction mechanism for the direct cyclization has been proposed (**Figure 3-6**). Firstly, the starting material reacts with 2.0 equivalent of DPPA and base to generate the mixed acid anhydride intermediate **M-1**. Subsequently, one of the acid anhydride groups transfers to isocyanate to give intermediate **M-2**. Then the isocyanate group might react with the phosphate ion generated in the reaction mixture to give the cyclic intermediate **M-3**. Then, the migration of the phosphate group might occur accompany with CO_2 release to give diphenylphosphate **7**. Finally, the phenanthridinone derivative **1** will be obtained after hydrolysis by treatment of aq. 2*N* NaOH in the second operation.

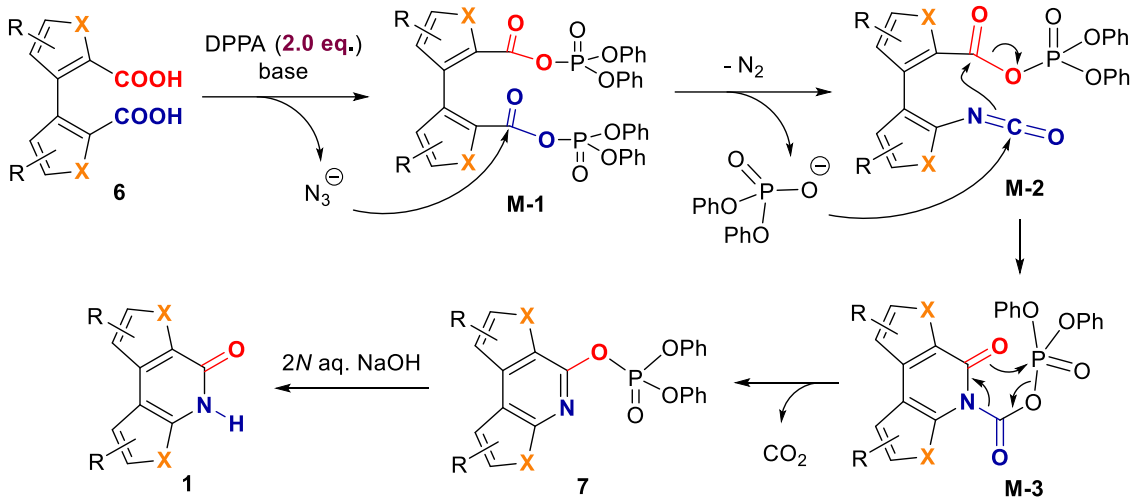

Figure 3-6. Proposed mechanism of one-pot cyclization

In the case of substrate **6l**, desired product **1l** was not detected. Instead, cyclic urea **15** was formed in 32% yield (**Scheme 3-7**).

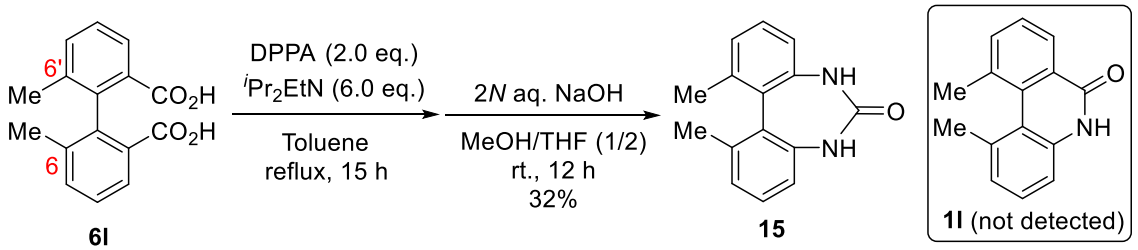

Scheme 3-7. Cyclic urea formation from substrate **6l**

It was supposed that the steric repulsion between the methyl groups at 6,6'- position led that the distance of two carboxy groups is too far to allow the nucleophilic attack of the nitrogen of isocyanate to the acid anhydride in **M-2** (**Figure 3-6**) to undergo smoothly.

Therefore, the expected cyclization to **1l** can not be proceeded. A plausible mechanism of formation of **15** was proposed (**Figure 3-7**). First of all, both carboxylic acid groups in **6l** react with DPPA and DIPEA to form two isocyanate groups in **M-4**, then one of the isocyanates reacts with the phosphate ion generated in the system to form **M-5**. The other isocyanate reacts with phosphate ion and mixted acid anhydride by nucleophilic attack to generate the cyclic intermediate **M-6**. Finally, **15** will be furnished with releasing of phosphate group and CO_2 in sodium hydroxide solution (**Figure 3-7**). For another possibility, after treating sodium hydroxide solution, **M-4** may directly form cyclic intermediate by nucleophilic attack from hydroxide, then **15** was furnished through decarboxylation.

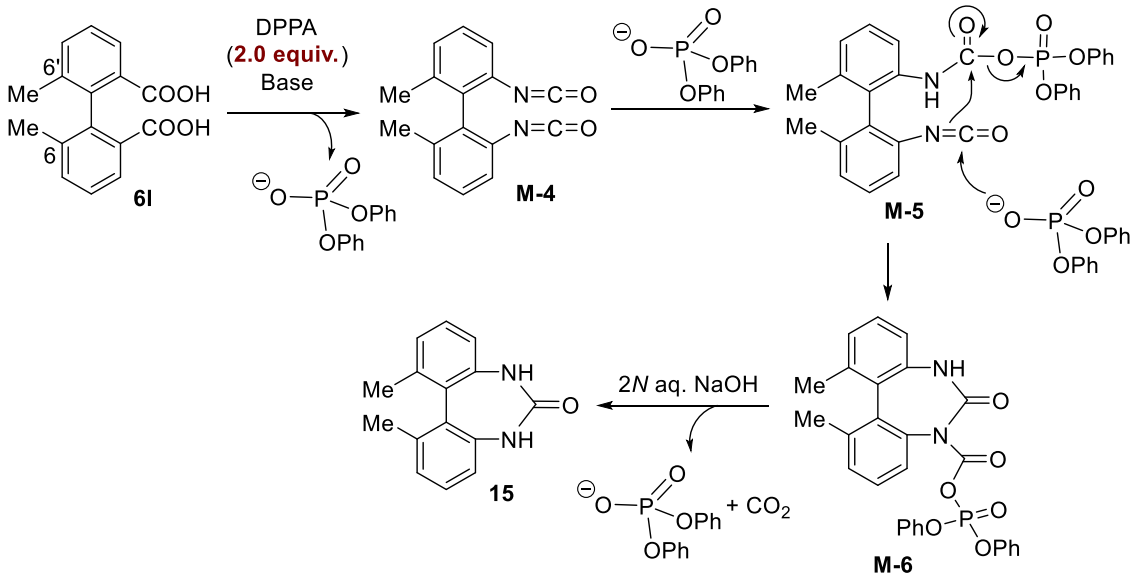

Figure 3-7. Proposed mechanism of formation of **15**

Combined with lactamization (**Chapter 2**) and direct one-pot cyclization (**Chapter 3**) strategies, the author has made some progress in the synthesis of amide-functionalized helicene-like molecules without metal catalyst or photo-irradiation. However, recent years, palladium-catalyzed coupling reaction has developed a lot and still remains as convenient and suitable methods to synthesize helicenes and helicene-like molecules. The author also developed an efficient palladium-catalyzed domino reaction towards sulfur and amide-functionalized [7]helicene-like molecule **1b** with C–N and C–C formation together with the following deprotection of PMB group.

Chapter 4
Preparation of amide-functionalized helicene-like molecules by palladium-catalyzed domino reactions

Referring to a series of palladium-catalyzed domino reactions of *ortho*-halobenzamide to phenanthridinone derivatives described in **Chapter 1** (Scheme 1-5), an strategy for the synthesis of sulfur and amide-functionalized [7]helicene-like molecule **1b** was designed and proposed (**Scheme 4-1**).

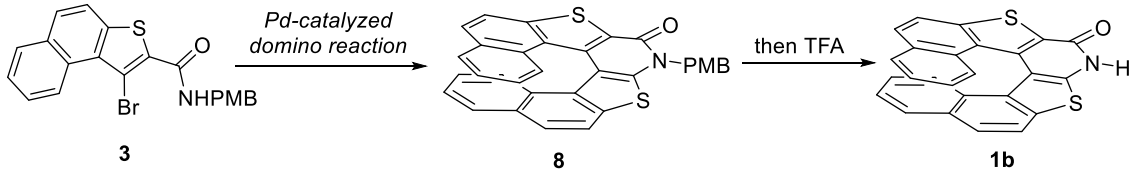

3 8 1b

Scheme 4-1. Strategy to synthesize **1b** via palladium-catalyzed domino reaction

4.1 Preparation of the substrates for palladium-catalyzed domino reaction

In order to investigate the proposed domino strategy, it is necessary to prepare **3** in large quantity. The author developed a pathway to synthesize **3** from commercially available starting materials in a total yield of 32% over 8 steps as shown in **Scheme 4-2**.

According to the literature procedure, naphtho[2,1-*b*]thiophene-2-carboxylic acid **18** was easily obtained after 3 steps via **16** and **17** without column chromatography.[24] After transformation to oxazoline derivative **20**, the bromination through *ortho*-lithiation gave **21**. Then, the hydrolysis under acidic conditions and the condensation with 4-methoxybenzylamine gave desired bromo naphthothiophene amide **3** (**Scheme 4-2**).

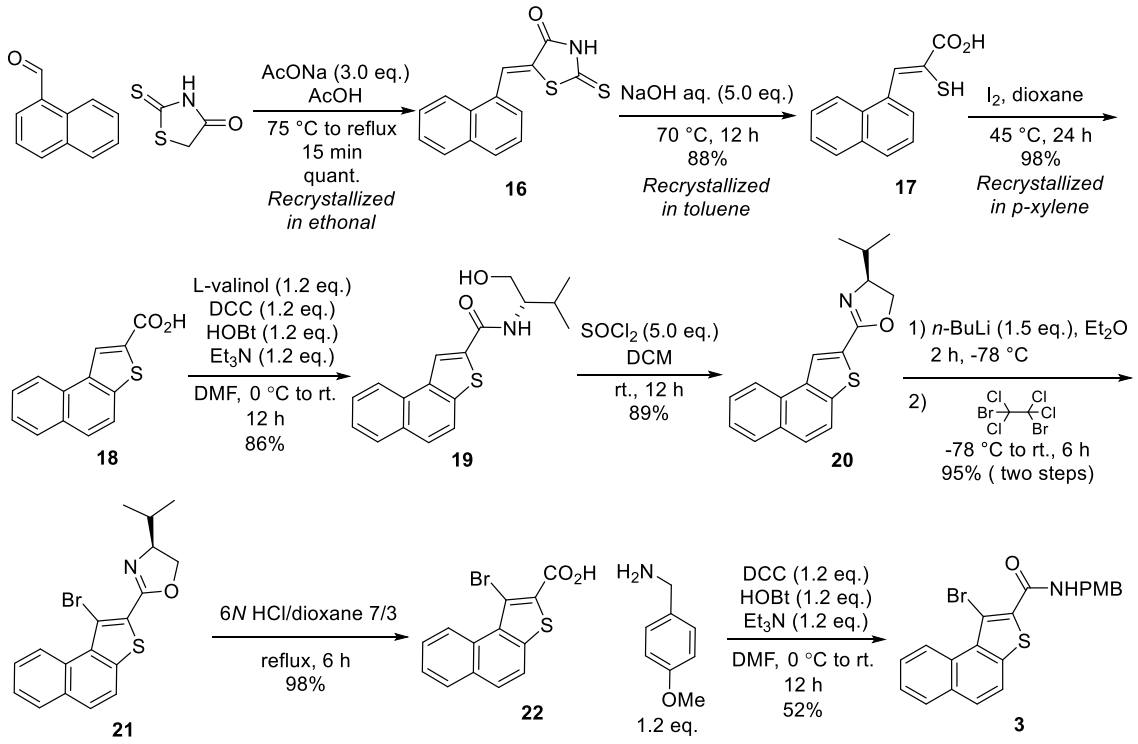

Scheme 4-2. Synthesis of substrate **3**

To investigate other substrates without sulfur, substrate **29** was synthesized (**Scheme 4-3**). **25** was prepared by the reported procedure through **23** and **24** from 2-acethyl naphthalene in 11% yield through 5 steps.[25] By Sandmeyer reaction, bromide **26** was obtained from **25**. After several failed attempts of direct conversion from cyano to carboxylic acid, **28** was generated through conversion of the nitrile group to aldehyde **27** and subsequent oxidation. Finally, condensation between carboxylic acid and *p*-methoxybenzyl (PMB) amine gave PMB amide **29**.

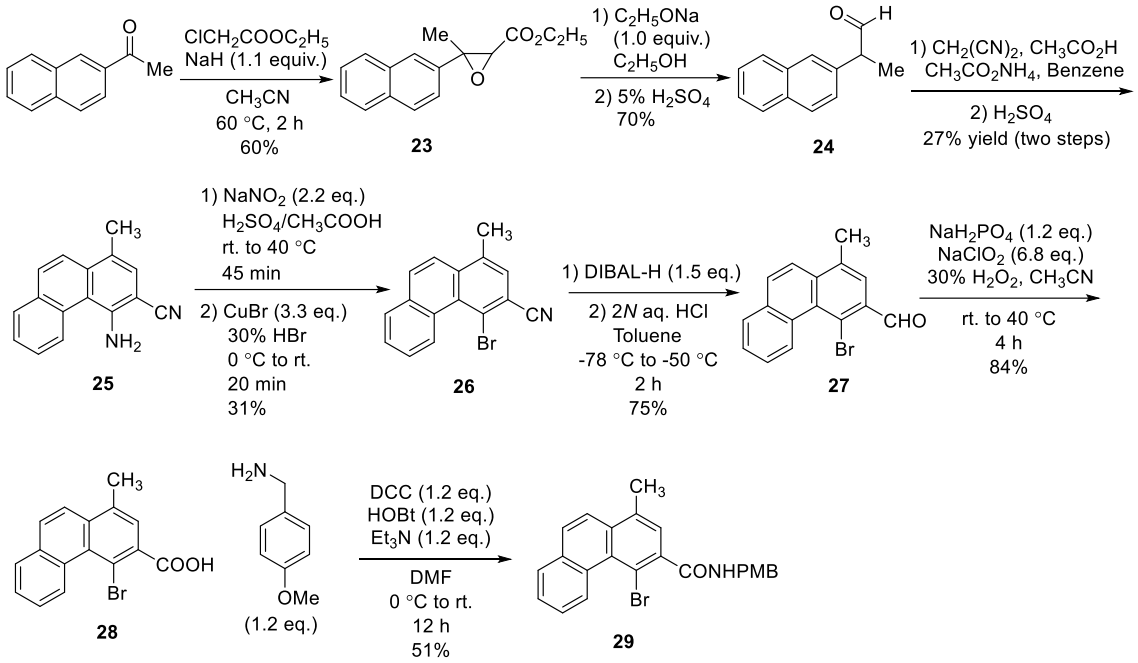

Scheme 4-3. Synthesis of substrate **29**

4.2 Synthesis of amide-functionalized [7]helicene-like molecule via palladium-catalyzed domino reaction

With substrate **3** in hand, several trials were conducted based on previous researches.[13-15] At first, the additive-ligand free catalytic system using Pd_2dba_3 (6 mol%), K_2CO_3 (1.1 equiv.) in DMF developed by the author's group, was applied, however, the desired product was not detected at all after heating at 100 °C or 140 °C for 24 hours (**Scheme 4-4**).

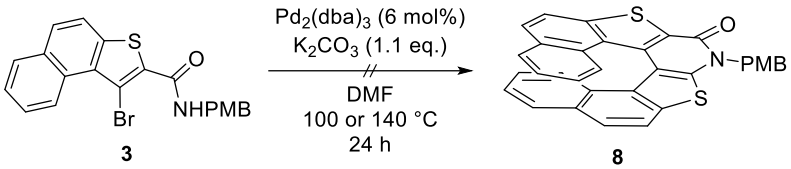

Scheme 4-4. Additive-ligand free palladium-catalyzed domino reaction

Then, by applying Chen's ligand-free conditions with $PdCl_2(PhCN)_2$ (5 mol%), CsF (4.0 equiv.) in DMA at 140 °C, target helicene-like compound **8** was detected by mass spectral analysis. However, the yield was found to be low after purification (**Table 4-1, Entry 1**). Then further reaction conditions were screened on the amount of catalyst, reaction temperature and reaction time were examined and it was found that the reactivity of substrate **3** is relatively low and more reaction time was needed. Moreover, the reaction temperature was shown to influence the reaction efficiency. When a reaction temperature over 100 °C was applied, the yield decreased. When the conditions in **entry 1** and **2** were applied, it was found that starting material would be remained partly. Therefore, 100 °C seemed to be a proper temperature for the reaction, and reaction time was increased twice. Finally, the product was obtained in 67% yield by carrying the reaction out at 100 °C in DMA for 48 hours with $PdCl_2(PhCN)_2$ (10 mol%), CsF (4.0 eq.) (**Table 4-1, Entry 6**).

Table 4-1. Preliminary conditions screening for palladium-catalyzed domino reaction

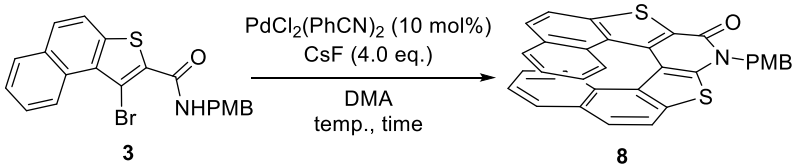

Entry	Temp. (°C)	Time (h)	Yield[a]
1	80	24	16%
2	100	24	35%
3	120	24	26%
4	140	24	16%
5	100	48	67%

a) NMR yield, 1,3,5-trimehoxybenzene as an internal standard.

Furthermore, some trials were performed in order to improve the yield by adding phosphine ligands. But the results were not satisfactory (**Table 4-2, entry 1-10**). Enantioselective synthesis of **8** by using chiral phosphine ligands were also attempted by using (*R*)-BINAP and (*R*)-MOP as chiral phosphine ligands, but the enantioselectivity was not observed at all (**Table 4-2, entry 11-12**).

Table 4-2. Attempts with phosphine ligands

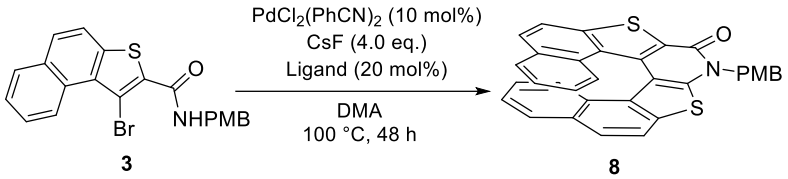

3 **8**

Entry	Ligand	Yield[a]
1	-	67%
5	$P(OMe)_3$	64%
6	$P(n\text{-}Bu)_3$	61%
7	Tri(*o*-tolyl)phosphine	61%
8	DPPP	60%
9	PCy_3	46%
10	Xantphos	61%
11	(*R*)-BINAP	66%(*dl*)
12	(*R*)-MOP	69%(*dl*)

a) NMR yield, 1,3,5-trimethoxybenzene as an internal standard.

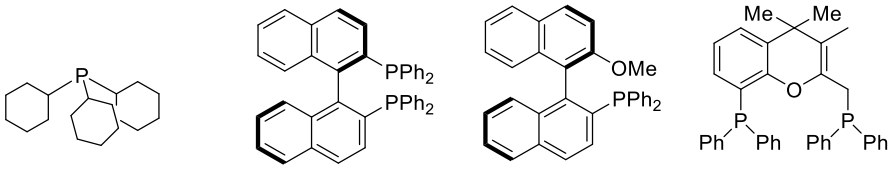

PCy_3: Tricyclohexylphosphine (*R*)-BINAP (*R*)-MOP Xantphos

In order to investigate the applicability of the domino reaction to the different substrates, several substrates **30**-**32** with same naphtho[2,1-*b*]thiophene nucleus were synthesized and tested (**Figure 4-1**). The substrates **31** bearing furylmethyl amide moiety was also found to be inapplicable to the conditions, although the reported domino reaction (**Scheme 1-5D, Chapter 1**) showed the corresponding *ortho*-bromo phenylamides gave the product in 92% yield.[15] The naphthothiophene substrate **32** with *n*-butyl amide moiety generated *n*-butyl [7]helicene-like molecule **36** in 11% yield (**Scheme 4-5**). Aryl chloride **30** did not give the helicene-like compound.

To investigate the possibility of diastereoselective synthesis of **8**, the substrates **33**, **34**, **35** bearing chiral amine moieties were examined (**Figure 4-1**). However, corresponding helicene-like molecules were failed to be obtained clearly.

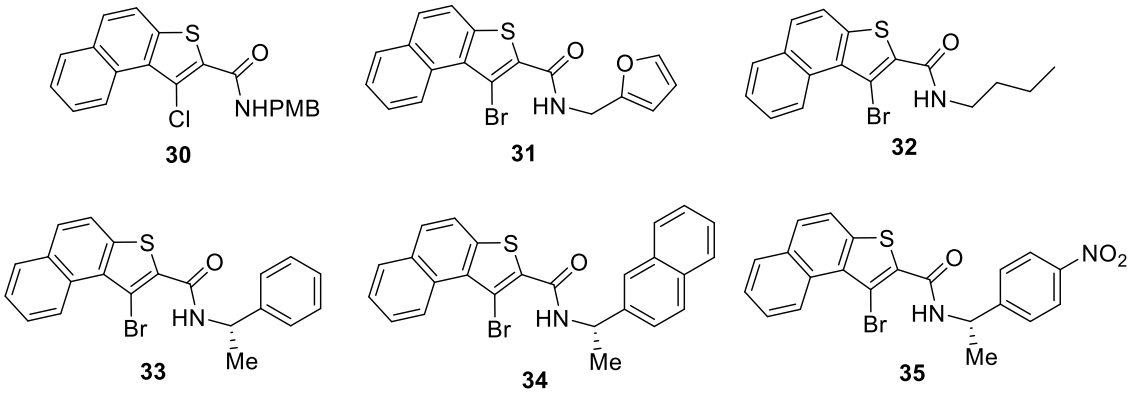

Figure 4-1. Expanded substrates for palladium-catalyzed domino reaction

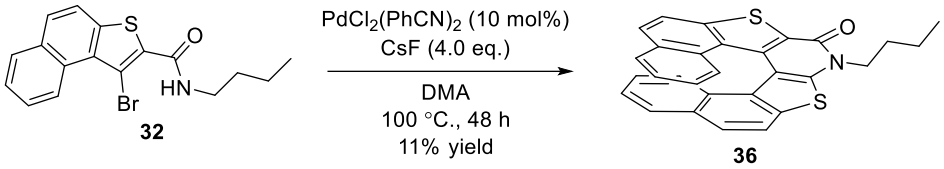

Scheme 4-5. Palladium-catalyzed domino reaction with **32**

Furthermore, palladium-catalyzed domino reaction of phenanthryl bromide **29** as the substrate without sulfur was examined. However, desired helicene-like product **37** could not be detected. Instead, the debrominated product **38** was yielded in 19% yield (**Scheme 4-6**).

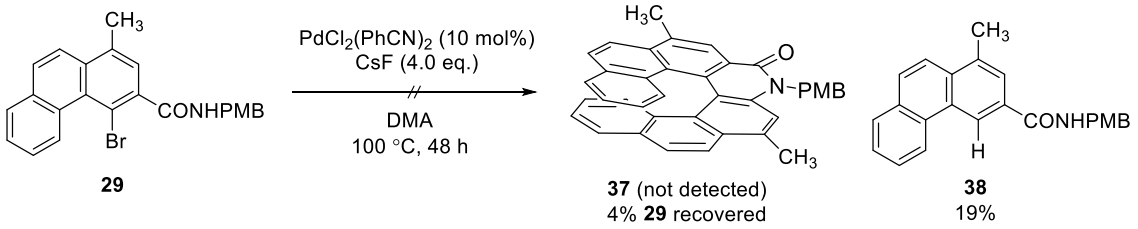

Scheme 4-6. Palladium-catalyzed domino reaction from **29**

The palladium-catalyzed reaction was considered as one-pot domino C–C and C–N formation reaction involving an *ipso* substitution procedure. In 2011, Gandon and Porée conducted a detailed mechanistic study to characterize Pd(II) palladacycle and biaryl species as common intermediates for the domino processes.[26] On that basis, C(sp^2)–C(sp^2) bond formation is expected

and calculated by DFT to be generated from a Pd(IV) complex **B** after oxidation addition of the substrate into the Pd(II) palladacycle intermediate **A**. Based on these considerations, a plausible mechanism has been proposed (**Figure 4-2**).

After successive oxidative addition of Pd(0) to the substrate **2**, a Pd(II) intermediate **A** and Pd(IV) intermediate **B** will be furnished continuously. Intermediate **B** will lead to the C-C coupling accompanying reductive elimination of Pd(IV) to Pd(II). The resulted intermediate **C** will undergo the key step of electrophilic aromatic substitution with deamidation reaction to give intermediate **D**. And then after the leaving of isocyanate group, palladacycle **E** will be furnished. Finally the product **8** will be released by reductive elimination with Pd(0) entering to the catalytic cycle back.

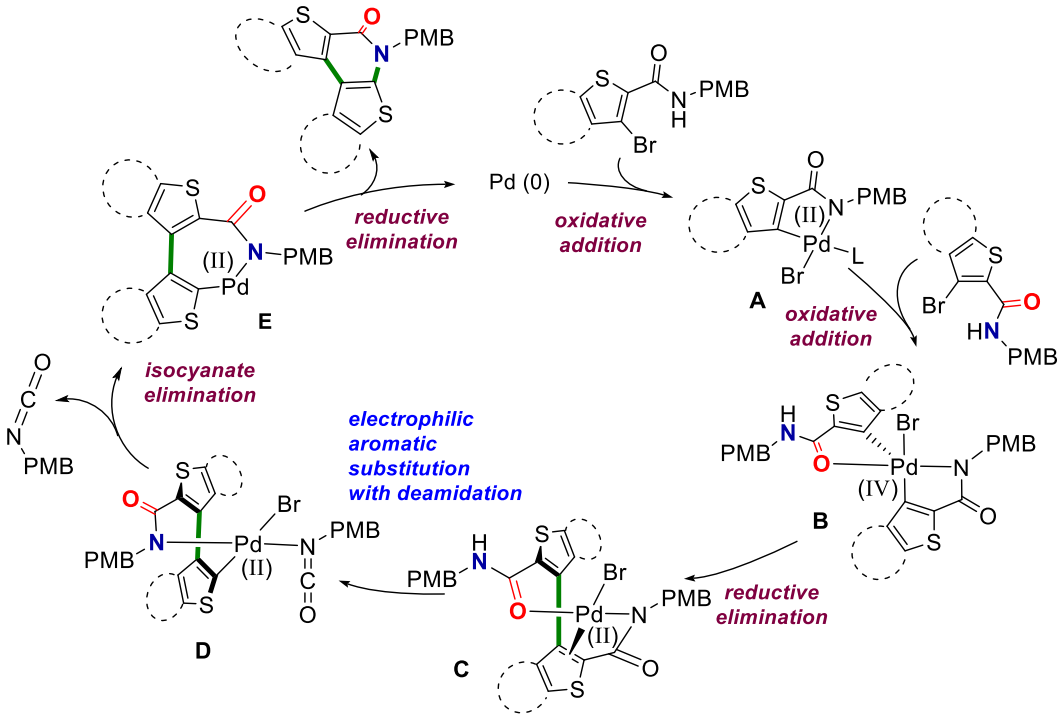

Figure 4-2. Proposed mechanism for palladium-catalyzed domino reaction from **3**

In both case of **3** and **29** as substrate, the first oxidative addition seemed to function well. However, during the second oxidative addition, in the intermediate **B'** (**Figure 4-3**), the steric repulsion between PMB and the terminal ring in phenanthrene was stronger than the case of naphthothiophene intermediate **B**.

Therefore, in the case of **29** as substrate, the formation of intermediated **B'** should be quite difficult which might be the reason why phenanthrene **29** didn't furnish corresponding helicene-like product **37**.

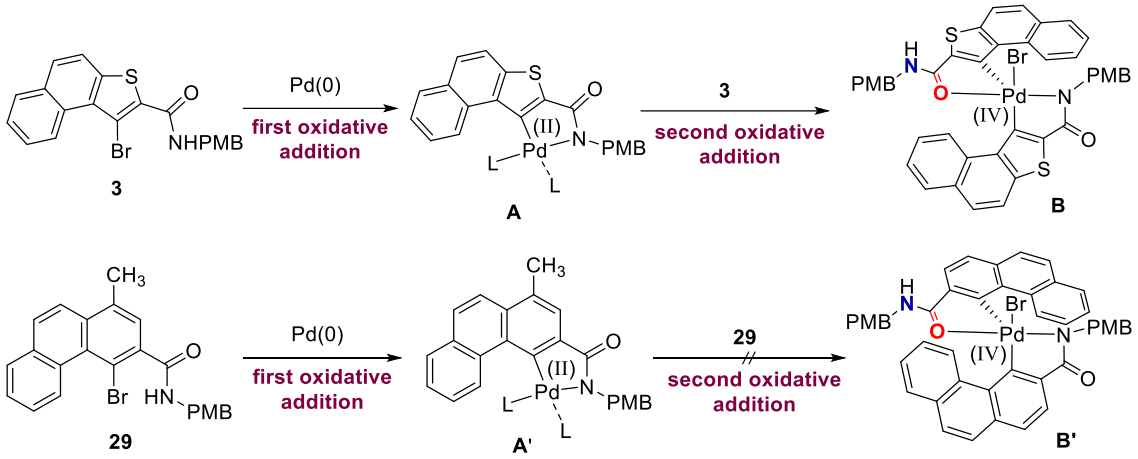

Figure 4-3. Comparison of substrate **3** and **29** during domino procedure

Above all, the racemic PMB type helicene-like molecule **8** was obtained in 67% yield via palladium-catalyzed domino reaction with subsequent C–C and C–N bond formations, although the diversity of substrates is quite limited and enatioselective and diastereoselective synthesis failed to be achieved. A proposed mechanism may offer some clues how the steric effects dominate the formation of a Pd(IV) intermediate, which could show an explanation for the substrate limitation. Further study for screening the conditions and substrates should be performed to expand the application scale and confirm the mechanism.

4.3 Deprotection of PMB group of the domino reaction product and oxidation of the sulfur atoms

The sulfur containing amide-functionalized [7]helicene-like molecule **1b** was furnished smoothly from **8** by refluxing in TFA for 48 h with deprotection of PMB group in 82% yield (**Scheme 4-7**).

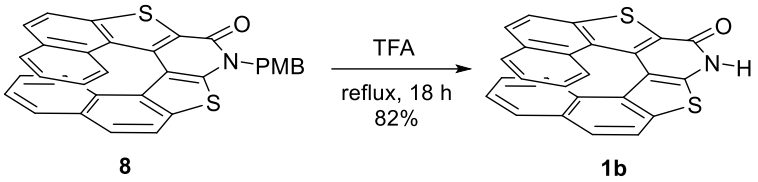

Scheme 4-7. Deprotection of PMB group

With the introduction of sulfur atom to the out ridge of helicene backbone, it offers a possibility to change the electronic properties and potential chiropotical properties by further modification of the helicene structure on sulfur atoms.[27] Therefore, further oxidation of sulfur atoms towards sulfonyl groups has been performed from both racemic and (*M*)-amide-functionalized [7]helicene-like molecule **1b** (**Scheme 4-8**).

For the oxidation procedure, excess amount of trifluoroperacetic acid, which was generated *in situ* by mixing trifluoroacetic anhydride and H_2O_2, was used to oxidize the sulfur atoms in DCM at room temperature. Although the reaction took long time (7 days), both of the sulfur atoms of **1b** were completely oxidized to the corresponding sulfonyl groups. The specific rotation of (*M*)-**39** was also recorded: $[\alpha]_D^{19}$ = -983.6 (c = 0.5, DMSO).

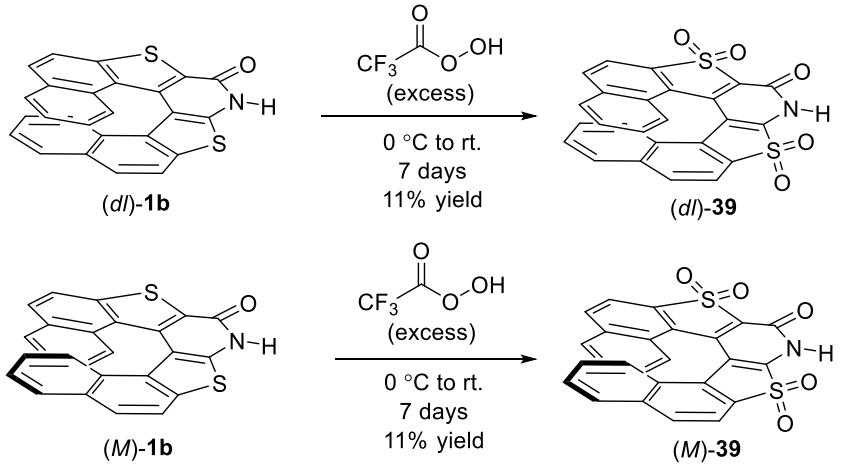

Scheme 4-8. Oxidation of the sulfur atoms of **1b**

The new oxidized helicene-like molecule **39** may exhibit interesting properties, eg., the acidity of amide group will be increased with the sulfonyl groups located nearby as electron withdrawing groups. And the sulfonyl groups might function as sterically hindered group, or a molecular recognition site as hydrogen-bonding acceptor site.

4.4 Racemization barriers and chiroptical properties

4.4.1 Racemization barriers of amide-functionalized helicene-like molecules

The racemization of helicenes is one of the intriguing properties.[28] To evaluate the configurational stability of helical chirality of the optically active amide-functionalized helicene-like molecules, the author intended to check the racemization barrier energy for each molecule.

In the racemization process of helicenes, two transition states of pentahelicene have been proposed as shown in **Figure 4-4**. One is the C_{2v} transition state, in which all of the atoms of the helicene locate in the same plane. The other one is the C_s transition state, in which the terminal rings bending to the same side. In the most theoretical calculations, the transition state with C_s symmetry has been adopted. It means that the ground state firstly twists into the nonchiral C_s-transition state and subsequently transforms to each configuration with equal possibility, resulting in racemization.

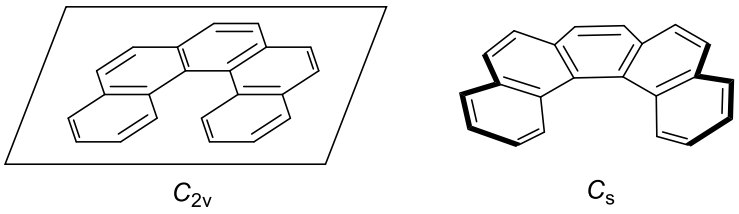

Figure 4-4. Two different transition states for racemization of pentahelicene

Firstly, it was intended to examine the racemization barrier energy of **1a** by experiment. However, the racemization barrier was proved to be too high to be measured practically. With continuous heating under reflux conditions in chlorobenzene (bp. 132 °C), no racemization was observed even after 3 days. Therefore, an estimation of the racemization barrier was undertaken using density functional theory (DFT) calculations at the wB97xd/6-311+G(d,p)//B3LYP/6-31G(d,p) level of theory (see the experimental part) in chlorobenzene as solvent. The calculation was performed by the use of the dihedral angle (**Figure 2-1**, ϕa,b–c,d: 23°) from the X-Ray analysis as the ground state structure. The results of the calculation showed the C_s-symmetric transition-state structure with 41.4 kcal/mol of the racemization barrier as shown in **Figure 4-5**. This theoretical result confirmed that the configurational stability of **1a** is enough to be optically active form without racemization under ambient temperature.

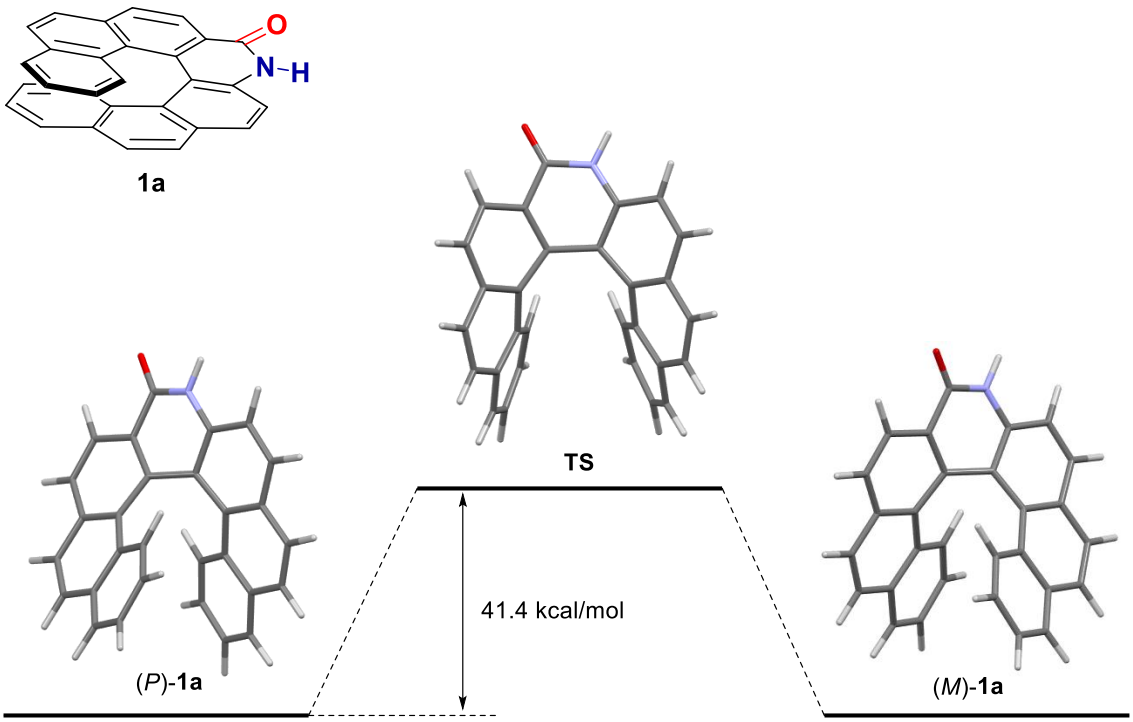

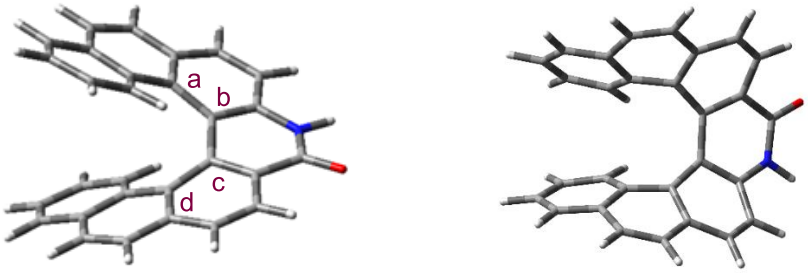

Ground state (0.0) TS-structure (41.4)

Figure 4-5. Ground state and TS state of **1a** (Relative Gibbs free energies (kcal/mol) are given in parentheses; Dihedral angle (ϕa,b–c,d: 23°) was frozen using a crystal structure by X-Ray analysis)

On the other hand, the sulfur and amide-functionalized [7]helicene-like molecule **1b**, the racemization barrier energy has been successfully measured by heating the (*P*)-**1b** in PhCl under refluxing conditions. By monitoring the ee value at continuous time points, the plot of $\ln(ee_0/ee_t)$ to time was obtained as shown in **Table 4-1**.

Table 4-1. Racemization rate constant measurement (in chlorobenzene)

Time (min)	ee (%)
0	100
125	97.3
240	93.8
360	90.2
1020	72.2
1140	69.6
1810	55.9
2044	52.4

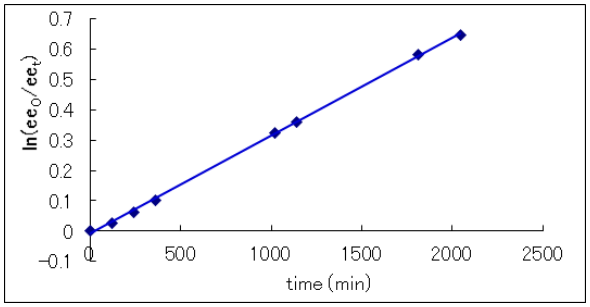

The first-order plot was shown as $\ln(ee_0/ee_t) = 0.0003t - 0.0088$ ($R^2 = 0.9996$). After calculation, the racemization rate constant was resulted as $k_{rac} = 2.716\times10^{-6}$ (s^{-1}). Then, the racemization barrier energy $\Delta G^{\ddagger}_{rac}$ was figured out as 34.3 kcal/mol by the following Eyring equation:

$$\Delta G^{\ddagger}_{rac} = -RT \ln(hk_{rac}/\kappa Tk_B)$$

Where, k_{rac} = racemization rate constant, $\Delta G^{\ddagger}_{rac}$ = energy barrier for racemization, T = temperature, R = gas constant, h = Planck constant, k_B = Boltzmann constant, and κ = kappa, transmission coefficient (which is usually unity for this calculation).

On the other hand, DFT calculation of **1b** was performed in chlorobenzene as solvent. The racemization barrier ($\Delta G^{\ddagger}$ = 36.3 kcal/mol) was found to be similar value to the result determined by experiment. These consistent results indicate the reliability of the DFT calculation.

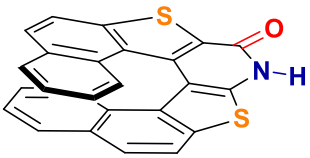

1b

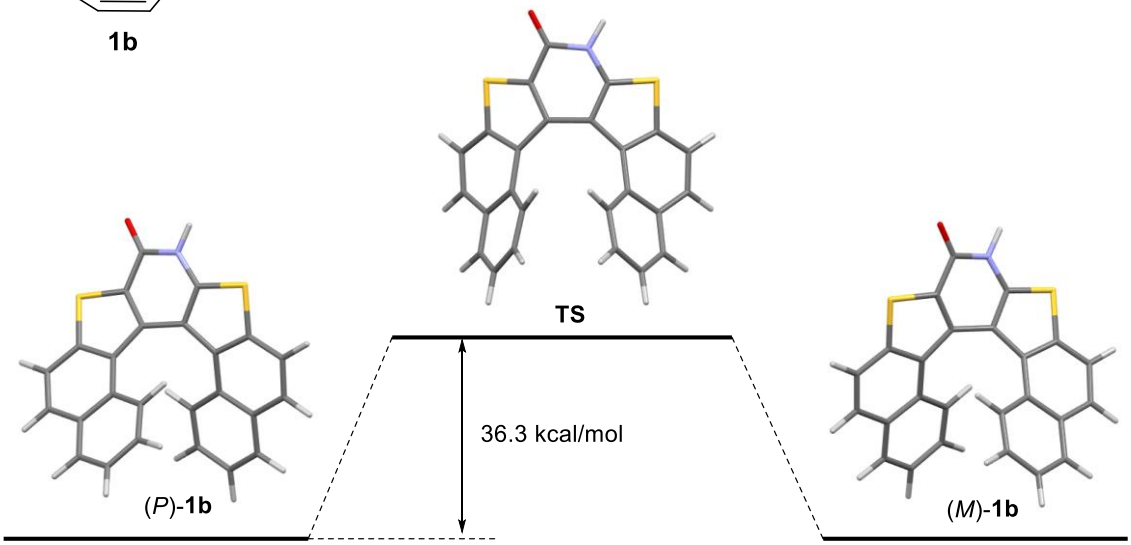

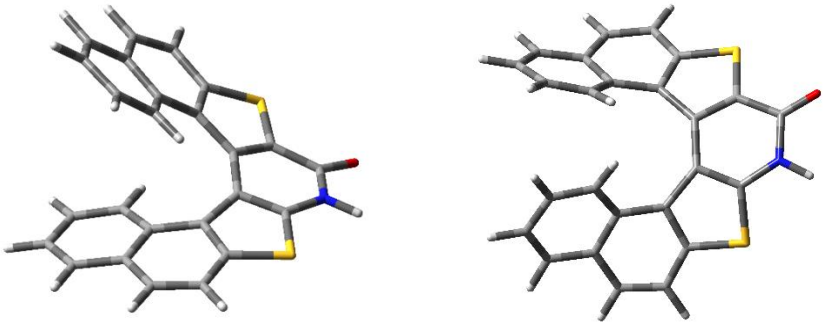

Ground state (0.0) TS-structure (34.3)

Figure 4-6. Ground state and TS state of **1b**. (The optimized structures of the ground state and the transition state were depicted by DFT calculation; Relative Gibbs free energies (kcal/mol) are given in parentheses)

The racemization barrier energy of sulfur and amide-functionalized [5]helicene-like molecule **1n** was turn out to be 3.1 kcal/mol by DFT calculation. The stability is much lower than sulfur and amide-functionalized [7]helicene-like molecules ($\Delta G^{\ddagger}_{rac}$ = 34.3 kcal/mol).

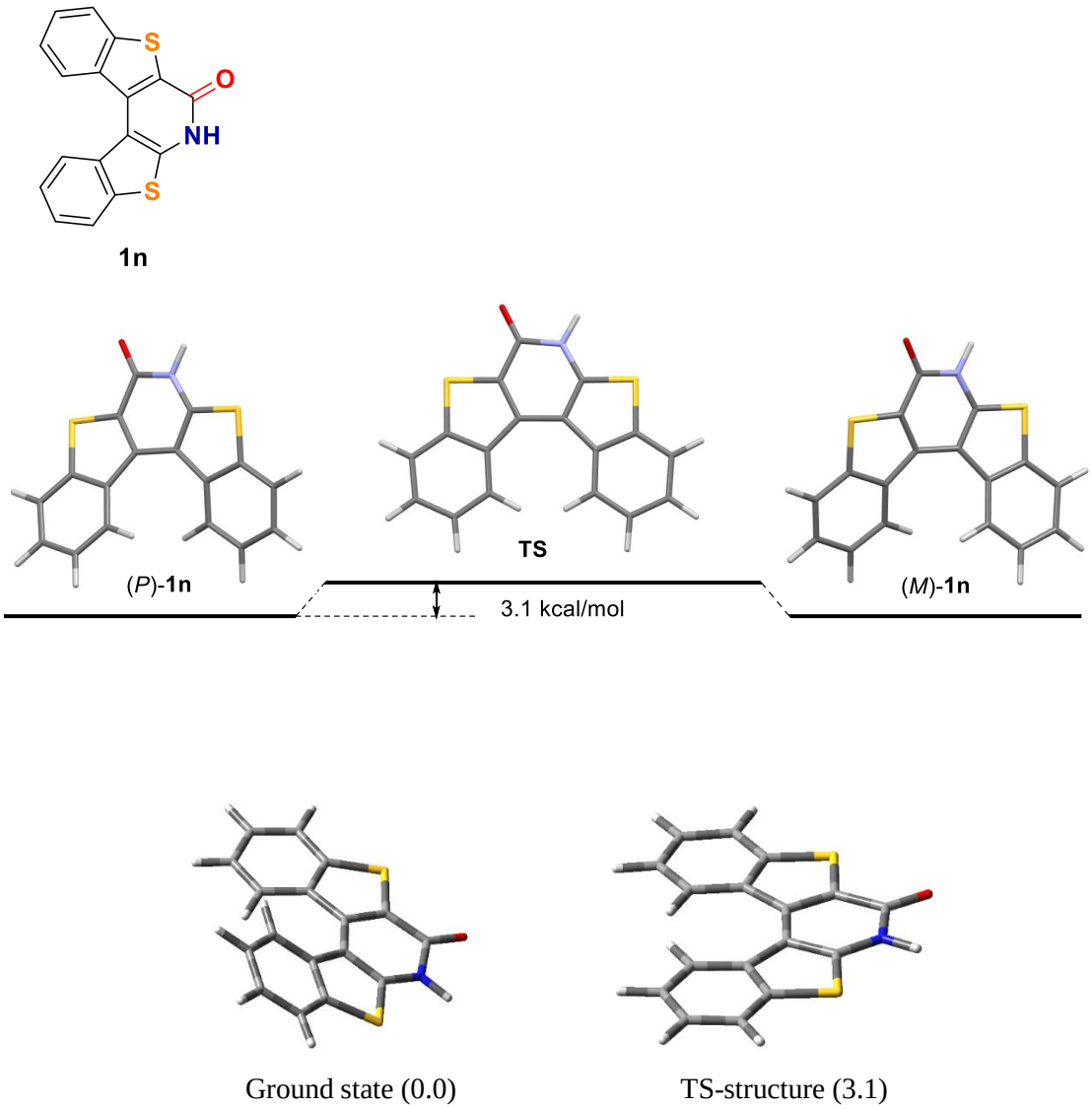

Figure 4-7. Ground state and TS state of **1n** (The optimized structures of the ground state and the transition state were depicted by DFT calculation; Relative Gibbs free energies (kcal/mol) are given in parentheses)

With the calculated and experimental racemization barrier energies in hand, a contradistinction and summary was conducted with other reported examples (**Figure 4-8**).[29]

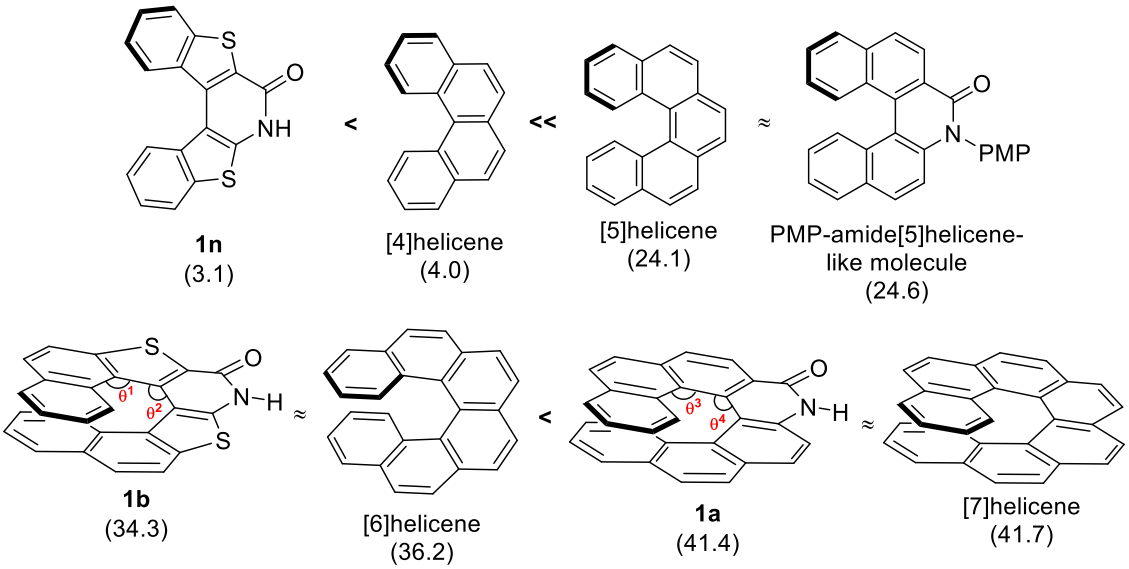

Figure 4-8. Comparison of the racemization barriers among amide-functionalized helicene-like molecules and carbohelicenes. Racemization barriers (kcal/mol) are shown in parentheses (see: ref. 29)

1) Generally, [6] and [7]helicenes are considered as configurationally stable, whereas helicenes with less than 5 aromatic rings might not keep their helical chirality very well at high temperature for a long time. It is because, as the length of helicene and helicene-like molecules ([4]helicenes to [7]helicenes) increase, the interplanar angles (**Figure 1-2C**) are larger, making it more difficult to reach the TS structure from the ground state.

2) It was found that the racemization barrier energies are similar for amide-functionalized helicene-like molecules without sulfur atoms than these normal carbohelicenes with same number of rings in backbone, indicating that pyridone ring inserted in the helicene outer core shows nearly no influence on the configurational stability of helical chirality. (24.6 kcal/mol for PMP-amide [5]helicene-like molecule, 24.1 kcal/mol for [5]helicene; 41.4 kcal/mol for **1a**, 41.7 kcal/mol for [7]helicene)

3) Another point worth noting is the significantly reduced racemization barrier energies for helicene-like molecules by introducing thiophene rings into the helical backbone. One thiophene ring replacing one benzene ring at each side will greatly decrease the helical stability to even a lower level relating to the number of fused aromatic rings of carbohelicenes. (34.3 kcal/mol for **1b**, similar with 36.2 kcal/mol for [6]helicene; 3.1 kcal/mol for **1n**, similar with 4.0 kcal/mol for [4]helicene)

For the reasons why sulfur containing amide functionalized helicene-like molecules show lower racemization barriers, two factors are suggested.

Firstly, with **1a** and **1b** taken as example, the introduction of thiophene ring as a five number ring instead of six-number benzene ring will cause an increase of the inside angle (θ^1 = 130.92°,θ^2 = 133.12°,θ^3 = 124.55°,θ^4 = 127.21° in **Figure 4-8**) for at thiophene ring postion. With a larger inner angle ($\theta^1 > \theta^3$; $\theta^2 > \theta^4$) at corresponding position, the terminal ring will be further apart from each other and the overlapping area will be less as shown in **Figure 4-9**, thus the steric interactions between the two terminal rings will be smaller during racemization. This leads to a smaller racemization barrier energy of **1b** than **1a** (34.3 kcal/mol for **1b**; 41.4 kcal/mol for **1a**).

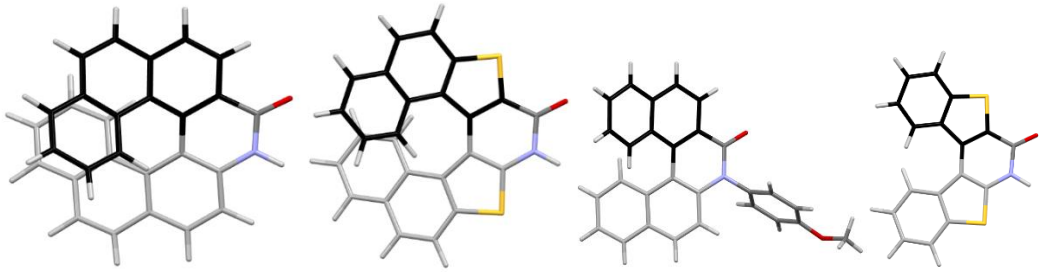

(*P*)-**1a** (*P*)-**1b** (*P*)-PMP-[5]helicene (*P*)-**1n**

Figure 4-9. Comparison of overlapping area in **1a**, **1b**, PMP-[5]helicene and **1n**

Secondly, it is indicated that twisting distributed over a large number of aromatic bonds of the helicenes enables the racemization,[28h] therefore, the extent of aromacity of fused rings will also contribute to the racemization barrier energy. The sulfur containing amide functionalized helicene-like molecules show smaller racemization barriers as thiophene ring has a smaller aromacity compared with benzene ring.

With the combination of differences of π overlapping area at terminal part and total helicene aromacity, sulfur containing amide-functionalized helicene-like molecules show lower racemization barrier energies.

4.4.2 Comparison with optical rotations of helicene and helicene-like molecules

With three new kinds of optically active [7]helicene-like molecules **1a**, **1b**, **39** in hand, the optical rotations of each molecule were measured in DMSO (**Figure 4-10**).

Obviously, all of them show relatively high optical rotation values. Even though the amide-functionalized [7]helicene-like molecules seem to present a smaller optical rotation ($[\alpha]_D^{18}$ = +1954.5, c = 0.2 in DMSO) than carbo[7]helicene ($[\alpha]_D^{25}$ = +5577, c = 1.0 in $CHCl_3$),[29] their optical rotation values are still much higher than most usual chiral molecules.

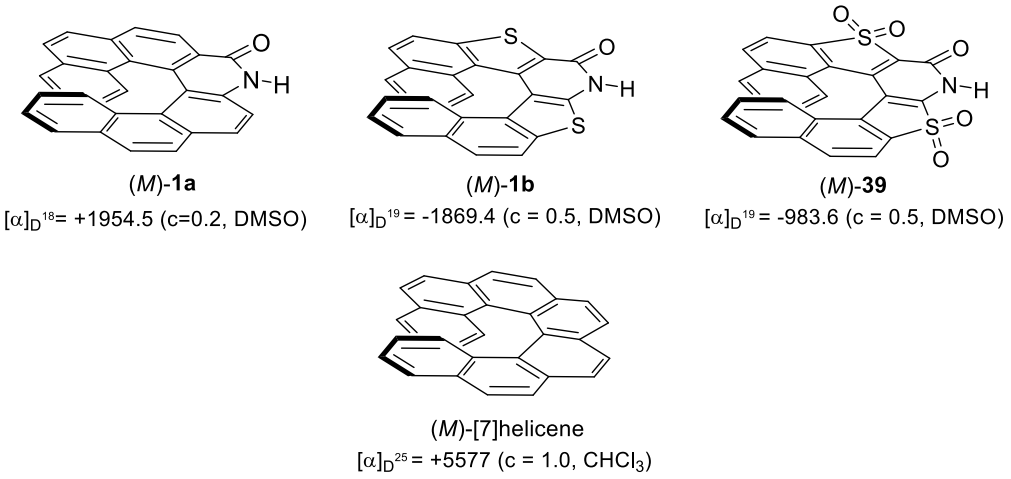

Figure 4-10. Comparison of optical rotations

4.4.3 CD spectra of amide-functionalized [7]helicene-like molecules

For investigating the chiroptical properties of **1a** and **1b**, their circular dichroism (CD) spectrums were measured, as well as UV spectra in THF (**Figure 4-11; 4-12**).

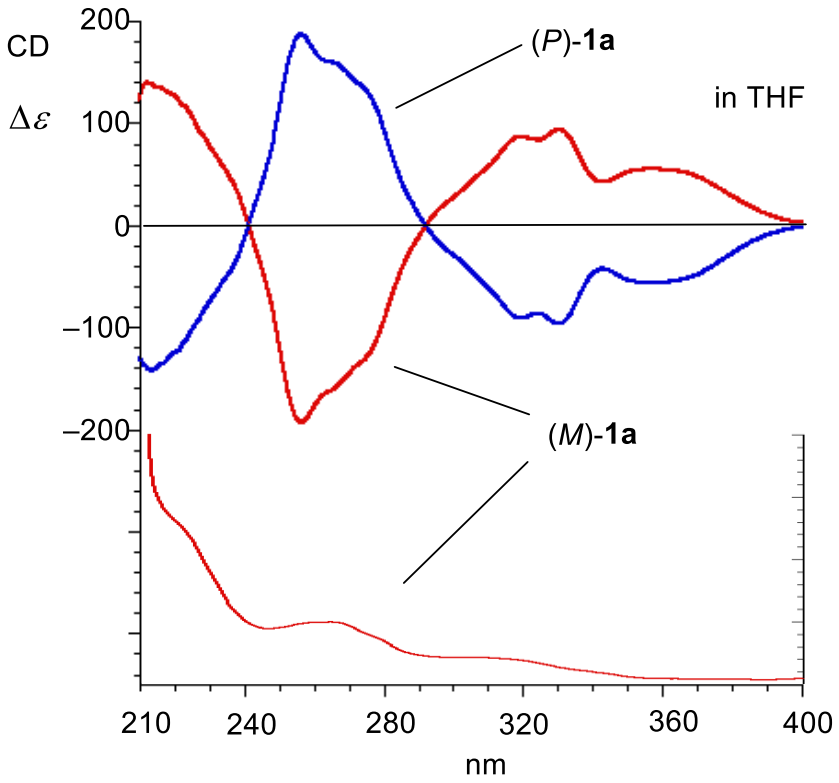

Figure 4-11. CD and UV spectra of amide-functionalized [7]helicene-like molecule **1a** (0.85×10^{-5} M for (*P*)-**1a**; 1.15×10^{-5} M for (*M*)-**1a**, in THF)

The CD spectra of (*M*)-enantiomer **1a** (**Figure 4-11**) was revealed to show a small positive Cotton around 330.4 nm ($\Delta\varepsilon = +93.7$ $M^{-1}cm^{-1}$), a large negative Cotton around 256.4 nm ($\Delta\varepsilon = -193.4$ $M^{-1}cm^{-1}$), and a large positive band at 212.2 nm ($\Delta\varepsilon = +139.7$ $M^{-1}cm^{-1}$). The CD spectra of (*P*)-**1a** showed opposite Cotton, being exactly mirrored image. For (*M*)-**1a**, between 292 nm to 210 nm, the wavelength dependence of the CD curve shows characteristic shapes. Along with the decreasing of wavelength, the plot decreases to a minimum and then increases, passing through zero where the maximum of absorption occurs, as the wavelength is decreased further, it becomes positive, until reaching a maximum. A typical negative Cotton effect pattern is acknowledged. On the contrary, (*P*)-**1a** shows a positive Cotton effect.

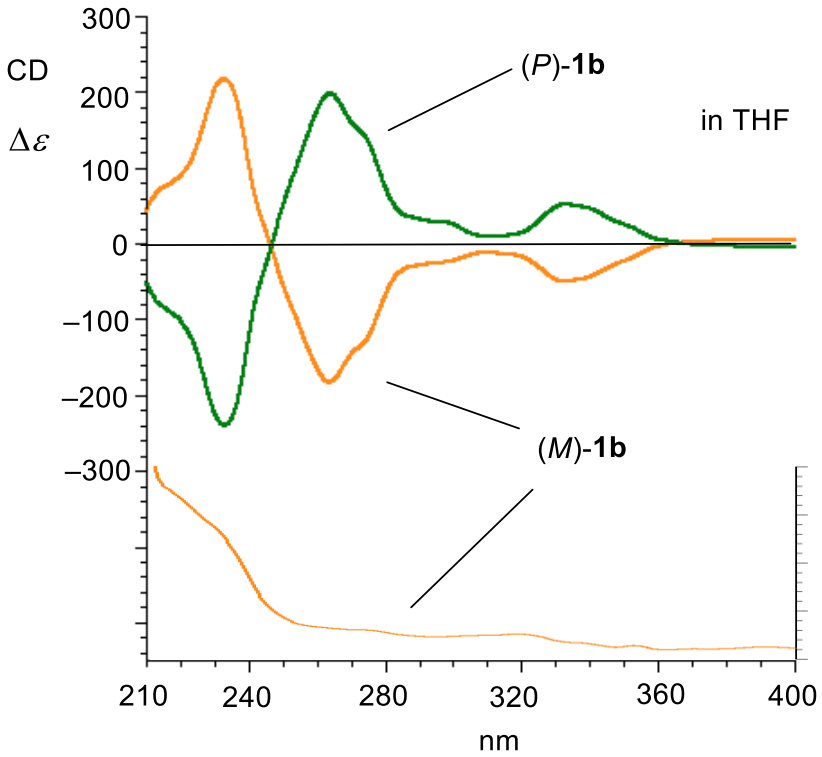

Figure 4-12. CD and UV spectra of amide-functionalized thia[7]helicene-like molecule **1b** (1.65×10^{-5} M for (*P*)-**1b**; 1.45×10^{-5} M for (*M*)-**1b**, in THF)

The CD spectra of (*M*)-enantiomer **1b** (**Figure 4-12**) was revealed to show a small negative Cotton around 333.2 nm ($\Delta\varepsilon$ = -50.2 $M^{-1}cm^{-1}$), a large negative Cotton around 263.7 nm ($\Delta\varepsilon$ = -182.9 $M^{-1}cm^{-1}$), and a large positive Cotton around 232.8 nm ($\Delta\varepsilon$ = +217.2 $M^{-1}cm^{-1}$). (*P*)-**1b** showed opposite Cotton, being exactly mirrored image. Being similar with (*M*)-**1a**, (*M*)-**1b** also presents a negative Cotton effect whereas (*P*)-**1b** shows positive Cotton effect between 292 nm to 210 nm wavelenghth.

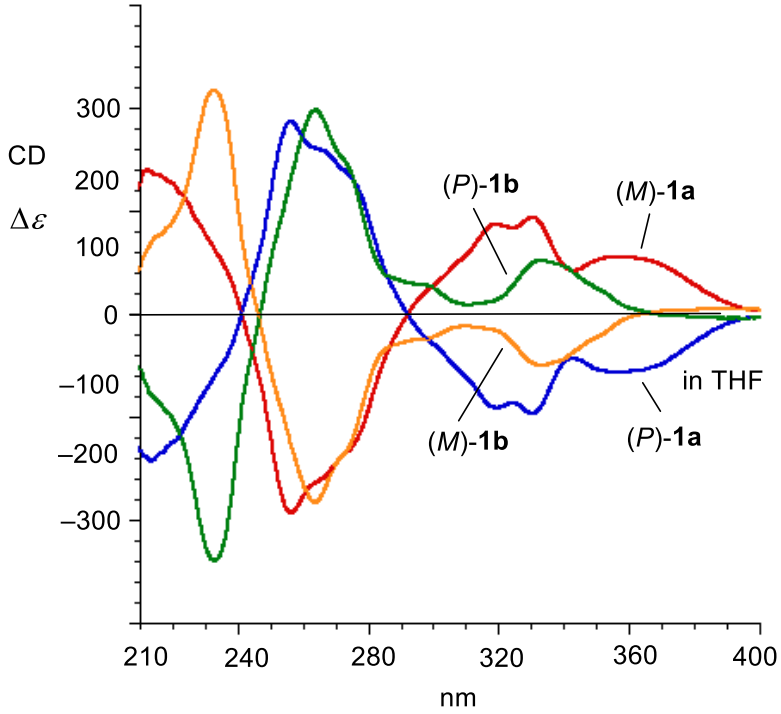

Figure 4-13. Combined CD spectra of **1a** and **1b** in THF

Both mirror-image plots for the (*M*)- and (*P*)-enantiomers of **1a** or **1b** are obtained. Thus, the combined CD spectra of [7]helicene-like molecules **1a** and **1b** can be smoothly obtained (**Figure 4-13**), which makes it clear to compare with each other. The appearance of same Cotton effect for (*M*)-enantiomers or (*P*)-enantiomers with same trend in CD spectra should be referable for other similar helicene or helicene-like structures in determination of their absolute configurations.

Conclusion and perspective

In summary, two cyclization methods from biaryl substrates with retention of optical purity was developed to synthesize amide-functionalized [7]helicene-like molecule **1a**, which is optically pure and configurationally stable, showing a special self-assembly behavior caused by common π-π stacking interactions and unusual hydrogen bonding function together in helicene aggregation. The unique aggregation construction is quite promising in material chemistry, presenting special properties and applications.

Sulfur containing amide-functionalized [7]helicene-like molecule **1b** was synthesized through one-pot cyclization and a more direct palladium-catalyzed domino reaction with following deprotection of PMB group, which could be further modified chemically such as sufficient oxidation of sulfur atoms. The sterically hindered and electron withdrawing sulfonyl groups inserted in helical structure might not only improve the acidity of amide group but also function as new hydrogen bonding recognition site.

For newly prepared helicene-like molecules, the racemization barrier energies were revealed to show that amide-functionalized [7]helicene-like molecules are configurationally stable in umbient termperature. CD spectra might be used for deducing the absolute configuration of similar amide-functionalized helicene-like molecules.

Besides, a variety of biologically important phenantheridinone derivatives were prepared by direct one-pot cyclization, during which, increased stability of phosphate derivatives generated in the first stage was turn out to be originated from the combination of chalcogen bonding interaction and pnictogen bonding interaction.

The author expects that more efficient and applicable methodologies to prepare amide-functionalized helicene-like molecules could be developed and more interesting properties and applications of these molecules would be discovered.

References:

1. For selected reviews of helicene and heterohelicene synthesis, see:
   (a) Collins, S. K.; Vachon, M. P. *Org. Biomol. Chem*. **2006**, *4*, 2518.
   (b) Gingras, M. *Chem. Soc. Rev*. **2013**, *42*, 968.
   (c) Gingras, M.; Félix, G.; Peresutti, R. *Chem. Soc. Rev*. **2013**, *42*, 1007.
   (d) Shen, Y.; Chen, C.-F. *Chem. Rev*. **2012**, *112*, 1463.
   (e) Laarhoven, W. H.; Prinsen, W. J. C. *Top. Curr. Chem*. **1984**, *125*, 63.
   (f) Urbano, A. *Angew. Chem. Int. Ed*. **2003**, *42*, 3986.
   (g) Saito, N.; Yamaguchi, M. *Molecules*, **2018**, *23*, 277.
   (h) Hoffman, N. J. *Photochem. Photobiol. C Photochem. Rev*. **2014**, *19*, 1.
   (i) Virieux, D.; Sevrain, N.; Ayad, T.; Pirat, J.-L. Helical phosphorus derivatives. In *Advancesin Heterocyclic Chemistry*; Eric, F.V.S.; Christopher, A.R., Eds.; *Academic Press*: Cambridge, MA, USA, 2015; Vol. 116.
   (j) Dhbaibi, K.; Favereau, L.; Crassous, J. *Chem. Rev*. **2019**, *119*, 8846.
   (k) Hiroto, S. *Bull. Chem. Soc. Jpn*. **2018**, *91*, 829.
   (l) Gataullin, R. R. *Russ. J. Org. Chem*. **2019**, *55*, 1247.
   (m) Starý, I.; Stará, I. G. *Targets Heterocycl. Syst*. **2017**, *21*, 23.
   (n) Wang, H. *Imaging Science and Photochemistry*, **2017**, *35*, 603.
   (o) Hoffman, N. *Chem. Rev*. **2008**, *108*, 1052.
   (p) Jørgensen, K. B. *Molecules*, **2010**, *15*, 4334.
   (q) Stará, I. G.; Starý, I. In *Aromatic Ring Assemblies, Polycyclic Aromatic Hydrocarbons, and Conjugated Polyenes*; Siegel, J. S., Tobe, Y., Eds.; Thieme: Stuttgart, 2010; Vol. 45b, pp. 885.
   (r) Dumitrascu, F.; Dumitrescu, D. G.; Aronb, I. *ARKIVOC*, **2010**, *1*, 1.
   (s) Tanaka, K.; Kimura, Y.; Murayama, K. *Bull. Chem. Soc. Jpn*. **2015**, *88*, 375.
   (t) Katz, T. J. *Angew. Chem. Int. Ed*. **2000**, *39*, 1921.
2. For selected reviews of helicene properties, see:
   (a) Gingras, M. *Chem. Sov. Rev*. **2013**, *42*, 1051.
   (b) Sawato, T.; Yamaguchi, M. *ChemplusChem*. **2020**, *85*, 2017.
   (c) Starý, I.; Stará, I. G.; Alexandrova, Z.; Sehnal, P.; Teply, F.; Saman, D.; Rulisek, L. *Pure Appl. Chem*. **2006**, 78, 495.
   (d) Wynberg, H. *Acc. Chem. Res*. **1971**, *4*, 65.
   (e) Rajca, A.; Miyasaka, M. *Functional Organic Materials*; Wiley-VCH Verlag GmbH & Co. KGaA: Weinheim, Germany, 2007; Chapter 15, pp. 547.
   (f) Licandro, E.; Cauteruccio, S.; Dova, D. *In Advances in Heterocyclic Chemistry*; Scriven,

E. F. V.; Ramsden, C. A., Eds.; *Academic Press*, 2016; Vol. 118.

(g) Zhao, W.-L.; Li, M.; Lu, H.-Y.; Chen, C.-F. *Chem. Commun*. **2019**, *55*, 13793.

3. For selected reviews of helicene applications, see:

(a) Brandt, J. R.; Salerno, F.; Fuchter, M. J. *Nat. Rev. Chem*. **2017**, *1*, 0045.

(b) Demmer, C. S.; Voituriez, A.; Marinetti, A. *C. R. Chimie*. **2017**, *20*, 860.

(c) OuYang, J.; Crassous, J. *Coordination Chemistry Reviews*, **2018**, *376*, 533.

(d) Usui, K. *YAKUGAKU ZASSHI*, **2017**, *137*, 1381.

(e) Borovkov, V.; Hasan, M. *Symmetry*, **2018**, *10*, 10.

(f) Saleh, N.; Shen, C.; Crassous, *J. Chem. Sci*. **2014**, *5*, 3680.

(g) Aillard, P.; Voituriez, A.; Marinetti, A. *Dalton Trans*. **2014**, *43*, 15263.

(h) Fang, L.; Lin, W.; Shen, Y.; Chen, C.-F. *Chin. J. Org. Chem*. **2018**, *38*, 541.

(i) Chen, J.; Takenaka, N. *Chem. Eur. J*. **2009**, *15*, 7268.

4. For selected articles of organic material study of helicenes, see:

(a) Verbiest, T.; Elshocht, S. V.; Persoons, A.; Nuckolls, C.; Phillips, K. E.; Katz, T. J. *Langmuir*. **2001**, *17*, 4685.

(b) Verbiest, T.; Elshocht, S. V.; Kauranen, M.; Hellemans, L.; Snauwaert, J.; Nuckolls, C.; Katz, T. J.; Persoons, A. *Science*, **1998**, *282*, 913.

(c) Kaseyama, T.; Furumi, S.; Zhang, X.; Tanaka, K.; Takeuchi, M. *Angew. Chem. Int. Ed*. **2011**, *50*, 3684.

(d) Phillips, K. E. S.; Katz, T. J.; Jockusch, S.; Lovinger, A. J.; Turro, N. J. *J. Am. Chem. Soc*. **2001**, *123*, 11899.

(e) Okuyama, T.; Tani, Y.; Miyake, K.; Yokoyama, Y. *J. Org. Chem*. **2007**, *72*, 1634.

(f) Hatakeyama, T.; Hashimoto, S.; Oba, T.; Nakamura, M. *J. Am. Chem. Soc*. **2012**, *134*, 19600.

(g) Shcherbina, M. A.; Zeng, X.-B.; Tadjiev, T.; Ungar, G.; Eichhorn, S. H.; Phillips, K. E. S.; Katz, T. J. *Angew. Chem. Int. Ed*. **2009**, *48*, 7837.

(f) Busson, B.; Kauranen, M.; Nuckolls, C.; Katz, T. J.; Persoons, A. *Phys. Rev. Lett*. **2000**, *84*, 79.

5. For selected articles of heterohelicene used as catalyst, see:

(a) Takenaka, N.; Sarangthem, R. S.; Captain, B. *Angew. Chem. Int. Ed*. **2008**, *47*, 9708.

(b) Takaneka, N.; Chen, J.; Captain, B.; Sarangthem, R. S.; Chandrakumar, A. *J. Am. Chem. Soc*. **2010**, *132*, 4536.

(c) Chen, J.; Captain, B.; Takenaka, N. *Org. Lett*. **2011**, *13*, 1654.

(d) Crittall, M. R.; Rzepa, H. S.; Carbery, D. R. *Org. Lett*. **2011**, *13*, 1250.

(e) Yamamoto, T.; Shimizu, T.; Igawa, K.; Tomooka, K.; Hirai, G.; Suemune, H.; Usui, K. *Sci. Rep*. **2016**, *6*, 36211.

(f) Magne, V.; Sanogo, Y.; Demmer, C. S.; Retailleau, P.; Marinetti, A.; Guinchard, X.; Voituriez, A. *ACS Catal*. **2020**, *10*, 8141.

6. For selected articles for biological applications of helicenes, see:
   (a) Nakagawa, H.; Yoshida, M.; Kobori, Y.; Yamada, K. *Chirality*, **2003**, *15*, 703.
   (b) Honzawa, S.; Okubo, H.; Anzai, S.; Yamaguchi, M.; Tsumoto, K.; Kumagai, I. *Bioorg. Med. Chem*. **2002**, *10*, 3213.
   (c) Nakagawa, H.; Kobori, Y.; Yoshida, M.; Yamada, K. *Chem. Commun*. **2001**, *24*, 2692.
   (d) Nakagawa, H.; Gomi, K.; Yamada, K. *Chem. Pharm. Bull*. **2001**. *49*, 49.
   (e) Nakagawa, H.; Yamada, K. *Chem. Pharm. Bull*. **2005**, *53*, 52.
   (f) Shinohara, K.; Sannohe, Y.; Kaieda, S.; Tanaka, K.; Osuga, H.; Tahara, H.; Xu, Y.; Kawase, T.; Bando, T.; Sugiyama, H. *J. Am. Chem. Soc*. **2010**, *132*, 3778.
   (g) Xu, Y.; Zhang, Y.-X.; Sugiyama, H.; Umano, T.; Osuga, H.; Tanaka, K. *J. Am. Chem. Soc*. **2004**, *126*, 6566.
7. For other examples of self-assembly of helicenes, see: ref. 4 and
   (a) Usui, K.; Yamamoto, K.; Ueno, Y.; Igawa, K.; Hagihara, R.; Masuda, T.; Ojida, A.; Karasawa, S.; Tomooka, K.; Hirai, G.; Suemune, H. *Chem. Eur. J*. **2018**, *24*, 14617.
   (b) Hirao, T.; Ono, Y.; Kawata, N.; Haino, T. *Org. Lett*. **2020**, *22*, 5294.
   (c) Nakano, K.; Oyama, H.; Nishimura, Y.; Nakasako, S.; Nozaki, K. *Angew. Chem. Int. Ed.* **2012**, *51*, 695.
   (d) Murguly, E.; McDonald, R.; Branda, N. R. *Org. Lett*. **2000**, *2*, 3169.
8. Abbate, B.; Bazzini, C.; Caronna, T.; Fontana, F.; Gambarotti, C.; Gangemi, F.; Longhi, G.; Mele, A.; Sora, I. N.; Panzeri, W. *Tetrahedron* **2006**, *62*, 139.
9. Talele, H. R.; Sahoo, S.; Bedekar, A. V. *Org. Lett*. **2012**, *14*, 3166.
10. Murase, T.; Suto, T.; Suzuki, H. *Chem. Asian J*. **2017**, *12*, 726.
11. For selected articles of catalytic asymmetric syntheses by chiral transition-metal catalysts, see:
   (a) Grandbois, A.; Collins, S. K. *Chem. Eur. J*. **2008**, *14*, 9323.
   (b) Nkamura, T.; Frumi, S.; Takeuchi, M; Shibuya, T.; Tanaka, K. *J. Am. Chem. Soc*. **2014**, *136*, 5555.
   (c) Sako, M.; Takeuchi, Y.; Tsujihara, T.; Kodera, J.; Kawano, T.; Takazawa, S.; Sasai, H. *J. Am. Chem. Soc*. **2016**, *138*, 11481.
   (d) Kinoshita, S.; Yamano, R.; Shibata, Y.; Tanaka, Y.; Hanada, K.; Matsumoto, T.; Miyamoto, K.; Muranaka, A.; Uchiyama, M.; Tanaka, K. *Angew. Chem. Int. Ed*. **2020**, *59*, 11020.

12. For our previous researches about axially chiral biaryl amino acid compound, see:
   (a) Furuta, T.; Yamamoto, J.; Kitamura, Y.; Hashimoto, A.; Masu, H.; Azumaya, I.; Kan, T.;

Kawabata, T. *J. Org. Chem*. **2010**, *75*, 7010.

(b) Furuta, T.; Nikaido, M.; Yamamoto, J.; Kuribayashi, T.; Kawabata, T. *Synthesis*, **2013**, *45*, 1312.

(c) Murai, T.; Xing, Y.; Kuribayashi, T.; Lu, W.; Guo, J.-D.; Yella, R.; Hamada, S.; Sasamori, T.; Tokitoh, N.; Kawabata, T.; Furuta, T. *Chem. Pharm. Bull*. **2018**, *66*, 1203.

13. Ferraccioli, R.; Grenzi, D.; Motti, E.; Catellani, M. *J. Am. Chem. Soc*. **2006**, *128*, 722.
14. Furuta, T.; Kitamura, Y.; Hashimoto, A.; Fujii, S.; Tanaka, K.; Kan, T. *Org. Lett*. **2007**, *9*, 183.
15. Liu, H.; Han, W.; Li, C.; Ma, Z.; Li, R.; Zheng, X.; Fu, H.; Chen, H. *Eur. J. Org. Chem*. **2016**, 389.
16. Fu, W. C.; Wang, Z.; Chan, W. T. K.; Lin, Z.; Kwong, F. Y. *Angew. Chem. Int. Ed*. **2017**, *56*, 7166.
17. Hayashi, T.; Iwamura, H.; Uozumi, Y.; Matumoto, Y.; Ozawa, F. *Synthesis*, **1994**, 526.
18. Nakano, K.; Hidehira, Y.; Takahashi, K.; Hiyama, T.; Nozaki, K. Angew. Chem. Int. Ed. 2005, 44, 7136.
19. Konishi, H.; Hoshino, F.; Manabe, K. *Chem. Pharm. Bull*. **2016**, *64*, 1438.
20. For chiral recognition and self-sorting of π-faces in helicenes with flexible π-core, see:
    (a) Amemiya, R.; Yamaguchi, M. Org. Biomol. Chem. 2008, 6, 26.
    (b) Safont-Sempere, M. M.; Osswald, P.; Stolte, M.; Grüne, M.; Renz, M.; Kaupp, M.; Radacki, K.; Braunschweig, H.; Würthner, F. J. Am. Chem. Soc. 2011, 133, 9580.
21. For amide tautomerization, see:
    (a) Forlani, L.; Cristoni, G.; Boga, C.; Todesco, P. E.; Vecchio, E. D.; Selva, S.; Monari, M. ARKIVOC, 2002, 198.
    (b) Schlegel, H. B.; Gund, P.; Fluder, E. M. J. Am. Chem. Soc. 1982, 104, 5347.
22. For selected examples of biological activity of phenanthridinone derivatives, see:
    (a) Shnyder, S. D.; Cooper, P. A.; Millington, N. J.; Gill, J. H.; Bibby, M. C. *Nat. Prod*. **2008**, *71*, 321.
    (b) Nakamura, M.; Aoyama, A.; Salim, T. A. *Bioorg. Med. Chem*. **2010**, *18*, 2420.
    (c) Patil, S.; Kamath, S.; Sanchez, T.; Neamati, N.; Schinazi, R. F.; Buolamwini, J. K. *Bioorg. Med. Chem*. **2007**, *15*, 1212.
    (d) Ishida, J.; Hattori, K.; Yamamoto, H.; Iwashita, A.; Mihara, K.; Matsuoka, N. *Bioorg. Med. Chem. Lett*. **2005**, *15*, 4221.
    (e) Grese, T. A.; Adrian, M. D.; Phillips, D. L.; Shelter, P. K.; Short, L. L. *J. Med. Chem*. **2001**, *44*, 2857.
    (f) Dow, R. L.; Chou, T. T.; Bechle, B. M.; Goddard, C.; Larson, E. R. *J. Med. Chem*. **1994**, *37*, 2224.

(h) Vangrevelinghe, E.; Zimmermann, K.; Schoepfer, J.; Portmann, R.; Fabbro, D.; Furet, P. *J. Med. Chem.* **2003**, *46*, 2656.

(i) Pierre, F.; Chua, P. C.; O'Brien, S. E.; Siddiqui-Jain, A.; Bourbon, P.; Haddach, M. *J. Med. Chem*. **2011**, *54*, 635.

(j) Pierre, F.; Stefan, E.; Nédellec, A.-S.; Chevrel, M.-C.; Regan, C. F.; Siddiqui-Jain, A. *Bioorg. Med. Chem. Lett*. **2011**, *21*, 6687.

(k) Antony, S.; Agama, K. K.; Miao, Z.-H.; Takagi, K.; Mollie, H.; Wright, M. H. *Cancer Res*. **2007**, *67*, 10397.

(l) Ruchelman, A. L.; Kerrigan, J. E.; Li, T.-K.; Zhou, N.; Liu, A.; Liu, L. F.; LaVoie, E. J. *Bioorg. Med. Chem*. **2004**, *12*, 3731.

(m) Lehtiö, L.; Jemth, A.-S.; Collins, R.; Loseva, O.; Johansson, A.; Markova, N. *J. Med. Chem*. **2009**, *52*, 3108.

23. For chalcogen-bonding function and pnictogen-bonding function, see:

(a) Cavallo, G.; Metrangolo, P.; Pilati, T.; Resnati, G.; Terraneo, G. *Cryst. Growth Des*. **2014**, *14*, 2697.

(b) Nagao, Y.; Hirata, T.; Goto, S.; Sano, S.; Kakehi. A.; Iizuka, K.; Shiro. M. *J. Am. Chem. Soc*. **1998**, *120*, 3104.

(c) Scilabra, P.; Terraneo, G.; Resnati, G. *Acc. Chem. Res*. **2019**, *52*, 1313.

(d) Brammer, L. *Faraday Discuss*. **2017**, *203*, 485.

(e) Abbenseth, J.; Goicoechea, J. M. *Chem. Sci*. **2020**, *11*, 9728.

24. Carpino, L. A.; Abdel-Maksoud, A. A.; Dumitru, L.; Mansour, E. M. E.; Zewail, M. A. *J. Org. Chem*. **2007**, *72*, 1729.

25. Krasodomski, W.; Łuczyn´ski, M. K.; Wilamowski, J.; Sepioł, J. J. *Tetrahedron*, **2003**, *59*, 5677.

26. Donati, L.; Leproux, P.; Prost, E.; Michel, S.; Tillequin, F.; Gandon, V.; Porée, F.-H. *Chem. Eur. J*. **2011**, *17*, 12809.

27. Yamamoto, Y.; Sakai, H.; Yuasa, J.; Araki, Y.; Wada, T.; Sakanoue, T.; Takenobu, T.; Kawai, T.; Hasobe, T. *J. Phys. Chem. C*, **2016**, *120*, 7421.

28. For articles of racemization study of helicene, see:

(a) Martin, R. H. *Angew. Chem., Int. Ed. Engl*. **1974**, *13*, 649.

(b) Meurer, K. P.; Vögtle, F. *Top. Curr. Chem*. **1985**, *127*, 1.

(c) Wynberg, H.; Groen, M. B. *J. Chem. Soc. D: Chem. Commun*. **1969**, 964.

(d) Yamada, K.; Nakagawa, H.; Kawazura, H. *Bull. Chem. Soc. Jpn*. **1986**, *59*, 2429.

(e) Lindner, H. J. *Tetrahedron*, **1975**, *31*, 281.

(f) Grimme, S.; Peyerimhoff, S. D. *Chem. Phys*. **1996**, *204*, 411.

(g) Johansson, M. P.; Patzschke, M. *Chem. -Eur. J*. **2009**, *15*, 13210.

(h) Janke, R. H.; Haufe, G.; Würthwein, E. U.; Borkent, J. H. *J. Am. Chem. Soc*. **1996**, *118*, 6031.

(i) Lebon, F.; Longhi, G.; Gangemi, F.; Abbate, S.; Priess, J.; Juza, M.; Bazzini, C.; Caronna, T.; Mele, A. *J. Phys. Chem. A*, **2004**, *108*, 11752.

29. Martin, R. H., Marchant, M. J. *Tetrahedron*, **1974**, *30*, 347.

Experimental Section

General Information

Melting points were measured by using a Yanagimoto micro melting point apparatus and BUCHI Melting Point M-565 and were uncorrected. NMR spectra were obtained with a JEOL ECX-400 PKT spectrometeror or JEOL ECA-600 spectrometer, chemical shift being given in ppm units (^{1}H NMR in $CDCl_3$: tetramethylsilane as internal standards, indicating 0, ^{13}C NMR in $CDCl_3$: $CDCl_3$ as internal standards, indicating 77.0) and spin-spin coupling constants being given in Hz units. IR spectra were recorded with a JASCO FT-IR 4200 spectrometer. The mass spectra (MS) and high-resolution mass spectra (HRMS) were recorded with a JEOL MStation JMS-700 spectrometer (for FAB) or Bruker Daltonics impact HD-KC (for ESI). Specific rotation was measured with JASCO P-2200 polarimeter.

Silica gel column chromatography was carried out by using Silica gel 60 N (spherical, neutral, 63 ~ 210 μm, Kanto Chemical Co., Inc.). TLC analysis and preparative TLC (PTLC) were performed on commercial glass plates bearing a 0.25 mm layer and 0.5 mm layer of Merck Kiesel–gel 60 F_{254}, respectively. Analytical HPLC was run with a JASCO PU-2089 Plus instrument, equipped with a Daicel CHIRALPAK IC (4.6 mm × 250 mm), or CHIRALPAK AD-H (4.6 mm × 250 mm) and a JASCO UV-2075 Plus UV/Vis detector (detection: 254 nm). Preparative HPLC was run with a JASCO PU-2086 Plus instrument, equipped with a COSMOSIL 5SL-II (20 mm × 250 mm) and a JASCO UV-2075 Plus UV/Vis detector (detection: 254 nm).

All chemical reagents were commercially purchased and used without further purification.

Chapter 2

Scheme S2-1. One-pot synthesis of 3-methoxyphenanthrene **9**

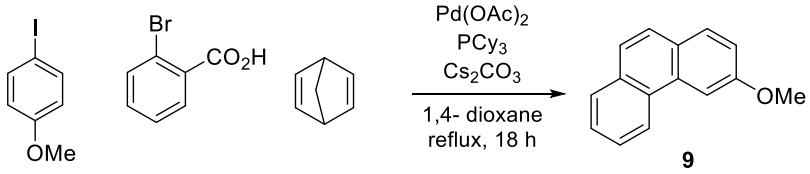

3-Methoxyphenanthrene (**9**)

Cs_2CO_3 (9.8 g, 30 mmol, 3.0 equiv.), 2-bromobenzoic acid (4.2 g, 20 mmol, 2.0 equiv.), $Pd(OAc)_2$ (115 mg, 0.5 mmol, 5mol%), PCy_3 (420 mg, 1.5 mmol, 15mol%), 4-iodoanisole (2.3 g, 10 mmol, 1.0 equiv.) and magnetic stir bar were loaded to a 500 mL flask. The flask was carefully evacuated and backfilled with Argon for three cycles. Norbornadiene (2.6 mL, 25 mmol, 2.5 equiv.) and 1,4-dioxane (200 mL) were added by syringe and the flask was placed into oil bath (130 °C) and stirred for 18 h. After completion of reaction, the reaction flask was allowed to reach rt. gradually. Then after filtration and the residue being washed by AcOEt, the collected filtrate was concentrated to obtain crude oil. The resulting oil was then diluted with AcOEt and washed sequentially with 1*N* aq. HCl, sat. aq. NH_4Cl and brine. The separated organic layer was dried over Na_2SO_4 and then filtered to collect the filtrate which was concentrated *in vacuo* to give crude product. The resulting crude product was purified by column chromatography (SiO_2, *n*-hexane) to furnish **9** (1.3 g, 64%).

The spectral data was identical to the literature data[1].

Scheme S2-2. Demethylation of 3-methoxyphenanthrene **9**

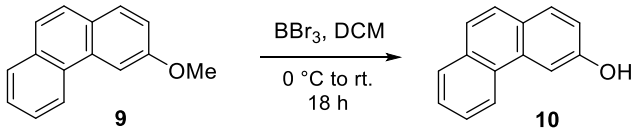

3-Phenanthrenol (**10**)

3-Methoxyphenanthrene **9** (1.3 g, 6.4 mmol, 1.0 equiv.) was dissolved in dry DCM (30 mL). The solution was chilled to 0 °C, and BBr_3 (12.8 mL, 12.8 mmol, 2.0 equiv.) was added dropwise. After finishing adding, the ice bath was removed and the resulting mixture was stirred at rt. for 18 h. The reaction was allowed to stopped until TLC showed a complete consume. MeOH (20 mL) was added to the reaction mixture to decompose excess BBr_3 while cooled to 0 °C. Next, the solvent was removed under reduced pressure. The resulting residue was finally purified by column chromatography (SiO_2, *n*-hexane : AcOEt = 9 : 1) to give target compound **10** (1.1 g, 86%).

The spectral data was identical to the literature data[2].

Scheme S2-3. Synthesis of diol (*dl*)-**11** by oxidative coupling

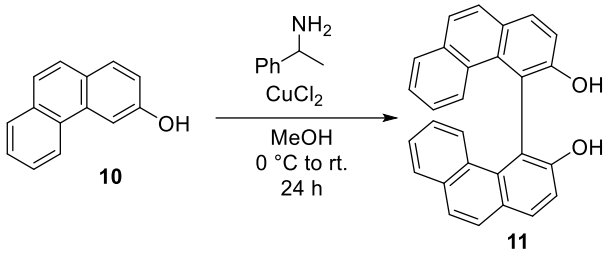

(*dl*)-4,4'-Bisphenanthryl-3,3'-diol (**11**)

A solution of 3-phenanthrenol **10** (1.1 g, 5.5 mmol, 1.0 equiv.) and $CuCl_2$ (1.5 g, 10.9 mmol, 2.0 equiv.) in degassed MeOH (30 mL) was stirred at Argon atmosphere at ice bath for 30 min. A solution of 1-phenylethylamine (5.6 mL, 43.7 mmol, 8.0 equiv.) in MeOH (20 mL) was added slowly over a period of 5 min under Argon protection at ice bath. The resulted solution was allowed to stir at rt. for 24 h until TLC showed a complete reaction. Then, the reaction mixture was cooled down to 0 °C and 6*N* aq. HCl was carefully added until the mixture turn to be clear solution. The resulting solution was quenched by water (50 mL) and then extracted by AcOEt (50 mL) for three times. The organic layers were combined and washed with sat. aq. NH_4Cl and brine. Next, the organic phase was dried over Na_2SO_4 and filtered to collect the filtrate which was concentrated *in vacuo* to obtain the crude product. The resulted crude product was further purified by column chromatography (SiO_2, *n*-hexane : AcOEt = 4 : 1) to give (*dl*)-**11** (0.9 g, 82%).

The spectral data was identical to the literature data[3].

Scheme S2-4. Optical resolution of diol (*dl*)-**11**

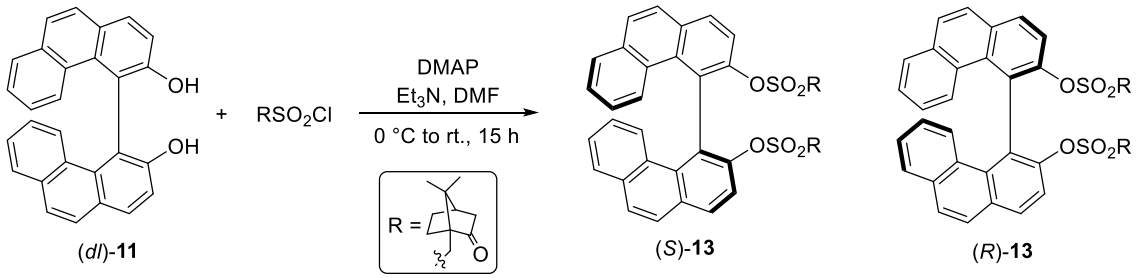

Synthesis of (*S*)- and (*R*)-3,3'-bis{[(1*S*,4*R*)-7,7-dimethyl-2-oxobicyclo[2.2.1]hept-1-yl]-methanesulfonyloxy}-4,4'-biphenanthryl [(*S*,*S*,*R*)-**13** and (*R*,*S*,*R*)-**13**].

A 30 mL flask was fitted with a 10 mL addition funnel containing a solution of (*1S*)-camphor-10-sulfonyl chloride (1.8 g, 7.0 mmol, 3.0 equiv.) in DMF (2.5 mL) was charged with dialcohol (*dl*)-**11** (0.9 g, 2.33 mmol, 1.0 equiv.), 4-(*N*, *N*-dimethylamino)pyridine (14.2 mg, 0.12 mmol, 5 mol%), triethylamine (5 mL), and DMF (2.5 mL). After a solution of acid chloride in DMF was slowly

added with stirring at ice bath, the resulted mixture was stirred at rt. for 15 h. The reaction was quenched with water, and then the organic layer was separated. After the aqueous layer was extracted with AcOEt (20 mL × 3), the combined organic layers were washed with water and brine, dried over Na_2SO_4, filtered and concentrated *in vacuo*. Purification of the crude residue by column chromatography (SiO_2, toluene : AcOEt = 10 : 1) gave (*R*,*S*,*R*)-**13** (930.5 mg, 49%), and (*S*,*S*,*R*)-**13** (892.5 mg, 47%).

Absolute configurations of (*S*,*S*,*R*)-**13** and (*R*,*S*,*R*)-**13** were identified by the reported ^{1}H NMR data[3].

Scheme S2-5. Hydrolysis of disulfonate (*S*,*S*,*R*)-**13**

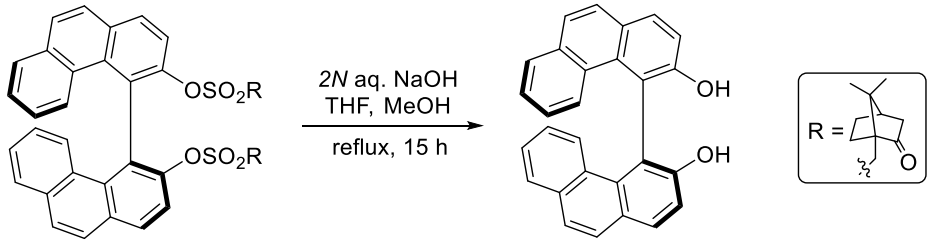

(*S*)-**13** (*S*)-**11**

(*S*)-4,4'-Biphenanthryl-3,3'-diol (**11**)

A 30 mL round bottom flask fitted with reflux condenser was charged with (*S*)-**13** (892.5 mg, 1.1 mmol), THF (7 mL), MeOH (3 mL) and 2 *N* aq. NaOH (3 mL). The reaction mixture was refluxed for 15 h. The whole mixture was cooled to r.t. and concentrated under reduced pressure to remove most of THF and MeOH. The resulting mixture was diluted by water and then acidified with 1 *N* aq. HCl. The aqueous phase was extracted by AcOEt three times (10 mL), and the combined organic layers were then washed by water and brine. Then organic layer was dried over Na_2SO_4, filtered, and concentrated under reduced pressure. Purification of the crude residue by column chromatography (SiO_2, AcOEt : *n*-hexane = 1 : 2) gave (*S*)-**11** (402 mg, 97%, >99% ee).

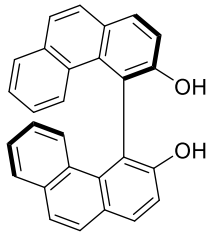

(*R*)-**11**

Optically pure (*R*)-**11** (97% yield) was obtained as the same procedure of hydrolysis of (*R,S,R*)-**13**.

Scheme S2-6. Preparation of triflate from diol (*dl*)-**11**

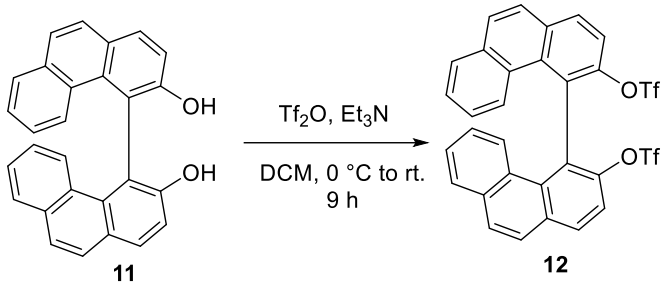

11 **12**

(*dl*)-3,3'-Bis(trifluoromethanesulfonyloxy)-4,4'-biphenanthryl (**12**)

A mixture of (*dl*)-diol **11** (403.8 mg, 1.0 mmol, 1.0 equiv.) and pyridine (0.4 mL, 5.0 mmol, 5.0 equiv.) in DCM (10 mL) was placed in a 50 mL flask at ice bath. To this solution was added trifluoromethanesulfonic acid anhydride (0.7 mL, 4.0 mmol, 4.0 equiv.) at ice bath. After the reaction mixture was stirred at rt. for 9 h, AcOEt (30 mL) was added. The resulted mixture was washed with 1*N* aq. HCl (30 mL) twice, sat. aq. $NaHCO_3$ and brine. The organic layer was separated and dried over Na_2SO_4, filtered and evaporated *in vacuo* to obtain crude residue. The resulted residue was purified by column chromatography (SiO_2, *n*-hexane : AcOEt = 4 : 1) to give a colorless solid (*dl*)-**12** (552 mg, 85%).

The spectral data was identical to the literature data[4].

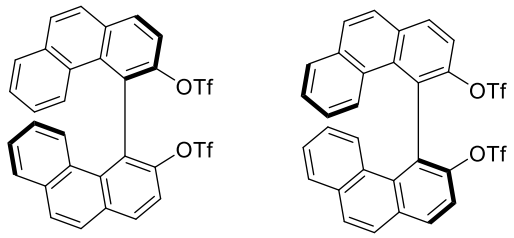

(*R*)-**12** (*S*)-**12**

Synthesis of optically pure **12** by the substitution of corresponding optically pure **11** was as same as racemic form.

(*R*)-**12**, 77% yield; (*S*)-**12**, 83% yield.

Scheme S2-7. Preparation of phenyl formate

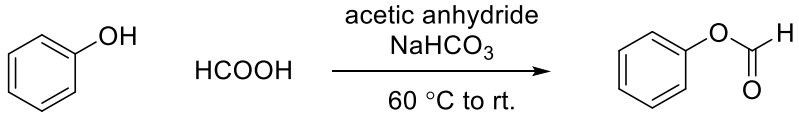

Phenyl formate

Formic acid (16.2 mL, 420.8 mmol, 10.0 equiv.) was added to acetic anhydride (32.0 mL, 328.4 mmol, 7.8 equiv.) at rt. The resulted mixture was stirred at 60 °C for 1 h and was cooled to rt. Phenol (4.0 g, 42.2 mmol, 1.0 equiv.) and $NaHCO_3$ (7.2 g, 84.8 mmol, 2.0 equiv.) were added to the solution, and the mixture was stirred for about 4 h until starting material was consumed. The reaction was quenched adding a mixture of DCM (50 mL) and water (100 mL), and the biphasic system was stirred vigorously. The organic phase was separated, and the aqueous phase was extracted with DCM (50 mL) twice. The combined organic phases were washed with water (3 × 100 mL) and brine (100 mL), and dried over Na_2SO_4. The solvent was removed under reduced pressure for giving a resulting residue which was purified by column chromatography (SiO_2, *n*-hexane : AcOEt = 95 : 5) to afford phenyl formate as colorless oil (4.02 g, 78%).

The spectral data was identical to the literature data[5].

Scheme S2-8. Esterification of ditriflate (*dl*)-**12**

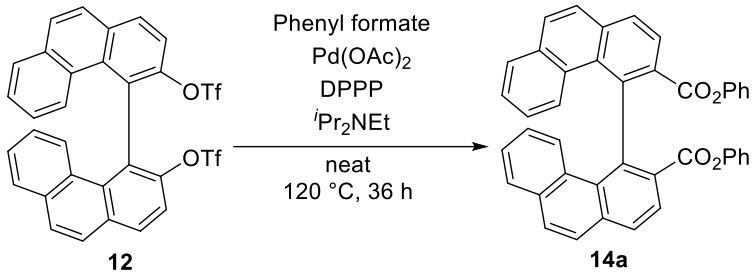

(*dl*)-Diphenyl 4,4'-biphenanthryl-3,3'-dicarboxylate (**14a**)

(*dl*)-Ditriflate **12**[10] (552 mg, 0.85 mmol. 1.0 equiv.), $Pd(OAc)_2$ (19 mg, 0.085 mmol, 10 mol%) and DPPP (53 mg, 0.128 mmol, 15 mol%) were added to a screw-capped 30 mL reaction tube containing a magnetic stirring bar. The tube was evacuated and backfilled with Argon for three times. Phenyl formate (762 µL, 6.79 mmol, 8.0 equiv.) and DIPEA (1.8 mL, 10.2 mmol, 12 equiv.) were added to the tube under a flow of Argon and the tube was equipped with a screw cap. The reaction mixture was heated to 120 °C in an oil bath and stirred for 36 h. The reaction mixture was cooled to rt. and diluted with CH_2Cl_2, washed with water and brine, dried over Na_2SO_4, filtered and concentrated *in vacuo* to give a residue. The resulted residue was purified by column chromatography (SiO_2, *n*-hexane : AcOEt = 5 : 1) to afford (*dl*)-**14a** (170 mg, 34%).

Colorless prisms (*n*-hexane–AcOEt); m.p. 229–230 ºC;

^{1}H NMR (400 MHz, $CDCl_3$) δ 8.20 (d, *J* = 8.2 Hz, 2H), 8.12 (d, *J* = 8.2 Hz, 2H), 7.87 (d, *J* = 9.2 Hz, 4H), 7.84–7.81 (m, 2H), 7.66 (d, *J* = 8.7 Hz, 2H), 7.37 (t, *J* = 7.1 Hz, 2H), 7.15–7.11 (m, 4H), 7.03 (t, *J* = 7.3 Hz, 2H), 6.95–6.91 (m, 2H), 6.40–6.37 (m, 4H);

^{13}C NMR (100 MHz, $CDCl_3$) δ 166.4, 150.4, 140.6, 136.0, 133.7, 130.8, 130.2, 130.1, 129.9, 129.4, 129.0, 128.9, 127.6, 127.2, 126.8, 126.6, 126.3, 125.4, 121.1;

IR (neat) 3057, 1750, 1725, 1587, 1495, 1260, 1189, 1161, 1120, 1049, 1024, 921, 841, 746 cm^{-1}.;

HRMS (ESI) *m/z* calcd for $C_{42}H_{26}NaO_4$ $(M+Na)^+$ 617.1723, found. 617.1721.

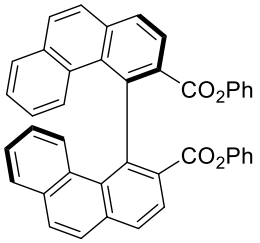

(*R*)-**14a**

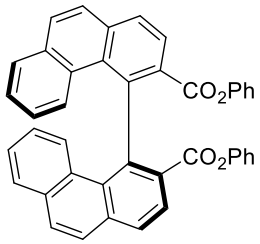

(*S*)-**14a**

Synthesis of optically pure **14a** by the esterification of corresponding optically pure **12** was as same as racemic form.

(*R*)-**14a**, 34% yield, m.p. 84–85 °C, $[\alpha]_D^{22}$ = –125.8 (c = 0.46, $CHCl_3$); (*S*)-**14a**, 32% yield.

Scheme S2-9. Hydrolysis of diester (*dl*)-**14a**

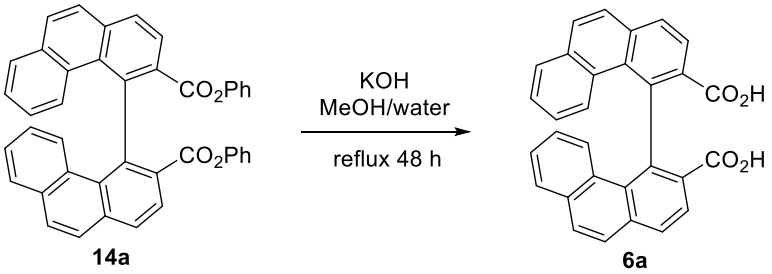

14a **6a**

(*dl*)-4,4'-Biphenanthryl-3,3'-dicarboxylic acid (**6a**)

To a solution of (*dl*)-dicarboxylic acid **14a** (170 mg, 0.29 mmol, 1.0 equiv.) dissolved in MeOH (20 mL) was added the solution of KOH (651 mg, 11.6 mmol, 40 equiv.) in water (5.0 mL). The resulting mixture was allowed to stir for 48 h under reflux conditions. The resulting mixture was concentrated under reduced pressure to remove solvent, giving crude residue. Then the residue was dissolved in water (50 mL). The aqueous phase was washed by Et_2O (10 mL), and then the aqueous phase was acidified by 6.0 M aq. HCl until the pH turn to be 1~2. The resulting suspension was extracted by AcOEt (15 mL) for three times. The combined organic layer was washed with H_2O, brine, and dried over Na_2SO_4, filtered, and evaporated *in vacuo* to give (*dl*)-**6a** (108 mg, 82%).

Colorless prisms (AcOEt); m.p. 264–265 ºC;

^{1}H NMR (400 MHz, acetone-d_6) δ 8.11 (d, *J* = 8.2 Hz, 2H), 7.99 (d, *J* = 8.2 Hz, 2H), 7.85 (d, *J* = 9.2 Hz, 2H), 7.74 (d, *J* = 8.7 Hz, 2H), 7.67 (d, *J* = 7.8 Hz, 2H), 7.20–7.10 (m, 4H), 6.65 (q, *J* = 8.2 Hz, 2H);

^{13}C NMR (100 MHz, acetone-d_6) δ 169.3, 142.0, 136.8, 134.8, 132.4, 132.2, 131.0, 130.6, 130.3, 130.0, 128.6, 128.4, 127.6, 127.3, 126.8;

IR (neat) 3050, 1696, 1592, 1556, 1517, 1419, 1375, 1317, 1269, 1227, 1201, 1170, 1068, 1008, 888, 867, 849, 745 cm^{-1};

HRMS (EI) *m/z* calcd for $C_{30}H_{18}O_4$ $(M)^+$ 442.1205, found. 442.1208.

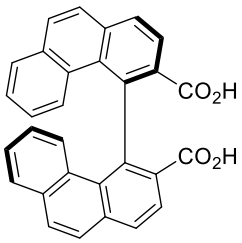

(*R*)-**6a**

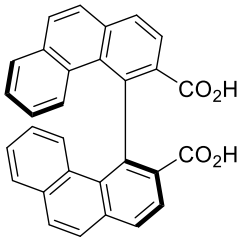

(*S*)-**6a**

Synthesis of optically pure **6a** by hydrolysis of corresponding optically pure diester **14a** was as same as racemic form.

(*R*)-**6a**, 87% yield, m.p. 250–251 °C, $[\alpha]_D^{22}$ = –44.2 (c = 0.59, acetone); (*S*)-**6a**, 84% yield.

Scheme S2-10. Selective monomethylation of dicarboxylic acid (*dl*)-**6a**

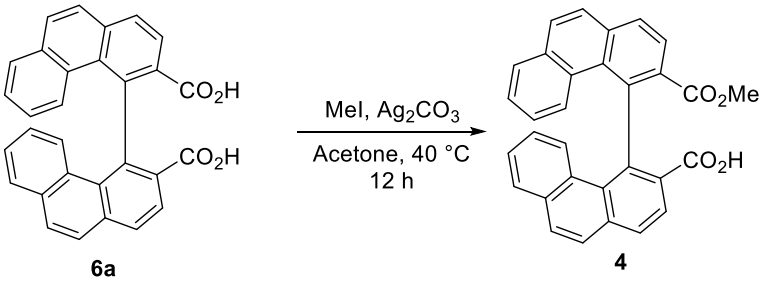

6a **4**

(*dl*)-3'-(Methoxycarbonyl)-4,4'-biphenanthrene-3-carboxylic acid (**4**)

To a solution of (*dl*)-dicarboxylic acid **6a** (108 mg, 0.24 mmol, 1.0 equiv.), and Ag_2CO_3 (33 mg, 0.12 mmol, 0.5 equiv.) in acetone (5.0 mL) was added MeI (45 μL, 0.72 mmol, 3.0 equiv.) at rt. After stirring at 40 °C for 12 h, the reaction was diluted by water (20 mL) and quenched with 1*N* aq. HCl (5.0 mL), and extracted with AcOEt (10 mL) for three times. The combined organic layer was washed with water, brine, and dried over Na_2SO_4, filtered and evaporated *in vacuo* to give a residue, which was purified by column chromatography (SiO_2, *n*-hexane : AcOEt : AcOH = 100 : 100 : 1) to afford (*dl*)-**4** (60 mg, 54%).

Colorless prisms (AcOEt); m.p. 265–266 ºC;

^{1}H NMR (400 MHz, $CDCl_3$) δ 8.12–8.01 (m, 3H), 7.91 (d, *J* = 8.2 Hz, 1H), 7.87–7.77 (m, 6H), 7.51 (d, *J* = 8.7 Hz, 1H), 7.43 (d, *J* = 8.7 Hz, 1H), 7.36–7.32 (m, 2H), 6.90–6.83 (m, 2H), 3.19 (d, *J* = 15.6 Hz, 3H);

^{13}C NMR (100 MHz, $CDCl_3$) δ 170.7, 169.4, 140.4, 139.7, 135.9, 135.7, 133.7, 133.6, 130.9, 130.6, 130.2, 130.1, 130.0, 129.7, 129.5, 129.4, 129.0, 128.9, 127.4, 127.12, 127.09, 126.8, 126.7, 126.59, 126.56, 126.54, 126.34, 126.29, 52.1 (Two carbon signals were overlapped.);

IR ($CHCl_3$) 3426, 1691, 1542, 1383, 1266, 1058, 745 cm^{-1};

HRMS (FAB) *m/z* calcd for $C_{31}H_{20}O_4$ $(M)^+$ 456.1362, found 456.1362.

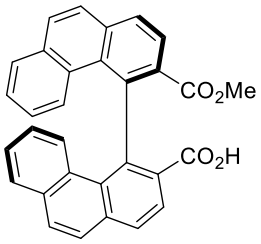

(*R*)-**4**

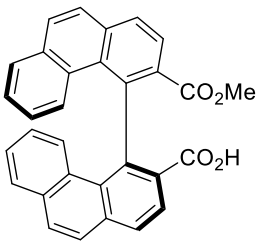

(*S*)-**4**

Synthesis of optically pure **4** by monomethylation of corresponding dicarboxylic acid **6a** was as same as racemic form.

(*R*)-**4**, 40% yield, m.p. 252–253 °C, $[\alpha]_D^{22}$ = –79.8 (c = 0.11, $CHCl_3$); (*S*)-**4**, 43% yield.

Scheme S2-11. Intramolecular cyclization to amide-functionalized [7]helicene-like molecule (*dl*)-**1a** from monomethyl ester (*dl*)-**4**

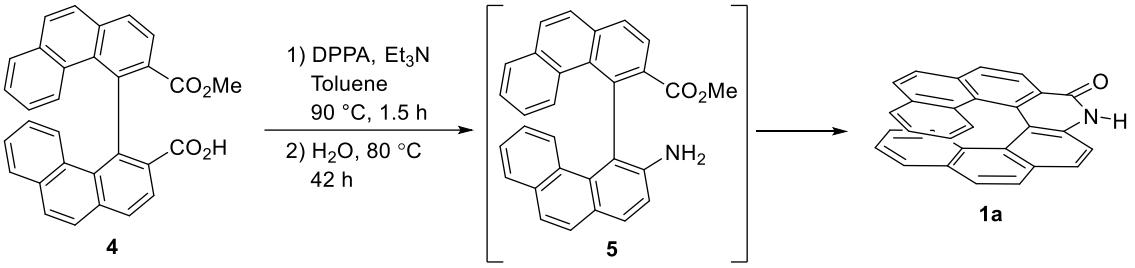

(*dl*)-Amide-functionalized [7]helicene-like molecule (**1a**)

To a solution of monomethyl ester (*dl*)-**4** (25 mg, 55 μmol, 1.0 equiv.) in toluene (2.0 mL) were added DPPA (17 μL, 77 μmol, 1.4 equiv.) and Et_3N (13 μL, 0.17 mmol, 3.0 equiv.) at 0 °C under argon atmosphere. Then, the mixture was stirred for 1.5 h at 90 °C. After cooling to rt., the mixture was treated with H_2O (1.0 mL) and then the resulted solution was stirred at 80 °C for 42 h. Then the reaction was extracted with EtOAc (5.0 mL) for three times. The combined organic layer was dried over Na_2SO_4, filtered, and evaporated *in vacuo* to give the crude product. The crude product

was purified by column chromatography (SiO_2, *n*-hexane : AcOEt = 3 : 1) to afford (*dl*)-**1a** (11 mg, 51%).

Yellow prisms (*n*-hexane-AcOEt); m.p. >300 °C;
^{1}H NMR (400 MHz, DMSO-d_6) δ 12.23 (s, 1H), 8.43 (d, *J* = 8.2 Hz, 1H), 8.13 (d, *J* = 8.2 Hz, 1H), 8.07 (d, *J* = 8.7 Hz, 1H), 7.88 (d, *J* = 8.7 Hz, 1H), 7.76–7.69 (m, 3H), 7.49 (d, *J* = 8.7 Hz, 1H), 7.42 (d, *J* = 7.3 Hz, 1H), 7.36 (d, *J* = 7.8 Hz, 1H), 7.05 (d, *J* = 8.7 Hz, 1H), 6.99–6.92 (m, 2H), 6.84 (d, *J* = 8.2 Hz, 1H), 6.40–6.30 (m, 2H);
^{13}C NMR (100 MHz, DMSO-d_6) δ 161.9, 136.8, 134.6, 132.5, 132.3, 132.0, 131.1, 129.8, 129.5, 129.1, 128.8, 128.7, 128.3, 127.5, 127.44, 127.39, 126.7, 126.4, 126.3, 126.25, 126.19, 125.9, 124.2, 124.10, 124.06, 123.4, 116.8, 111.9 (One carbon signal was overlapped.);
IR ($CHCl_3$) 3049, 2872, 1657, 1603, 794, 719 cm^{-1};
HRMS (FAB) *m/z* calcd for $C_{29}H_{18}NO$ $(M+H)^+$ 396.1373, found 396.1388.

Crystallographic data for the single crystal of racemic **1a** obtained by recrystallization from toluene and *n*-hexane: $C_{29}H_{17}NO$, M = 395.43, monoclinic, $P2_1$, a = 9.0465(2), b = 11.3071(3), c = 19.1900(5) Å, α = 90°, β = 95.411(2)°, γ = 90°, V = 1954.19(8) Å^3, Z = 4, ρ_{calcd} = 1.317 gcm^{-3}, T = 103 K, 22156 reflections measured, 7194 unique. The final R_1 and *wR* were 0.0587 and 0.1787 (all data). These data have been deposited with the Cambridge Crystallographic Data Center as CCDC 2031916.

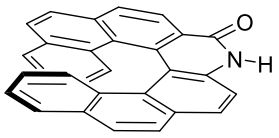

(*M*)-**1a**

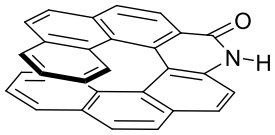

(*P*)-**1a**

(*M*)- and (*P*)-**1a** were prepared by intramolecular cyclization of monomethyl ester (*R*)- and (*S*)-**4** in 53% and 48%, respectively, according to the same procedure as racemic form.
(*M*)-**1a**, >99% ee, 53% yield, m.p. >300 °C; $[\alpha]_D^{18}$ = +1954.5 (c = 0.2, DMSO); CD λ_{ext} (THF) nm (Δε): 356 (55.01), 330 (93.66), 319 (87.21), 256 (–193.38), 212 (139.71). UV λ_{max} (THF) nm (log ε): 310sh (4.26), 263 (4.64), 225sh (4.97).
(*P*)-**1a**, >98% ee, 48% yield, m.p. >300 °C; $[\alpha]_D^{19}$ = +1660 (c = 0.1, $CHCl_3$); CD λ_{ext} (THF) nm (Δε): 356 (–56.64), 330 (–96.89), 319 (–90.88), 256 (186.7), 213 (–142.84).

Scheme S2-12. Isolation of amine intermediate (*dl*)-**5** during intramolecular cyclization towards (*dl*)-**1a**

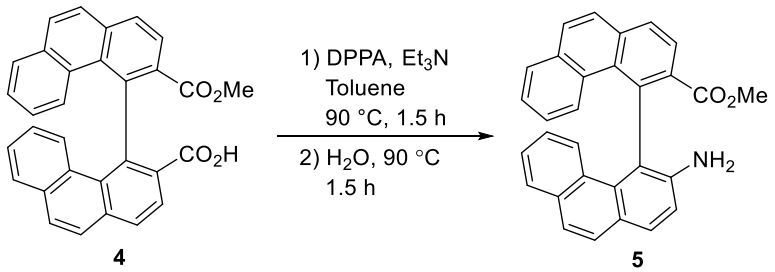

4 **5**

(*dl*)-methyl 3'-amino-[4,4'-biphenanthrene]-3-carboxylate (**5**)

To a solution of monomethyl ester (*dl*)-**4** (25 mg, 55 μmol, 1.0 equiv.) in toluene (2.0 mL) were added DPPA (17 μL, 77 μmol, 1.4 equiv.) and Et_3N (13 μL, 0.17 mmol, 3.0 equiv.) at 0 °C under argon atmosphere. Then, the mixture was stirred for 1.5 h at 90 °C. Then, H_2O (1.0 mL) was added, the reaction was stopped after stirring at 90 °C for another 1.5 h. After cooling to rt, the mixture was quenched with 1*N* aq. HCl (5 mL). Then the reaction was extracted with AcOEt (5.0 mL) for three times. The combined organic layer was dried over Na_2SO_4, filtered, and evaporated *in vacuo* to give the crude product. The crude product was purified by column chromatography (SiO_2, *n*-hexane : AcOEt = 3 : 1) to afford (*dl*)-**5** (15 mg, 64%).

Green prisms (n-hexana-AcOEt); m.p. > 300 °C;

^{1}H NMR (400 MHz, $CDCl_3$) δ 8.48 (d, *J* = 8.7 Hz, 1H), 8.17–8.00 (m, 1H), 7.97–7.81 (m, 5H), 7.78–7.69 (m, 2H), 7.67–7.62 (m, 1H), 7.57–7.52 (m, 1H), 7.45 (t, *J* = 7.6 Hz, 1H), 7.30–7.26 (m, 1H), 7.10–6.99 (m, 2H), 6.86–6.79 (m, 1H), 3.41 (s, 2H), 3.00 (s, 3H);

^{13}C NMR (100 MHz, $CDCl_3$) δ 169.1, 143.2, 137.3, 135.6, 134.0, 133.4, 133.2, 131.2, 130.7, 130.5, 130.4, 129.9, 129.5, 129.3, 128.9, 128.4, 127.5, 127.4, 127.2, 127.1, 126.6, 125.9, 125.5, 125.2, 124.3, 121.2, 117.2, 51.8 (Two carbon signals were overlapped.);

IR (neat) 3470, 2960, 2853, 1730, 1603, 1157, 1129, 842, 798, 746 cm^{-1};

HRMS (ESI) *m/z* calcd for $C_{30}H_{22}NO_2$ $(M+H)^+$ 428.1645, found. 428.1633.

Chapter 3

Optimization of reaction conditions for direct one-pot cyclization to phenanthridinone 1d

Scheme S3-1. Preparation of biaryl dicarboxylic acid

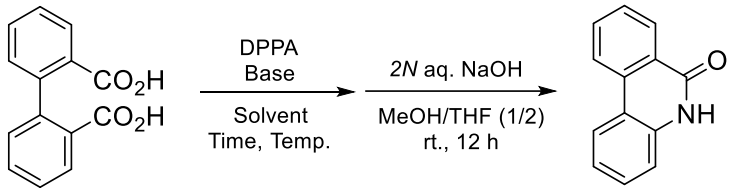

6d **1d**

General procedure for synthesis of phenanthridinone **1d** by one-pot cyclization

To a solution of diphenic acid **6d** (24.2 mg, 0.1 mmol, 1.0 equiv.) in dry solvent (5.0 mL), DPPA and base were added at rt. under Argon atmosphere. Then, the mixture was stirred and heated for scheduled time. After cooling to rt, the mixture was concentrated *in vacuo* to obtain the residue. Next, the crude residue was dissolved in the mixed solvent of MeOH/THF (3 mL/6mL) and 2*N* aq. NaOH (0.5 mL, 1.0 mmol, 10.0 equiv.) was added. The resulted mixture was allowed to stir at rt. for 12 h. The resulted mixture was concentrated and then diluted with AcOEt (10 mL). The organic phase was washed with water (5 mL) for three times and brine (5 mL), and the resulted organic layer was dried over Na_2SO_4 and then filtered to collect the filtrate which was concentrated *in vacuo* to obtain the crude product. Finally the crude product was purified by column chromatography (SiO_2, *n*-hexane : AcOEt = 3 : 2) to afford phenanthridinone **1d**.

Scheme S3-2. Scale-up reaction to synthesize **1d** with optimized conditions

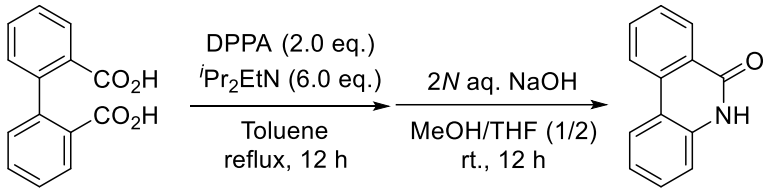

6d **1d**

To a solution of diphenic acid **6d** (2.0 g, 8.26 mmol, 1.0 equiv.) in toluene (60 mL), DPPA (3.6 mL, 16.5 mmol, 2.0 equiv.) and DIPEA (8.7 mL, 49.6 mmol, 6.0 equiv.) were added at rt. under Argon atmosphere. Then, the mixture was stirred and heated for 12 h. After cooling to rt., the mixture was concentrated *in vacuo* to obtain the residue. Next, the crude residue was dissolved in the mixed solvent of MeOH/THF (30 mL/60 mL) and 2*N* aq. NaOH (41 mL, 82.6 mmol, 10.0 equiv.) was added. The resulted mixture was allowed to stir at rt. for 12 h. The resulted mixture was concentrated and then diluted with AcOEt (50 mL). The organic phase was washed with 1*N* aq. HCl (30 mL) for three times, water (50 mL) and brine (20 mL), and the resulted organic layer was dried over Na_2SO_4 and then filtered to collect the filtrate which was concentrated *in vacuo* to

obtain the crude product. The crude product was washed by mixture of $CHCl_3$: *n*-hexane (1 : 1). Finally the preliminarily purified product was further purified by column chromatography (SiO_2, *n*-hexane : AcOEt = 1 : 1) to afford phenanthridinone **1d** (1.3 g, 80%).

The spectral data was identical to the literature data[6].

Scheme S3-3. Preparation of dicarboxylic acid **6**

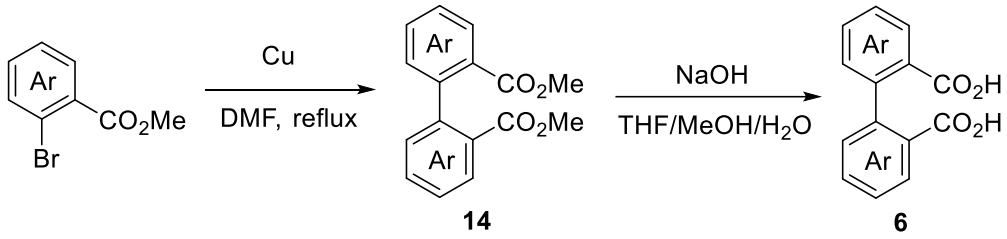

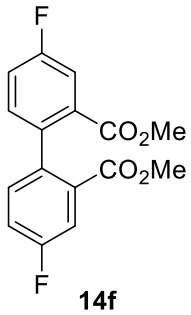

14f

Dimethyl 4,4'-difluoro-[1,1'-biphenyl]-2,2'-dicarboxylate (**14f**)

A solution of methyl 2-bromo-5-fluorobenzoate (3.16 g, 13.6 mmol, 1.0 equiv.) and Cu powder (6.89 g, 108 mmol, 8.0 equiv.) in DMF (10 mL) was refluxed under N_2 atmosphere for 16 h. After the reaction was cooled to rt, the mixture was added H_2O and extracted with $CHCl_3$. The organic layer was washed with brine and dried over Na_2SO_4, filtered and concentrated *in vacuo* to give a residue. The residue was purified by column chromatography (SiO_2, *n*-hexane : AcOEt = 9 : 1) to afford **14f** (1.85 g, 89%).

Colorless oil.

^{1}H NMR (300 MHz, $CDCl_3$) δ 7.71 (dd, J = 9.3, 2.8 Hz, 2H), 7.20–7.30 (m, 2H), 7.15 (dd, J = 8.4, 5.5 Hz, 2H), 3.66 (s, 6H);

^{13}C NMR (75 MHz, $CDCl_3$) δ 166.2 (d, J = 2.3 Hz), 161.7 (d, J = 246 Hz), 138.3 (d, J = 3.8 Hz), 132.1 (d, J = 7.5 Hz), 131.2 (d, J = 7.5 Hz), 118.8 (d, J = 21 Hz), 117.0 (d, J = 23 Hz), 52.3;

IR (neat) 1718, 1479, 1436, 1238, 1185, 1069, 980, 826, 787, 753 cm^{-1};

HRMS (EI) *m/z* calcd for $C_{16}H_{12}F_2O_4$ $(M)^+$ 306.0704, found. 306.0707.

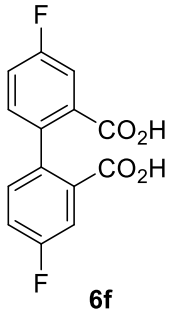

6f

4,4’-Difluoro-[1,1’-biphenyl]-2,2’-dicarboxylic acid (**6f**)

To a solution of **14f** (1.75 g, 5.71 mmol) in THF/MeOH (2 : 1, 30 mL), 2*N* aq. NaOH (10 mL) was added at rt. After being stirred at rt. for 68 h, the reaction mixture was washed with CPME. The aqueous layer was acidified with 2*N* aq. HCl, and extracted with AcOEt. The organic layer was washed with brine, dried over Na_2SO_4, filtered and concentrated *in vacuo* to give **6f** (1.51 g, 95%). This dicarboxylic acid was used for one-pot cyclization reaction without further purification.

White solid; m.p. 240–241 ºC;

^{1}H NMR (500 MHz, acetone-d_6) δ 11.22 (s, 2H), 7.74 (dd, J = 9.6, 2.9 Hz, 2H), 7.39–7.35 (m, 2H), 7.29 (dd, J = 8.5, 5.5 Hz, 2H);

^{13}C NMR (125 MHz, acetone-d_6) δ 166.7 (d, J = 2.5 Hz), 162.4 (d, J = 244 Hz), 139.9 (d, J = 3.8 Hz), 133.5 (d, J = 7.5 Hz), 132.8 (d, J = 7.5 Hz), 119.0 (d, J = 21 Hz), 117.3 (d, J = 24 Hz);

IR (neat) 2851, 1707, 1421, 1250, 1201, 929, 885, 825, 758, 517 cm^{-1};

HRMS (EI) *m/z* calcd for $C_{14}H_8F_2O_4$ $(M)^+$ 278.0391, found. 278.0394.

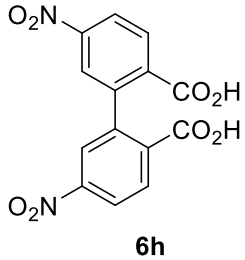

6h

5,5’-Dinitro-[1,1'-biphenyl]-2,2'-dicarboxylic acid (**6h**)

To a solution of **14h**[7] (2.87 g, 7.96 mmol) in THF/MeOH (1 : 1, 80 mL), 1*N* aq. NaOH (40 mL) was added at rt. After being stirred at rt. for 72 h, the reaction mixture was washed with CPME. The aqueous layer was acidified with conc. HCl, and extracted with AcOEt. The organic layer was washed with brine, dried over Na_2SO_4, filtered and concentrated *in vacuo* to give the residue. The residue was recrystallized from acetone/ *n*-hexane to give **6h** (2.26 g, 85%).

Yellow solid; m.p. 266–267 ºC;

^{1}H NMR (300 MHz, DMSO-d_6) δ 8.39 (dd, *J* = 2.4, 8.4 Hz, 2H), 8.22 (d, *J* = 8.4 Hz, 2H), 8.16 (d, *J* = 2.4 Hz, 2H);

^{13}C NMR (75 MHz, DMSO-d_6) δ 167.1, 149.7, 143.1, 136.9, 132.1, 125.9, 123.8;

IR (neat) 3430, 3092, 2642, 1711, 1682, 1527, 1352, 1296, 1256, 806, 742 cm^{-1};

HRMS (ESI-) m/z calcd for $C_{14}H_7N_2O_8$ $(M-H)^+$ 331.0208, found. 331.0207.

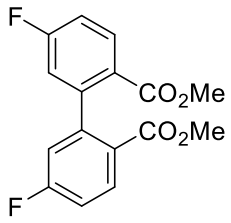

14i

Dimethyl 5,5'-difluoro-[1,1'-biphenyl]-2,2'-dicarboxylate (**14i**)

A solution of methyl 2-bromo-4-fluorobenzoate (5.56 g, 23.9 mmol, 1.0 equiv.) and Cu powder (12.1 g, 191 mmol, 8.0 equiv.) in DMF (10 mL) was refluxed under N_2 atmosphere for 16 h. After the reaction was cooled to rt., the mixture was added H_2O and extracted with $CHCl_3$. The organic layer was washed with brine and dried over Na_2SO_4, filtered and concentrated *in vacuo* to give a residue. The residue was purified by column chromatography (SiO_2, *n*-hexane : AcOEt = 4 : 1) to afford **14i** (2.79 g, 76%).

Colorless oil.

^{1}H NMR (300 MHz, $CDCl_3$) δ 8.07 (dd, *J* = 8.8, 5.8 Hz, 2H), 7.05–7.20 (m, 2H), 6.90 (dd, *J* = 9.0, 2.6 Hz, 2H), 3.64 (s, 6H);

^{13}C NMR (75 MHz, $CDCl_3$) δ 166.1, 164.4 (d, *J* = 253 Hz), 145.4 (dd, *J* = 9.0, 1.5 Hz), 132.8 (d, *J* = 9.0 Hz), 125.4 (d, *J* = 3.0 Hz), 117.3 (d, *J* = 22 Hz), 114.7 (d, *J* = 21 Hz), 52.1;

IR (KBr) 1719, 1578, 1434, 1252, 1100, 873, 844, 778, 699, 602 cm^{-1};

HRMS (EI) *m/z* calcd for $C_{16}H_{12}F_2O_4$ $(M)^+$ 306.0704, found. 306.0707.

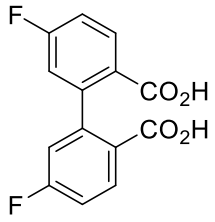

6i

5,5'-Difluoro-[1,1'-biphenyl]-2,2'-dicarboxylic acid (**6i**)

To a solution of **14i** (2.71 g, 8.85 mmol) in THF/MeOH (2 : 1, 30 mL), 2*N* aq. NaOH (10 mL) was added at rt. After being stirred at rt. for 67 h, the reaction mixture was washed with CPME. The aqueous layer was acidified with 2*N* aq. HCl, and extracted with AcOEt. The organic layer was washed with brine, dried over Na_2SO_4, filtered and concentrated *in vacuo* to give **6i** (2.37 g, 96%). This dicarboxylic acid was used for one-pot cyclization reaction without further purification.

White solid; m.p. 236–237 ºC;

^{1}H NMR (500 MHz, acetone-d_6) δ 11.02 (s, 2H), 8.13 (dd, J = 8.7, 6.0 Hz, 2H), 7.29–7.14 (m, 2H), 7.04 (dd, J = 9.5, 2.6 Hz, 2H);

^{13}C NMR (125 MHz, acetone-d_6) δ 166.7, 165.0 (d, J = 250 Hz), 146.8 (dd, J = 10, 1.3 Hz), 133.8 (d, J = 10 Hz), 126.9 (d, J = 2.5 Hz), 117.9 (d, J = 23 Hz), 114.9 (d, J = 21 Hz);

IR (neat) 2815, 1675, 1575, 1403, 1253, 1211, 887, 838, 785, 603 cm^{-1};

HRMS (EI) *m/z* calcd for $C_{14}H_8F_2O_4$ $(M)^+$ 278.0391, found. 278.0393.

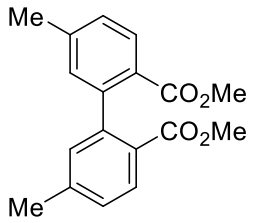

14j

Dimethyl 5,5'-dimethyl-[1,1'-biphenyl]-2,2'-dicarboxylate (**14j**)

A solution of methyl 2-bromo-4-methylbenzoate (2.09 g, 9.12 mmol, 1.0 equiv.) and activated Cu (4.64 g, 73.0 mmol, 8.0 equiv.) in DMF (10 mL) was refluxed under N_2 atmosphere for 63 h. After the reaction was cooled to rt., the mixture was added H_2O and extracted with $CHCl_3$. The organic layer was washed with brine and dried over Na_2SO_4, filtered and concentrated *in vacuo* to give a residue. The residue was purified by column chromatography (SiO_2, *n*-hexane : AcOEt = 4 : 1) to afford **14j** (1.20 g, 88%).

White solid; m.p. 85–86 ºC;

^{1}H NMR (300 MHz, $CDCl_3$) δ 7.90 (d, J = 8.0 Hz, 2H), 7.28–7.12 (m, 2H), 7.01–6.84 (m, 2H), 3.60 (s, 6H), 2.39 (s, 6H);

^{13}C NMR (75 MHz, $CDCl_3$) δ 167.3, 143.7, 142.0, 130.9, 129.9, 127.8, 126.5, 51.6, 21.5;

IR (neat) 1721, 1604, 1427, 1278, 1247, 1077, 1050, 834, 775, 701 cm^{-1};

HRMS (EI) *m/z* calcd for $C_{18}H_{18}O_4$ $(M)^+$ 298.1205, found. 298.1205.

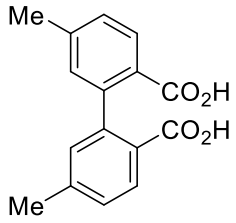

6j

5,5'-Dimethyl-[1,1'-biphenyl]-2,2'-dicarboxylic acid (**6j**)

To a solution of **14j** (1.06 g, 3.55 mmol) in THF/MeOH (2 : 1, 15 mL), 2*N* aq. NaOH (5 mL) was added at rt. After being stirred at 60 ºC for 18 h, the reaction mixture was washed with CPME. The aqueous layer was acidified with 2*N* aq. HCl, and extracted with AcOEt. The organic layer was washed with brine, dried over Na_2SO_4, filtered and concentrated *in vacuo* to give **6j** (937 mg, 98%). This dicarboxylic acid was used for one-pot cyclization reaction without further purification.

White amorphous;

^{1}H NMR (500 MHz, acetone-d_6) δ 10.80 (s, 2H), 7.89 (d, J = 7.9 Hz, 2H), 7.24 (dd, J = 8.0, 1.8 Hz, 2H), 6.98 (d, J = 1.8 Hz, 2H), 2.39 (s, 6H);

^{13}C NMR (75 MHz, acetone-d_6) δ 168.2, 145.1, 142.4, 131.9, 131.0, 128.3, 127.8, 21.3;

IR (neat) 2869, 1690, 1604, 1570, 1413, 1290, 1265, 787, 603, 440 cm^{-1};

HRMS (EI) *m/z* calcd for $C_{16}H_{14}O_4$ $(M)^+$ 270.0892, found. 270.0892.

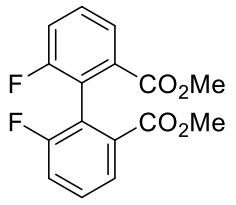

14k

Dimethyl 6,6'-difluoro-[1,1'-biphenyl]-2,2'-dicarboxylate (**14k**)

A solution of methyl 2-bromo-3-fluorobenzoate (4.64 g, 19.9 mmol, 1.0 equiv.) and Cu powder (10.1 g, 159 mmol, 8.0 equiv.) in DMF (20 mL) was refluxed under N_2 atmosphere for 15 h. After the reaction was cooled to rt., the mixture was added H_2O and extracted with $CHCl_3$. The organic layer was washed with brine and dried over Na_2SO_4, filtered and concentrated *in vacuo* to give a residue. The residue was purified by column chromatography (SiO_2, *n*-hexane : AcOEt = 4 : 1) to afford **14k** (2.47 g, 81%).

White solid; m.p. 109–110 ºC;

^{1}H NMR (300 MHz, $CDCl_3$) δ 7.93–7.87 (m, 2H), 7.52–7.42 (m, 2H), 7.37–7.28 (m, 2H), 3.66 (s, 6H);
^{13}C NMR (75 MHz, $CDCl_3$) δ 166.2–166.0 (m), 159.8 (d, *J* = 244.9 Hz), 131.6 (t, *J* = 1.9 Hz), 129.7–129.3 (m), 126.2 (d, *J* = 2.9 Hz), 123.9 (d, *J* = 19.0 Hz), 119.2 (d, *J* = 23.4 Hz), 52.3;
IR (neat) 3431, 2952, 1725, 1443, 1276, 1200, 1145, 1010, 893, 826, 759 cm^{-1};
HRMS (EI) *m/z* calcd for $C_{16}H_{12}F_2O_4$ $(M)^+$ 306.0704, found. 306.0704.

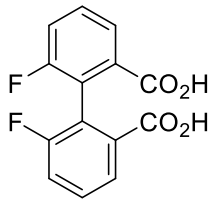

6k

6,6'-Difluoro-[1,1'-biphenyl]-2,2'-dicarboxylic acid (**6k**)
To a solution of **14k** (2.42 g, 7.90 mmol) in THF/MeOH (2 : 1, 30 mL), 2*N* aq. NaOH (10 mL) was added at rt. After being stirred at 60 ºC for 62 h, the reaction mixture was washed with CPME. The aqueous layer was acidified with 2*N* aq. HCl, and extracted with AcOEt. The organic layer was washed with brine, dried over Na_2SO_4, filtered and concentrated *in vacuo* to give **6k** (2.14 g, 97%).This dicarboxylic acid was used for one-pot cyclization reaction without further purification.

White amorphous;
^{1}H NMR (300 MHz, methanol-d_4) δ 7.91–7.85 (m, 2H), 7.55–7.45 (m, 2H), 7.39–7.33 (m, 2H);
^{13}C NMR (75 MHz, methanol-d_4) δ 168.8, 161.1 (d, *J* = 242.9 Hz), 133.7, 130.3 (d, *J* = 9.0 Hz), 127.2 (d, *J* = 2.9 Hz), 125.4 (d, *J* = 19.0 Hz), 119.7 (d, *J* = 23.7 Hz);
IR (neat) 2992, 2873, 2662, 2539, 1686, 1440, 1412, 1264, 933, 767 cm^{-1};
HRMS (EI) *m/z* calcd for $C_{14}H_8F_2O_4$ $(M)^+$ 278.0391, found. 278.0391.

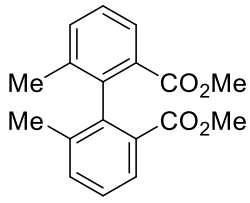

14l

Dimethyl 6,6'-dimethyl-[1,1'-biphenyl]-2,2'-dicarboxylate (**14l**)
A solution of methyl 2-bromo-3-methylbenzoate (4.60 g, 20.1 mmol, 1.0 equiv.) and Cu powder (10.2 g, 161 mmol, 8.0 equiv.) in DMF (20 mL) was refluxed under N_2 atmosphere for 15 h. After

the reaction was cooled to rt, the mixture was added H_2O and extracted with $CHCl_3$. The organic layer was washed with brine and dried over Na_2SO_4, filtered and concentrated *in vacuo* to give a residue. The residue was purified by column chromatography (SiO_2, *n*-hexane : AcOEt = 4 : 1) to afford **14l** (2.19 g, 73%).

White solid; m.p. 39–40 ºC;
^{1}H NMR (300 MHz, $CDCl_3$) δ 7.89–7.84 (m, 2H), 7.46–7.42 (m, 2H), 7.33 (t, *J* = 7.7 Hz, 2H), 3.58 (s, 6H), 1.91 (d, *J* = 0.7 Hz, 6H);
^{13}C NMR (75 MHz, $CDCl_3$) δ 167.6, 141.3, 136.7, 133.7, 129.4, 127.8, 127.0, 51.8, 20.1;
IR (neat) 3430, 2952, 1726, 1432, 1264, 1193, 1145, 1010, 870, 763 cm^{-1};
HRMS (EI) *m/z* calcd for $C_{18}H_{18}O_4$ $(M)^+$ 298.1205, found. 298.1203.

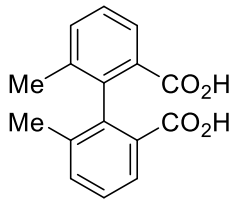

6l

6,6'-Dimethyl-[1,1'-biphenyl]-2,2'-dicarboxylic acid (**6l**)
To a solution of **14l** (234 mg, 784 μmol) in THF/MeOH (2 : 1, 15 mL), 2*N* aq. NaOH (5.0 mL) was added at rt. After being stirred at 60 ºC for 168 h, the reaction mixture was washed with CPME. The aqueous layer was acidified with 2*N* aq. HCl, and extracted with AcOEt. The organic layer was washed with brine, dried over Na_2SO_4, filtered and concentrated *in vacuo* to give **6l** (205 mg, 97%).This dicarboxylic acid was used for one-pot cyclization reaction without further purification.

White solid; m.p. 232–233 ºC;
^{1}H NMR (500 MHz, methanol-d_4) δ 7.82 (d, *J* = 7.9 Hz, 2H), 7.47–7.41 (m, 2H), 7.32 (t, *J* = 7.7 Hz, 2H), 1.88 (s, 6H);
^{13}C NMR (125 MHz, methanol-d_4) δ 170.9, 142.5, 137.8, 134.5, 131.5, 128.8, 127.9, 20.2;
IR (neat) 3008, 2662, 2554, 1694, 1300, 1276, 1184, 1157, 937, 909, 759 cm^{-1};
HRMS (EI) *m/z* calcd for $C_{16}H_{14}O_4$ $(M)^+$ 270.0892, found. 270.0892.

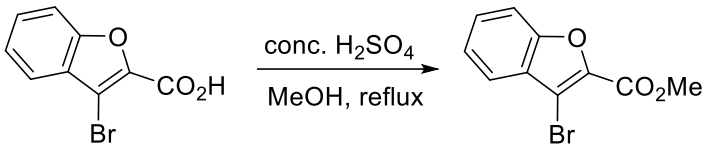

S1 **S2**

Methyl 3-bromobenzofuran-2-carboxylate (**S2**)

A solution of 3-bromobenzofuran-2-carboxylic acid[8] (1.03 g, 4.27 mmol) and a few drops of conc. H_2SO_4 in MeOH (10 mL) was refluxed under N_2 atmosphere for 71 h. After the reaction was cooled to rt, the mixture was added sat. aq. $NaHCO_3$ and extracted with AcOEt. The organic layer was washed with brine and dried over Na_2SO_4, filtered and concentrated *in vacuo* to give a residue. The residue was purified by short column chromatography (SiO_2, *n*-hexane : AcOEt = 9 : 1) to afford **S2** (1.08 g, 99%).

White solid; m.p. 49–50 ºC;

^{1}H NMR (300 MHz, $CDCl_3$) δ 7.69–7.61 (m, 1H), 7.52–7.48 (m, 2H), 7.44–7.34 (m, 1H), 4.02 (s, 3H);

^{13}C NMR (75 MHz, $CDCl_3$) δ 159.4, 154.1, 141.4, 129.1, 128.2, 124.5, 121.9, 112.6, 106.4, 52.7;

IR (neat) 1719, 1549, 1436, 1326, 1298, 1157, 1143, 1024, 841, 741 cm^{-1};

HRMS (EI) *m/z* calcd for $C_{10}H_7BrO_3$ $(M)^+$ 253.9579, found. 253.9580.

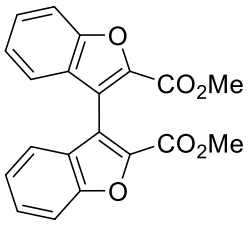

14m

Dimethyl [3,3'-bibenzofuran]-2,2'-dicarboxylate (**14m**)

A solution of **S2** (4.28 g, 16.8 mmol, 1.0 equiv.) and activated Cu (8.53 g, 134 mmol, 8.0 equiv.) in DMF (15 mL) was refluxed under N_2 atmosphere for 27 h. After the reaction was cooled to rt., the mixture was added H_2O and extracted with $CHCl_3$. The organic layer was washed with brine and dried over Na_2SO_4, filtered and concentrated *in vacuo* to give a residue. The residue was purified by column chromatography (SiO_2, *n*-hexane : AcOEt = 4 : 1) to afford **14m** (1.99 g, 68%).

Yellow solid; m.p. 187–188 ºC;

^{1}H NMR (300 MHz, $CDCl_3$) δ 7.75–7.68 (m, 2H), 7.55–7.46 (m, 2H), 7.43–7.38 (m, 2H), 7.33 – 7.21 (m, 2H), 3.79 (s, 6H);

^{13}C NMR (75 MHz, $CDCl_3$) δ 159.9, 154.8, 142.1, 128.3, 127.7, 124.1, 122.3, 118.3, 112.7, 52.4;
IR (neat) 1720, 1556, 1438, 1296, 1152, 1138, 970, 840, 757, 741 cm^{-1};
HRMS (EI) *m/z* calcd for $C_{20}H_{14}O_6$ $(M)^+$ 350.0790, found. 350.0789.

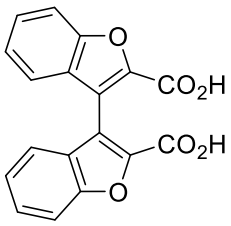

6m

[3,3'-Bibenzofuran]-2,2'-dicarboxylic acid (**6m**)
To a solution of **14m** (413 mg, 1.18 mmol) in THF/MeOH (2 : 1, 15 mL), 2*N* aq. NaOH (5 mL) was added at rt. After being stirred at rt. for 67 h, the reaction mixture was washed with CPME. The aqueous layer was acidified with 2*N* aq. HCl, and extracted with AcOEt. The organic layer was washed with brine, dried over Na_2SO_4, filtered and concentrated *in vacuo* to give **6m** (368 mg, 97%). This dicarboxylic acid was used for one-pot cyclization reaction without further purification.

Pale yellow solid; m.p. 245–246 °C;
^{1}H NMR (500 MHz, methanol-d_4) δ 7.70 (d, J = 8.4 Hz, 2H), 7.58–7.51 (m, 2H), 7.40 (d, J = 5.0 Hz, 2H), 7.35–7.23 (m, 2H);
^{13}C NMR (75 MHz, methanol-d_4) δ 162.4, 156.1, 144.1, 129.2, 129.1, 125.0, 123.1, 119.3, 113.2,
IR (neat) 2848, 1682, 1565, 1450, 1288, 1171, 1144, 950, 840, 739 cm^{-1};
HRMS (EI) *m/z* calcd for $C_{18}H_{10}O_6$ $(M)^+$ 322.0477, found. 322.0476.

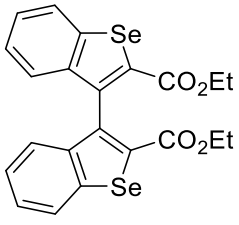

14o

Diethyl [3,3'-bibenzo[*b*]selenophene]-2,2'-dicarboxylate (**14o**)
A solution of ethyl 3-bromobenzo[*b*]selenophene-2-carboxylate[9] (1.50 g, 4.52 mmol, 1.0 equiv.) and Cu powder (2.30 g, 36.1 mmol, 8.0 equiv.) in DMF (10 mL) was refluxed under N_2 atmosphere for 34.5 h. After the reaction was cooled to rt., the mixture was added H_2O and extracted with $CHCl_3$. The organic layer was washed with brine and dried over Na_2SO_4, filtered

and concentrated *in vacuo* to give a residue. The residue was purified by column chromatography (SiO_2, *n*-hexane : AcOEt = 9 : 1) to afford **14o** (956 mg, 84%).

Pale yellow solid; m.p. 158–159 ºC;

^{1}H NMR (500 MHz, $CDCl_3$) δ 7.96 (d, J = 8.0 Hz, 2H), 7.37–7.43 (m, 2H), 7.24–7.29 (m, 4H), 4.03 (q, J = 7.1 Hz, 4H), 0.90 (t, J = 7.1 Hz, 6H);

^{13}C NMR (125 MHz, $CDCl_3$) δ 163.5, 142.2, 141.9, 141.2, 133.5, 127.3, 126.8, 125.8, 125.2, 61.4, 13.7;

IR (neat) 1707, 1681, 1279, 1233, 1100, 1071, 1041, 1017, 757, 732 cm^{-1};

HRMS (EI) *m/z* calcd for $C_{22}H_{18}O_4Se_2$ $(M)^+$ 505.9535, found. 505.9535.

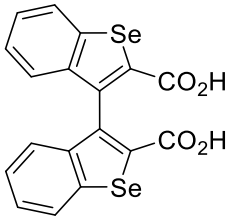

6o

[3,3'-Bibenzo[*b*]selenophene]-2,2'-dicarboxylic acid (**6o**)

To a solution of **14o** (600 mg, 1.19 mmol) in THF/MeOH (2 : 1, 30 mL), 2*N* aq. NaOH (10 mL) was added at rt. After being stirred at rt. for 19 h, the reaction mixture was washed with CPME. The aqueous layer was acidified with 2*N* aq. HCl, and extracted with AcOEt. The organic layer was washed with brine, dried over Na_2SO_4, filtered and concentrated *in vacuo* to give **6o** (477 mg, 90%). This dicarboxylic acid was used for one-pot cyclization reaction without further purification.

Pale yellow solid; m.p. 274–275 ºC;

^{1}H NMR (500 MHz, acetone-d_6) δ 11.34 (s, 2H), 8.17 (d, J = 8.0 Hz, 2H), 7.52–7.42 (m, 2H), 7.37–7.29 (m, 2H), 7.21 (dd, J = 8.1, 1.1 Hz, 2H);

^{13}C NMR (125 MHz, acetone-d_6) δ 164.4, 143.2, 142.8, 142.1, 134.5, 128.1, 127.2, 126.9, 126.1;

IR (neat) 1715, 1661, 1513, 1292, 1246, 1174, 756, 748, 733, 722 cm^{-1};

HRMS (EI) *m/z* calcd for $C_{18}H_{10}O_4Se_2$ $(M)^+$ 449.8909, found. 449.8909.

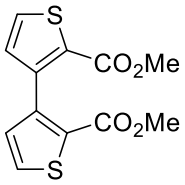

14p

Dimethyl [3,3'-bithiophene]-2,2'-dicarboxylate (**14p**)

A solution of methyl 3-bromothiophene-2-carboxylate (4.05 g, 18.3 mmol, 1.0 equiv.) and activated Cu (9.31 g, 147 mmol, 8.0 equiv.) in DMF (10 mL) was refluxed under N_2 atmosphere for 63 h. After the reaction was cooled to rt., the mixture was added H_2O and extracted with $CHCl_3$. The organic layer was washed with brine and dried over Na_2SO_4, filtered and concentrated *in vacuo* to give a residue. The residue was purified by column chromatography (SiO_2, *n*-hexane : AcOEt = 4 : 1 to 3 : 1) to afford **14p** (1.71 g, 66%).

White solid; m.p. 194–195 ºC;

^{1}H NMR (300 MHz, $CDCl_3$) δ 7.51 (d, J = 5.0 Hz, 2H), 7.05 (d, J = 5.1 Hz, 2H), 3.74 (s, 6H);

^{13}C NMR (75 MHz, $CDCl_3$) δ 162.3, 141.8, 131.2, 129.7, 128.8, 52.1;

IR (neat) 1702, 1433, 1283, 1237, 1097, 1072, 864, 782, 767, 671 cm^{-1};

HRMS (EI) *m/z* calcd for $C_{12}H_{10}O_4S_2$ $(M)^+$ 282.0021, found. 282.0022.

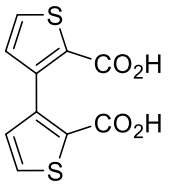

6p

[3,3'-Bithiophene]-2,2'-dicarboxylic acid (**6p**)

To a solution of **14p** (382 mg, 1.35 mmol) in THF/MeOH (2 : 1, 15 mL), 2*N* aq. NaOH (5 mL) was added at rt. After being stirred at rt. for 16 h, the reaction mixture was washed with CPME. The aqueous layer was acidified with 2*N* aq. HCl, and extracted with AcOEt. The organic layer was washed with brine, dried over Na_2SO_4, filtered and concentrated *in vacuo* to give **6p** (335 mg, 97%). This dicarboxylic acid was used for one-pot cyclization reaction without further purification.

White amorphous;

^{1}H NMR (500 MHz, methanol-d_4) δ 7.63 (d, J = 5.1 Hz, 2H), 7.04 (d, J = 5.1 Hz, 2H);

^{13}C NMR (75 MHz, methanol-d_4) δ 165.1, 143.1, 132.3, 131.1, 130.8;

IR (neat) 2521, 1651, 1423, 1302, 1265, 867, 768, 731, 665, 514 cm^{-1};

HRMS (EI) *m/z* calcd for $C_{10}H_6O_4S_2$ $(M)^+$ 253.9708, found. 253.9711.

Substrate Scope for One-pot Cyclization

Scheme S3-4. Substrate scope for one-pot cyclization.

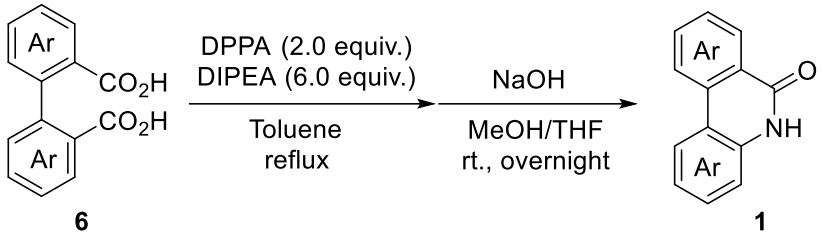

6 **1**

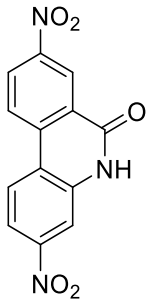

1e

3,8-Dinitrophenanthridin-6(5*H*)-one (**1e**)

To a solution of **6e**[10] (101 mg, 305 μmol, 1.0 equiv.) in toluene (10 mL), DPPA (130 μL, 605 μmol, 1.98 equiv.) and DIPEA (320 μL, 1.84 mmol, 6.03 equiv.) were added at rt. After being refluxed for 12 h under N_2 atmosphere, the reaction mixture was concentrated *in vacuo* to give a residue. Then, a solution of the residue in THF/MeOH/2*N* aq. NaOH (2 : 1 : 1, 8 mL) was stirred at rt. for 12 h, and the reaction mixture was extracted with AcOEt. The organic layer was washed with brine, dried over Na_2SO_4, filtered and concentrated *in vacuo* to give a residue. The residue was purified by column chromatography (SiO_2, *n*-hexane : AcOEt = 5 : 1 to 2 : 1 to 1 : 1 to 1 : 2 to 1 : 5), and then washed with *n*-hexane for 3 times to obtain **1e** (50.5 mg, 58%).

Yellow solid; m.p. >300 ºC;

^{1}H NMR (300 MHz, DMSO-d_6) δ 12.28 (s, 1H), 8.97–8.71 (m, 2H), 8.71–8.50 (m, 2H), 8.11 (d, *J* = 2.1 Hz, 1H), 8.01–7.97 (m, 1H);

^{13}C NMR (75 MHz, DMSO-d_6) δ 159.5, 148.4, 147.5, 137.9, 137.6, 127.2, 126.9, 126.4, 126.2, 122.7, 121.3, 116.7, 111.4;

IR (neat) 3371, 3084, 2960, 2877, 1679, 1615, 1519, 1348, 846, 735, 452 cm^{-1};

HRMS (ESI) *m/z* calcd for $C_{13}H_8N_3O_5$ $(M+H)^+$ 286.0458, found. 286.0456.

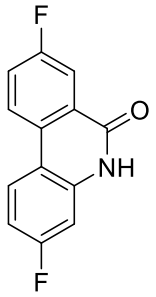

1f

3,8-Difluorophenanthridin-6(5*H*)-one (**1f**)

To a solution of **6f** (278 mg, 1.00 mmol, 1.0 equiv.) in toluene (20 mL), DPPA (430 μL, 2.00 mmol, 2.0 equiv.) and DIPEA (1.05 mL, 6.0 mmol, 6.0 equiv.) were added at rt. After being refluxed for 15 h under N_2 atmosphere, the reaction mixture was concentrated *in vacuo* to give a residue. Then, a solution of the residue in THF/MeOH/2*N* aq. NaOH (1 : 1 : 1, 60 mL) was stirred at rt. for 12 h, and the reaction mixture was extracted with AcOEt. The organic layer was washed with H_2O and brine, dried over Na_2SO_4, filtered and concentrated *in vacuo* to give a residue. The residue was washed with $CHCl_3$ to obtain **1f** (175 mg, 76%).

White amorphous;

^{1}H NMR (300 MHz, DMSO-d_6) δ 11.90 (s, 1H), 8.52 (dd, J = 9.0, 5.1 Hz, 1H), 8.34–8.46 (m, 1H), 7.92 (dd, J = 9.3, 2.9 Hz, 1H), 7.72 (td, J = 8.7, 2.9 Hz, 1H), 7.04–7.16 (m, 2H);

^{13}C NMR (125 MHz, DMSO-d_6) δ 102.1 (d, J = 25 Hz), 110.1 (d, J = 23 Hz), 112.5 (d, J = 21 Hz), 114.0 (d, J = 2.5 Hz), 162.3 (d, J = 244 Hz), 161.4 (d, J = 245 Hz), 160.1 (d, J = 3.8 Hz), 137.6 (d, J = 11 Hz), 130.6 (d, J = 2.5 Hz), 126.9 (d, J = 7.5 Hz), 125.9 (d, J = 1.3 Hz), 125.8 (d, J = 3.8 Hz), 121.2 (d, J = 24 Hz);

IR (neat) 2969, 2885, 1690, 1670, 1627, 1487, 1260, 1169, 870, 795, 524, 468 cm^{-1};

HRMS (EI) *m/z* calcd for $C_{13}H_7F_2NO$ $(M)^+$ 231.0496, found 231.0496.

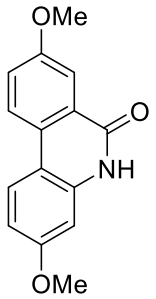

1g

3,8-Dimethoxyphenanthridin-6(5*H*)-one (**1g**)

To a solution of **6g** (52.3 mg, 0.173 mmol, 1.0 equiv.) in toluene (8 mL), DPPA (76 µL, 0.346 mmol, 2.0 equiv.) and DIPEA (185 µL, 1.04 mmol, 6.0 equiv.) were added at rt. After being refluxed for 12 h under N_2 atmosphere, the reaction mixture was concentrated *in vacuo* to give a residue. Then, a solution of the residue in THF/MeOH/2*N* aq. NaOH (2 : 1 : 1, 8 mL) was stirred at rt. for 12 h, and the reaction mixture was extracted with AcOEt. The organic layer was washed with brine, dried over Na_2SO_4, filtered and concentrated *in vacuo* to give a residue. The residue was purified by column chromatography (SiO_2, *n*-hexane : AcOEt = 1 : 1) to afford **1g** (33 mg, 75%).

White amorphous;
^{1}H NMR (500 MHz, DMSO-d_6) δ 11.60 (s, 1H), 8.32 (d, J = 8.9 Hz, 1H), 8.20 (d, J = 8.8 Hz, 1H), 7.70 (d, J = 2.9 Hz, 1H), 7.40 (dd, J = 8.9, 2.9 Hz, 1H), 6.90–6.78 (m, 2H), 3.89 (s, 3H), 3.81 (s, 3H);
^{13}C NMR (75 MHz, DMSO-d_6) δ 160.9, 159.5, 158.2, 136.9, 128.1, 125.7, 124.1, 124.0, 121.8, 111.3, 110.1, 108.5, 99.5, 55.4, 55.3;
IR (neat) 2835, 1658, 1612, 1485, 1365, 1265, 1196, 1169, 1045, 799, 777 cm^{-1};
HRMS (EI) *m/z* calcd for $C_{15}H_{13}NO_3$ $(M)^+$ 255.0895, found. 255.0895.

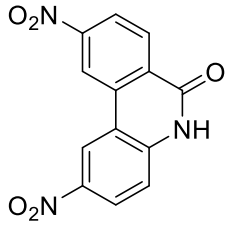

1h

2,9-Dinitrophenanthridin-6(5*H*)-one (**1h**)
To a solution of **6h** (332 mg, 1.00 mmol, 1.0 equiv.) in toluene (20 mL), DPPA (430 µL, 2.00 mmol, 2.0 equiv.) and DIPEA (1.00 mL, 5.74 mmol, 5.75 equiv.) were added at rt. After being refluxed for 15 h under N_2 atmosphere, the reaction mixture was concentrated *in vacuo* to give a residue. Then, a solution of the residue in THF/MeOH/2*N* aq. NaOH (1 : 1 : 1, 60 mL) was stirred at rt. for 5 h, and the reaction mixture was extracted with AcOEt. The organic layer was washed with H_2O and brine, dried over Na_2SO_4, filtered and concentrated *in vacuo* to give a residue. The residue was washed with $CHCl_3$/ *n*-hexane (1 : 1) to obtain **1h** (188 mg, 66%).

Yellow solid; m.p. >300 ºC;
^{1}H NMR (300 MHz, DMSO-d_6) δ 12.43 (s, 1H), 9.48–9.11 (m, 2H), 8.61 – 8.20 (m, 3H), 7.43 (d, J = 8.9 Hz, 1H);

^{13}C NMR (75 MHz, DMSO-d_6) δ 160.0, 150.8, 142.6, 142.0, 134.4, 134.4, 130.0, 125.8, 123.2, 120.8, 119.3, 117.5, 116.9;

IR (neat) 3100, 2889, 2857, 1666, 1615, 1531, 1335, 1148, 846, 786, 559 cm^{-1};

HRMS (ESI) *m/z* calcd for $C_{13}H_8N_3O_5$ $(M+H)^+$ 286.0458, found. 286.0458.

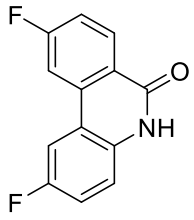

1i

2,9-Difluorophenanthridin-6(5*H*)-one (**1i**)

To a solution of **6i** (278 mg, 1.00 mmol, 1.0 equiv.) in toluene (20 mL), DPPA (430 μL, 2.00 mmol, 2.0 equiv.) and DIPEA (1.05 mL, 6.00 mmol, 6.0 equiv.) were added at rt. After being refluxed for 15 h under N_2 atmosphere, the reaction mixture was concentrated *in vacuo* to give a residue. Then, a solution of the residue in THF/MeOH/2*N* aq. NaOH (1 : 1 : 1, 60 mL) was stirred at rt. for 12 h, and the reaction mixture was extracted with AcOEt. The organic layer was washed with H_2O and brine, dried over Na_2SO_4, filtered and concentrated *in vacuo* to give a residue. The residue was washed with $CHCl_3$ to obtain **1i** (168 mg, 73%).

White amorphous;

^{1}H NMR (300 MHz, DMSO-d_6) δ 11.75 (s, 1H), 8.29–8.41 (m, 2H), 8.25 (dd, *J* = 10.4, 2.5 Hz, 1H), 7.49 (td, *J* = 8.6, 2.4 Hz, 1H), 7.30–7.44 (m, 2H);

^{13}C NMR (125 MHz, DMSO-d_6) δ 165.0 (d, *J* = 249 Hz), 159.9, 157.7 (d, *J* = 236 Hz), 136.4 (dd, *J* = 10, 2.5 Hz), 133.6 (d, *J* = 1.3 Hz), 130.9 (d, *J* = 10 Hz), 122.7 (d, *J* = 1.3 Hz), 118.2 (dd, *J* = 8.1, 2.5 Hz), 118.0 (d, *J* = 18 Hz), 117.8 (d, *J* = 2.5 Hz), 116.6 (d, *J* = 24 Hz), 109.7 (d, *J* = 24 Hz), 109.3 (d, *J* = 24 Hz);

IR (neat) 3428, 3175, 3143, 3040, 2997, 2861, 1686, 1610, 1507, 1443, 1367, 1208, 866, 818, 671, 587 cm^{-1};

HRMS (EI) *m/z* calcd for $C_{13}H_7F_2NO$ $(M)^+$ 231.0496, found. 231.0497.

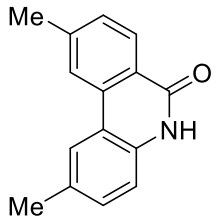

1j

2,9-Dimethylphenanthridin-6(5*H*)-one (**1j**)

To a solution of **6j** (270 mg, 1.00 mmol, 1.0 equiv.) in toluene (20 mL), DPPA (430 µL, 2.00 mmol, 2.0 equiv.) and DIPEA (1.05 mL, 6.00 mmol, 6.0 equiv.) were added at rt. After being refluxed for 15 h under N_2 atmosphere, the reaction mixture was concentrated *in vacuo* to give a residue. Then, a solution of the residue in THF/MeOH/2*N* aq. NaOH (1 : 1 : 1, 60 mL) was stirred at rt. for 12 h, and the reaction mixture was extracted with AcOEt. The organic layer was washed with H_2O and brine, dried over Na_2SO_4, filtered and concentrated *in vacuo* to give a residue. The residue was purified by column chromatography (SiO_2, *n*-hexane : AcOEt = 7 : 3 to 1 : 1), and then washed with $CHCl_3$/ *n*-hexane (1 : 2) to obtain **1j** (93 mg, 41%).

White solid; m.p. 269–270 ºC;

^{1}H NMR (300 MHz, DMSO-d_6) δ 11.50 (s, 1H), 8.30 (s, 1H), 8.23–8.13 (m, 2H), 7.49–7.38 (m, 1H), 7.33–7.25 (m, 2H), 2.52 (s, 3H), 2.41 (s, 3H);

^{13}C NMR (75 MHz, DMSO-d_6) δ 160.7, 142.9, 134.6, 134.2, 131.1, 130.5, 129.0, 127.5, 123.5, 123.0, 122.5, 117.4, 116.0, 21.5, 20.7;

IR (neat) 2856, 1658, 1613, 1364, 827, 778, 687, 659, 624, 530, 445 cm^{-1};

HRMS (EI) *m/z* calcd for $C_{15}H_{13}NO$ $(M)^+$ 223.0997, found. 223.0998.

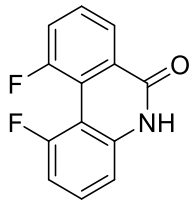

1k

1,10-Difluorophenanthridin-6(5*H*)-one (**1k**)

To a solution of **6k** (278 mg, 1.00 mmol, 1.0 equiv.) in toluene (20 mL), DPPA (430 µL, 2.00 mmol, 2.0 equiv.) and DIPEA (1.05 mL, 6.00 mmol, 6.0 equiv.) were added at rt. After being refluxed for 15 h under N_2 atmosphere, the reaction mixture was concentrated *in vacuo* to give a residue. Then, a solution of the residue in THF/MeOH/2*N* aq. NaOH (1 : 1 : 1, 60 mL) was stirred at rt. for 12 h, and the reaction mixture was extracted with AcOEt. The organic layer was washed

with H_2O and brine, dried over Na_2SO_4, filtered and concentrated *in vacuo* to give a residue. The residue was purified by column chromatography (SiO_2, *n*-hexane : AcOEt = 7 : 3 to AcOEt only), and then washed with $CHCl_3$/ *n*-hexane (1 : 1) to obtain **1k** (113 mg, 49%).

White solid; m.p. >300 °C;
^{1}H NMR (500 MHz, DMSO-d_6) δ 11.96 (s, 1H), 8.25–8.21 (m, 1H), 7.77–7.71 (m, 2H), 7.58–7.53 (m, 1H), 7.24 (dd, *J* = 8.2, 1.2 Hz, 1H), 7.12–7.08 (m, 1H);
^{13}C NMR (125 MHz, DMSO-d_6) δ 159.6 (d, *J* = 1.9Hz), 158.6 (d, *J* = 251.2 Hz), 157.7 (d, *J* = 253.8 Hz), 138.6 (d, *J* = 6.3 Hz), 131.1 (d, *J* = 11.3 Hz), 129.8 (d, *J* = 10.0 Hz), 128.7, 123.6, 120.6 (dd, *J* = 17.8, 7.7 Hz), 118.9 (d, *J* = 12.5 Hz), 111.9, 109.7 (dd, *J* = 16.4, 9.0 Hz), 103.2 (d, *J* = 15.0 Hz);
IR (neat) 3044, 3008, 2873, 1683, 1618, 1559, 1380, 1268, 791, 731, 516, 492 cm^{-1};
HRMS (APCI) *m/z* calcd for $C_{13}H_8F_2NO$ $(M+H)^+$ 232.0568, found. 232.0570.

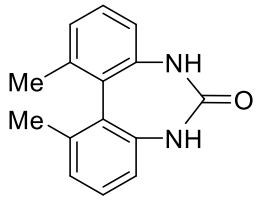

15

1,11-Dimethyl-5,7-dihydro-6*H*-dibenzo[*d*,*f*][1,3]diazepin-6-one (**15**)
To a solution of **6l** (270 mg, 1.00 mmol, 1.0 equiv.) in toluene (20 mL), DPPA (430 μL, 2.00 mmol, 2.0 equiv.) and DIPEA (1.05 mL, 6.00 mmol, 6.0 equiv.) were added at rt. After being refluxed for 15 h under N_2 atmosphere, the reaction mixture was concentrated *in vacuo* to give a residue. Then, a solution of the residue in THF/MeOH/2*N* aq. NaOH (1 : 1 : 1, 60 mL) was stirred at rt. for 12 h, and the reaction mixture was extracted with AcOEt. The organic layer was washed with H_2O and brine, dried over Na_2SO_4, filtered and concentrated *in vacuo* to give a residue. The residue was purified by column chromatography (SiO_2, *n*-hexane : AcOEt = 7 : 3 to AcOEt only), and then washed with $CHCl_3$/ *n*-hexane (1 : 1) to obtaine the urea **15** (76 mg, 32%).

White amorphous;
^{1}H NMR (500 MHz, DMSO-d_6) δ 8.58 (s, 2H), 7.19 (t, *J* = 7.7 Hz, 2H), 7.06–7.00 (m, 2H), 6.95–6.87 (m, 2H), 2.07 (s, 6H);
^{13}C NMR (125 MHz, DMSO-d_6) δ 165.9, 143.0, 137.5, 128.7, 128.0, 125.9, 118.8, 20.0;
IR (neat) 3240, 3143, 3025, 2925, 1929, 1690, 1567, 1427, 1380, 874, 798, 687 cm^{-1};
HRMS (APCI) *m/z* calcd for $C_{15}H_{15}N_2O$ $(M+H)^+$ 239.1179, found. 239.1181.

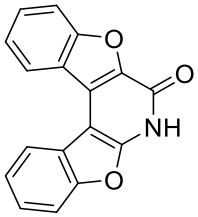

1m

Bis(benzofuro)[2,3-*b*:3',2'-*d*]pyridin-7(6*H*)-one (**1m**)

To a solution of **6m** (58 mg, 0.18 mmol, 1.0 equiv.) in toluene (5 mL), DPPA (77 μL, 0.36 mmol, 2.0 equiv.) and DIPEA (188 μL, 1.08 mmol, 6.0 equiv.) were added at rt. After being refluxed for 12 h under Argon atmosphere, the reaction mixture was concentrated *in vacuo* to give a residue. Then, a solution of the residue in THF/MeOH/2*N* aq. NaOH (2 : 1 : 1, 16 mL) was stirred at rt. for 12 h, and the reaction mixture was extracted with AcOEt. The organic layer was washed with water and brine, dried over Na_2SO_4, filtered and concentrated *in vacuo* to give a residue. The residue was purified by column chromatography (SiO_2, *n*-hexane : AcOEt = 1 : 1 and then $CHCl_3$) and then washed with $CHCl_3$/ *n*-hexane (1 : 1) to obtaine **1m** (33 mg, 67%).

White solid; m.p. >300 ºC;

^{1}H NMR (600 MHz, DMSO-d_6) δ 8.62 (d, *J* = 7.8 Hz, 1H), 8.41 (s, 1H), 7.93 (d, *J* = 8.3 Hz, 1H), 7.80–7.72 (m, 2H), 7.65–7.57 (m, 1H), 7.53–7.46 (m, 2H);

^{13}C NMR (150 MHz, DMSO-d_6) δ 156.6, 152.9, 151.9, 130.0, 130.0, 124.2, 124.2, 124.1, 124.0, 123.8, 122.9, 122.2, 121.6, 121.5, 112.9, 111.7 (One carbon signal was overlapped.);

IR (neat) 3435, 3029, 2590, 1655, 1599, 1451, 1180, 1053, 750, 499 cm^{-1};

HRMS (ESI) *m/z* calcd for $C_{17}H_{10}NO_3$ $(M+H)^+$ 276.0655, found. 276.0654.

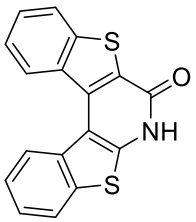

1n

Benzo[4,5]thieno[2,3-*b*]benzo[4,5]thieno[3,2-*d*]pyridin-7(6*H*)-one (**1n**)

To a solution of [3,3'-bibenzo[*b*]thiophene]-2,2'-dicarboxylic acid[11] (354 mg, 1.00 mmol, 1.0 equiv.) in toluene (20 mL), DPPA (430 μL, 2.00 mmol, 2.0 equiv.) and DIPEA (1.05 mL, 6.00 mmol, 6.0 equiv.) were added at rt. After being refluxed for 15 h under N_2 atmosphere, the reaction mixture was concentrated *in vacuo* to give a residue. Then, a solution of the residue in

THF/MeOH/2*N* aq. NaOH (1 : 1 : 1, 60 mL) was stirred at rt. for 12 h, and the reaction mixture was extracted with AcOEt. The organic layer was washed with H_2O and brine, dried over Na_2SO_4, filtered and concentrated *in vacuo* to give a residue. The residue was washed with $CHCl_3$ to obtain **1n** (158 mg, 52%).

Pale yellow solid; m.p. >300 ºC;

^{1}H NMR (500 MHz, DMSO-d_6) δ 13.21 (s, 1H), 8.78–8.91 (m, 1H), 8.58 (d, J = 8.2 Hz, 1H), 8.30–8.19 (m, 1H), 8.08 (d, J = 7.9 Hz, 1H), 7.81-7.56 (m, 2H), 7.57 (t, J = 7.7 Hz, 1H), 7.43 (t, J = 7.6 Hz, 1H);

^{13}C NMR (75 MHz, DMSO-d_6) δ 158.1, 141.5, 137.2, 134.5, 133.3, 133.2, 128.0, 126.3, 125.2, 125.0, 124.3, 124.2, 123.5, 123.0 (Three carbon signals were overlapped);

IR (neat) 2657, 1635, 1453, 1120, 903, 748, 718, 615, 575, 410 cm^{-1};

HRMS (EI) *m/z* calcd for $C_{17}H_9NOS_2$ $(M)^+$ 307.0126, found. 307.0125.

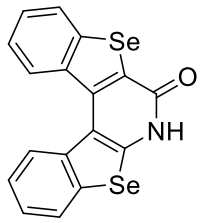

1o

Benzo[4,5]selenopheno[2,3-*b*]benzo[4,5]selenopheno[3,2-*d*]pyridin-7(6*H*)-one (**1o**)

To a solution of **6o** (448 mg, 1.00 mmol, 1.0 equiv.) in toluene (20 mL), DPPA (430 µL, 2.00 mmol, 2.0 equiv.) and DIPEA (1.05 mL, 6.00 mmol, 6.0 equiv.) were added at rt. After being refluxed for 15 h under N_2 atmosphere, the reaction mixture was concentrated *in vacuo* to give a residue. Then, a solution of the residue in THF/MeOH/2*N* aq. NaOH (1 : 1 : 1, 30 mL) was stirred at rt. for 12 h, and the reaction mixture was extracted with AcOEt. The organic layer was washed with H_2O and brine, dried over Na_2SO_4, filtered and concentrated *in vacuo* to give a residue. The residue was purified by column chromatography (SiO_2, *n*-hexane : AcOEt = 7 : 3 to 3 : 2), and then washed with $CHCl_3$ to obtain **1o** (237 mg, 59%).

Yellow solid; m.p. >300 ºC;

^{1}H NMR (500 MHz, DMSO-d_6) δ 12.90 (s, 1H), 8.79–8.62 (m, 1H), 8.36 (d, J = 8.2 Hz, 1H), 8.31–8.19 (m, 1H), 8.13 (d, J = 7.8 Hz, 1H), 7.71–7.58 (m, 2H), 7.48 (t, J = 7.6 Hz, 1H), 7.32 (t, J = 7.5 Hz, 1H);

^{13}C NMR (125 MHz, DMSO-d_6) δ 159.2, 142.6, 140.9, 137.2, 135.5, 135.0, 127.9, 127.8, 127.5, 126.7, 124.8, 124.6, 124.3 (Three carbon signals were overlapped.);

IR (neat) 3431, 2833, 1651, 1523, 1443, 1113, 750, 711, 603, 535, 428 cm^{-1};
HRMS (EI) *m/z* calcd for $C_{17}H_9NOSe_2$ $(M)^+$ 402.9014, found. 402.9019.

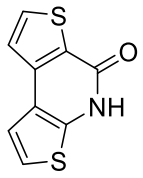

1p

Dithieno[2,3-*b*:3',2'-*d*]pyridin-5(4*H*)-one (**1p**)

To a solution of **6p** (254 mg, 1.00 mmol, 1.0 equiv.) in toluene (20 mL), DPPA (430 µL, 2.00 mmol, 2.0 equiv.) and DIPEA (1.05 mL, 6.00 mmol, 6.0 equiv.) were added at rt. After being refluxed for 15 h under N_2 atmosphere, the reaction mixture was concentrated *in vacuo* to give a residue. Then, a solution of the residue in THF/MeOH/2*N* aq. NaOH (1 : 1 : 1, 60 mL) was stirred at rt. for 12 h, and the reaction mixture was extracted with AcOEt. The organic layer was washed with H_2O and brine, dried over Na_2SO_4, filtered and concentrated *in vacuo* to give a residue. The residue was purified by column chromatography (SiO_2, *n*-hexane : AcOEt = 3 : 2 to 1 : 1), and then washed with $CHCl_3$/ *n*-hexane (1 : 9) to obtain **1p** (114 mg, 55%).

Pale yellow amorphous;
^{1}H NMR (300 MHz, DMSO-d_6) δ 12.58 (s, 1H), 8.15 (d, J = 5.2 Hz, 1H), 7.78 (d, J = 5.1 Hz, 1H), 7.56 (d, J = 5.6 Hz, 1H), 7.28 (d, J = 5.6 Hz, 1H);
^{13}C NMR (75 MHz, DMSO-d_6) δ 157.9, 142.3, 141.3, 134.7, 126.8, 123.4, 121.0, 117.4, 117.4;
IR (neat) 2781, 1621, 1180, 1112, 883, 845, 714, 643, 580, 453 cm^{-1};
HRMS (EI) *m/z* calcd for $C_9H_5NOS_2$ $(M)^+$ 206.9813, found. 206.9815.

Scheme S3-5. Syntheses of *O*-phosphated helicenes.

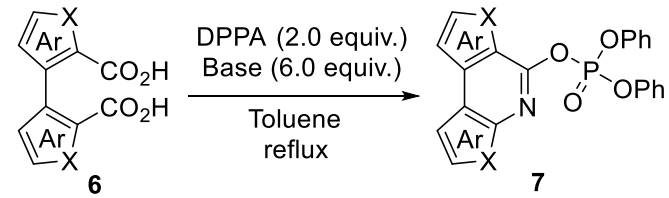

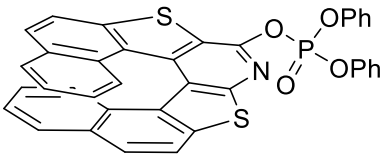

7b

Phosphate sulfur containing amide-functionalized [7]helicene-like molecule (**7b**)

To a solution of **6b** (114 mg, 0.25 mmol, 1.0 equiv.) in toluene (10 mL), DPPA (108 µL, 0.5 mmol, 2.0 equiv.) and Et_3N (192 µL, 1.5 mmol, 6.0 equiv.) were added at rt. After being refluxed for 4 h under N_2 atmosphere, the reaction mixture was quenched with 2*N* aq. HCl and extracted with AcOEt. The organic layer was washed with brine, dried over Na_2SO_4, filtered and concentrated *in vacuo* to give a residue. The residue was purified by column chromatography (SiO_2, *n*-hexane : AcOEt = 4 : 1 to 3 : 1) to afford **7b** (24 mg, 15%).

Yellow solid; m.p. 126–127 ºC;

^{1}H NMR (600 MHz, $CDCl_3$) δ 8.07 (d, *J* = 8.6 Hz, 1H), 8.05–8.00 (m, 2H), 7.98 (d, *J* = 8.6 Hz, 1H), 7.90–7.81 (m, 2H), 7.56–7.49 (m, 4H), 7.47–7.40 (m, 4H), 7.33–7.27 (m, 2H), 7.25–7.22 (m, 1H), 7.21–7.19 (m, 1H), 7.18–7.11 (m, 2H), 6.49–6.44 (m, 1H), 6.42–6.31 (m, 1H);

^{13}C NMR (150 MHz, $CDCl_3$) δ 155.2, 150.9 (d, *J* = 7.4 Hz), 149.7 (d, *J* = 6.7 Hz), 141.2, 140.2, 136.0, 130.9, 130.8 (d, *J* = 4.8 Hz), 130.6, 130.5 (d, *J* = 6.4 Hz), 130.0, 129.0, 128.1 (d, *J* = 16.6 Hz), 127.9, 127.0, 126.6, 125.9, 125.6, 125.1, 124.8, 124.2, 122.5, 121.8 (d, *J* = 9.4 Hz), 120.8 (d, *J* = 4.9 Hz), 120.5 (d, *J* = 11.1 Hz) (Four carbon signals were overlapped.);

IR (neat) 3057, 2969, 2328, 2164, 1487, 1308, 1184, 1073, 961, 942, 802, 679, 516 cm^{-1};

HRMS (EI) *m/z* calcd for $C_{37}H_{22}NO_4PS_2$ $(M)^+$ 639.0728, found. 639.0741.

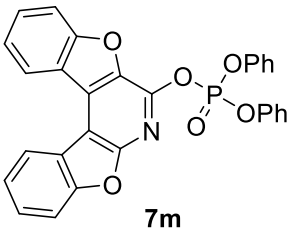

7m

Bis(benzofuro)[2,3-*b*:3',2'-*d*]pyridin-7-yl diphenyl phosphate (**7m**)

To a solution of **6m** (100 mg, 0.31 mmol, 1.0 equiv.) in toluene (20 mL), DPPA (133 µL, 0.62 mmol, 2.0 equiv.) and DIPEA (324 µL, 1.86 mmol, 6.0 equiv.) were added at rt. After being refluxed for 15 h under N_2 atmosphere, the reaction mixture was quenched with 2*N* aq. HCl and extracted with AcOEt. The organic layer was washed with brine, dried over Na_2SO_4, filtered and concentrated *in vacuo* to give a residue. The residue was purified by column chromatography (SiO_2, *n*-hexane : AcOEt = 4 : 1 to 3 : 1) to afford **7m** (109 mg, 69%).

Pale yellow solid; m.p. 163–164 ºC;

^{1}H NMR (500 MHz, $CDCl_3$) δ 8.37 (d, J = 5.0 Hz, 1H), 8.24 (d, J = 5.0 Hz, 1H), 7.73–7.63 (m, 3H), 7.59–7.50 (m, 11H), 7.30–7.17 (m, 2H);

^{13}C NMR (75 MHz, $CDCl_3$) δ 157.8, 155.4 (d, J = 0.8 Hz), 155.1, 150.8 (d, J = 7.5 Hz), 139.3 (d, J = 6.8 Hz), 138.2 (d, J = 7.5 Hz), 130.7, 130.0 (d, J = 0.8 Hz), 127.9, 125.9 (d, J = 1.5 Hz), 124.1 (d, J = 0.8 Hz), 123.8, 122.6, 122.3 (d, J = 2.3 Hz), 120.7 (d, J = 5.3 Hz), 113.1, 112.5, 130.3, 108.6 (Two carbon signals were overlapped.);

^{31}P NMR (200 MHz, $CDCl_3$) δ –18.3;

IR (neat) 1640, 1597, 1485, 1450, 1395, 1310, 1184, 1048, 939, 741, 519 cm^{-1};

HRMS (EI) *m/z* calcd for $C_{29}H_{18}NO_6P$ $(M)^+$ 507.0872, found. 507.0873.

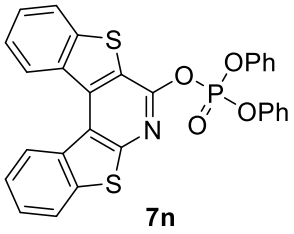

7n

Benzo[4,5]thieno[2,3-*b*]benzo[4,5]thieno[3,2-*d*]pyridin-7-yl diphenyl phosphate (**7n**)

To a solution of [3,3'-bibenzo[*b*]thiophene]-2,2'-dicarboxylic acid[x] (400 mg, 1.13 mmol, 1.0 equiv.) in toluene (40 mL), DPPA (485 µL, 2.26 mmol, 2.0 equiv.) and DIPEA (1.17 mL, 6.77 mmol, 6.0 equiv.) were added at rt. After being refluxed for 16.5 h under N_2 atmosphere, the reaction mixture was quenched with 2*N* aq. HCl and extracted with AcOEt. The organic layer was washed with brine, dried over Na_2SO_4, filtered and concentrated *in vacuo* to give a residue. The residue was purified by column chromatography (SiO_2, *n*-hexane : AcOEt = 9 : 1 to 4 : 1) to afford **7n** (235 mg, 39%).

Purified **7n** was recrystallized from AcOEt to give white solid.

White solid; m.p. 155–156 ºC;

The chemical shifts of the ^{1}H NMR signals were found to depend on the concentration as follows:

^{1}H NMR (500 MHz, $CDCl_3$, 0.005 M) δ 9.09 (d, J = 8.1 Hz, 1H), 8.91 (d, J = 7.8 Hz, 1H), 8.05–7.95 (m, 2H), 7.71–7.52 (m, 4H), 7.47–7.40 (m, 7H), 7.30–7.21 (m, 3H);

^{1}H NMR (500 MHz, $CDCl_3$, 0.1 M) δ 8.94 (d, J = 8.2 Hz, 1H), 8.75–8.80 (m, 1H), 7.85–7.95 (m, 2H), 7.55–7.60 (m, 1H), 7.38–7.54 (m, 11H), 7.23–7.29 (m, 2H);

^{13}C NMR (75 MHz, $CDCl_3$, 0.1 M) δ 155.4, 150.8 (d, J = 7.5 Hz), 150.3 (d, J = 6.8 Hz), 141.7, 141.2, 138.0, 134.0, 132.5, 130.0 (d, J = 0.8 Hz), 129.0, 126.6, 126.2, 125.9 (d, J = 1.5 Hz), 124.9, 124.6, 124.4, 123.7, 123.4, 123.1, 121.6 (d, J = 9.0 Hz), 120.8 (d, J = 4.5 Hz);

^{31}P NMR (200 MHz, $CDCl_3$) δ –18.7;
IR (neat) 1588, 1525, 1487, 1342, 1300, 1181, 1161, 936, 751, 687 cm^{-1};
HRMS (EI) *m/z* calcd for $C_{29}H_{18}NO_4PS_2$ $(M)^+$ 539.0415, found. 539.0411.

Crystallographic data for the single crystal of racemic **1n** obtained by recrystallization from $CHCl_3$ and *n*-hexane: $C_{29}H_{18}NO_{18}PS_2$, M = 539.53, monoclinic, $P2_1$, a = 7.58210(10), b = 30.1544(7) Å, c = 10.5015(2) Å, α = 90°, β = 95.411(2)°, γ = 90°, V = 2399.65(8) $Å^3$, Z = 4, ρ_{calcd} = 1.493 gcm^{-3}, T = 103 K, 43732 reflections measured, 4708 unique. The final R_1 and wR were 0.0626 and 0.1297 (all data).

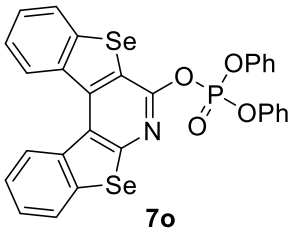

7o

Benzo[4,5]selenopheno[2,3-*b*]benzo[4,5]selenopheno[3,2-*d*]pyridin-7-yl diphenyl phosphate (**7o**)
To a solution of **6o** (428 mg, 0.96 mmol, 1.0 equiv.) in toluene (60 mL), DPPA (411 µL, 1.91 mmol, 2.0 equiv.) and DIPEA (998 µL, 5.73 mmol, 6.0 equiv.) were added at rt. After being refluxed for 18 h under N_2 atmosphere, the reaction mixture was quenched with 2*N* aq. HCl and extracted with AcOEt. The organic layer was washed with brine, dried over Na_2SO_4, filtered and concentrated *in vacuo* to give a residue. The residue was purified by column chromatography (SiO_2, *n*-hexane : AcOEt = 4 : 1 to 7 : 3) to afford **7o** (286 mg, 47%).
Purified **7o** was recrystallized from AcOEt/ *n*-hexane to give pale yellow solid.

Pale yellow solid; m.p. 149–150 ºC;
The chemical shifts of the ^{1}H NMR signals were found to depend on the concentration as follows
^{1}H NMR (500 MHz, $CDCl_3$, 0.005 M) δ 8.98 (d, J = 7.9 Hz, 1H), 8.78 (d, J = 7.9 Hz, 1H), 7.94–8.05 (m, 2H), 7.37–7.60 (m, 11H), 7.21–7.31 (m, 3H);
^{1}H NMR (500 MHz, $CDCl_3$, 0.1 M) δ 8.89 (d, J = 8.0 Hz, 1H), 8.70 (dd, J = 7.1, 2.1 Hz, 1H), 7.87–7.98 (m, 2H), 7.34–7.52 (m, 12H), 7.19–7.30 (m, 2H);
^{13}C NMR (75 MHz, $CDCl_3$, 0.1 M) δ 157.9 (d, J = 0.8 Hz), 151.8 (d, J = 6.8 Hz), 150.9 (d, J = 7.5 Hz), 145.0 (d, J = 0.6 Hz), 142.0, 139.0, 136.5, 134.9, 130.0 (d, J = 1.5 Hz), 129.1, 127.7, 127.6, 126.9, 126.8, 126.7, 126.4, 125.9 (d, J = 1.5 Hz), 124.4, 124.3, 121.7 (d, J = 5.3 Hz), 120.7 (d, J = 4.5 Hz);
^{31}P NMR (200 MHz, $CDCl_3$) δ –18.7;
IR (neat) 1487, 1341, 1300, 1276, 1177, 962, 930, 755, 687, 522 cm^{-1};

HRMS (ESI) *m/z* calcd for $C_{29}H_{18}NaNO_4PSe_2$ $(M+Na)^+$ 657.9202, found. 657.9217.

Crystallographic data for the single crystal of racemic **7o** obtained by recrystallization from $CHCl_3$ and *n*-hexane: $C_{29}H_{18}NO_{18}PSe_2$, M = 633.33, monoclinic, $P2_1/n$, a = 8.34950(10) Å, b = 18.8577(2) Å, c = 15.9730(2) Å, α = 90°, β = 103.7580(10)°, γ = 90°, V = 2442.83(5) Å^3, Z = 4, ρ_{calcd} = 1.722 gcm^{-3}, T = 103 K, 44328 reflections measured, 4794 unique. The final R_1 and wR were 0.0568 and 0.1351 (all data).

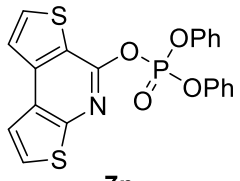

7p

Dithieno[2,3-*b*:3',2'-*d*]pyridin-5-yl diphenyl phosphate (**7p**)

To a solution of **6p** (300 mg, 1.18 mmol, 1.0 equiv.) in toluene (25 mL), DPPA (507 µL, 2.36 mmol, 2.0 equiv.) and DIPEA (1.23 mL, 7.08 mmol, 6.0 equiv.) were added at rt. After being refluxed for 15 h under N_2 atmosphere, the reaction mixture was quenched with 2*N* aq. HCl and extracted with AcOEt. The organic layer was washed with brine, dried over Na_2SO_4, filtered and concentrated *in vacuo* to give a residue. The residue was purified by column chromatography (SiO_2, *n*-hexane : AcOEt = 3 : 2) to afford **7p** (306 mg, 59%).

Pale yellow solid; m.p. 138–139 ºC;

^{1}H NMR (300 MHz, $CDCl_3$) δ 7.78 (d, J = 5.3 Hz, 1H), 7.64–7.66 (m, 1H), 7.55 (d, J = 5.9 Hz, 1H), 7.51 (d, J = 5.9 Hz, 1H), 7.34–7.46 (m, 8H), 7.20–7.28 (m, 2H);

^{13}C NMR (75 MHz, $CDCl_3$) δ 153.4 (d, J = 0.8 Hz), 150.9 (d, J = 7.5 Hz), 149.2 (d, J = 6.8 Hz), 143.8 (d, J = 0.8 Hz), 133.2, 129.9 (d, J = 0.8 Hz), 126.3, 125.81 (d, J = 1.5 Hz), 125.76, 122.1, 121.8 (d, J = 9.8 Hz), 120.7 (d, J = 5.3 Hz), 119.4;

^{31}P NMR (200 MHz, $CDCl_3$) δ –18.7;

IR (neat) 1584, 1481, 1311, 1179, 1154, 1065, 942, 737, 687, 507 cm^{-1};

HRMS (EI) *m/z* calcd for $C_{21}H_{14}NO_4PS_2$ $(M)^+$ 439.0102, found. 439.0099.

Synthesis of Amide-functionalized [7]Helicene-like Molecules 1a and 1b via Direct One-pot Cyclization Method.

Scheme S3-6. Synthesis of **1a** via direct one-pot cyclization

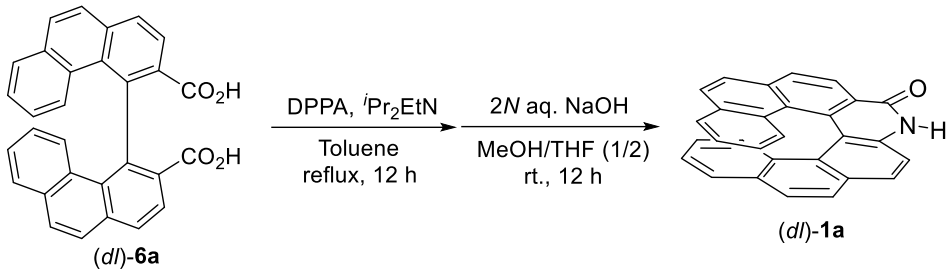

(*dl*)-**6a** (*dl*)-**1a**

Amide-functionalized [7]helicene-like molecule (*dl*)-**1a**

To a solution of (*dl*)-**6a** (10 mg, 0.023 mmol, 1.0 equiv.) in toluene (2 mL), DPPA (10 µL, 0.046 mmol, 2.0 equiv.) and DIPEA (24 µL, 0.14 mmol, 6.0 equiv.) were added at rt. After being refluxed for 12 h under N_2 atmosphere, the reaction mixture was concentrated *in vacuo* to give a residue. Then, a solution of the residue in THF/MeOH/2*N* aq. NaOH (2 : 1 : 1, 4 mL) was stirred at rt. for 12 h, and the reaction mixture was extracted with AcOEt. The organic layer was washed with 1*N* aq. HCl, sat. aq. $NaHCO_3$ and brine, dried over Na_2SO_4, filtered and concentrated *in vacuo* to give a residue. The residue was further purified by column chromatography (SiO_2, *n*-hexane : AcOEt = 3 : 1) to afford (*dl*)-**1a** (3.8 mg, 42%).

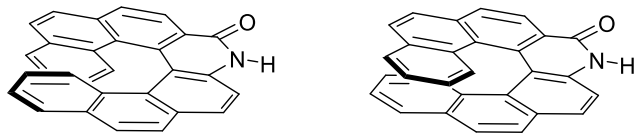

(*M*)-**1a** (*P*)-**1a**

(*M*)- and (*P*)-**1a** were prepared by direct one-pot cyclization from dicarboxylic acid (*R*)- and (*S*)-**6a** in 37% and 38%, respectively, according to the same procedure as racemic form.

(*M*)-**1a**, >99% ee, 37% yield, m.p. >300 °C; (*P*)-**1a**, >98% ee, 38% yield, m.p. >300 °C;

The physical data is consistent with the data reported in **Chapter 2**.

Scheme S3-7. Synthesis of (*dl*)-**1b** via direct one-pot cyclization

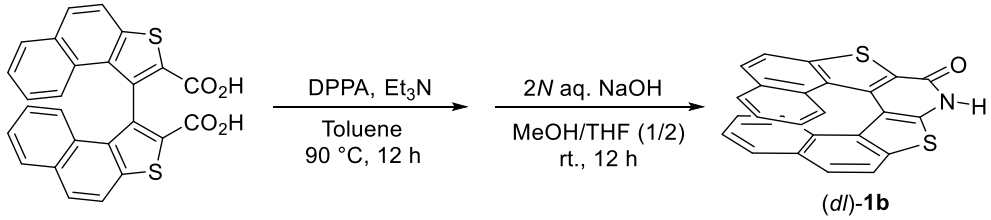

(*dl*)-**6b** (*dl*)-**1b**

Sulfur containing amide functionalized [7]helicene-like molecule (*dl*)-**1b**

To a solution of (*dl*)-**6b** (64.7 mg, 0.143 mmol, 1.0 equiv.) in toluene (5 mL), DPPA (61 µL, 0.285 mmol, 2.0 equiv.) and Et_3N (119 µL, 0.855 mmol, 6.0 equiv.) were added at rt. After being refluxed for 12 h under N_2 atmosphere, the reaction mixture was concentrated *in vacuo* to give a

residue. Then, a solution of the residue in THF/MeOH/2*N* aq. NaOH (2 : 1 : 1, 8 mL) was stirred at rt. for 12 h, and the reaction mixture was extracted with AcOEt. The organic layer was washed with 1*N* aq. HCl, sat. aq. $NaHCO_3$ and brine, dried over Na_2SO_4, filtered and concentrated *in vacuo* to give a residue. The residue was further purified by column chromatography (SiO_2, *n*-hexane : AcOEt = 3 : 1 to 1 : 1) to afford (*dl*)-**1b** (14.6 mg, 25%).

Yellow solid; m.p. >300 ºC;

^{1}H NMR (400 MHz, DMSO-d_6) δ 8.29 (d, J = 8.7 Hz, 1H), 8.19–8.10 (m, 2H), 8.05–7.97 (m, 1H), 7.95–7.91 (m, 2H), 7.41–7.32 (m, 1H), 7.30–7.21 (m, 2H), 7.17–7.11 (m, 1H), 6.55–6.45 (m, 1H), 6.42–6.31 (m, 1H);

^{13}C NMR (100 MHz, DMSO-d_6) δ 158.0, 140.9, 137.1, 131.0, 130.8, 130.6, 130.1, 130.0, 129.6, 128.9, 127.9, 127.8, 126.0, 125.7, 125.5, 125.4, 125.0, 124.3, 123.4, 121.2, 120.7. (Four carbon signals were overlapped);

IR (neat) 3048, 2924, 1647, 1515, 1440, 1360, 1225, 1137, 608 cm^{-1};

HRMS (ESI) *m/z* calcd for $C_{25}H_{14}NOS_2$ $(M+H)^+$ 408.0511, found. 408.0510.

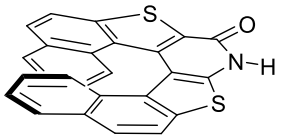

(*M*)-**1b**

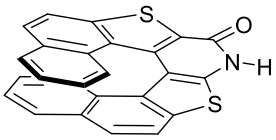

(*P*)-**1b**

(*M*)- and (*P*)-**1b** were prepared by direct one-pot cyclization from dicarboxylic acid (*R*)- and (*S*)-**6b** in 26% and 24%, respectively, according to the same procedure as racemic form.

(*M*)-**1b**, >99% ee, 26% yield, m.p. > 300 °C, $[\alpha]_D^{19}$ = –1869.5 (c = 0.5, DMSO); CD λ_{ext} (THF) nm (Δε): 333 (–50.16), 330 (93.66), 264 (–182.89), 234 (217.18). UV λ_{max} (THF) nm (log ε): 318 (4.25), 230sh (4.97).

(*P*)-**1b**, >99% ee, 24% yield, m.p. >300 ºC, $[\alpha]_D^{22}$ = +1874.6 (c = 0.04, THF); CD λ_{ext} (THF) nm (Δε): 333 (52.04), 330 (93.66), 264 (187.93) 234 (–236.91).

Scheme S3-8. Hydrolysis of **7b**

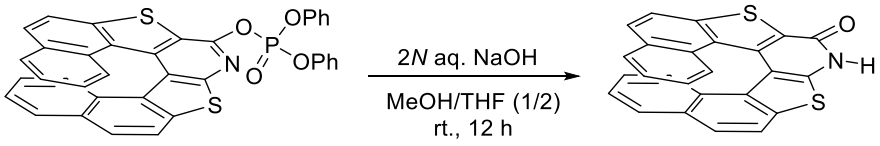

(*dl*)-**7b** (*dl*)-**1b**

The solution of (*dl*)-**7b** (24 mg, 37.5 μmol) in THF/MeOH/2*N* aq. NaOH (2 :1 : 1, 4 mL) was allowed to be stirred at rt. for 12 h. And the reaction mixture was extracted with AcOEt (5 mL × 3). The organic layers were combined and washed with 1*N* aq. HCl, sat. aq. $NaHCO_3$ and brine,

dried over Na_2SO_4, filtered and concentrated *in vacuo* to give a residue. The residue was further purified by column chromatography (SiO_2, *n*-hexane : AcOEt = 3 : 1 to 1 : 1) to afford (*dl*)-**1b** (15 mg, quant.).

The physical data of (*dl*)-**1b** was consistent with reported in **Chapter 3**.

Chapter 4.

Scheme S4-1. Preparation for substrate **3**

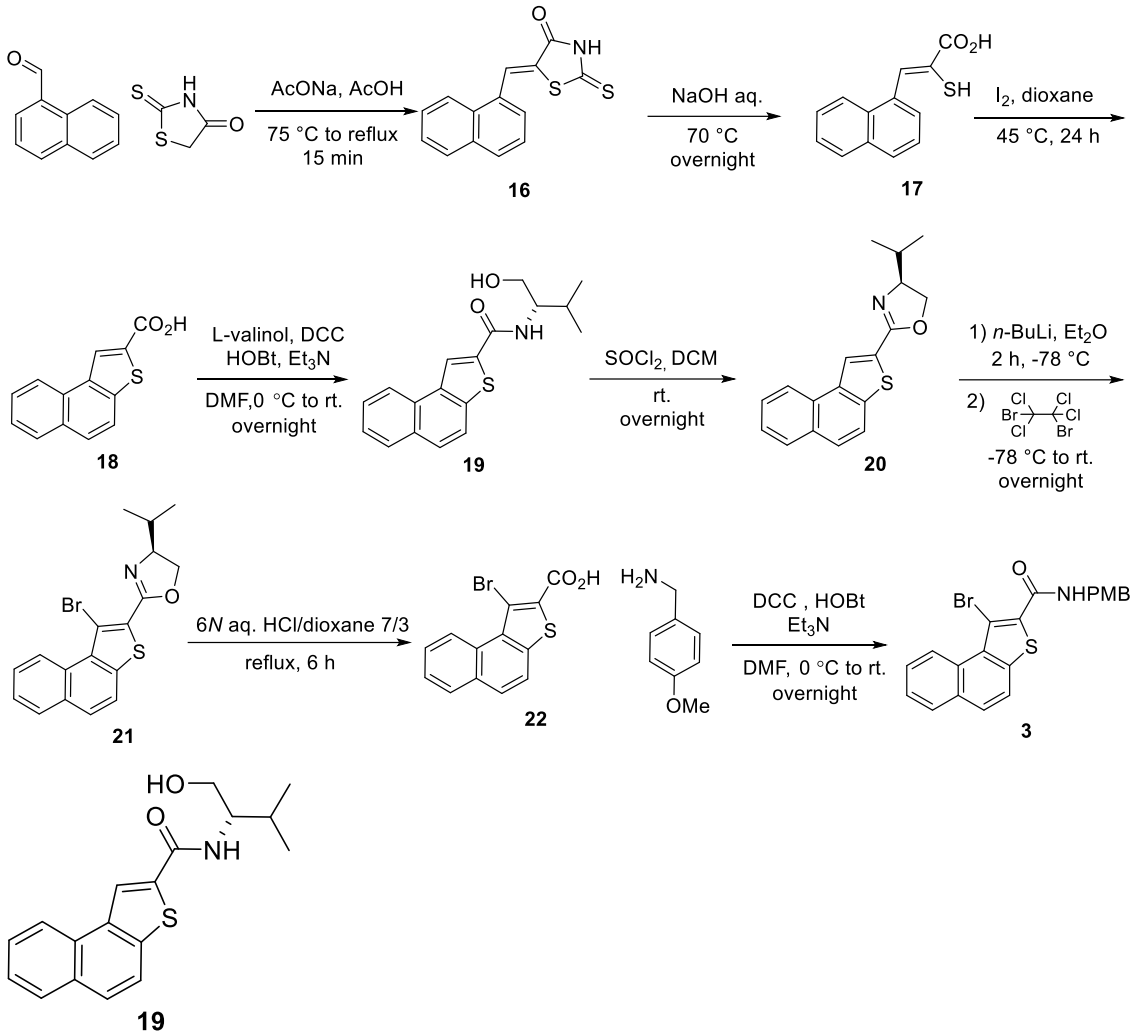

(*S*)-*N*-(1-hydroxy-3-methylbutan-2-yl)naphtho[2,1-*b*]thiophene-2-carboxamide (**19**)

To a mixture of **18**[12] (2.77 g, 12.12 mmol, 1.0 equiv.) and HOBt (2.0 g, 14.54 mmol, 1.2 equiv.) in DMF (20 mL) chilled in an ice-water bath, added DCC (3.0 g, 14.54 mmol, 1.2 equiv.) in one portion. Stir the mixture for 30 min, and remove the ice bath. Formation of white precipitate (DCU) was observed. Add L-valinol (1.5 g, 14.54 mmol, 1.2 equiv.) and Et_3N (2.0 mL, 14.54 mmol, 1.2 equiv.). Continue stirring the mixture at rt. for 12 h. Remove DCU by filtration and wash the precipitates on a fritted funnel with AcOEt (150 mL). The filtrate was washed with 1*N* aq. HCl (30 mL×3), sat. aq. $NaHCO_3$ (30 mL) and brine (20 mL). Organic layer was dried over Na_2SO_4 and then filtered to collect the filtrate which was concentrated *in vacuo* to obtain the crude product. The residue was further purified by column chromatography (SiO_2, *n*-hexane : AcOEt = 1 : 1) to obtain **19** (3.3 g, 86%).

White solid; m.p. 152–153 °C;

^{1}H NMR (600 MHz, $CDCl_3$) δ 8.41 (s, 1H), 8.29–8.24 (m, 1H), 7.98–7.87 (m, 1H), 7.84–7.73 (m, 2H), 7.61–7.57 (m, 1H), 7.55–7.51 (m, 1H), 6.47 (d, *J* = 8.8 Hz, 1H), 4.11–3.94 (m, 1H), 3.89–3.81 (m, 2H), 2.62 (t, *J* = 5.4 Hz, 1H), 2.09–2.06 (m, 1H), 1.08–1.06 (m, 6H);

^{13}C NMR (100 MHz, $CDCl_3$) δ 163.2, 139.5, 137.6, 135.6, 131.1, 129.8, 128.9, 127.6, 127.2, 126.0, 123.5, 123.4, 120.6, 63.8, 57.8, 29.5, 19.8, 19.3;

IR (neat) 3295, 3048, 2937, 1631, 1543, 1193, 1073, 802, 746, 683 cm^{-1};

HRMS (ESI) *m/z* calcd for $C_{18}H_{20}NO_2S$ $(M+H)^+$ 314.1209, found. 314.1208.

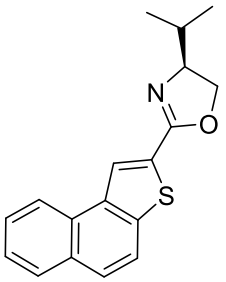

20

(*S*)-4-Isopropyl-2-(naphtho[2,1-*b*]thiophen-2-yl)-4,5-dihydrooxazole (**20**)

To a solution of **19** (3.3 g, 10.3 mmol, 1.0 equiv.) in DCM (20 mL), $SOCl_2$ (3.7 mL, 51 mmol, 5.0 equiv.) was added dropwise at rt. After being stirred at rt. for 12 h, the reaction was quenched with sat. aq. $NaHCO_3$ (50 mL) and then diluted with $CHCl_3$ (30 mL). After separation, the organic layer was washed with sat. aq. $NaHCO_3$ (10 mL×3), water (20 mL×3) and brine (20 mL). Organic phase was dried over Na_2SO_4, and filtered to collect the filtrate which was evaporated in vacuo to obtain the crude residue. Recrystallization in hot *n*-hexane of the residue gave pure product **20** (2.7 g, 89%)

White solid; m.p. 104–105 °C;

^{1}H NMR (600 MHz, $CDCl_3$) δ 8.48 (s,1H), 8.38 (d, *J* = 8.4 Hz, 1H), 7.93 (d, *J* = 6.0 Hz, 1H), 7.88–7.83 (m, 1H), 7.81–7.73 (m, 1H), 7.68–7.61 (m, 1H), 7.58–7.47 (m, 1H), 4.51–4.36 (m, 1H), 4.27–4.14 (m, 2H), 2.00–1.87 (m, 1H), 1.07 (d, *J* = 6.0 Hz, 3H), 0.97 (d, *J* = 6.7 Hz, 3H);

^{13}C NMR (150 MHz, $CDCl_3$) δ 159.6, 139.7, 135.8, 131.1, 130.0, 129.7, 128.8, 127.2, 127.1, 125.9, 125.2, 123.6, 120.6, 73.2, 70.9, 32.9, 19.2, 18.2;

IR (neat) 3052, 2952, 2865, 1651, 1356, 1029, 954, 814, 742, 484 cm^{-1};

HRMS (ESI) *m/z* calcd for $C_{18}H_{18}NOS$ $(M+H)^+$ 296.1104, found. 296.1105.

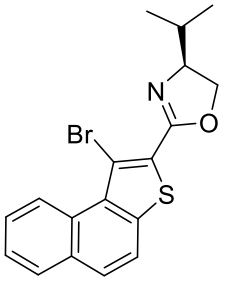

21

(*S*)-2-(1-Bromonaphtho[2,1-*b*]thiophen-2-yl)-4-isopropyl-4,5-dihydrooxazole (**21**)

To a solution of **20** (2.7 g, 9.2 mmol, 1.0 equiv.) in dry ether (60 mL), *n*BuLi (9.3 mL, 14.7 mmol, 1.6 equiv.) was added slowly at –78 °C under Argon atmosphere. The resulted mixture was stirred –78 °C for 1 h. A solution of 1,2-dibromotetrachloroethane (4.8 g, 14.7 mmol, 1.6 equiv.) was added to the resulted mixture at –78 °C under Argon atmosphere. The resulted mixture was stirred for 6 h from –78°C to rt., and evaporated *in vacuo* to remove the solvent. The residue was diluted with AcOEt (50 mL) and washed with 1*N* aq. HCl (20 mL×3), sat. aq. $NaHCO_3$ (20 mL) and brine (20 mL). Organic layer was dried over Na_2SO_4 and then filtered to collect the filtrate which was concentrated *in vacuo* to obtain the crude product. The residue was further purified by column chromatography (SiO_2, *n*-hexane : AcOEt = 4 : 1) to obtain **21** (3.3 g, 95%).

Pale yellow solid; m.p. 87–88 °C;

^{1}H NMR (600 MHz, $CDCl_3$) δ 9.86 (d, *J* = 8.6 Hz, 1H), 7.94 (dd, *J* = 8.1, 1.5 Hz, 1H), 7.81 (d, *J* = 8.7 Hz, 1H), 7.77 (d, *J* = 8.7 Hz, 1H), 7.72–7.67 (m, 1H), 7.62–7.57 (m, 1H), 4.53–4.43 (m, 1H), 4.29–4.14 (m, 2H), 2.03–1.88 (m, 1H), 1.09 (d, *J* = 6.8 Hz, 3H), 0.99 (d, *J* = 6.8 Hz, 3H);

^{13}C NMR (150 MHz, $CDCl_3$) δ 158.7, 138.7, 132.3, 131.4, 130.1, 129.2, 128.6, 126.8, 126.1, 125.6, 122.9, 120.2, 110.3, 73.0, 70.5, 32.9, 19.0, 18.2;

IR (neat) 3060, 2965, 2885, 1638, 1499, 1208, 1045, 982, 810, 671 cm^{-1};

HRMS (ESI) *m/z* calcd for $C_{18}H_{17}BrNOS$ $(M+H)^+$ 374.0209, found. 374.0210.

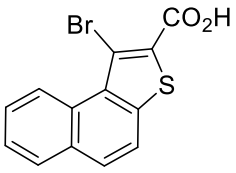

22

1-Bromonaphtho[2,1-*b*]thiophene-2-carboxylic acid (**22**)

The solution of **21** (3.3 g, 8.74 mmol) in 150 mL mixed solvent (6*N* aq. HCl : 1,4-dioxane = 7 : 3) was allowed to be stirred for 6 h under refluxing at Argon atmosphere. Then the suspension was cooled to rt. and filtered to collect the residue and the filtrate. The filtrate was washed with

water (30 mL × 3) and brine (20 mL × 3). Organic layer was dried over Na_2SO_4 and then filtered to collect the filtrate which was concentrated *in vacuo* to obtain the crude product. The residue was further purified by column chromatography (SiO_2, *n*-hexane : AcOEt :AcOH = 90 : 30 : 1) to obtain **22**. The solid was dried under reduced pressure at 80 °C for 12 hours. After combination, the total resulted compound **22** was obtained (2.6 g, 98%).

White solid; m.p. 250–251 °C;

^{1}H NMR (600 MHz, DMSO-d_6) δ 9.79 (d, *J* = 8.5 Hz, 1H), 8.15–8.05 (m, 2H), 8.05–7.99 (m, 1H), 7.78–7.71 (m, 1H), 7.69–7.58 (m, 1H);

^{13}C NMR (100 MHz, DMSO-d_6) δ 162.3, 139.1, 131.9, 130.5, 129.5, 129.4, 129.2, 127.0, 126.3, 122.0, 120.9, 111.8 (One carbon signal was overlapped.);

IR (neat) 2965, 2590, 1690, 1479, 1436, 1249, 890, 802, 679, 464 cm^{-1};

HRMS (ESI) *m/z* calcd for $C_{13}H_8BrO_2S$ $(M+H)^+$ 306.9423, found. 306.9425.

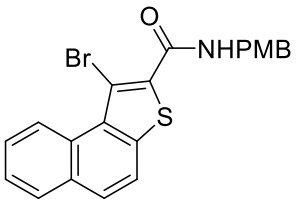

3

1-Bromo-*N*-(4-methoxybenzyl)naphtho[2,1-*b*]thiophene-2-carboxamide (**3**)

To a mixture of **22** (2.6 g, 8.6 mmol, 1.0 equiv.) and HOBt (1.4 g, 10.32 mmol, 1.2 equiv.) in DMF (30 mL) chilled in an ice-water bath, added DCC (2.1 g, 10.32 mmol, 1.2 equiv.) in one portion. Stir the mixture for 30 min, and remove the ice bath. Formation of white precipitate (DCU) was observed. Add 4-methoxybenzylamine (1.5 g, 10.32 mmol, 1.2 equiv.) and Et_3N (1.4 mL, 10.32 mmol, 1.2 equiv.). Continue stirring the mixture at rt. for 12 h. Remove DCU by filtration and wash the precipitates on a fritted funnel with AcOEt (100 mL). The filtrate was washed with 1*N* aq. HCl (30 mL×3), sat. aq. $NaHCO_3$ (30 mL) and brine (20 mL). Organic layer was dried over Na_2SO_4 and then filtered to collect the filtrate which was concentrated *in vacuo* to obtain the crude product. The residue was further purified by column chromatography (SiO_2, *n*-hexane : AcOEt = 3 : 1 to 2 : 1) to obtain **3** (1.9 g, 4.5 mmol, 52%).

White solid; m.p. 144–145 °C;

^{1}H NMR (400 MHz, $CDCl_3$) δ 9.63 (dd, *J* = 8.7, 1.2 Hz, 1H), 7.96 (dd, *J* = 8.0, 1.6 Hz, 1H), 7.87 – 7.76 (m, 2H), 7.70–7.62 (m, 1H), 7.61–7.55 (m, 1H), 7.52 (s, 1H), 7.41–7.32 (m, 2H), 6.96 – 6.86 (m, 2H), 4.69 (d, *J* = 5.5 Hz, 2H), 3.82 (d, *J* = 0.7 Hz, 3H);

^{13}C NMR (100 MHz, $CDCl_3$) δ 161.4, 159.3, 139.0, 134.9, 132.3, 131.0, 130.1, 129.8, 129.5, 129.5, 128.8, 126.9, 126.2, 122.4, 120.5, 114.4, 55.5, 44.1. (One carbon signal was overlapped.); **IR** (neat) 3303, 3064, 2889, 2833, 1619, 1543, 1511, 1300, 1244, 810, 503 cm^{-1};
HRMS (ESI) *m/z* calcd for $C_{21}H_{17}BrNO_2S$ $(M+H)^+$ 426.0158, found. 426.0157.

Scheme S4-2. Preparation of phenanthrene substrate **29**

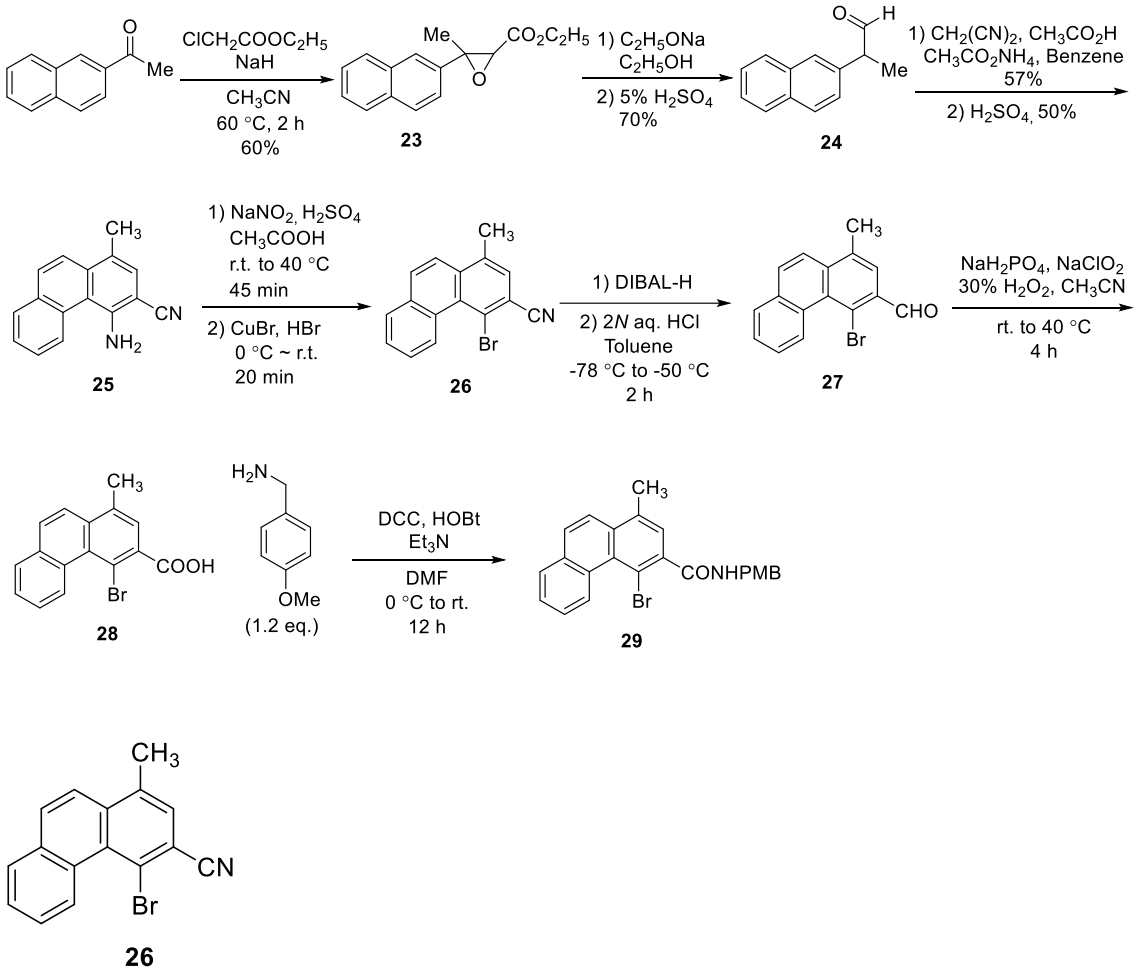

26

4-Bromo-1-methylphenanthrene-3-carbonitrile (**26**)

To a solution of $NaNO_2$ (138 mg, 2.0 mmol, 2.2 equiv.) in conc. H_2SO_4 (2 mL) and CH_3COOH (2 mL) at 40 °C, **25**[14] (216 mg, 0.93 mmol, 1.0 equiv.) was added portionwise and slowly. The resulted mixture was allowed to be stirred at 40 °C for 1 h to obtain a brown solution. After cooling to rt., the brown solution was added dropwise to another solution of CuBr (430.5 mg, 3.0 mmol, 3.3 equiv.) in 30% HBr (3 mL) at ice bath. The finally resulted mixture was stirred for 20 min at ice bath. Then the mixture was poured into ice water and basified with 6*N* aq. NaOH under stirring. The solution was then extracted by AcOEt (20 mL × 3). The organic layers were combined and washed with water (20 mL) and brine (10 mL). After being dried over Na_2SO_4, the

organic phase was filtered to collect filtrate which was evaporated *in vacuo* to obtain crude residue. The residue was purified by column chromatography (SiO_2, *n*-hexane : AcOEt = 5 : 1) to give **26** (85.5 mg, 31%).

Brown solid; m.p. 120–121 °C;
^{1}H NMR (600 MHz, $CDCl_3$) δ 9.84–9.79 (m, 1H), 7.96–7.89 (m, 2H), 7.87 (d, *J* = 9.1 Hz, 1H), 7.74–7.66 (m, 2H), 7.62 (q, *J* = 0.9 Hz, 1H), 2.72 (d, *J* = 0.9 Hz, 3H);
^{13}C NMR (150 MHz, $CDCl_3$) δ 136.0, 135.6, 133.3, 131.4, 130.7, 129.9, 129.6, 128.7, 128.2, 127.6, 126.2, 122.1, 120.8, 119.2, 116.4, 20.3;
IR (neat) 3068, 2984, 2220, 1503, 1376, 822, 746, 639, 587, 555 cm^{-1};
HRMS (APCI) *m/z* calcd for $C_{16}H_{11}BrN$ $(M+H)^+$ 296.0069, found. 296.0068.

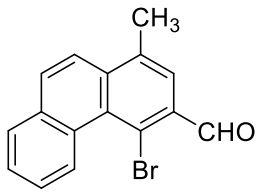

27

4-Bromo-1-methylphenanthrene-3-carbaldehyde (**27**)
To a solution of **26** (85.5 mg, 0.3 mmol, 1.0 equiv.) in toluene (8 mL) at -78 °C under Argon atmosphere, DIBAL-H (435 μL, 0.435 mmol, 1.0 equiv.) was added. The resulted solution was stirred for 3 h at -50 °C. Then 2*N* aq. HCl (5 mL) was added at rt. After being stirred for 1 h, the mixture was extracted by AcOEt (5 mL×3). Organic layers were combined and washed with water (10 mL×3) and brine (5 mL). After being dried over Na_2SO_4, the organic phase was filtered to collect the filtrate which was concentrated *in vacuo* to obtain the crude residue. The residue was purified by column chromatography (SiO_2, *n*-hexane : AcOEt = 10 : 1) to give **27** (67 mg, 75%)

White solid; m.p. 122–123 °C;
^{1}H NMR (600 MHz, $CDCl_3$) δ 10.75 (s, 1H), 9.76–9.65 (m, 1H), 7.95–7.92 (m, 1H), 7.92–7.89 (m, 2H), 7.86 (d, *J* = 9.0 Hz, 1H), 7.70–7.64 (m, 2H), 2.73 (d, *J* = 0.9 Hz, 3H);
^{13}C NMR (150 MHz, $CDCl_3$) δ 193.9, 137.6, 134.9, 133.4, 131.1, 130.5, 129.9, 128.6, 128.3, 127.7, 127.2, 125.5, 124.0, 122.4, 20.2 (One carbon signal was overlapped.);
IR (neat) 2928, 1679, 1587, 1372, 1260, 989, 818, 742, 531, 444 cm^{-1};
HRMS (APCI) *m/z* calcd for $C_{16}H_{12}BrO$ $(M+H)^+$ 299.0066, found. 299.0067.

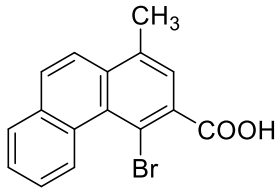

28

4-Bromo-1-methylphenanthrene-3-carboxylic acid (**28**)

To a solution of $NaClO_2$ (137.8 mg, 1.5mmol, 6.8 equiv.) in water (1.5 mL) was added dropwise to a stirred mixture of **27** (67 mg, 0.224 mmol, 1.0 equiv.), NaH_2PO_4 (32.3 mg, 0.269 mmol, 1.2 equiv.), 30% H_2O_2 (112 μL, 1.12 mmol, 5.0 equiv.) in water (0.5 mL) and acetonitrile (1 mL). The resulted mixture was stirred at 40 °C for 5 h. Then Na_2SO_3 (112.9 mg, 0.896 mmol, 6.8 equiv.) was added to the system. The obtained solution was evaporated *in vacuo* to give a crude residue. The residue was purified by column chromatography (SiO_2, $CHCl_3$: MeOH = 10 : 1) to give **28** (59 mg, 84%)

White solid; m.p. 211–212 °C;

^{1}H NMR (600 MHz, acetone-d_6) δ 9.82 (d, *J* = 8.0 Hz, 1H), 8.07–8.02 (m, 1H), 8.02–7.96 (m, 2H), 7.78–7.70 (m, 2H), 7.63 (d, *J* = 1.0 Hz, 1H), 2.77 (s, 3H);

^{13}C NMR (150 MHz, acetone-d_6) δ 136.1, 134.9, 134.4, 131.0, 130.1, 129.4, 128.5, 128.4, 127.9, 126.0, 123.2, 113.9, 20.0 (Three carbon signals were overlapped.);

IR (neat) 2969, 2614, 1694, 1419, 1272, 926, 818, 750, 635, 456 cm^{-1};

HRMS (ESI-) *m/z* calcd for $C_{16}H_{10}BrO_2$ $(M-H)^+$ 312.9870, found. 312.9872.

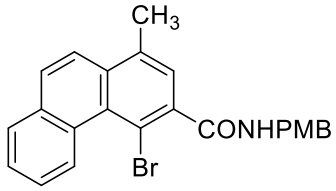

29

4-Bromo-*N*-(4-methoxybenzyl)-1-methylphenanthrene-3-carboxamide (**29**)

To a mixture of **28** (59 g, 0.188 mmol, 1.0 equiv.) and HOBt (30.5 mg, 0.226 mmol, 1.2 equiv.) in DMF (5 mL) chilled in an ice-water bath, added DCC (46.6 mg, 0.226 mmol, 1.2 equiv.) in one portion. Stir the mixture for 30 min, and remove the ice bath. Formation of white precipitate (DCU) was observed. Add 4-methoxybenzylamine (41.1 mg, 0.24 mmol, 1.2 equiv.) and Et_3N (32 μL, 0.226 mmol, 1.2 equiv.). Continue stirring the mixture at rt. for 12 h. Remove DCU by filtration and wash the precipitates on a fritted funnel with AcOEt (10 mL). The filtrate was washed with 1*N* aq. HCl (5 mL×3), sat. aq. $NaHCO_3$ (5 mL) and brine (5 mL). Organic layer was

dried over Na_2SO_4 and then filtered to collect the filtrate which was concentrated *in vacuo* to obtain the crude product. The residue was further purified by column chromatography (SiO_2, *n*-hexane : AcOEt = 3 : 1 to 3 : 2) to obtain **29** (41.5 mg, 0.1 mmol, 51%).

White amorphous;

^{1}H NMR (600 MHz, $CDCl_3$) δ 9.78 (d, *J* = 8.4 Hz, 1H), 7.93–7.87 (m, 1H), 7.87–7.78 (m, 2H), 7.69–7.57 (m, 2H), 7.43 (d, *J* = 0.9 Hz, 1H), 7.38 (d, *J* = 8.7 Hz, 2H), 6.95–6.86 (m, 2H), 6.04 (s, 1H), 4.67 (d, *J* = 5.6 Hz, 2H), 3.82 (s, 3H), 2.70 (d, *J* = 0.9 Hz, 3H);

^{13}C NMR (100 MHz, $CDCl_3$) δ 169.5, 159.3, 139.7, 135.2, 134.0, 133.4, 130.3, 129.8, 129.7, 129.5, 129.1, 128.4, 127.9, 127.5, 126.8, 125.2, 122.3, 114.3, 113.6, 55.5, 44.9, 20.2;

IR (neat) 3267, 3052, 2925, 1634, 1511, 1249, 1034, 810, 750, 576, 444 cm^{-1};

HRMS (ESI) *m/z* calcd for $C_{24}H_{21}BrNO_2$ $(M+H)^+$ 434.0750, found. 434.0749.

Scheme S4-3. Palladium-catalyzed domino reaction with conditions developed by Furuta

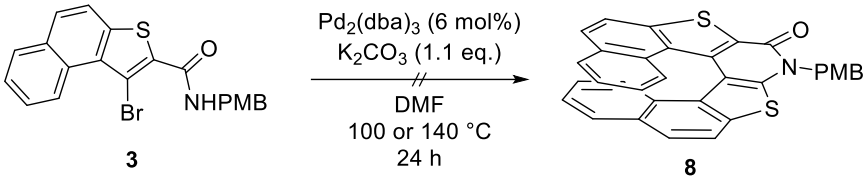

The mixture of **3** (30 mg, 0.07 mmol, 1.0 equiv.), $Pd_2(dba)_3$ (3.9 mg, 4 μmol, 6 mol%) and K_2CO_3 (11.1 mg, 0.08 mmol, 1.1 equiv.) in DMF (2 mL) was stirred at 100 °C under Argon atmosphere. After cooling the reaction to rt, H_2O (5 mL) was added, and extracted with AcOEt (5 mL×2). The organic layers were combined and washed with H_2O, brine, dried over Na_2SO_4, and evaporated *in vacuo* to give the residue. However, the target compound **8** couldn't been detected. **3** almost remained. After increase the temperature to 140 °C, the target compound **8** was still failed to be detected. But **3** disappeared.

Scheme S4-4. Conditions screening for palladium-catalyzed domino reaction

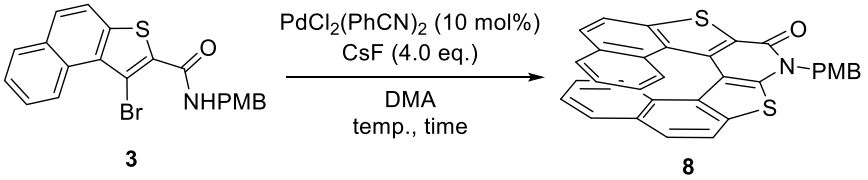

General procedure towards **8**

$PdCl_2(PhCN)_2$ (1.8 mg, 0.0047 mmol, 0.1 equiv.), **3** (20 mg, 0.047 mmol, 1.0 equiv.), CsF (28.6 mg, 0.188 mmol, 4.0 equiv.) were added in a reaction tube, and the mixture was dissolved in anhydrous DMA (2 mL) under Argon atmosphere. The reaction mixture was stirred at scheduled temperature for 24 h or 48 h, then AcOEt (10 mL) was added to dissolve the mixture as much as

possible (except for inorganic salts). Celatom was used to filter undissolved substances. The solvent was then evaporated *in vacuo*, and the mixture was purified by PTLC (SiO_2, *n*-hexane : AcOEt = 5 : 1) to afford the crude product. 1,3,5-Trimethoxybenzene was used as internal standard to determine the yield.

Yellow solid; m.p. 210–211 °C;
^{1}H NMR (600 MHz, $CDCl_3$) δ 8.03 (d, *J* = 8.7 Hz, 1H), 7.98 (d, *J* = 8.7 Hz, 1H), 7.89–7.83 (m, 2H), 7.83–7.79 (m, 2H), 7.55–7.51 (m, 2H), 7.42–7.34 (m, 2H), 7.21–7.11 (m, 2H), 6.91–6.86 (m, 2H), 6.49–6.37 (m, 2H), 5.94 (d, *J* = 15.4 Hz, 1H), 5.38 (d, *J* = 15.4 Hz, 1H), 3.76 (s, 3H);
^{13}C NMR (150 MHz, $CDCl_3$) δ 159.7, 158.6, 146.3, 142.3, 137.2, 131.7, 131.4, 131.2, 130.9, 130.8, 130.0, 129.8, 129.8, 129.7, 127.8, 127.7, 127.1, 126.9, 126.6, 125.7, 125.5, 125.3, 124.5, 123.8, 120.8, 119.7, 114.3, 113.8, 55.4, 50.6 (One carbon signal was overlapped.);
IR (neat) 2960, 1627, 1511, 1475, 1256, 1034, 806, 742, 675, 524 cm^{-1};
HRMS (ESI) *m/z* calcd for $C_{33}H_{22}NO_2S_2$ $(M+H)^+$ 528.1086, found. 528.1085.

Scheme S4-5. Phosphine ligands screening for palladium-catalyzed domino reaction

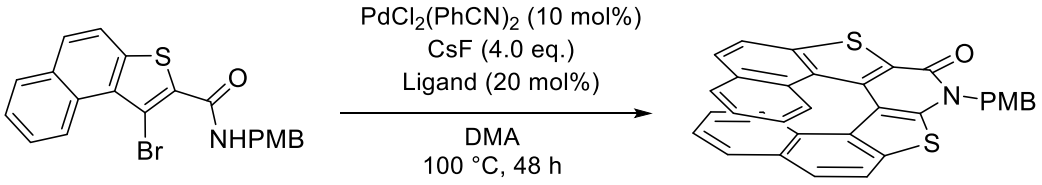

3 **8**

General procedure
$PdCl_2(PhCN)_2$ (1.8 mg, 0.0047 mmol, 0.1 equiv.), **3** (20 mg, 0.047 mmol, 1.0 equiv.), CsF (28.6 mg, 0.188 mmol, 4.0 equiv.), and phosphine ligand (0.0094 mmol, 0.2 equiv.) were added in a reaction tube, and the mixture was dissolved in anhydrous DMA (2 mL) under Argon atmosphere. The reaction mixture was stirred at 100 °C for 48 h, then AcOEt (10 mL) was added to dissolve the mixture as much as possible (except for inorganic salts). Celatom was used to filter undissolved substances. The solvent was then evaporated *in vacuo*, and the mixture was purified by PTLC (SiO_2, *n*-hexane : AcOEt = 5 : 1) to afford the crude product. 1,3,5-Trimethoxybenzene was used as internal standard to determine the yield.

Preparation for other Naphthothiophene Substrates for Palladium-catalyzed Domino Reaction

Scheme S4-6. Synthesis of substrate **30**

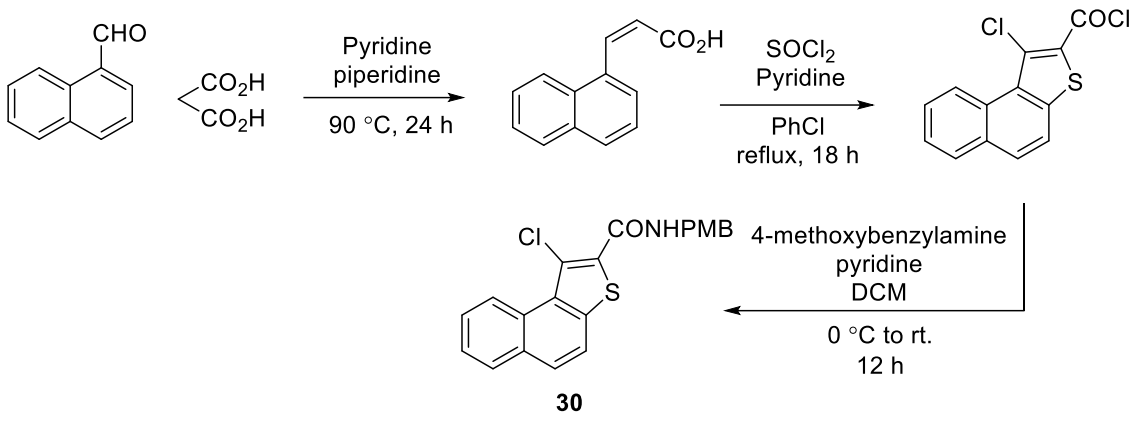

30

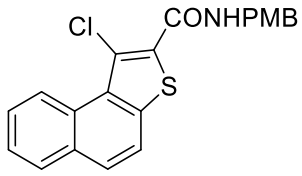

30

1-Chloro-*N*-(4-methoxybenzyl)naphtho[2,1-*b*]thiophene-2-carboxamide (**30**)

To a mixture of 1-chloronaphtho[2,1-*b*]thiophene-2-carbonyl chloride[13] (281.2 mg, 1 mmol, 1.0 equiv.) and 4-methoxybenzylamine (130 μL, 1 mmol, 1.0 equiv.) in DCM (10 mL) chilled in an ice-water bath, added pyridine (0.4 g, 5 mmol, 5.0 equiv.). Continue stirring the mixture at rt. for 12 h. The mixture was concentrated in vacuo to remove DCM and then diluted with AcOEt (20 mL). Organic phase was washed with 1*N* aq. HCl (10 mL), sat. aq. $NaHCO_3$ (10 mL) and brine (5 mL). Organic layer was dried over Na_2SO_4 and then filtered to collect the filtrate which was concentrated *in vacuo* to obtain the crude product. The residue was further purified by column chromatography (SiO_2, *n*-hexane : AcOEt = 3 : 1) to obtain **30** (313 mg, 82%).

White solid; m.p. 131–132 °C;

^{1}H NMR (400 MHz, $CDCl_3$) δ 9.37 (d, *J* = 8.5 Hz, 1H), 8.01–7.92 (m, 1H), 7.88–7.77 (m, 2H), 7.71–7.55 (m, 2H), 7.50 (s, 1H), 7.36 (d, *J* = 9.2 Hz, 2H), 6.92 (d, *J* = 9.2 Hz, 2H), 4.69 (d, *J* = 5.5 Hz, 2H), 3.82 (d, *J* = 2.3 Hz, 3H);

^{13}C NMR (100 MHz, $CDCl_3$) δ 161.1, 159.3, 138.5, 133.2, 132.2, 130.2, 129.9, 129.9, 129.4, 128.9, 127.2, 126.3, 122.6, 120.7, 119.9, 114.4, 55.5, 44.0 (One carbon signal was overlapped.);

IR (neat) 3427, 3315, 2925, 2837, 1647, 1527, 1292, 1253, 806, 511 cm^{-1};

HRMS (ESI) *m/z* calcd for $C_{21}H_{17}ClNO_2S$ $(M+H)^+$ 382.0663, found. 382.0661.

Scheme S4-7. Synthesis of substrates **31-35**

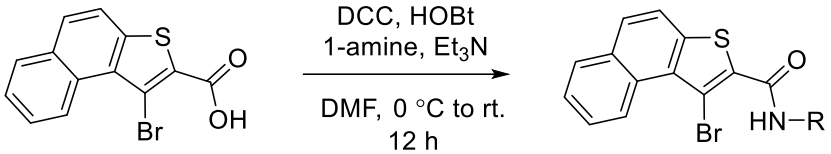

22 **31-35**

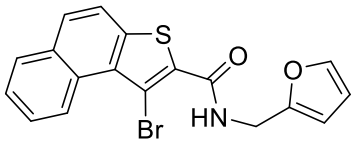

31

1-Bromo-*N*-(furan-2-ylmethyl)naphtho[2,1-*b*]thiophene-2-carboxamide (**31**)

To a mixture of **22** (80.1 mg, 0.261 mmol, 1.0 equiv.) and HOBt (43.2 mg, 0.32 mmol, 1.2 equiv.) in DMF (5 mL) chilled in an ice-water bath, added DCC (66 mg, 0.32 mmol, 1.2 equiv.) in one portion. Stir the mixture for 30 min, and remove the ice bath. Formation of white precipitate (DCU) was observed. Add furfurylamine (28 μL, 0.32 mmol, 1.2 equiv.) and Et_3N (44.6 μL, 0.32 mmol, 1.2 equiv.). Continue stirring the mixture at rt. for 12 h. Remove DCU by filtration and wash the precipitates on a fritted funnel with AcOEt (20 mL). The filtrate was washed with 1*N* aq. HCl (5 mL×3), sat. aq. $NaHCO_3$ (5 mL) and brine (5 mL). Organic layer was dried over Na_2SO_4 and then filtered to collect the filtrate which was concentrated *in vacuo* to obtain the crude product. The residue was further purified by column chromatography (SiO_2, *n*-hexane : AcOEt = 4 : 1) to obtain **31** (90 mg, 89%).

White solid; m.p. 119–120 °C;

^{1}H NMR (400 MHz, $CDCl_3$) δ 9.73–9.56 (m, 1H), 7.97 (dd, *J* = 7.9, 1.6 Hz, 1H), 7.89–7.76 (m, 2H), 7.72–7.68 (m, 1H), 7.65–7.54 (m, 2H), 7.43 (t, *J* = 1.4 Hz, 1H), 6.38 (d, *J* = 1.4 Hz, 2H), 4.75 (d, *J* = 5.4 Hz, 2H);

^{13}C NMR (100 MHz, $CDCl_3$) δ 161.4, 150.8, 142.6, 139.1, 134.6, 132.3, 131.0, 130.1, 129.5, 128.9, 126.9, 126.2, 122.4, 120.5, 110.7, 108.1, 105.8, 37.4;

IR (neat) 3279, 1615, 1527, 1284, 1200, 1146, 814, 750, 675, 603 cm^{-1};

HRMS (ESI) *m/z* calcd for $C_{18}H_{13}BrNO_2S$ $(M+H)^+$ 385.9845, found. 385.9841.

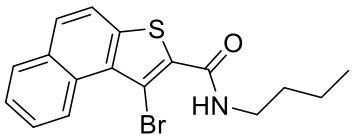

32

1-Bromo-*N*-butylnaphtho[2,1-*b*]thiophene-2-carboxamide (**32**)

To a mixture of **22** (83.7 mg, 0.273 mmol, 1.0 equiv.) and HOBt (44.3 mg, 0.328 mmol, 1.2 equiv.) in DMF (5 mL) chilled in an ice-water bath, added DCC (67.7 mg, 0.328 mmol, 1.2 equiv.) in one portion. Stir the mixture for 30 min, and remove the ice bath. Formation of white precipitate (DCU) was observed. Add *n*Butylamine (32 μL, 0.328 mmol, 1.2 equiv.) and Et_3N (46 μL, 0.328 mmol, 1.2 equiv.). Continue stirring the mixture at rt. for 12 h. Remove DCU by filtration and wash the precipitates on a fritted funnel with AcOEt (10 mL). The filtrate was washed with 1*N* aq. HCl (5 mL×3), sat. aq. $NaHCO_3$ (5 mL) and brine (5 mL). Organic layer was dried over Na_2SO_4 and then filtered to collect the filtrate which was concentrated *in vacuo* to obtain the crude product. The residue was further purified by column chromatography (SiO_2, *n*-hexane : AcOEt = 5 : 1) to obtain **32** (81 mg, 82%).

White solid; m.p. 128– 129 °C;
^{1}H NMR (400 MHz, $CDCl_3$) δ 9.67 (d, *J* = 8.6 Hz, 1H), 7.97 (dd, *J* = 8.0, 1.6 Hz, 1H), 7.87–7.78 (m, 2H), 7.72–7.64 (m, 1H), 7.63–7.56 (m, 1H), 3.70–3.51 (m, 2H), 1.75–1.60 (m, 2H), 1.53–1.41 (m, *J* = 14.9, 7.4 Hz, 2H), 1.00 (t, *J* = 7.4 Hz, 3H);
^{13}C NMR (100 MHz, $CDCl_3$) δ 161.5, 138.9, 135.4, 132.3, 131.0, 130.1, 129.5, 128.7, 126.9, 126.2, 122.4, 120.6, 105.1, 40.3, 31.6, 20.4, 14.0;
IR (neat) 3327, 2960, 2929, 2865, 1619, 1535, 1288, 802, 746, 675, 571 cm^{-1};
HRMS (ESI) *m/z* calcd for $C_{17}H_{17}BrNOS$ $(M+H)^+$ 362.0209, found. 362.0206.

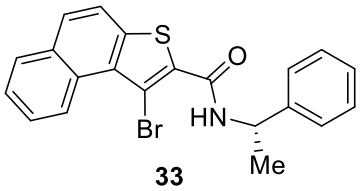

33

(*S*)-1-Bromo-*N*-(1-phenylethyl)naphtho[2,1-*b*]thiophene-2-carboxamide (**33**)
To a mixture of **22** (307 mg, 1 mmol, 1.0 equiv.) and HOBt (162.1 mg, 1.2 mmol, 1.2 equiv.) in DMF (10 mL) chilled in an ice-water bath, added DCC (247.6 mg, 1.2 mmol, 1.2 equiv.) in one portion. Stir the mixture for 30 min, and remove the ice bath. Formation of white precipitate (DCU) was observed. Add (*S*)-(-)-1-phenylethylamine (155 μL, 1.2 mmol, 1.2 equiv.) and Et_3N (167.3 μL, 1.2 mmol, 1.2 equiv.). Continue stirring the mixture at rt. for 12 h. Remove DCU by filtration and wash the precipitates on a fritted funnel with AcOEt (20 mL). The filtrate was washed with 1*N* aq. HCl (5 mL×3), sat. aq. $NaHCO_3$ (5 mL) and brine (5 mL). Organic layer was dried over Na_2SO_4 and then filtered to collect the filtrate which was concentrated *in vacuo* to obtain the crude product. The residue was further purified by column chromatography (SiO_2, *n*-hexane : AcOEt = 4 : 1) to obtain **33** (373 mg, 91%).

White solid; m.p.195–196 °C;

^{1}H NMR (600 MHz, $CDCl_3$) δ 9.69–9.60 (m, 1H), 7.99–7.95 (m, 1H), 7.86–7.79 (m, 2H), 7.70–7.65 (m, 1H), 7.63–7.55 (m, 2H), 7.49–7.44 (m, 2H), 7.42–7.38 (m, 2H), 7.33–7.28 (m, 1H), 5.51–5.42 (m, 1H), 1.70 (d, *J* = 6.9 Hz, 3H);

^{13}C NMR (150 MHz, $CDCl_3$) δ 160.7, 142.9, 139.0, 132.4, 131.1, 130.1, 129.5, 129.0, 128.8, 127.7, 126.9, 126.4, 126.2, 122.4, 120.6, 50.3, 22.4 (Two carbon signals were overlapped.);

IR (neat) 3303, 3025, 1627, 1543, 1308, 1276, 1200, 806, 699, 552 cm^{-1};

HRMS (ESI) *m/z* calcd for $C_{21}H_{17}BrNOS$ $(M+H)^+$ 410.0209, found. 410.0208.

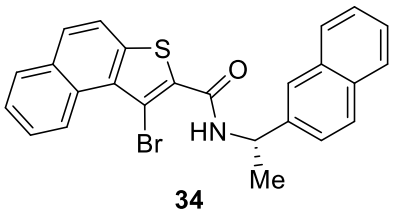

34

(*S*)-1-Bromo-*N*-(1-(naphthalen-2-yl)ethyl)naphtho[2,1-*b*]thiophene-2-carboxamide (**34**)

To a mixture of **22** (60 g, 0.2 mmol, 1.0 equiv.) and HOBt (33 mg, 0.24 mmol, 1.2 equiv.) in DMF (5 mL) chilled in an ice-water bath, added DCC (50 mg, 0.24 mmol, 1.2 equiv.) in one portion. Stir the mixture for 30 min, and remove the ice bath. Formation of white precipitate (DCU) was observed. Add (*S*)-1-(2-naphthyl) ethylamine (41.1 mg, 0.24 mmol, 1.2 equiv.) and Et_3N (33 μL, 0.24 mmol, 1.2 equiv.). Continue stirring the mixture at rt. for 12 h. Remove DCU by filtration and wash the precipitates on a fritted funnel with AcOEt (10 mL). The filtrate was washed with 1*N* aq. HCl (5 mL×3), sat. aq. $NaHCO_3$ (5 mL) and brine (5 mL). Organic layer was dried over Na_2SO_4 and then filtered to collect the filtrate which was concentrated *in vacuo* to obtain the crude product. The residue was further purified by column chromatography (SiO_2, chloroform) to obtain **34** (28.3 mg, 31%).

White solid; m.p. 217–218 °C;

^{1}H NMR (600 MHz, $CDCl_3$) δ 9.65 (d, *J* = 8.6 Hz, 1H), 7.96 (d, *J* = 8.0 Hz, 1H), 7.92 –7.87 (m, 2H), 7.87–7.82 (m, 3H), 7.81 (d, *J* = 8.8 Hz, 1H), 7.70–7.65 (m, 2H), 7.64–7.56 (m, 2H), 7.52–7.46 (m, 2H), 5.59–5.44 (m, 1H), 1.79 (d, *J* = 6.9 Hz, 3H);

^{13}C NMR (150 MHz, $CDCl_3$) δ 160.7, 140.2, 139.0, 135.1, 133.6, 133.0, 132.3, 131.1, 130.1, 129.5, 128.9, 128.8, 128.1, 127.8, 126.9, 126.5, 126.2, 126.2, 125.0, 124.8, 122.4, 120.5, 105.5, 50.3, 22.2;

IR (neat) 3331, 2973, 2921, 1623, 1531, 1264, 798, 739, 627, 479 cm^{-1};

HRMS (ESI) *m/z* calcd for $C_{25}H_{19}BrNOS$ $(M+H)^+$ 460.0365, found. 460.0362.

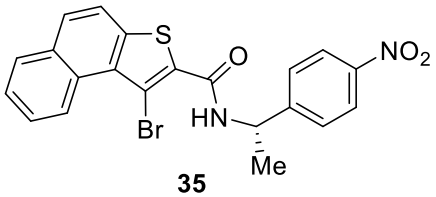

35

(*S*)-1-Bromo-*N*-(1-(4-nitrophenyl)ethyl)naphtho[2,1-*b*]thiophene-2-carboxamide (**35**)

To a mixture of **22** (66 g, 0.215 mmol, 1.0 equiv.) and HOBt (35 mg, 0.258 mmol, 1.2 equiv.) in DMF (5 mL) chilled in an ice-water bath, added DCC (54.2 mg, 0.258 mmol, 1.2 equiv.) in one portion. Stir the mixture for 30 min, and remove the ice bath. Formation of white precipitate (DCU) was observed. Add (*S*)-α-methyl-4-nitroenzylamine · HCl (52.3 mg, 0.258 mmol, 1.2 equiv.) and Et_3N (36 μL, 0.258 mmol, 1.2 equiv.). Continue stirring the mixture at rt. for 12 h. Remove DCU by filtration and wash the precipitates on a fritted funnel with AcOEt (10 mL). The filtrate was washed with 1*N* aq. HCl (5 mL × 3), sat. aq. $NaHCO_3$ (5 mL) and brine (5 mL). Organic layer was dried over Na_2SO_4 and then filtered to collect the filtrate which was concentrated *in vacuo* to obtain the crude product. The residue was further purified by column chromatography (SiO_2, *n*-hexane : AcOEt = 3 : 1) to obtain **35** (98 mg, quant.).

White solid; m.p. 205–206 °C;

^{1}H NMR (400 MHz, $CDCl_3$) δ 9.68 (d, *J* = 8.6 Hz, 1H), 8.39–8.17 (m, 2H), 8.09–7.93 (m, 1H), 7.92–7.78 (m, 2H), 7.78–7.68 (m, 2H), 7.63–7.55 (m, 3H), 5.58–5.26 (m, 1H), 1.75 (d, *J* = 7.2 Hz, 3H);

^{13}C NMR (100 MHz, $CDCl_3$) δ 161.0, 150.5, 147.4, 139.2, 134.3, 132.3, 131.0, 130.0, 129.6, 129.1, 127.2, 127.1, 126.3, 124.3, 122.4, 120.5, 105.8, 50.0, 22.4;

IR (neat) 3327, 3235, 2925, 2849, 1627, 1519, 1344, 858, 802, 746, 679 cm^{-1};

HRMS (ESI) *m/z* calcd for $C_{21}H_{16}BrN_2O_3S$ $(M+H)^+$ 455.0060, found. 455.0060.

Scheme S4-8. Palladium-catalyzed domino reaction with **32**

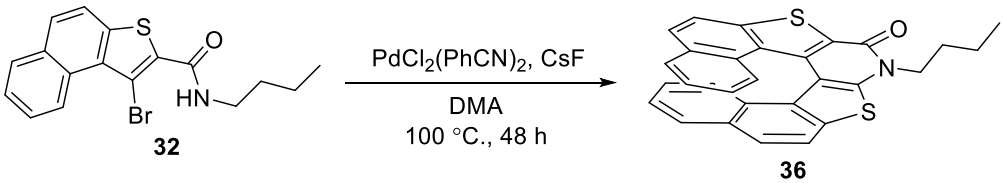

32 **36**

$PdCl_2(PhCN)_2$ (2.1 mg, 0.0056 mmol, 0.1 equiv.), **32** (20.1 mg, 0.0555 mmol, 1.0 equiv.), CsF (34 mg, 0.222 mmol, 4.0 equiv.) were added in a reaction tube, and the mixture was dissolved in anhydrous DMA (2 mL) under Argon atmosphere. The reaction mixture was stirred at scheduled temperature for 48 h, then AcOEt (10 mL) was added to dissolve the mixture as much as possible

(except for inorganic salts). Celatom was used to filter undissolved substances. The solvent was then evaporated *in vacuo*, and the mixture was purified by PTLC (SiO_2, *n*-hexane : AcOEt = 5 : 1) to afford the crude product **36** (0.3 mg, 11%). 1,3,5-Trimethoxybenzene was used as internal standard to determine the yield.

Yellow solid; m.p. 263–264 °C;

^{1}H NMR (600 MHz, $CDCl_3$) δ 8.03 (d, *J* = 8.7 Hz, 1H), 7.98 (d, *J* = 8.7 Hz, 1H), 7.92 (d, *J* = 8.6 Hz, 1H), 7.89–7.81 (m, 3H), 7.53–7.42 (m, 1H), 7.40–7.35 (m, 1H), 7.22–7.13 (m, 2H), 6.51–6.46 (m, 1H), 6.44–6.39 (m, 1H), 4.76–4.64 (m, 1H), 4.34–4.25 (m, 1H), 2.13–1.94 (m, 2H), 1.62–1.57 (m, 2H), 1.06 (t, *J* = 7.4 Hz, 3H);

^{13}C NMR (150 MHz, $CDCl_3$) δ 158.3, 146.5, 142.1, 137.0, 131.8, 131.7, 131.3, 130.9, 130.8, 130.0, 129.8, 129.7, 129.6, 127.8, 127.7, 126.9, 126.7, 125.7, 125.4, 125.3, 124.5, 123.8, 120.9, 119.8, 113.5, 48.4, 29.8, 20.5, 14.0;

IR (neat) 3431, 3057, 2928, 1642, 1503, 1483, 1169, 802, 746, 675 cm^{-1};

HRMS (ESI) *m/z* calcd for $C_{29}H_{20}NNaOS_2$ $(M+Na)^+$ 486.0957, found. 486.0950.

Scheme 4S-9. Palladium-catalyzed domino reaction with **29**

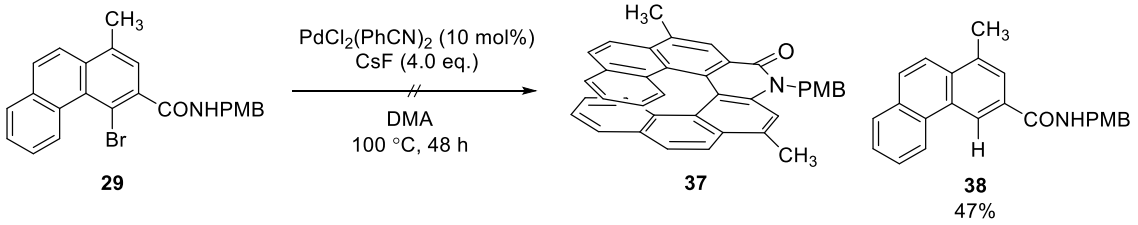

$PdCl_2(PhCN)_2$ (1.3 mg, 0.00345 mmol, 0.1 equiv.), **29** (15 mg, 0.0345 mmol, 1.0 equiv.), CsF (21 mg, 0.138 mmol, 4.0 equiv.) were added in a reaction tube, and the mixture was dissolved in anhydrous DMA (2 mL) under Argon atmosphere. The reaction mixture was stirred at scheduled temperature for 48 h, then AcOEt (10 mL) was added to dissolve the mixture as much as possible (except for inorganic salts). Celatom was used to filter undissolved substances. The solvent was then evaporated *in vacuo*, and the mixture was purified by PTLC (SiO_2, *n*-hexane : AcOEt = 5 : 1) to afford the crude product. Target compound **37** was not found, while 2.3 mg of debrominated product **38** was collected in 19% yield.

Pal yellow solid; m.p. 216–217 °C;

^{1}H NMR (400 MHz, $CDCl_3$) δ 9.06 (s, 1H), 8.77 (d, *J* = 8.2 Hz, 1H), 7.99–7.90 (m, 2H), 7.87 (d, *J* = 9.1 Hz, 1H), 7.77 (dd, *J* = 1.7, 0.9 Hz, 1H), 7.72–7.60 (m, 2H), 7.40–7.32 (m, 2H), 6.97–6.90 (m, 2H), 6.54 (s, 1H), 4.69 (d, *J* = 5.5 Hz, 2H), 3.82 (s, 3H), 2.78 (d, *J* = 0.7 Hz, 3H);

^{13}C NMR (100 MHz, $CDCl_3$) δ 167.8, 159.3, 135.7, 132.9, 132.0, 131.6, 130.9, 130.5, 130.2, 129.6, 128.8, 127.2, 127.1, 125.4, 123.3, 122.5, 120.6, 114.4, 55.5, 44.0, 20.2 (One carbon signal was overlapped.);

IR (neat) 3272, 2921, 1634, 1515, 1244, 1176, 1041, 822, 746, 580 cm^{-1};

HRMS (ESI) *m/z* calcd for $C_{24}H_{22}NO_2$ $(M+H)^+$ 356.1645, found. 356.1643.

Scheme 4S-10. Deprotection of PMB group

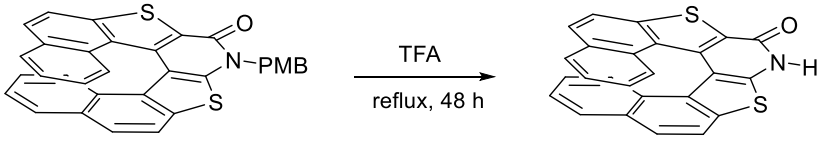

8 **1b**

Sulfur containing amide-functionalized [7]helicene-like molecule **1b**

The solution of **8** (12 mg, 0.023 mmol) in TFA (2 mL) was refluxed for 48 h under Argon atmosphere. The reaction was cooled to rt. and quenched with sat. aq. $NaHCO_3$ (10 mL) and extracted with AcOEt (5 mL×3). Organic layers were combined and washed with water (10 mL) and brine (5 mL). Organic phase was then dried over Na_2SO_4 and filtered to collect the filtrate which was concentrated *in vacuo* to obtain the residue. The residue was purified by column chromatography (SiO_2, *n*-hexane : AcOEt = 1 : 1) to obtain **1b** (7.6 mg, 82%)

Scheme 4S-11. Oxidation of sulfur atoms in **1b**

Preparation of TFPAA (trifluoroperoxyacetic acid)

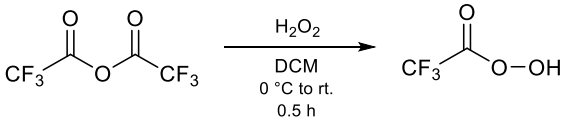

Trifluoroacetic anhydride (1.4 mL, 10 mmol, 1.0 equiv.) was added dropwise to a solution of 30% H_2O_2 (1.0 mL, 10 mmol, 1.0 equiv.) in DCM (2 mL) under stirring at ice bath during more than 10 min. Then the mixture was allowed to stir at rt. for 0.5 h. The resulted solution of TFPAA in DCM was used directly for the following oxidation reaction immediately.

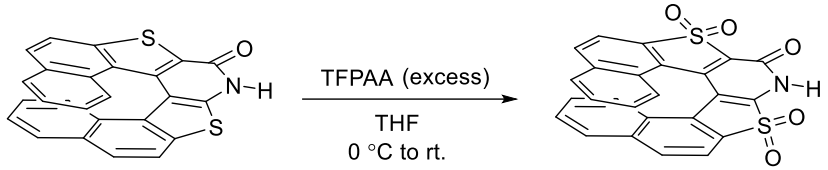

1b **39**

Sulfonyl groups containing amide-functionalized [7]helicene-like molecule **39**

TFPAA solution in DCM prepared immediately was added dropwise to the solution of **1b** (15 mg, 0.037 mmol) in dry THF (10 mL) under stirring at ice bath. The resulted solution was allowed to

stir at rt. for 7 days. The reaction was quenched with sat. aq. $Na_2S_2O_3$ (20 mL) and stirred at rt. for 2 h. The resulted solution was extracted by AcOEt (10 mL × 3). Organic layers were combined and washed with sat. aq. $NaHCO_3$ (5 mL × 3), water (5 mL × 3) and brine (5 mL). Organic phase was dried over Na_2SO_4 and filtered to collect the filtrate which was evaporated *in vacuo* to obtain the residue. The residue was purified by column chromatography (SiO_2, AcOEt) to obtain **39** (1.9 mg, 11%)

Yellow solid; m.p. > 300 °C;

^{1}H NMR (600 MHz, DMSO-d_6) δ 8.35 (d, J = 8.4 Hz, 1H), 8.06 (d, J = 8.4 Hz, 1H), 8.03–8.00 (m, 2H), 7.99–7.92 (m, 2H), 7.35–7.23 (m, 2H), 7.05 (d, J = 8.6 Hz, 1H), 6.96 (d, J = 8.5 Hz, 1H), 6.67–6.55 (m, 2H), 5.38 (s, 1H);

^{13}C NMR (150 MHz, DMSO-d_6) δ 174.5, 139.6, 138.0, 135.4, 135.0, 133.7, 131.7, 130.1, 128.8, 128.7, 128.6, 128.3, 128.1, 127.9, 127.9, 126.8, 126.3, 126.1, 125.7, 125.6, 118.7, 117.1, 116.7 (Two carbon signals were overlapped.);

IR (neat) 3435, 3064, 1655, 1543, 1447, 1384, 1125, 746, 599, 523 cm^{-1};

HRMS (ESI) *m/z* calcd for $C_{25}H_{14}NO_5S_2$ $(M+H)^+$ 472.0308, found. 472.0309.

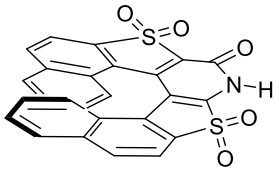

(*M*)-**39**

(*M*)-**39** (11% yield) was obtained, following the same procedure of oxidation of (*dl*)-**1b**.

Yellow solid, m.p. > 300 °C, $[\alpha]_D^{22}$ = -983.6 (c = 0.5, DMSO).

References:

1. Fu, W. C.; Wang, Z.; Chan, W. T. K.; Lin, Z.; Kwong, F. Y. *Angew. Chem. Int. Ed*. **2017**, *56*, 7166.
2. Wu, R.; 'Pete'Silks, L. A.; Olivault-Shiflett, M.; Williams, R. F.; Ortiz, E. G.; Stotter, P.; Kimball, D. B.; Martinez, R. A. *J. Label Compd. Radiopharm*, **2013**, *56*, 581.
3. Nakano, K.; Hidehira, Y.; Takahashi, K.; Hiyama, T.; Nozaki, K. *Angew. Chem. Int. Ed*. **2005**, *44*, 7136.
4. Hayashi, T.; Iwamura, H.; Uozumi, Y.; Matumoto, Y.; Ozawa, F. *Synthesis* **1994**, 526.
5. María, J.; Álvarez-Calero; Jorge, Z. D.; Massanet, G. M. *Org. Lett.* **2016**, *18*, 6344.
6. Banwell, M. G.; Lupton, D. W.; Ma, X.; Renner, J.; Sydnes, M. O. *Org. Lett*. **2004**, *6*, 2741.
7. Nelson, T. D.; Crouch, R. D. Organic Reactions (Hoboken, NJ, United States), **2004**, *63*, 265.
8. Ferraccioli, R.; Carenzi, D.; Motti, E.; Catellani, M. *J. Am. Chem. Soc*. **2006**, *128*, 722.
9. Paegle, E.; Belyakov, S.; Arsenyan, P. *Eur. J. Org. Chem*. **2014**, 3831.
10. Vergura, S.; Scafato, P.; Belviso, S.; Suprechi, S. *Chem. Eur. J*. **2019**, *25*, 5682.
11. Mézlová, M.; Petříčkováb, H.; Maloňc, P.; Kozmíka, V.; Svoboda, J. Collect. Czech. *Chem. Commun*. **2003**, *68*, 1020.
12. Carpino, L. A.; Abdel-Maksoud, A. A.; Dumitru, L.; Mansour, E. M. E.; Zewail, M. A. *J. Org. Chem*. **2007**, *72*, 1729.
13. Irgashev, R. A.; Demina, N. S.; Rusinov, G. L. *Org. Biomol. Chem*. **2020**, *18*, 3164.
14. Krasodomski, W.; Łuczyn´ski, M. K.; Wilamowski, J.; Sepioł, J. J. *Tetrahedron*, **2003**, *59*, 5677.

HPLC chart

For amide-functionalized [7]helicene-like molecule **1a**: CHIRALPAK AD-H (4.6 mm × 250 mm), *n*-hexane : IPA = 9 : 1, flow : 1.0 mL/min, UV : 254 nm.

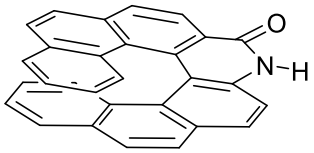

(*dl*)-**1a**

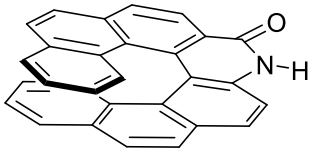

(*P*)-**1a**

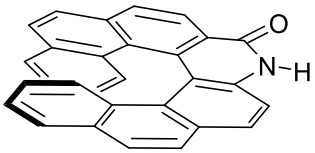

(*M*)-**1a**

(1) Chromatogram of racemic amide-functionalized [7]helicene **1a**

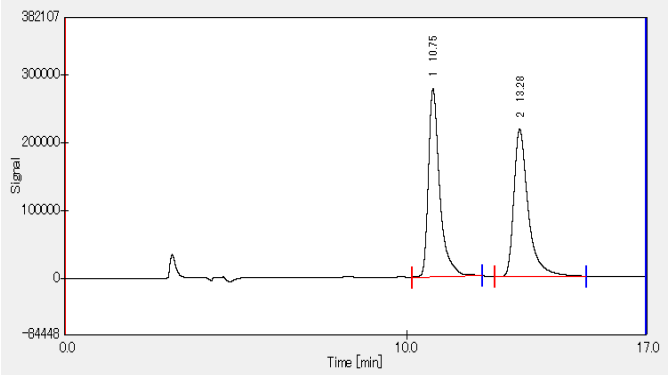

	Retention time (min)	Peak area (%)
1	10.7	50.3
2	13.3	49.7

(2) Chromatogram of (*P*)-amide-functionalized [7]helicene-like molecule **1a**

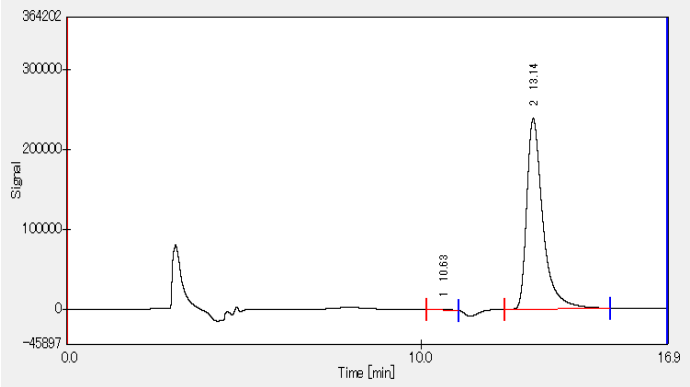

	Retention time (min)	Peak area (%)
1	10.6	0.3
2	13.1	99.7

(3) Chromatogram of (*M*)-amide-functionalized [7]helicene-like molecule **1a**

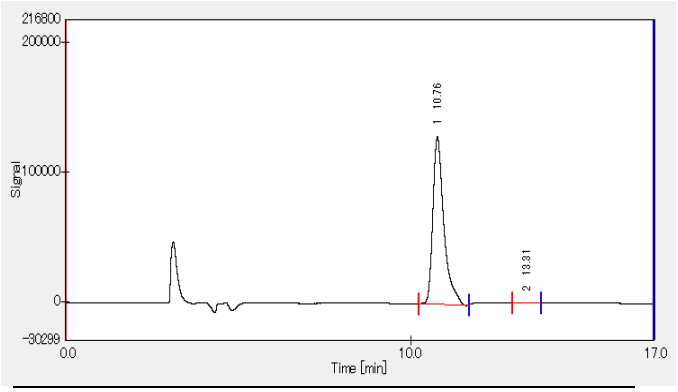

	Retention time (min)	Peak area (%)
1	10.8	99.5
2	13.3	0.5

For sulfur containing amide-functionalized [7]helicene **1b**: CHIRALPAK IC (4.6 mm × 250 mm), *n*-hexane : IPA = 9 : 1, flow : 1.0 mL/min, UV : 254 nm.

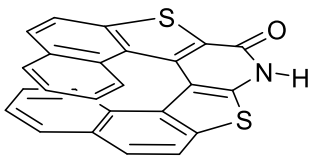

(*dl*)-**1b**

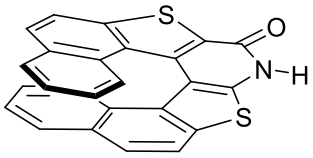

(*P*)-**1b**

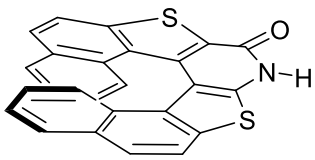

(*M*)-**1b**

(1) Chromatogram of racemic sulfur containing amide-functionalized [7]helicene-like molecule **1b**

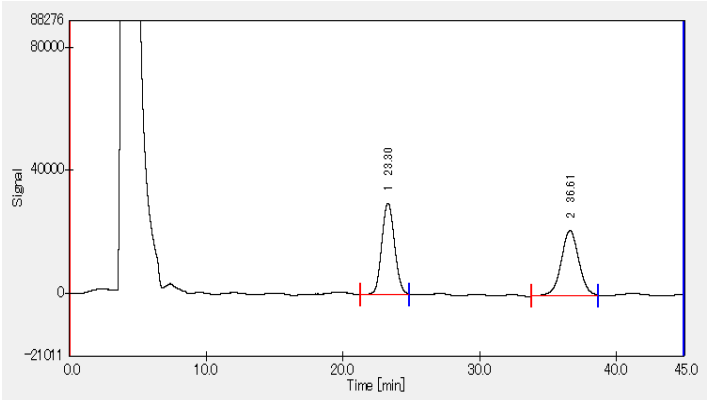

	Retention time (min)	Peak area (%)
1	23.3	50.5
2	36.6	49.5

(2) Chromatogram of (*P*)-sulfur-containing amide-functionalized [7]helicene-like molecule **1b**

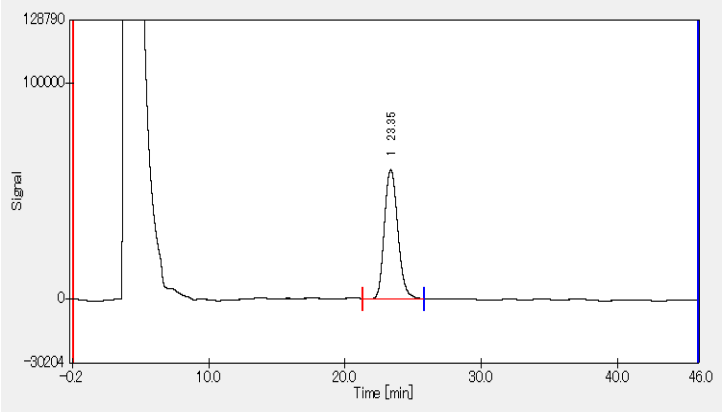

	Retention time (min)	Peak area (%)
1	23.5	100
2		

(3) Chromatogram of (*M*)-sulfur containing amide-functionalized [7]helicene-like molecule **1b**

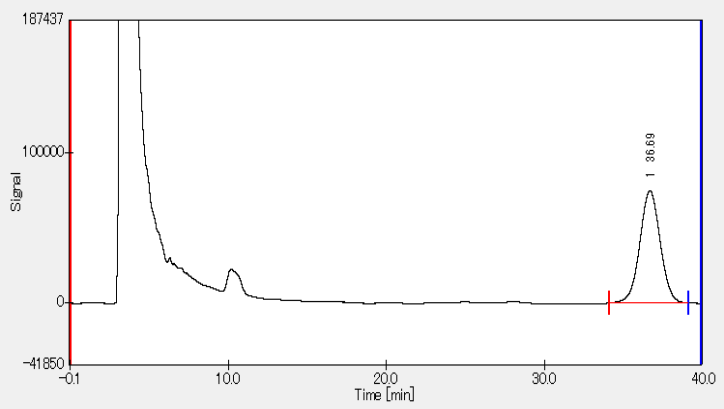

	Retention time (min)	Peak area (%)
1		
2	36.7	100

Calculation

Density functional theory (DFT) calculations were performed using the Gaussian 16 software package. [1] The molecular geometries for the transition states (TS) were first estimated with the *Reaction plus* software package, based on the nudged elastic band method,[2] and were subsequently re-optimized using the Gaussian 16 software package. Once the stationary points were obtained at B3LYP/6-31G (d,p) level,[3] the harmonic vibrational frequencies were calculated at the same level to estimate the Gibbs free energy. The nature of the stationary points was characterized via vibrational analysis. All of the Gibbs free energy values reported in this paper were calculated for a temperature of 298.15 K. All of the transition structures reported were optimized without constraints and the intrinsic reaction coordinate (IRC) routes were calculated in both directions toward the corresponding minima for the transition-state structure. For each gas-phase optimized structure (potential energy minimum or transition state computed at B3LYP/6-31G (d,p) level of theory), additional single-point energy calculations were performed at ωB97XD/6-311+G(d,p) level of theory,[4] in which solvent effects were also taken into account by estimating the solvation free energies (for chlorobenzene as solvent).

1. Gaussian 16, Revision C.01, Frisch, M. J.; Trucks, G. W.; Schlegel, H. B.; Scuseria, G. E.; Robb, M. A.; Cheeseman, J. R.; Scalmani, G.; Barone, V.; Petersson, G. A.; Nakatsuji, H.; Li, X.; Caricato, M.; Marenich, A. V.; Bloino, J.; Janesko, B. G.; Gomperts, R.; Mennucci, B.; Hratchian, H. P.; Ortiz, J. V.; Izmaylov, A. F.; Sonnenberg, J. L.; Williams-Young, D.; Ding, F.; Lipparini, F.; Egidi, F.; Goings, J.; Peng, B.; Petrone, A.; Henderson, T.; Ranasinghe, D.; Zakrzewski, V. G.; Gao, J.; Rega, N.; Zheng, G.; Liang, W.; Hada, M.; Ehara, M.; Toyota, K.; Fukuda, R.; Hasegawa, J.; Ishida, M.; Nakajima, T.; Honda, Y.; Kitao, O.; Nakai, H.; Vreven, T.; Throssell, K.; Montgomery, J. A., Jr.; Peralta, J. E.; Ogliaro, F.; Bearpark, M. J.; Heyd, J. J.; Brothers, E. N.; Kudin, K. N.; Staroverov, V. N.; Keith, T. A.; Kobayashi, R.; Normand, J.; Raghavachari, K.; Rendell, A. P.; Burant, J. C.; Iyengar, S. S.; Tomasi, J.; Cossi, M.; Millam, J. M.; Klene, M.; Adamo, C.; Cammi, R.; Ochterski, J. W.; Martin, R. L.; Morokuma, K.; Farkas, O.; Foresman, J. B.; Fox, D. J. Gaussian, Inc., Wallingford CT, 2016.

2. Henkelman, G.; Jónsson, H.; *J. Chem. Phys.* **2000**, *113*, 9978–9985.

3. (a) Becke, A. D. *J. Chem. Phys.* **1993**, *98*, 5648 − 5652. (b) Lee, C.; Yang, W.; Parr, R. G. *Phys. Rev. B* **1988**, *37*, 785−789. (c) Stephens, P. J.; Devlin, F. J.; Chabalowski, C. F.; Frisch, M. J. J. *Phys. Chem.* **1994**, *98*, 11623−11627.

4. Chai, J.-D.; Head-Gordon, M. *Phys. Chem. Chem. Phys.* **2008**, *10*, 6615−6620.

The energies and coordinates of each structure

1a

(1) Transition state

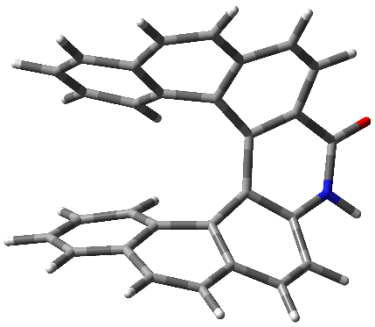

Calculation Method = RB3LYP

Formula = $C_{29}H_{17}NO$

Basis Set = 6-31G(d,p)

Charge = 0

Spin = Singlet

Solvation = None

Imaginary Freq = 1

Temperature = 298.15 Kelvin

Pressure = 1 atm

E(RB3LYP) = -1245.3257 Hartree

Zero-point Energy Correction = 0.373085 Hartree

Thermal Correction to Energy = 0.393337 Hartree

Thermal Correction to Enthalpy = 0.394282 Hartree

Thermal Correction to Free Energy = 0.326251 Hartree

EE + Zero-point Energy = -1244.9526 Hartree

EE + Thermal Energy Correction = -1244.9324 Hartree

EE + Thermal Enthalpy Correction = -1244.9314 Hartree

EE + Thermal Free Energy Correction = -1244.9995 Hartree

E (Thermal) = 246.823 kcal/mol

Heat Capacity (Cv) = 88.801 cal/mol-kelvin

Entropy (S) = 143.182 cal/mol-kelvin

Calculation Type = SP

Calculation Method = RwB97XD

Formula = $C_{29}H_{17}NO$

Basis Set = 6-311+G(d,p)

Charge = 0

Spin = Singlet

Solvation = scrf=solvent=chlorobenzene

E(RwB97XD) = -1245.1765 Hartree

0 1

H	4.33509800	-2.34277800	-0.05816300
C	3.29227900	-2.09425800	-0.21623300
H	2.92099600	-3.49329500	-1.80224900
C	2.51203600	-2.73329400	-1.14300700
C	1.43950600	-0.51565200	0.29919100
C	1.12109700	-2.46545900	-1.17187600
C	2.78215900	-0.95145800	0.44243900
C	0.54918900	-1.53407200	-0.25615600
C	0.26466300	-3.18955400	-2.07136600
H	-0.58888600	-1.20755000	2.16846500
C	-1.08770700	-3.16611600	-1.93407900
H	0.73566100	-3.76954600	-2.86027200
H	-1.73139600	-3.70104300	-2.62673200
C	-1.65792900	-2.59202100	-0.75162200
C	-2.96561900	-2.93875600	-0.34430800
C	-0.82550400	-1.82259900	0.12127900
C	-3.39808200	-2.67979900	0.94240800
H	-3.59834300	-3.48667800	-1.03759200
H	-4.38808200	-2.99262200	1.26053300
C	-2.52122500	-2.07148200	1.85692600
H	-2.82170700	-1.94412300	2.89248500
C	-1.27415200	-1.63614700	1.44721000
H	3.50788400	3.53215900	-0.03034300
C	2.55784000	3.01761600	-0.14120600
H	1.76925700	4.36097500	-1.60797500
C	1.59827100	3.47575700	-1.00265300
C	1.21640000	0.97284100	0.32635700
C	0.33665100	2.83493300	-1.04932700

C	2.39504600	1.74837500	0.46585800
C	0.07697700	1.72495600	-0.19419800
C	-0.70369500	3.34693400	-1.89565500
H	-0.88166000	0.93705900	2.19660100
C	-1.99043000	2.92432600	-1.77050400
H	-0.43044100	4.09073700	-2.63938100
H	-2.77147100	3.29619500	-2.42733800
C	-2.34986600	2.13277700	-0.63254300
C	-3.69620300	2.05448400	-0.20907900
C	-1.31774200	1.58339100	0.19346100
C	-4.01519800	1.60204300	1.05662600
H	-4.47152800	2.43492000	-0.86885500
H	-5.04886900	1.59165200	1.38937100
C	-2.98616600	1.22179300	1.93593600
H	-3.22175500	0.94957000	2.96020000
C	-1.67356000	1.19325400	1.50343000
N	3.51322500	1.21283900	1.08571800
H	4.28959300	1.82226600	1.31129200
C	3.80694000	-0.13386300	1.11444900
O	4.86090300	-0.55268300	1.58117400

(2) Ground state 1 [(*P*)-1a]

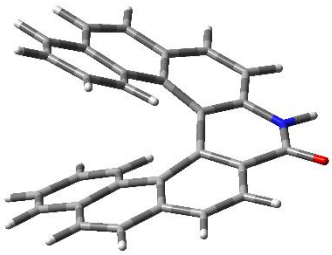

Calculation Method = RB3LYP

Formula = $C_{29}H_{17}NO$

Basis Set = 6-31G(d,p)

Charge = 0

Spin = Singlet

Solvation = None

Imaginary Freq = 0

Temperature = 298.15 Kelvin

Pressure = 1 atm

E(RB3LYP) = -1245.3915 Hartree
Zero-point Energy Correction = 0.374556 Hartree
Thermal Correction to Energy = 0.395583 Hartree
Thermal Correction to Enthalpy = 0.396527 Hartree
Thermal Correction to Free Energy = 0.326018 Hartree
EE + Zero-point Energy = -1245.0169 Hartree
EE + Thermal Energy Correction = -1244.9959 Hartree
EE + Thermal Enthalpy Correction = -1244.9949 Hartree
EE + Thermal Free Energy Correction = -1245.0654 Hartree
E (Thermal) = 248.232 kcal/mol
Heat Capacity (Cv) = 90.374 cal/mol-kelvin
Entropy (S) = 148.399 cal/mol-kelvin

Calculation Type = SP
Calculation Method = RwB97XD
Formula = $C_{29}H_{17}NO$
Basis Set = 6-311+G(d,p)
Charge = 0
Spin = Singlet
Solvation = scrf=solvent=chlorobenzene
E(RwB97XD) = -1245.2447 Hartree

0 1

O	5.13088000	-0.15456800	0.35915600
C	3.95329500	0.11942700	0.14828200
C	2.82445300	-0.81946600	0.29367800
C	3.14287300	-2.13709700	0.68556300
C	2.14867600	-3.07547300	0.77299500
H	2.35351400	-4.07234200	1.15280100
C	0.84816600	-2.78379400	0.28586700
C	0.54142100	-1.49316200	-0.23814600
C	1.50254400	-0.43389100	-0.02134400
C	-0.15639600	-3.80670300	0.30739100
H	0.08919600	-4.75248800	0.78231600

C	-1.38084300	-3.60445100	-0.24656600
H	-2.14331600	-4.37767000	-0.20713400
C	-1.65611700	-2.40633700	-0.97980000
C	-0.68068900	-1.36268600	-1.02563100
C	-2.85182200	-2.28886500	-1.72718900
H	-3.58707000	-3.08607200	-1.65570200
C	-3.06796300	-1.21092600	-2.55991900
H	-3.98444100	-1.13717500	-3.13761300
C	-2.06920700	-0.22753300	-2.68559900
H	-2.20330500	0.59536000	-3.38131200
C	-0.90851500	-0.30448400	-1.93938000
H	-0.14688000	0.44968400	-2.08066600
N	3.59015800	1.35239900	-0.36580900
H	4.36376500	1.97548400	-0.55991600
C	2.29982000	1.85052100	-0.39808900
C	1.21724400	1.01658900	-0.04625600
C	-0.05165500	1.66210800	0.20340100
C	-0.25486600	2.97578000	-0.31058600
C	0.83863100	3.70845000	-0.83703200
H	0.66521700	4.71257000	-1.21309500
C	2.10646100	3.19041400	-0.80583200
H	2.96286600	3.77764000	-1.12518300
C	-1.11705200	1.10234800	1.02813000
C	-2.40686100	1.71946900	1.02107100
C	-2.61085200	2.93770000	0.29791300
H	-3.60190700	3.38267900	0.29257700
C	-1.55849500	3.56988500	-0.28577900
H	-1.68459600	4.54295200	-0.75292000
C	-0.91178300	0.03827200	1.94090700
H	0.07862200	-0.37981500	2.05663800
C	-1.93906100	-0.45783600	2.72017300
H	-1.74038800	-1.26818600	3.41506300
C	-3.23266600	0.08984600	2.62925500
H	-4.04077600	-0.31364300	3.23212300
C	-3.45251700	1.17053600	1.80132700
H	-4.43096600	1.64183800	1.75934700

H 4.17497500 -2.35292300 0.93725200

(3) Ground state 2 [(*M*)-1a]

Calculation Method = RB3LYP

Formula = $C_{29}H_{17}NO$

Basis Set = 6-31G(d,p)

Charge = 0

Spin = Singlet

Solvation = None

Imaginary Freq = 0

Temperature = 298.15 Kelvin

Pressure = 1 atm

E(RB3LYP) = -1245.3915 Hartree

Zero-point Energy Correction = 0.374558 Hartree

Thermal Correction to Energy = 0.395586 Hartree

Thermal Correction to Enthalpy = 0.39653 Hartree

Thermal Correction to Free Energy = 0.326018 Hartree

EE + Zero-point Energy = -1245.0169 Hartree

EE + Thermal Energy Correction = -1244.9959 Hartree

EE + Thermal Enthalpy Correction = -1244.9949 Hartree

EE + Thermal Free Energy Correction = -1245.0654 Hartree

E (Thermal) = 248.234 kcal/mol

Heat Capacity (Cv) = 90.374 cal/mol-kelvin

Entropy (S) = 148.405 cal/mol-kelvin

Calculation Type = SP

Calculation Method = RwB97XD

Formula = $C_{29}H_{17}NO$

Basis Set = 6-311+G(d,p)

Charge = 0

Spin = Singlet

Solvation = scrf=solvent=chlorobenzene

E(RwB97XD) = -1245.2447 Hartree

0 1

H -4.17535500 -2.35207200 0.93756400

C	-3.14320100	-2.13651300	0.68585400
H	-2.35427300	-4.07194500	1.15296700
C	-2.14922100	-3.07510500	0.77320000
C	-1.50255800	-0.43364500	-0.02116700
C	-0.84868700	-2.78370500	0.28599300
C	-2.82453200	-0.81896200	0.29395700
C	-0.54167100	-1.49316200	-0.23803600
C	0.15560400	-3.80688500	0.30747000
H	0.14705200	0.44938600	-2.08075500
C	1.38008000	-3.60493200	-0.24648000
H	-0.09027600	-4.75262800	0.78232800
H	2.14236500	-4.37833000	-0.20710200
C	1.65563300	-2.40687600	-0.97970700
C	2.85136500	-2.28973300	-1.72710400
C	0.68047300	-1.36299600	-1.02554600
C	3.06774500	-1.21189600	-2.55990200
H	3.58643600	-3.08709300	-1.65554800
H	3.98423400	-1.13838000	-3.13760500
C	2.06920300	-0.22831500	-2.68566400
H	2.20343700	0.59446100	-3.38149000
C	0.90851500	-0.30493500	-1.93939700
H	-2.96222700	3.77778300	-1.12595200
C	-2.10590100	3.19053300	-0.80643200
H	-0.66449500	4.71244900	-1.21387700
C	-0.83801500	3.70841500	-0.83763800
C	-1.21698200	1.01674100	-0.04645100
C	0.25534800	2.97573800	-0.31094200
C	-2.29946200	1.85080400	-0.39832800
C	0.05199300	1.66213800	0.20315000
C	1.55899700	3.56979400	-0.28601900
H	-0.07849400	-0.37978100	2.05645700
C	2.61121800	2.93763700	0.29790100
H	1.68517400	4.54282300	-0.75321300
H	3.60228000	3.38259700	0.29275400
C	2.40709100	1.71946200	1.02111000
C	3.45264100	1.17059600	1.80154200

C	1.11728900	1.10234500	1.02801300
C	3.23268100	0.08994700	2.62950200
H	4.43110100	1.64187900	1.75964800
H	4.04069400	-0.31348400	3.23253300
C	1.93908100	-0.45772300	2.72026500
H	1.74029800	-1.26802400	3.41518300
C	0.91190500	0.03833300	1.94082300
N	-3.58985900	1.35297800	-0.36561900
H	-4.36339200	1.97604500	-0.56001200
C	-3.95315600	0.12010300	0.14850200
O	-5.13080000	-0.15372000	0.35932900

1o

(1) Transition state

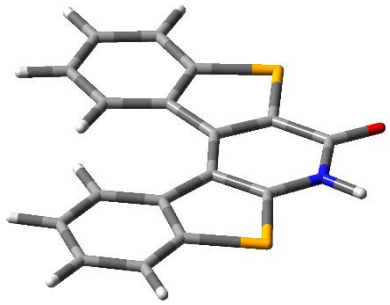

Calculation Method = RB3LYP

Formula = $C_{17}H_9NOSe_2$

Basis Set = 6-31G(d,p)

Charge = 0

Spin = Singlet

Solvation = None

E(RB3LYP) = -5582.0054 Hartree

Imaginary Freq = 1

Temperature = 298.15 Kelvin

Pressure = 1 atm

Electronic Energy (EE) = -5582.0054 Hartree

Zero-point Energy Correction = 0.213254 Hartree
Thermal Correction to Energy = 0.228574 Hartree
Thermal Correction to Enthalpy = 0.229518 Hartree
Thermal Correction to Free Energy = 0.169638 Hartree
EE + Zero-point Energy = -5581.7921 Hartree
EE + Thermal Energy Correction = -5581.7768 Hartree
EE + Thermal Enthalpy Correction = -5581.7758 Hartree
EE + Thermal Free Energy Correction = -5581.8357 Hartree
E (Thermal) = 143.432 kcal/mol
Heat Capacity (Cv) = 62.04 cal/mol-kelvin
Entropy (S) = 126.029 cal/mol-kelvin

Calculation Type = SP
Calculation Method = RwB97XD
Formula = $C_{17}H_9NOSe_2$
Basis Set = 6-311+G(d,p)
Charge = 0
Spin = Singlet
Solvation = scrf=solvent=chlorobenzene
E(RwB97XD) = -5586.2993 Hartree

0 1

C	3.00912400	3.20429300	0.00013600
C	1.85193600	2.43293600	0.00011800
C	4.27342000	2.61298300	0.00007900
C	4.35886200	1.22716100	0.00001400
H	5.17336800	3.21926800	0.00008400
H	5.32482500	0.73160500	-0.00002400
C	3.18879300	0.47232800	0.00000200
C	1.87743800	1.02491600	0.00004000
C	0.78338200	0.01824900	-0.00001400
C	1.32759800	-1.26716700	-0.00007400
C	-2.61829800	3.44263700	0.00001600
C	-1.53716700	2.57360700	-0.00000400
C	-3.93168700	2.95877500	0.00004600
C	-4.14340300	1.59000100	0.00004700

H	-4.77344600	3.64421000	0.00007100
H	-5.15154500	1.18694800	0.00006500
C	-3.04866200	0.72085000	0.00002000
C	-1.69536500	1.17226200	0.00000400
C	-0.69974800	0.07190100	0.00000200
C	-1.35886400	-1.16038700	0.00000700
N	0.61292700	-2.42717900	-0.00012700
H	1.07865700	-3.32616700	-0.00015700
C	-0.77230300	-2.47611300	-0.00003400
O	-1.38487300	-3.54213900	-0.00001400
H	2.91446700	4.28580400	0.00019700
H	0.92413700	2.96774300	0.00018100
H	-0.56321800	3.01873000	-0.00004400
H	-2.43284400	4.51224300	0.00000500
Se	-3.22060800	-1.14139800	0.00002000
Se	3.19424800	-1.40649600	-0.00007300

(2) Ground state 1 [(*P*)-1o]

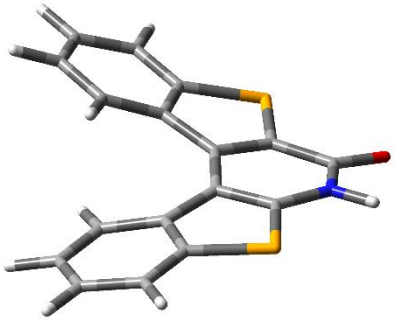

Calculation Method = RB3LYP

Formula = $C_{17}H_9NOSe_2$

Basis Set = 6-31G(d,p)

Charge = 0

Spin = Singlet

Solvation = None

E(RB3LYP) = -5582.0156 Hartree

RMS Gradient Norm = 1.4242e-05 Hartree/Bohr

Imaginary Freq = 0

Temperature = 298.15 Kelvin
Pressure = 1 atm
Frequencies scaled by = 1
Electronic Energy (EE) = -5582.0156 Hartree
Zero-point Energy Correction = 0.214049 Hartree
Thermal Correction to Energy = 0.229829 Hartree
Thermal Correction to Enthalpy = 0.230773 Hartree
Thermal Correction to Free Energy = 0.170023 Hartree
EE + Zero-point Energy = -5581.8015 Hartree
EE + Thermal Energy Correction = -5581.7857 Hartree
EE + Thermal Enthalpy Correction = -5581.7848 Hartree
EE + Thermal Free Energy Correction = -5581.8455 Hartree
E (Thermal) = 144.22 kcal/mol
Heat Capacity (Cv) = 63.31 cal/mol-kelvin
Entropy (S) = 127.861 cal/mol-kelvin

Calculation Type = SP
Calculation Method = RwB97XD
Formula = $C_{17}H_9NOSe_2$
Basis Set = 6-311+G(d,p)
Charge = 0
Spin = Singlet
Solvation = scrf=solvent=chlorobenzene
E(RwB97XD) = -5586.3112 Hartree

0 1

C	2.72563500	3.11311200	0.80262900
C	1.62563400	2.27546600	0.65006400
C	4.01907800	2.66404700	0.51287600
C	4.21772400	1.34342200	0.12077100
H	4.86976400	3.32849600	0.62626400
H	5.22033700	0.96476000	-0.05188900
C	3.11186900	0.50836000	-0.01474000
C	1.78161700	0.95602800	0.18266900
C	0.76365700	-0.07935600	-0.01263400
C	1.32515600	-1.33813000	-0.16725400

C	-2.30825400	3.35932800	-0.76359800
C	-1.30017000	2.41685500	-0.61766700
C	-3.64332800	3.02993800	-0.48428900
C	-3.97738400	1.73391400	-0.11443700
H	-4.42240700	3.77861600	-0.59099000
H	-5.01483800	1.45922000	0.04894100
C	-2.96529500	0.77822100	0.01001400
C	-1.59687000	1.11104700	-0.17528500
C	-0.69034800	-0.02414400	0.00215100
C	-1.37837200	-1.22243000	0.14760800
N	0.59220200	-2.48915600	-0.16388200
H	1.03625600	-3.39371700	-0.26100400
C	-0.78494500	-2.53813200	0.09991700
O	-1.37307000	-3.61015000	0.20803000
H	2.57421400	4.12539100	1.16481300
H	0.64588500	2.63697400	0.93121900
H	-0.28601500	2.68086200	-0.88486700
H	-2.05961100	4.35780500	-1.10963800
Se	-3.23597700	-1.06242100	0.30655600
Se	3.19842300	-1.35400300	-0.34957600

(3) Ground state 2 [(*M*)-1o]

Calculation Method = RB3LYP

Formula = $C_{17}H_9NOSe_2$

Basis Set = 6-31G(d,p)

Charge = 0

Spin = Singlet

Solvation = None

E(RB3LYP) = -5582.0156 Hartree

RMS Gradient Norm = 1.4254e-05 Hartree/Bohr

Imaginary Freq = 0

Temperature = 298.15 Kelvin

Pressure = 1 atm

Electronic Energy (EE) = -5582.0156 Hartree

Zero-point Energy Correction = 0.214049 Hartree
Thermal Correction to Energy = 0.229829 Hartree
Thermal Correction to Enthalpy = 0.230773 Hartree
Thermal Correction to Free Energy = 0.170023 Hartree
EE + Zero-point Energy = -5581.8015 Hartree
EE + Thermal Energy Correction = -5581.7857 Hartree
EE + Thermal Enthalpy Correction = -5581.7848 Hartree
EE + Thermal Free Energy Correction = -5581.8455 Hartree
E (Thermal) = 144.22 kcal/mol
Heat Capacity (Cv) = 63.31 cal/mol-kelvin
Entropy (S) = 127.861 cal/mol-kelvin

Calculation Type = SP
Calculation Method = RwB97XD
Formula = $C_{17}H_9NOSe_2$
Basis Set = 6-311+G(d,p)
Charge = 0
Spin = Singlet
Solvation = scrf=solvent=chlorobenzene
E(RwB97XD) = -5586.3112 Hartree

0 1

C	2.72563600	3.11311300	-0.80262700
C	1.62563400	2.27546700	-0.65006300
C	4.01907900	2.66404600	-0.51287500
C	4.21772400	1.34342200	-0.12077000
H	4.86976500	3.32849500	-0.62626200
H	5.22033800	0.96476000	0.05188900
C	3.11186900	0.50836000	0.01474100
C	1.78161800	0.95602800	-0.18266900
C	0.76365700	-0.07935600	0.01263300
C	1.32515600	-1.33813000	0.16725400
C	-2.30825500	3.35932800	0.76359700
C	-1.30017000	2.41685600	0.61766600
C	-3.64332900	3.02993800	0.48428800
C	-3.97738500	1.73391400	0.11443700

H	-4.42240700	3.77861600	0.59098900
H	-5.01483900	1.45922000	-0.04894000
C	-2.96529500	0.77822100	-0.01001400
C	-1.59687000	1.11104700	0.17528500
C	-0.69034900	-0.02414400	-0.00215200
C	-1.37837200	-1.22243000	-0.14760800
N	0.59220200	-2.48915600	0.16388200
H	1.03625600	-3.39371700	0.26100400
C	-0.78494500	-2.53813200	-0.09991600
O	-1.37307000	-3.61015000	-0.20803000
H	2.57421500	4.12539200	-1.16481100
H	0.64588600	2.63697500	-0.93121800
H	-0.28601500	2.68086300	0.88486600
H	-2.05961200	4.35780500	1.10963600
Se	-3.23597700	-1.06242100	-0.30655500
Se	3.19842300	-1.35400300	0.34957500

1n

(1) Transition state

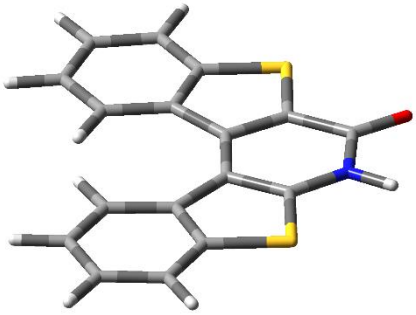

Calculation Method = RB3LYP

Formula = $C_{17}H_9NOS_2$

Basis Set = 6-31G(d,p)

Charge = 0

Spin = Singlet

Solvation = None

E(RB3LYP) = -1579.6334 Hartree

Imaginary Freq = 1

Imaginary Freq = 1
Temperature = 298.15 Kelvin
Pressure = 1 atm

Electronic Energy (EE) = -1579.6334 Hartree
Zero-point Energy Correction = 0.214228 Hartree
Thermal Correction to Energy = 0.228924 Hartree
Thermal Correction to Enthalpy = 0.229868 Hartree
Thermal Correction to Free Energy = 0.172545 Hartree
EE + Zero-point Energy = -1579.4192 Hartree
EE + Thermal Energy Correction = -1579.4045 Hartree
EE + Thermal Enthalpy Correction = -1579.4035 Hartree
EE + Thermal Free Energy Correction = -1579.4608 Hartree
E (Thermal) = 143.652 kcal/mol
Heat Capacity (Cv) = 61.269 cal/mol-kelvin
Entropy (S) = 120.647 cal/mol-kelvin

Calculation Type = SP
Calculation Method = RwB97XD
Formula = $C_{17}H_9NOS_2$
Basis Set = 6-311+G(d,p)
Charge = 0
Spin = Singlet
Solvation = scrf=solvent=chlorobenzene
E(RwB97XD) = -1579.56 Hartree

0 1

C	-3.13588600	-2.79637100	0.00039200
C	-1.93038400	-2.10330800	0.00039900
C	-4.36135300	-2.12340500	0.00007100
C	-4.37079300	-0.73432300	-0.00021300
H	-5.29542600	-2.67572300	0.00012600
H	-5.30540900	-0.18205600	-0.00044400
C	-3.15392300	-0.05511700	-0.00023700
C	-1.88437600	-0.69598700	0.00005100
S	-3.02982400	1.69612700	-0.00025600

C	-0.76784200	0.26972500	0.00009400
C	-1.28931300	1.56359700	-0.00002600
C	2.59878500	-3.18542500	-0.00009600
C	1.50662800	-2.33100500	0.00000900
C	3.90912400	-2.68545300	-0.00025500
C	4.11879200	-1.31618900	-0.00025200
H	4.75482500	-3.36602100	-0.00034400
H	5.12341200	-0.90488600	-0.00027000
C	3.01192500	-0.45987400	-0.00014700
C	1.66672000	-0.92974600	-0.00009200
S	3.13719400	1.27876700	0.00011800
C	0.70145200	0.18242100	-0.00001000
C	1.40240100	1.39297900	0.00015800
N	-0.54673500	2.70824200	-0.00016700
H	-0.99103100	3.61821700	-0.00034500
C	0.84546200	2.72681600	0.00019600
O	1.47542100	3.78016000	0.00036700
H	-3.11538400	-3.88182800	0.00069200
H	-1.02888100	-2.68700200	0.00065400
H	0.52940800	-2.77623900	0.00012900
H	2.42982200	-4.25773600	-0.00001700

(2) Ground state 1 [(*M*)-1n]

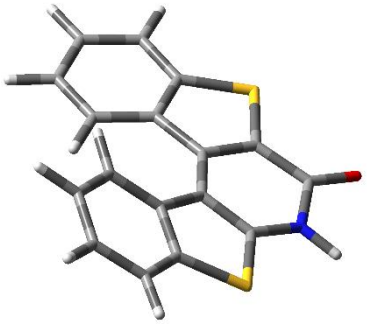

Calculation Method = RB3LYP

Formula = $C_{17}H_9NOS_2$

Basis Set = 6-31G(d,p)

Charge = 0

Spin = Singlet
Solvation = None
E(RB3LYP) = -1579.6389 Hartree
RMS Gradient Norm = 2.6809e-05 Hartree/Bohr
Imaginary Freq = 0
Imaginary Freq = 0
Temperature = 298.15 Kelvin
Pressure = 1 atm

Electronic Energy (EE) = -1579.6389 Hartree
Zero-point Energy Correction = 0.215429 Hartree
Thermal Correction to Energy = 0.230577 Hartree
Thermal Correction to Enthalpy = 0.231521 Hartree
Thermal Correction to Free Energy = 0.173132 Hartree
EE + Zero-point Energy = -1579.4235 Hartree
EE + Thermal Energy Correction = -1579.4083 Hartree
EE + Thermal Enthalpy Correction = -1579.4074 Hartree
EE + Thermal Free Energy Correction = -1579.4658 Hartree
E (Thermal) = 144.689 kcal/mol
Heat Capacity (Cv) = 62.334 cal/mol-kelvin
Entropy (S) = 122.89 cal/mol-kelvin

0 1

C	-2.97561200	-2.73849900	-0.57433200
C	-1.79852800	-2.00165300	-0.49436300
C	-4.21513800	-2.15732300	-0.27866800
C	-4.28699600	-0.80799300	0.05479000
H	-5.12408100	-2.74733700	-0.33859000
H	-5.24450600	-0.33071600	0.23839500
C	-3.10365800	-0.07498700	0.12126400
C	-1.82601700	-0.65204900	-0.09476000
S	-3.01505500	1.67025400	0.37680300
C	-0.75023300	0.32767900	0.03604800
C	-1.27406500	1.60363200	0.19189200
C	2.39653700	-3.15379800	0.53650200
C	1.35341300	-2.24209800	0.46279400

C	3.71651700	-2.76305000	0.25653700
C	4.00585400	-1.44080700	-0.05057300
H	4.51996200	-3.49126600	0.31026500
H	5.02883900	-1.12055600	-0.22134200
C	2.95574100	-0.51765400	-0.10634300
C	1.60303900	-0.90475900	0.09201900
S	3.14445200	1.21123800	-0.32212100
C	0.69788100	0.23334800	-0.02013300
C	1.41854400	1.41630700	-0.16283300
N	-0.51391300	2.73847500	0.17470700
H	-0.93520500	3.65344100	0.27742700
C	0.86444900	2.75248900	-0.09215400
O	1.48023600	3.80826900	-0.19035800
H	-2.92946200	-3.77758200	-0.88567700
H	-0.86498400	-2.46429300	-0.78325300
H	0.35451300	-2.55490200	0.73364000
H	2.18972100	-4.17883900	0.82799800

(3) Ground state 2 [(*P*)-1n]

Calculation Method = RB3LYP

Formula = $C_{17}H_9NOS_2$

Basis Set = 6-31G(d,p)

Charge = 0

Spin = Singlet

Solvation = None

E(RB3LYP) = -1579.6389 Hartree

Imaginary Freq = 0

Temperature = 298.15 Kelvin

Pressure = 1 atm

Electronic Energy (EE) = -1579.6389 Hartree

Zero-point Energy Correction = 0.215429 Hartree

Thermal Correction to Energy = 0.230577 Hartree

Thermal Correction to Enthalpy = 0.231521 Hartree

Thermal Correction to Free Energy = 0.173132 Hartree

EE + Zero-point Energy = -1579.4235 Hartree

EE + Thermal Energy Correction = -1579.4083 Hartree

EE + Thermal Enthalpy Correction = -1579.4074 Hartree

EE + Thermal Free Energy Correction = -1579.4658 Hartree

E (Thermal) = 144.689 kcal/mol

Heat Capacity (Cv) = 62.335 cal/mol-kelvin

Entropy (S) = 122.89 cal/mol-kelvin

Calculation Type = SP

Calculation Method = RwB97XD

Formula = $C_{17}H_9NOS_2$

Basis Set = 6-311+G(d,p)

Charge = 0

Spin = Singlet

Solvation = scrf=solvent=chlorobenzene

E(RwB97XD) = -1579.5659 Hartree

0 1

C	-2.97561900	-2.73849600	0.57433900
C	-1.79853200	-2.00165500	0.49436300
C	-4.21514400	-2.15732000	0.27867400
C	-4.28699800	-0.80799400	-0.05479900
H	-5.12408800	-2.74733300	0.33860100
H	-5.24450700	-0.33071800	-0.23840900
C	-3.10366000	-0.07499000	-0.12127000
C	-1.82601900	-0.65205200	0.09475700
S	-3.01505600	1.67025200	-0.37680800
C	-0.75023500	0.32767800	-0.03604600
C	-1.27406700	1.60363000	-0.19189000
C	2.39655000	-3.15379500	-0.53650500
C	1.35341900	-2.24210300	-0.46278800
C	3.71652800	-2.76304400	-0.25654500
C	4.00585800	-1.44080300	0.05057700
H	4.51997700	-3.49125500	-0.31027700
H	5.02884200	-1.12054800	0.22134800
C	2.95574300	-0.51765200	0.10634600
C	1.60304100	-0.90476100	-0.09201700

S	3.14445000	1.21124000	0.32212100
C	0.69788200	0.23334600	0.02013200
C	1.41854300	1.41630600	0.16282900
N	-0.51391600	2.73847600	-0.17469900
H	-0.93521300	3.65344100	-0.27741200
C	0.86444600	2.75248800	0.09215200
O	1.48023600	3.80826700	0.19036000
H	-2.92947000	-3.77757300	0.88570100
H	-0.86499000	-2.46430200	0.78324200
H	0.35452200	-2.55491700	-0.73362000
H	2.18973600	-4.17883200	-0.82801400

1b

(1) Transition state

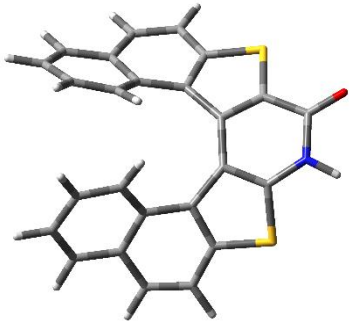

Calculation Method = RB3LYP

Formula = $C_{25}H_{13}NOS_2$

Basis Set = 6-31G(d,p)

Charge = 0

Spin = Singlet

Solvation = None

E(RB3LYP) = -1886.8609 Hartree

Imaginary Freq = 1

Temperature = 298.15 Kelvin

Pressure = 1 atm

Electronic Energy (EE) = -1886.8609 Hartree

Zero-point Energy Correction = 0.307594 Hartree

Thermal Correction to Energy = 0.327346 Hartree

Thermal Correction to Enthalpy = 0.32829 Hartree

Thermal Correction to Free Energy = 0.260559 Hartree
EE + Zero-point Energy = -1886.5533 Hartree
EE + Thermal Energy Correction = -1886.5336 Hartree
EE + Thermal Enthalpy Correction = -1886.5326 Hartree
EE + Thermal Free Energy Correction = -1886.6004 Hartree
E (Thermal) = 205.413 kcal/mol
Heat Capacity (Cv) = 84.055 cal/mol-kelvin
Entropy (S) = 142.553 cal/mol-kelvin

Calculation Type = SP
Calculation Method = RwB97XD
Formula = $C_{25}H_{13}NOS_2$
Basis Set = 6-311+G(d,p)
Charge = 0
Spin = Singlet
Solvation = scrf=solvent=chlorobenzene
E(RwB97XD) = -1886.7481 Hartree

0 1

H	5.67172900	-0.91835800	0.59791800
C	4.72183400	-0.40685700	0.47594200
H	5.37757400	0.77167600	-1.19075100
C	4.55185900	0.51790700	-0.53132100
C	2.45345700	-0.00846700	1.22053100
C	3.33414900	1.23031300	-0.67288600
C	3.67797600	-0.62075300	1.39696300
C	2.20400900	0.86264300	0.13809600
C	3.28470400	2.40689700	-1.47341900
H	3.84138000	-1.25827700	2.26024200
H	1.68516600	-0.11515100	1.97089500
C	2.22729000	3.26696600	-1.34405200
H	4.14027000	2.66645500	-2.08958800
H	2.22505200	4.23802600	-1.82873100
C	1.10351300	2.84903400	-0.59705600
C	0.95452000	1.57517700	-0.02658000
S	-0.25318900	3.90224000	-0.25702800

C	-0.44160100	1.32721100	0.42715700
C	-1.10023000	2.56166000	0.46900700
H	2.38551800	-5.19194400	0.55970500
C	1.65259900	-4.39984800	0.44100400
H	0.72384700	-5.28466000	-1.27850000
C	0.74194800	-4.44023500	-0.59465000
C	0.66254400	-2.33314700	1.22172300
C	-0.25074400	-3.44020200	-0.73258700
C	1.56522800	-3.36643600	1.39098700
C	-0.20896700	-2.28061500	0.11433200
C	-1.38700200	-3.67331500	-1.56536000
H	2.19776200	-3.38808900	2.27303500
H	0.54549300	-1.59057900	1.99704000
C	-2.50046300	-2.89339500	-1.42851000
H	-1.39679200	-4.54626100	-2.21151400
H	-3.42756600	-3.13559700	-1.93802400
C	-2.42218700	-1.72317100	-0.63124100
C	-1.22710700	-1.25876100	-0.04515600
S	-3.79527500	-0.71992600	-0.28086600
C	-1.36497200	0.14815300	0.39312800
C	-2.73534200	0.45767800	0.42862700
N	-2.41313600	2.74848200	0.80486400
H	-2.80369900	3.68136600	0.85854600
C	-3.35079300	1.72084700	0.76795300
O	-4.54695900	1.92990800	0.94202500

(2) Ground state 1 [(*P*)-1b]

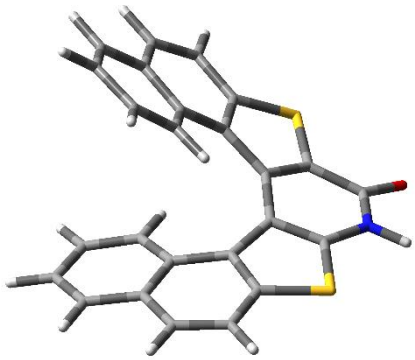

Calculation Method = RB3LYP
Formula = $C_{25}H_{13}NOS_2$
Basis Set = 6-31G(d,p)
Charge = 0
Spin = Singlet
Solvation = None
E(RB3LYP) = -1886.9162 Hartree
Imaginary Freq = 0
Temperature = 298.15 Kelvin
Pressure = 1 atm

Electronic Energy (EE) = -1886.9162 Hartree
Zero-point Energy Correction = 0.308501 Hartree
Thermal Correction to Energy = 0.329051 Hartree
Thermal Correction to Enthalpy = 0.329995 Hartree
Thermal Correction to Free Energy = 0.260135 Hartree
EE + Zero-point Energy = -1886.6077 Hartree
EE + Thermal Energy Correction = -1886.5872 Hartree
EE + Thermal Enthalpy Correction = -1886.5862 Hartree
EE + Thermal Free Energy Correction = -1886.6561 Hartree
E (Thermal) = 206.483 kcal/mol
Heat Capacity (Cv) = 85.944 cal/mol-kelvin
Entropy (S) = 147.034 cal/mol-kelvin

0 1

H	4.05515800	2.90981800	2.38089500
C	3.52125200	2.09349700	1.90377900
H	5.28316400	1.22235400	1.05025400
C	4.20333500	1.15989200	1.15656900
C	1.43407200	0.94602900	1.45767000
C	3.52663300	0.07567900	0.53946900
C	2.12632900	1.96660800	2.07452900
C	2.09661100	-0.00788100	0.64368900
C	4.26138400	-0.95282900	-0.11776200
H	1.59161400	2.67544800	2.69947400
H	0.36820500	0.85728700	1.61827800

C	3.63129000	-2.07708300	-0.58682500
H	5.34116900	-0.86066300	-0.18896000
H	4.19533200	-2.89860500	-1.01677500
C	2.22630900	-2.15005300	-0.49122900
C	1.42317000	-1.10729200	-0.00392900
S	1.29922700	-3.59595700	-0.88140900
C	-0.00153000	-1.42259100	-0.11720600
C	-0.17024300	-2.76883400	-0.42553100
H	0.97461900	4.91981800	-2.27411000
C	0.46210200	4.07411700	-1.82578400
H	-1.10480500	5.26328200	-0.97269000
C	-0.68976700	4.26619700	-1.09416200
C	0.32210500	1.68549700	-1.43720100
C	-1.38040300	3.17231000	-0.51512200
C	0.95417700	2.76740100	-2.01670900
C	-0.83722300	1.85081700	-0.64051500
C	-2.63940400	3.37355000	0.12766200
H	1.83689000	2.60630900	-2.62816800
H	0.70649400	0.69074800	-1.61616200
C	-3.39319800	2.31543600	0.55775200
H	-3.02020200	4.38713000	0.21666300
H	-4.38369400	2.46419700	0.97548800
C	-2.86139000	1.00934800	0.43788600
C	-1.55765600	0.75515200	-0.03153600
S	-3.77051800	-0.44155000	0.77752200
C	-1.23718100	-0.66469300	0.06243100
C	-2.38505900	-1.40471700	0.35698500
N	-1.36993500	-3.41902800	-0.34660800
H	-1.44535400	-4.40723000	-0.55307300
C	-2.52892100	-2.83624800	0.19142700
O	-3.53864600	-3.50155300	0.39491300

(3) Ground state 2 [(*M*)-1b]

Calculation Method = RB3LYP

Formula = $C_{25}H_{13}NOS_2$

Basis Set = 6-31G(d,p)
Charge = 0
Spin = Singlet
Solvation = None
E(RB3LYP) = -1886.9162 Hartree
Imaginary Freq = 0
Temperature = 298.15 Kelvin
Pressure = 1 atm

Electronic Energy (EE) = -1886.9162 Hartree
Zero-point Energy Correction = 0.3085 Hartree
Thermal Correction to Energy = 0.329049 Hartree
Thermal Correction to Enthalpy = 0.329993 Hartree
Thermal Correction to Free Energy = 0.26014 Hartree
EE + Zero-point Energy = -1886.6077 Hartree
EE + Thermal Energy Correction = -1886.5872 Hartree
EE + Thermal Enthalpy Correction = -1886.5862 Hartree
EE + Thermal Free Energy Correction = -1886.6561 Hartree
E (Thermal) = 206.481 kcal/mol
Heat Capacity (Cv) = 85.943 cal/mol-kelvin
Entropy (S) = 147.019 cal/mol-kelvin

Calculation Type = SP
Calculation Method = RwB97XD
Formula = $C_{25}H_{13}NOS_2$
Basis Set = 6-311+G(d,p)
Charge = 0
Spin = Singlet
Solvation = scrf=solvent=chlorobenzene
E(RwB97XD) = -1886.8055 Hartree

0 1

H	-4.05837000	2.90527900	2.37974600
C	-3.52343700	2.08944200	1.90294200
H	-5.28443500	1.21584100	1.05012000
C	-4.20452700	1.15469600	1.15619800

C	-1.43488300	0.94432000	1.45711700
C	-3.52655000	0.07106600	0.53944100
C	-2.12832700	1.96431700	2.07360100
C	-2.09638100	-0.01066300	0.64355300
C	-4.26006800	-0.95867500	-0.11736200
H	-1.59430900	2.67405400	2.69811200
H	-0.36889200	0.85691100	1.61772600
C	-3.62847200	-2.08227100	-0.58604300
H	-5.33996800	-0.86809200	-0.18848200
H	-4.19152900	-2.90468500	-1.01560900
C	-2.22339700	-2.15342800	-0.49053900
C	-1.42159600	-1.10937400	-0.00373900
S	-1.29424700	-3.59794200	-0.88118100
C	0.00356300	-1.42259400	-0.11725300
C	0.17412400	-2.76866700	-0.42562000
H	-0.98306700	4.91832000	-2.27237300
C	-0.46900000	4.07327000	-1.82458300
H	1.09637300	5.26484500	-0.97208700
C	0.68296000	4.26709600	-1.09348800
C	-0.32489800	1.68476600	-1.43670900
C	1.37563500	3.17418600	-0.51502800
C	-0.95903000	2.76579800	-2.01561200
C	0.83450100	1.85184100	-0.64051300
C	2.63473500	3.37719100	0.12716400
H	-1.84179100	2.60330900	-2.62662400
H	-0.70770800	0.68941700	-1.61582000
C	3.39024200	2.32005400	0.55668400
H	3.01421700	4.39124300	0.21613100
H	4.38082400	2.47020900	0.97374600
C	2.86024000	1.01317900	0.43712400
C	1.55668700	0.75716900	-0.03192600
S	3.77141600	-0.43645100	0.77682100
C	1.23807200	-0.66307800	0.06242900
C	2.38705900	-1.40142500	0.35700800
N	1.37475700	-3.41712300	-0.34649200
H	1.45142500	-4.40552000	-0.55166200

C	2.53294500	-2.83275200	0.19158600
O	3.54350300	-3.49672300	0.39546100

Acknowledgements

First and foremost, I am much obliged to Professor Takeo Kawabata (Kyoto University) for his guidance and encouragement in my academic and life. A special and sincere acknowledgement is given to him for great assistance in my study and also as a good role model in my future. The acquisition of independent thinking ability, diligent work attitude and many other corrections for my poor habits from him will be the most precious treasure in the rest of my life. I will never forget about it and keep his teaching and instructions in mind always.

I am also extremely grateful to Professor Takumi Furuta (Kyoto Pharmaceutical University) whose profound chemical knowledge, sophisticated experimental skills and meticulous work attitude have impressed me. Special thanks to his personal guidance to my research and kind care for my life. His encouragement and support are indispensable in the four years' life. I am especially grateful for his patience and kindness for my frequent interruptions.

I would like to express high appreciation to Assistant Professor Yoshihiro Ueda (Kyoto University), Assistant Professor Kazuhiro Morisaki (Kyoto University) for useful discussions. Their kind assistance for my daily life in laboratory is also highly appreciated, which helps me a lot to live a fulfilling and enjoyable life.

I am very thankful that Assistant Professor Shohei Hamada (Kyoto Pharmaceutical University) gives me lots of suggestions about my research topics and assistance for my experiments.

It is highly appreciated that Associate Professor Yusuke Kobayashi (Kyoto Pharmaceutical University) has done a plenty of perfect DFT calculation work and taught me a lot.

I am also much obliged to Professor Norihiro Tokitoh (Kyoto University) and Professor Takahiro Sasamori (University of Tsukuba) for their excellent X-Ray analysis of my compounds and valuable suggestions for the structural analysis.

I would like to sincerely express my gratitude to Professor Kiyosei Takasu (Kyoto University) and Professor Hiroaki Ohno (Kyoto University) for reviewing my thesis and providing valuable comments.

I would like to thank Mr. Takuya Murai and Miss Mayu Kurokawa for their contributions to the direct one-pot cyclization project. I am particularly grateful to Mr. Masanori Nikaido and Mr. Toshifumi Kuribayashi for their previous nice work in the synthesis of helicene-like molecules. I gratefully thank Mr. Chen Gong and Miss Wang Shuo who help me a lot when I just join the group. I am thankful to all of the members in Kawabata group and especially our secretary Ms. Kaori Hashimoto for her support to my daily life.

I would like to express my gratitude to *CSC China Scholarship Council* for financial supports.

I express my deep gratitude to my parents for all they have done for me. Their kind understanding and constant encouragement always support me to go forwards powerfully.